STRUCTURAL AND BIOPHYSICAL CHARACTERIZATION OF PENICILLIN V ACYLASE FROM *BACILLUS SUBTILIS* AND COMPARISON WITH RELATED HYDROLASES AS WELL AS STUDY OF SELECTED PROTEINS FROM MALARIAL PARASITE

THESIS SUBMITTED TO THE

UNIVERSITY OF PUNE

FOR THE DEGREE OF

DOCTOR OF PHILOSOPHY

IN

BIOTECHNOLOGY

BY

PRIYA R

DIVISION OF BIOCHEMICAL SCIENCES

NATIONAL CHEMICAL LABORATORY

PUNE – 411 008

DECEMBER 2006

DECLARATION

I hereby declare that the thesis entitled 'Structural and Biophysical Characterization of Penicillin V Acylase from *Bacillus subtilis* and Comparison with Related Hydrolases as well as Study of Selected Proteins from Malarial Parasite' submitted for Ph.D. degree to the University of Pune has not been submitted by me to any other university for a degree or diploma.

Priya R
Biochemical Sciences Division
National Chemical Laboratory
Dr. Homi Bhabha Road
Pune 411 008
India

Date:

CERTIFICATE

Certified that the work incorporated in this thesis entitled, 'Structural and Biophysical Characterization of Penicillin V Acylase from *Bacillus subtilis* and Comparison with Related Hydrolases as well as Study of Selected Proteins from Malarial Parasite' submitted by Ms. Priya R was carried out by the candidate under my supervision. The materials obtained from other sources have been duly acknowledged in the thesis.

(Dr. C. G. Suresh) Date:

Research Guide

Acknowledgments

I thank the Director and Head, Biochemical Sciences Division, NCL for permission to conduct my work here. I acknowledge financial support from Council of Scientific and Industrial Research, New Delhi. I thank the Commonwealth and the University of York for the split-site PhD scholarship.

I wish to express my sincere gratitude to my research Guide, Dr. C.G. Suresh, mainly for the academic freedom. He has been most understanding, considerate and caring. I am indebted to Dr. Archana V. Pundle for her able guidance and encouragement and Dr. Asmita A. Prabhune for constant support and care. I am grateful to Dr. Sushama Gaikwad for her help and guidance during crucial times.

I have been fortunate to work with Prof. Guy G. Dodson and Prof. Eleanor Dodson, who have been most kind; Dr. James A. Brannigan, who showed exemplary care, often bailing me out of cloning catastrophes and Prof. Antony J. Wilkinson, who provided kind support throughout the tenure at the University of York.

Dr. Shama Barnabas - I cherish the innumerable instances when she shared her wisdom –she is such a scholarly person, with lots of positive attitude, warmth and understanding. Dr. Anil Lachke has been an admirable source of advice and encouragement. I am most grateful to Dr C. SivaRaman for his scholarly suggestions and advice. I am thankful to Drs. Mala Rao and M I Khan for permission to use the spectrophotometer and fluorimeter.

I thank Prof. Marek Brozozowski for helping me even at unearthly hours, sorting out crystallisation problems. Dr. Claudia Schnick was the epitome of friend, philosopher and guide during my tenure at York. My thanks to Dr. Johan Turkenberg for help with collecting data and troubleshooting and Mr. Sam Hart for being so patient and helpful. I am also thankful to Dr. Elena Blagova, Mrs. Shirley Roberts for help with crystallisation. I thank Mr. Simon Grist, Mrs. Sally Lewis, Mrs. Wendy Offen and Mr Tim Kirk for all the ready help. I should mention Eric for magnanimously sharing work space. I thank Ms Caroline and Mrs Louise and the staff at commonwealth for ironing out difficulties. I should acknowledge Mrs Indira, Mr Trehan, Mr Karanjkar Mr Mari and Satyali for their help during all these years.

Dinesh, Rao, Bhushan, Rachna, Meena, Meena, Jayanthi, Jaspreet, Manish, Shivappa, Sulatha and all others have kept company and helped on innumerable occasions. I wish to acknowledge them and everyone from my lab and the division, especially Uma, Poorva, Sharmili, Suresh, Nishant, Anu, Raamesh, Urvashi, Nitin for all the timely help and Ashvini and Mrunal for being such great friends. I also am thankful to all the lovely friends, outside work who made life easier. I am indebted to Uming and her endearing family, especially Appa, Amma, Vekatesh and Sonali for constant support, encouragement and care. Though I have not mentioned all of them, I remember all the goodness each of my friends and family have showered on me.

I wish to mention with gratitude, my teachers at school and graduate studies, especially, Mr. H.H. Sheriff and Drs. K . Nirmala, S. Saroja and S. Annapurani –they were so caring and encouraging.

My family has always had an all- pervading, invisible presence in me, in the form of Hope I carry. I am privileged to be indebted to Aajima for unflinching love and to my TM, Ba for everything I treasure. I dedicate whatever little I have achieved to the loving memory of my beloved grandparents and for M-P, who stood by me, through thick and thin.

- Priya

Abbreviations

6APA	6-aminopenicillanic acid
AMoRe	Automated Molecular Replacement
AS	Ammonium sulphate
BLAST	Basic Local Alignment Search Tool
BSA	Bovine Serum Albumin
*Bsp*PVA	*Bacillus sphaericus* Penicillin V Acylase
*Bsu*PVA	*Bacillus subtilis* Penicillin V Acylase
CA	Cephalosporin acylase
CBH	Conjugated bile acid hydrolase
CCP4	Colloborative computational Project 4
CD	Circular Dichroism
CPB	Citrate Phosphate buffer
DNA	Deoxyribo Nucleic Acid
DTNB	5,5'-dithiobis-(2-nitrobenzoic) acid
DTT	DiThioThreitol
EDTA	Ethylene Diamine Tetra Acetic acid
FPLC	Fast protein liquid chromatography
GFC	Gel filtration chromatography
h /hr	hour
HEPES	N-(2-hydroxyethyl)-piperazine-N'-2-ethane sulfonic acid
HPLC	High performance liquid chromatography
IEF	Iso-electric focussing
IPTG	Isopropyl-β-D-thiogalactoside
kDa	kilo Dalton
K_i	Inhibition constant
K_m	Michaelis-Menten constant
LB	Lineweaver-Burke
M W / M_r	Molecular Weight
M	molar
MAD	Multi-wavelength anomalous dispersion
MALDI -MS	Matrix Assisted Laser Desorption Ionisation Mass Spectrometry
min	minute
MIR	Multiple isomorphous replacement
MR	Molecular replacement
NCS	Non-crystallographic symmetry

NIPOAB	2-nitro-5-(phenoxyacetamido)-benzoic acid
NMR	Nuclear Magnetic Resonance
Ntn	N-terminal hydrolase
O.D	Optical density
PAGE	Poly-acrylamide gel electrophoresis
PCR	Polymerase Chain Reaction
PDAB	Para Dimethyl Amino Benzaldehyde
PDB	Protein DataBank
PEG	poly ethylene glycol
PenG	Penicillin G
PenV	Penicillin V
Gdn HCl	Guanidine hydrochloride
PIPES	Piperazine -1,4–bis - (2-Ethane) Sulphonic Acid
PVA	Penicillin V Amidase
rmsd	root mean square deviation
rpm	revolution per minute
s	second
SDS	sodium dodecyl sulphate
SV	Stern-Volmer
TCA	TriChloro Acetic Acid
Tris	Tris-hydroxymethyl amino methane
V_M	Matthews number
α	(h,k,l) phase angle
μ	micro-
σ	sigma
Σ	summation
α	alpha
Å	Angstrom
β	beta
F(hkl)	structure factor
l	litre
^{o}C	degree centigrade

Abstract

The thesis is a result of the effort at characterising some proteins by using biochemical and biophysical techniques, especially crystallography to elucidate their structure and function. The aim was to characterize and conduct comparative study of a class of hydrolases called choloylglycine hydrolases. Understanding the atomic level contributions of various structural constituents towards activity and stability of penicillin acylase will help to improve the deacylase activity for the production of 6-aminopenicillanic acid, used in the semi-synthetic manufacture of various β-lactams. Similar objectives prompted studies on malarial proteins, which could find application in drug targeting.

The structure of *Bacillus subtilis* penicillin V acylase (*Bsu*PVA) has been elucidated and its enzymatic properties characterized. Biophysical studies using fluorimetry and circular dichroism have been conducted on this enzyme as well as a related hydrolase from *Bacillus sphaericus* (*Bsp*PVA) whose crystal structure was already known. By combining with kinetic studies, these studies have explained the differences between related enzymes at various levels considering molecular level observations obtained from X-ray crystallographic studies. Results will be discussed juxtaposed with the closely related conjugated bile salt hydrolases, which also belong to the family of choloylglycine hydrolases along with PAs. Three malarial proteins were cloned, another one purified and crystallization and crystal characterisation were carried out on one.

The thesis is divided into 9 chapters and structured in three parts. In the first part, characterization of a hypothetical protein from *B. subtilis*, its identification as a PVA and its three-dimensional structure determination are described in detail. Extensive comparative studies on related hydrolases from the choloylglycine family, by generating the relevant data on *Bsp*PVA, form the second part of the thesis. The third and final part deals with various studies carried out on proteins from the malarial parasite.

Chapter 1: General Introduction

Penicillin acylases (also called penicillin amidases or amidohydrolases) are enzymes that reversibly cleave the amide bond between the side chain and the β-lactam nucleus of penicillins, without affecting the amide bond of the β-lactam nucleus. PVA

is an industrially important enzyme that can be used in the manufacture of semi-synthetic penicillins. PVAs are remarkably similar to conjugated bile salt hydrolases in several aspects and the enzyme belongs to the same family. Comparative studies might help us to assign a function to penicillin acylases whose physiological role is still not understood.

The complete genome of the malarial parasite *Plasmodium falciparum* and that of the vector, mosquito have been reported. Along with the success of human genome project, the triumvirate genome data have been a shot in the arm for efforts to combat the disease. Various structural genomics consortia are trying to elucidate the proteome of the parasite and rational drug design. In an opportunity to work in one such consortium the author has tried to characterise selected proteins from the parasite. These efforts are described in the last chapter.

Chapter 2: Biochemical characterization of YxeI as a Penicillin V acylase

This chapter describes the biochemical characterization of YxeI, a hypothetical protein from *B. subtilis*, subsequently characterised as a PVA by us. *E. coli* BL21(DE3) cells were transformed with the *yxeI* gene, the protein was overproduced and purified. Molecular weight, pI and optimal conditions were estimated. PVA activity was detected against penicillin V and for the synthetic substrate 2-nitro-5-(phenoxyacetamido)-benzoic acid (NIPOAB). Chemical modification and site-directed mutation studies identified cysteine and arginine as active site residues.

Chapter 3: Crystallographic studies on YxeI from *B. subtilis* characterised as a PVA

*Bsu*PVA was crystallized and diffraction data were collected using R-AXIS IV^{++} Image Plate system under cryo conditions up to a resolution of 2.5 Å. Data were processed and scaled using *Denzo* and *Scalepack*. The structure has been determined using molecular replacement method using *Bsp*PVA (PDB code 2pva) as the search model. *Bsu*PVA forms a homotetramer by two symmetry-related dimers, in agreement with the existence of tetramer in gel filtration studies. The structure has the classical $\alpha\beta\beta\alpha$ Ntn hydrolase fold. Cysteine1 is the N-terminal nucleophilic residue. The final Rmerge and R factor were within the acceptable range. Geometry of the molecule, checked using *PROCHECK*, had no residue in the disallowed regions of the Ramachandran plot.

Chapter 4: Fluorimetric and kinetic studies of *Bsu*PVA

The decrease in fluorescence intensity upon titration with the substrates NIPOAB and penicillin V (PenV), without change in emission maxima, was made use of to calculate binding constants for these substrates at different temperatures. The temperature dependence of the association constants was used to determine the thermodynamic parameters. The accessibility of Trp fluorophores and their local environment were investigated using acrylamide, potassium iodide (KI) and cesium chloride (CsCl).

Chapter 5: Studies on conformational stability of *Bsu*PVA using fluorimetry and circular dichroism

Temperature, pH and Guanidine hydrochloride (Gdn HCl)- induced conformational changes were studied by monitoring the changes observed in Trp emission. Evidence for molecular aggregation at higher temperatures was obtained by the binding of 1-anilinonaphthalene-8-sulphonic acid (ANS) to the protein in a range of acidic pH 1-4. The secondary structure of the protein was studied using circular dichroism. Activity and denaturation studies were conducted at different concentrations of Gdn HCl.

Chapter 6: Comparative studies on related hydrolases- Part I. Specificity and substrate binding of the PVA from *Bacillus sphaericus*

This part of the thesis compares the kinetic, conformational and structural aspects and stability of *Bsu*PVA with other known hydrolases. Many PVAs have been reported but the only other PVA whose structure has been elucidated is the one from *B. sphaericus* (*Bsp*PVA). Conformational studies have not been reported on this enzyme. Such comparative studies have been carried out on this enzyme and the observed data are presented here. The binding constants for PenV and NIPOAB were calculated. Acrylamide was by far the most efficient quencher (81% quenching). Quenching by KI and CsCl are 20% and 14%, respectively.

Chapter 7: Comparative studies on related hydrolases- Part II. Comparison with the conformational stability of *Bsp*PVA

*Bsp*PVA has 3 Trp residues in hydrophobic environment. There are disturbances in secondary structure with increase in temperature and extremes of pH. The presence of molten globule as indicated by ANS binding is seen in the acidic pH range 1-4. PVA is active in this pH range. Increasing concentrations of Gdn HCl resulted in

decreased 333/356 intensity ratio. There is substantial loss of activity (80%) at 1 M Gdn HCl a complete loss of secondary structure at 6 M.

Chapter 8: Comparative studies on related hydrolases- Part III. Structure, function and evolution

*Bsu*PVA has good sequence homology with other PVAs and Conjugated Bile Acid Hydrolases. This chapter deals with comparison of structural, functional and evolutionary characteristics of *Bsu*PVA with other members of the choloylglycine hydrolase family. Major differences in the structure vis-à-vis substrate specificities, efficiency and relatedness of their sequences are discussed.

In conclusion, our studies have established that YxeI from *B. subtilis* is a PVA, belongs to choloylglycine hydrolase family of the Ntn-hydrolase superfamily and shares the $\alpha\beta\beta\alpha$ fold called the Ntn-fold and conserved residues especially at the oxyanion hole. Despite sharing relatively good sequence and structure homology, *Bsu*PVA and *Bsp*PVA are significantly different in their kinetic properties with respect to their hydrolase activities on penicillin V. Evidences show that the enzyme originated through divergent evolution from a common ancestor that possessed both penicillin acylase and conjugated bile acid hydrolase activities. This study enumerates the reasons and rationale behind designating the protein YxeI as a PVA.

Chapter 9: Studies on malarial proteins

Three calmodulin–like proteins from *Plasmodium falciparum,* MALP71.69, PF14_0181 and PF10_0301 were identified from PlasmoDB. Two of the genes could be expressed in *E. coli* BL21 cells, but were insoluble. Solubilization and purification using various methods were attempted. Macrophage migration inhibitory factor was purified, refolded and crystallisation attempted. A very crystalline precipitate was got. A translationally controlled tumour protein was purified and crystallized. Diffraction data were collected at the European Synchrotron Radiation Facility in France and could be processed very well. Though no new structures could be solved in the case of malarial proteins, the study helps in highlighting the challenges while working with eukaryotic proteins and the problems pertaining to malarial proteins in particular.

CHAPTER 1

INTRODUCTION

Background

The work presented in this thesis can be broadly segregated into two parts. The first part of this work is on penicillin V acylases, the enzymes used in the industrial production of semi-synthetic penicillins. The second part of the work is on selected proteins from the malarial parasite, *Plasmodium*. Accordingly, the background on this work is presented in two parts respectively.

Part I

1.1.1. Introduction to enzymes

Proteins, along with carbohydrates, lipids and nucleic acids are the major biological macromolecules. Enzymes are proteins specialized to perform biological catalytic functions. Some ribonucleic acids called ribozymes also can perform catalysis. The first commercial application of enzymes was in the form of organisms that possessed them, as in leavening or brewing with yeast. The word ‘enzyme’ originates from Greek *énsymo*, *én* meaning "at" or "in" and *simo* means "leaven" or "yeast" (Stryer, 1995). More than 2500 enzymes are known and 250 commercially used (Woodley, 2000). Enzymes are sometimes synthesized in inactive form called zymogen. E.g. Pepsinogen. Such zymogens need to be activated, often involving proteolytic cleavage, in this case, to pepsin. Two popular theories are used to explain binding of enzyme to its substrate:

Lock and key theory: Emil Fischer postulated in 1894 that the correct substrate of an enzyme acts as a key that fits into a specific pocket in the enzyme.

Induced fit theory: It was proposed by Daniel Koshland in 1958 that the substrate induces a change in the shape of the enzyme, which then fits it.

Enzymes speed up reactions by providing an alternate pathway of lower activation energy for a reaction without altering reaction equilibrium. The rates of enzyme turnover (number of substrate molecules converted to product per second) vary from 36 million per second for carbonic anhydrase to lysozyme, which processes merely 2 molecules per second. Their lifetime varies from a few minutes to weeks. They have optimal pH and temperatures where their efficiency is maximum. Some require cofactors or coenzymes for functioning- in such cases, the protein part is called apoenzyme and together with the cofactor, constitutes the holoenzyme. The main advantages of enzymes compared to most other catalysts are their chemoselectivity and steriospecificity. They are described by maximal velocity of the reaction they catalyze, V_{max}, and the affinity they have for the substrate, measured as substrate concentration at half maximal velocity, K_m, generally calculated using Michaelis-Menten equations proposed in 1913.

Enzymes are sensitive to molecules, which step up reaction called activators and inhibitors that reduce their activity. Inhibition can be reversible or irreversible. The different types are:

Competitive: Inhibitor binds to the same site as the substrate, K_m increases but V_{max} remains the same.

Uncompetitive: inhibitor binds only to the enzyme-substrate complex (ES), not to the free enzyme. This causes a decrease in both V_{max} and the K_m value.

Noncompetitive: Inhibitor binds to a site other than substrate binding site resulting in decreased V_{max}, but leaving K_m unchanged. The inhibition is mostly irreversible. E.g. Suicide inhibitors.

Partially competitive: The mechanism is similar to that of non-competitive inhibition except that the enzyme substrate inhibitor complex is active.

Mixed: Mixed inhibitors can bind to both the enzyme and the ES complex. It has the properties of both competitive and uncompetitive inhibition. Both, decrease in V_{max} and increase in K_m value occur.

Apart from *in vivo* functions, some enzymes have great commercial applications. Since reaction conditions are mild, and enzymes are specific, no unwanted by-products accumulate. Immobilization of enzymes has permitted repeated use of costly enzymes. Enzyme catalyzed reactions are thus cheaper than their chemical counterparts and the process more environment-friendly. Since enzymes help overcome energy barrier of activation, it has viable and economical industrial applications in textiles, petrochemicals, food, animal feed, detergents, pulp and paper, leather etc. For example, β-lactam acylases such as penicillin acylases, are used in the industrial production of semisynthetic β-lactam antibiotics.

1.1.2 Antibiotics

Antibiotics are chemicals produced by microorganisms or fungi that acts on other microorganisms. Antibiotics kill the bacteria (bactericidal) or arrest its growth (bacteriostatic). Majority of the clinically used antibiotics have been obtained from actinomycetes, especially *Streptomyces* species. *Bacillus* species and fungi also have yielded few useful antibiotics. They can be classified based on their chemical structure, microbial origin, spectrum of activity or mode of action. One class of antibiotics that work by inhibiting the synthesis of peptidoglycan in bacterial cell walls are β-lactam antibiotics, which can be classified based on their structure (nucleus) as

1. *Penicillin.* This can be classified into two types according to the source.

   Natural penicillins are penicillin G (PenG) and penicillin V (PenV)

   Semi-synthetic penicillins E.g. Amoxicillin, penicillinase-resistant cloxacillin, methicillin.

2. *Beta lactam inhibitors*. E.g. clavulanic acid, sulbactam
3. *Cephalosporin.* Generations – I, II, III and IV. Along with cephamycin, it forms a sub-group called cephems.
4. *Carbapenems*. E.g. imipenem and meropenem
5. *Monobactams*. E.g. Aztreonam

Penicillin G (6APA)

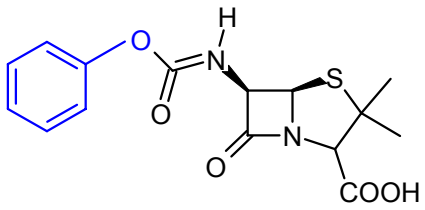

Clavulanic acid (Clavam)

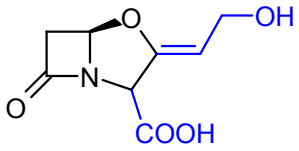

Cephalosporin C (Cephem)

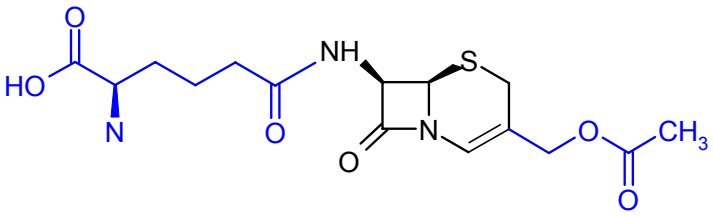

Imipenem (Carbapenem)

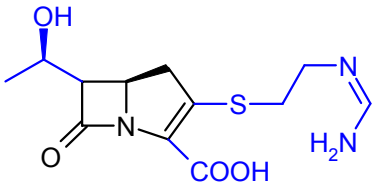

Carumonam (Monobactam)

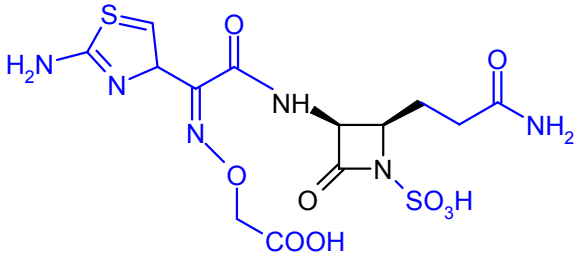

Fig. 1.1: Structures of different β-lactams. The nuclei of the different antibiotics are coloured black and indicated in brackets. The side chains are in blue. In another type of classification, the antibiotics are grouped according to their side chains.

Penicillins and cephalosporins are widely found in organisms especially, in fungi belonging to *Penicillium* and *Cephalosporium*. The basic component of penicillins and cephalosporins is a β-lactam nucleus which is formed by the fusion of a 4-membered β-lactam ring to a thiazolidine ring or a six carbon ring to form 6-aminopenicillanic acid (6APA) or 7-amino cephalosporanic acid (7ACA), respectively. They are the most widely used group of antibiotics. Modification of side chains yields different penicillins and cephalosporins. It is obvious that the side chain determines the antibacterial range and pharmacological properties of the β-lactams. The penicillin β-lactam nucleus is derived from valine and cysteine via a tripeptide intermediate. The β-lactams inhibit the transpeptidylation step in peptidoglycan (murein) synthesis.

Penicillin was discovered initially by a French medical student, Ernest Duchesne, in 1896, and subsequently rediscovered by Scottish physician Alexander Fleming in 1928, for which he was awarded the Nobel Prize along with Howard Florey and Ernst Chain who prepared the antibiotic in large quantities (Abraham, 1981; Bennet and Chung, 2001). Determination of X-ray structure of penicillin by Dorothy Crowfoot Hodgkin and co-workers in 1949 was made use of to find and develop more effective penicillins. Penicillins are used in the treatment of leptospirosis, syphilis, etc. The main disadvantage of using penicillin is allergy it causes in some people and narrow range of activity. They cause fatal allergies in around 300-500 people every year. Also, many penicillins display little activity against Gram negative bacteria, since they do not penetrate the outer membrane.

Cephalosporins are a group of broad-spectrum β-lactams. Cephalosporins and other newer penicillins are active against Gram negative bacteria. They are used as penicillin substitutes, and in surgical prophylaxis, and in the treatment of gonorrhea,

meningitis, pneumococcal, staphylococcal and streptococcal infections. Pharmacological characteristics of the antibiotic can be modified by substitution at 3 and 7 positions of its β-lactam ring. Newer generations of cephalosporin have progressively broader range of activity against gram-negative organisms but a narrower range of activity against gram-positive organisms than the preceding generation. They also have longer half-lives, reducing the dosing frequency. The advantages of cephalosporins over penicillins include low toxicity, resistance to β-lactamase (Abraham, 1987) and different antibacterial spectrum.

The peptidoglycan layer of bacteria is formed by cross-linked peptidoglycan chains, which are repeating alternating units of the sugars N-acetylglucosamine (NAG) and N-acetylmuramic acid (NAM) with a variable peptide chain attached to the carboxyl group of the NAM-unit. Individual peptidoglycan chains are covalently cross-linked to each other via short pentapeptide bridges connecting the third position of the first peptide chain to the carboxyl group of a D-alanyl-D-alanine residue from another peptide chain, catalyzed by transpeptidases (Fig. 1.2). Transpeptidases first bind to a D-alanyl-D-alanine unit forming a covalent acyl-enzyme complex with the release of terminal D-Ala. Attack on this complex by the terminal glycine of the cross-linking pentaglycine results in the recovery of active enzyme and formation of the bond between glycine and alanine (Scheme I, Fig. 1.3). Penicillin, being a structural analog of D-alanyl-D-alanine, interferes in this reaction by binding irreversibly to the enzyme (Scheme II, Fig. 1.3). As a result of faulty cell wall, cells are unable to divide inspite of growing, leading to accumulation of pressure and subsequent lysis of the cell by autolysins (Abraham, 1981).

1.1.3 Antibiotic Resistance

After a lot of initial failures, penicillin was finally prepared in large amounts. During the Second World War, it saved a lot of lives that could have succumbed to serious war wound infections. Complacency set in in the 1980s. Slowly, resistant microbes began to appear (Abraham, 1981). Now, diseases like tuberculosis, which were claimed to be vanquished before, are making a come back with renewed resistance. Antibiotics themselves increase the prevalence of resistance by selecting naturally occurring variants of organisms that are resistant. One can contract a resistant bug due to infection or the resistance can emerge within the body during treatment due to selection pressure of the antibiotic. The resistant organisms then transfer the resistance to other non-resistant organisms. Bacteria acquire genes conferring resistance by spontaneous DNA mutation, transformation, or from plasmids. Resistance may also arise from a change in the structure of penicillin binding proteins such that the antibiotic does not bind efficiently (Essack, 2001; Antignac *et al.,* 2003). In the case of Gram negative bacteria, penicillins pass across the outer membrane using porins. Resistance may develop from mutation leading to modified porins. The most efficient way for bacteria to withstand penicillin action is by producing ß-lactamases, which cleave ß-lactams, rendering them ineffective (Jacoby and Munoz-Price*,* 2005) (Scheme III, Fig. 1.3).

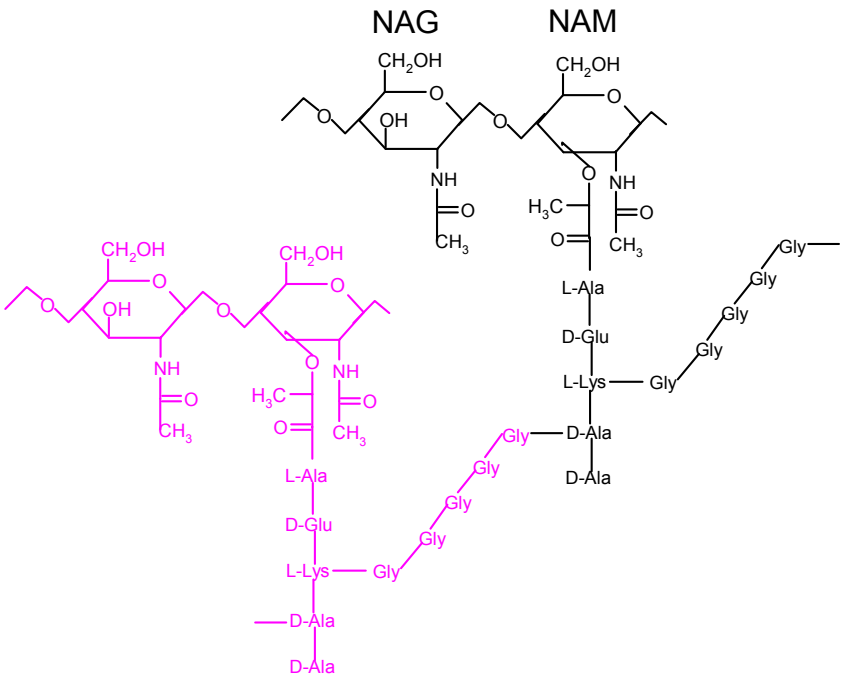

Fig. 1.2. The repeating unit of bacterial cell wall. The NAM units from different chains are joined together by a pentaglycine linker.

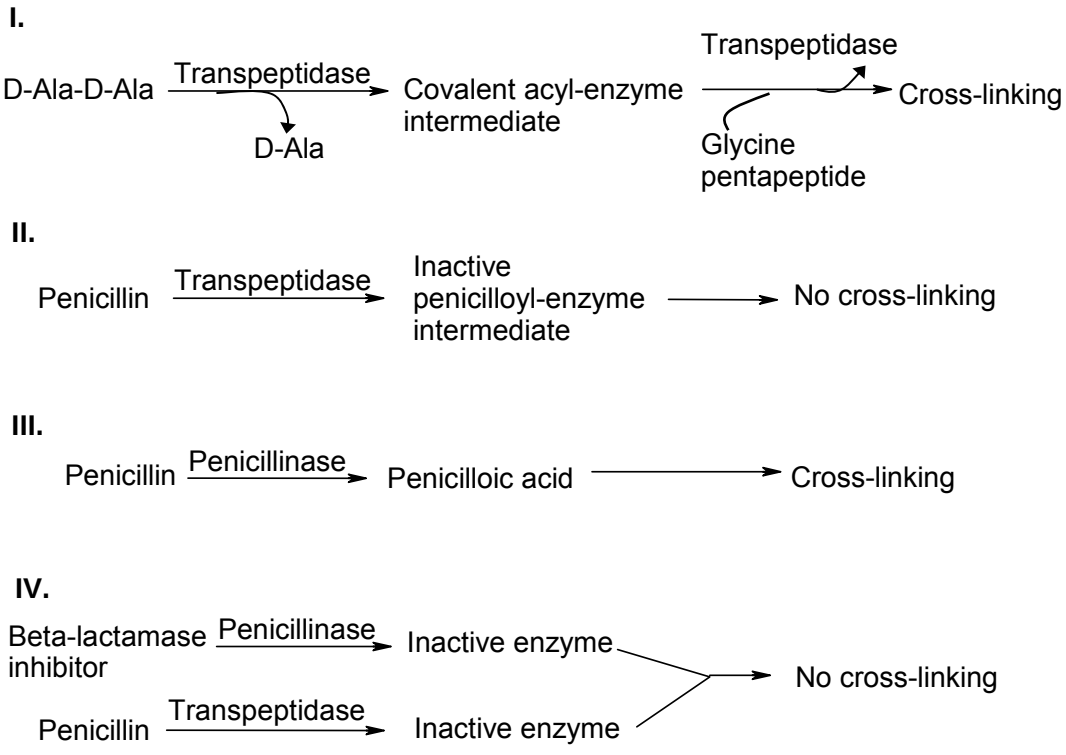

Fig. 1.3. Penicillin action

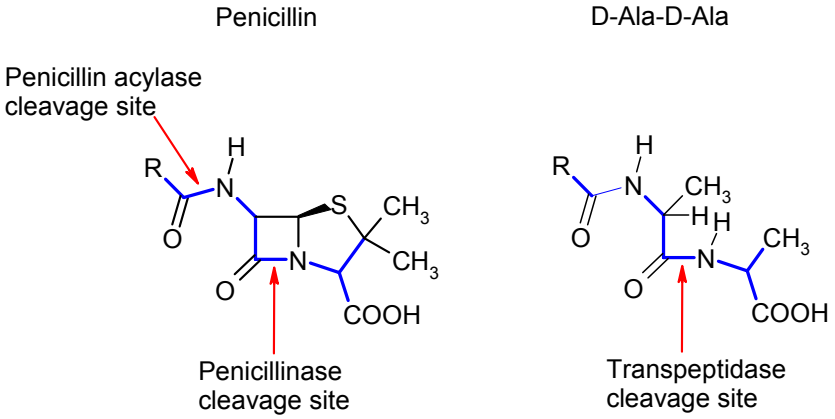

Fig. 1.4. Site of action of the enzymes. The backbone of penicillin and D-Alanyl alanine are very similar (coloured Blue), enabling penicillin to act as a structural analog for transpeptidase.

Consequently, β-lactamase resistant penicillins like flucloxacillin, dicloxacillin and methicillin and later vancomycin were developed and used. Methicillin and vancomycin resistant *Staphylococcus aureus* (referred to as MRSA and VRSA) have emerged now. This prompted the use of a group of structural analogs of ß-lactams, called ß-lactamase inhibitors in combination with β-lactams. Though they do not have antibacterial activity themselves, but bind tightly to ß-lactamases, allowing the other ß-lactam to act. E.g., the natural clavulanic acid or the synthetic sulbactam. These are effective against beta-lactamases commonly produced by a variety of organisms including *Staphylococcus* species, the *Enterobacteriaceae*, *Pseudomonas aeruginosa*, *Acinetobacter* species and some anaerobes. While using combination therapy with beta-lactamase inhibitors, the two ß-lactams act synergistically - one competitively inhibiting beta-lactamase, thus protecting the other from inactivation

(Scheme IV, Fig. 1.3). However, in some cases, penicillins antagonize each other; the antagonist blocks the more sensitive site but acts additively with the antagonized antibiotic at the less sensitive site (Acar *et al.,* 1975). A promising lead to new mechanism-based and transition state analogue inhibitors could be the retro-amide side chain of aryl malonamates, which fits the active site of P99 beta-lactamase (Cabaret *et al.,* 2003).

Though bacterial antibiotic resistance is a natural phenomenon, other factors can abet the problem. The most serious preventable cause is inappropriate antibiotic use. The need of the hour is firstly, to prevent the spread of resistance and the selection of resistant organisms, using narrow spectrum antibiotics and following proper regimen for the usage of antibiotics. Secondly, newer and effective antibiotics have to be found or developed. In the quest for new antibiotics, semi-synthetic penicillins, with a β-lactam nucleus and a custom-designed side chain, look promising, though resistance to some semi-synthetic penicillins are already reported.

1.1.4 Semi-synthetic penicillins

Since known natural penicillins were increasingly becoming ineffective for treatment of various pathogens, other forms were scouted for. It was first observed during fermentation of *E. coli* that it produced a mixture of penicillin isoforms. Later, it was discovered that it could be preferably induced to produce PenG by adding its side chain, phenylester, to the culture medium. It was observed that variations in the side chain alter the properties of a β-lactam antibiotic (Abraham, 1981; Vandamme and Voets, 1974) providing the first clue for more effective antibiotics. However, modifying the side chain chemically is expensive and generates by-products that have to be treated before disposal. In a multi-step reaction, natural penicillins have to be cleaved to yield the β-lactam nucleus 6APA and in the next scheme, the nucleus has to be

derivatised with the desired side chain. The amide link between the side chain and the nucleus can be hydrolyzed conventionally to yield 6APA but β-lactam ring also gets hydrolyzed. A significant discovery was that in the absence of any precursors, a particular *Penicillium* could produce the free β-lactam nucleus (Bruggink, 2001; Vandamme and Voets, 1974). Alternatively, Penicillin acylases can selectively hydrolyze the amide bond leaving the β-lactam ring intact. Penicillin acylase from *E. coli* could catalyze the breakdown of PenG to 6APA and its organic acid (Shewale, 1997). Later it was found that it could catalyze the second step also when it was found that under different conditions reverse reaction could occur (Vandamme and Voets, 1974). Thus the green method of semi-synthetic penicillin production was born. Other interesting discoveries included that Isopenicillin N synthase creates the bicyclic nucleus of penicillins in one step and deacetoxycephalosporin C synthase catalyses the expansion of the penicillin nucleus into the nucleus of cephalosporins.

The enzymatic method is regio- and stereo-specific and the reaction conditions are milder. Advances in immobilization techniques facilitated easy recovery and reuse of enzymes and increased their stability making it cost-effective (Woodley, 2000). In fact, in the hydrolysis of racemic iso-propylamide of mandelic acid, immobilization improved the enantioselectivity of PGA (Rocchietti *et al.,* 2002). Thus, enzymatic process is cheaper and safer than chemical processes. Today, penicillin G and V are fermentatively produced at an estimated annual market volume of 16,000 tons (Bruggink and Roy, 2001) worldwide using *Penicillium* strains. About 10,000 tons of this along with 30 tons of penicillin acylases are used for production of semi-synthetic β-lactam antibiotics (Demain, 2000, Elander, 2003). Major chunk of the 6APA produced is via the PGA route. The structures of all semi-synthetic penicillins and cephalosporins known are based on their respective beta-lactam nuclei, 6APA and 7ACA, respectively. Totally synthetic analogs are also known.

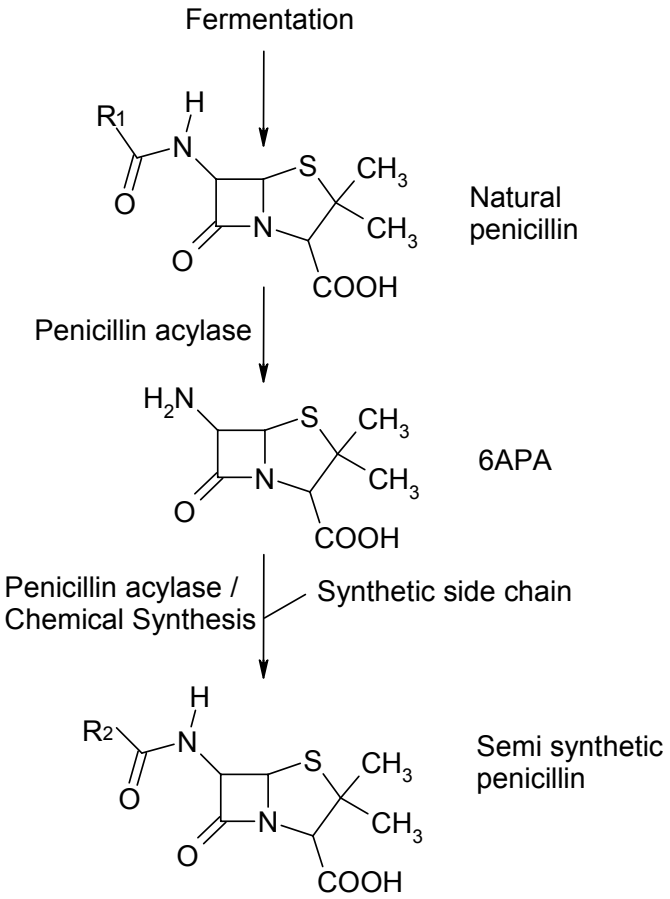

Fig. 1.5. Synthesis of semi-synthetic penicillin

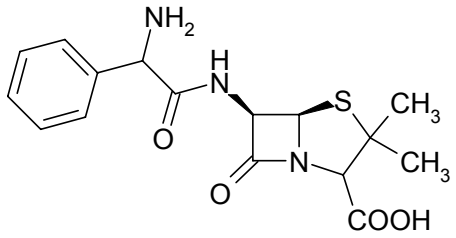

Fig. 1.6. Ampicillin, a semi-synthetic penicillin

The advantages of semi-synthetic penicillins are increased tolerance and diminished toxicity in humans, so they have fewer side effects; increased effectiveness due to greater selectivity against pathogens; increased resistance to β-lactamases; broader spectrum of antimicrobial activity, e.g., ampicillin is more useful than penicillin due to

broader spectrum (Bruggink and Roy, 2001); improved pharmacological properties like increased stability, better absorption from the gastro-intestinal tract resulting in less dosage and lower elimination rates from the patient, thus decreasing the frequency of administration of the drugs. The β-lactam acylases commonly used in pharmaceutical industry in the bulk manufacture of semi-synthetic β-lactams include penicillin acylases, cephalosporin acylase and glutaryl 7-aminocephalosporanic acid acylase reported from *Arthobacter viscosus, Bacillus laterosporus, Bacillus megaterium, Bacillus sphaericus, Kluyvera citrophila, Proteus rettgeri* and *Pseudomonas* sp. (Deshpande *et al.,* 1994).

1.1.5 β-lactam acylases

1.1.5.1 Penicillin acylases

Penicillin amidohydrolases (EC 3.5.1.24) also called penicillin acylases or penicillin amidases are enzymes that catalyze the hydrolysis of penicillin to a carboxylate and 6-aminopenicillanic acid (Sakaguchi and Murao, 1950). The EC number denotes that they are hydrolases acting on carbon-nitrogen bonds other than peptide bonds in linear amides. Apart from penicillin production, PAs are also used in other industries, in peptide synthesis or acyl group transfer reactions (Van Langen *et al.,* 2000). Amidase from *E. coli* is used in the synthesis of artificial sweetener aspartame (Fuganti *et al.,* 1986) and diphenyl dipeptides, whose derivatives are used as food additives, fungicidal, antiviral and anti-allergic compounds (Van Langen *et al.,* 2000). PAs can be used to resolve racemic mixtures of chiral compounds such as aminoacids (Bossi *et al.,* 1998), β-amino esters, amines and secondary alcohols (Svedas *et al.,* 1996).

According to the type of substrate preferably hydrolyzed, penicillin acylases are classified into Penicillin V acylase (PVA), Penicillin G acylase (PGA) and ampicillin

acylase which preferably cleave PenV, PenG and ampicillin, respectively. However, some PAs have broad substrate specificity, hydrolyzing more than one type of penicillin. PVA from *Streptomyces lavendulae* also acts on aliphatic penicillins like Penicillin F, dihydroF and K (Torres-Guzman *et al.,* 2002). Both PGA and PVA were found to be members of Ntn hydrolase superfamily.

1.1.5.1.1 Penicillin G acylase

PGA catalyses the hydrolysis of PenG and the condensation of Cα-substituted phenylacetic acids with β-lactam nucleophiles. PGA has been reported from *Achromobacter xylosoxidans* (Cai *et al.,* 2004), *Alcaligenes faecalis* (Verhaert *et al.,* 1997), *Arthrobacter viscosus* (Ohashi *et al.,*1988, Ohashi *et al.,*1989; Verhaert *et al.,* 1997). *Bacillus megaterium* (Martin *et al.,* 1995), *Bacillus megaterium, Escherichia coli, Kluyvera citrophila* (Barbero *et al.,* 1986; Martin *et al.,* 1991)*, Proteus rettgeri* (McDonough *et al.,*1999), *Streptomyces lavendulae*. Homologs of PAs are found throughout the whole kingdom of prokaryotes (Arroy *et al.,* 2003). Most PGAs in gram negative organisms are usually periplasmic. PGA of *B. megaterium* is extracellular (Martin *et al.,* 1995).

PGA from *E. coli* has been thoroughly investigated. In 1974, Kutzbach and Rauenbusch studied its general properties. The mature enzyme is a 80 kDa heterodimer of 24 kDa α-subunit and 64 kDa β-subunit comprising 209 and 566 aminoacids, respectively (Duggleby, 1995; McVey, 1997). It is produced as a 96 kDa cytoplasmic precursor pre-pro-protein. Post-translational processing requires translocation through the cytoplasmic membrane (Schumacher *et al.,* 1986, Hewitt *et al.,* 2000; Burtscher and Schumacher, 1992) to the periplasm using the 26-amino-acid signal peptide that is subsequently cleaved off. The 54-amino-acid spacer peptide that connects the α and β chains which may influence the final folding of the

chains (Oliver *et al.,* 1985), is cleaved on the carboxyl side first between Thr263 and Ser264 (Choi *et al.,* 1992), giving rise to the N-terminal of the β-subunit, serine, which is the active catalytic residue. However, the β-chain alone is not catalytic (Daumy, 1985). The C-terminal of the α-peptide is generated by another endopeptide cleavage (Bock *et al.,* 1983; Merino, *et al.,* 1992) and the α and β units are reconstituted to give an active enzyme. Kinetic studies showed that the autoproteolysis in PGA is intramolecular (Kasche *et al.,* 1999). These endopeptidase cleavages require an intact carboxy terminus. This type of processing is found in the synthesis and processing of preproinsulin and other eukaryotic hormones and is unique for a prokaryotic enzyme.

PGA from *Kluyvera citrophila* ATCC21285 is reported to be composed of two non-identical subunits of 23 and 62 kDa (Barbero *et al.,* 1986), in contrast with the previous findings (Shimizu *et al.,* 1975). Its nucleotide sequence is 80% similar to *E. coli* ATCC11105 PGA (Schumacher *et al.,* 1986), indicating a common ancestor. *Proteus rettgeri* is an 86 kDa enzyme composed of two essential non-identical subunits. Like *E. coli* PGA, the beta subunit contained a serine residue required for enzymatic activity, and the alpha subunit contained the domain that imparts specificity for the penicillin side chain (Daumy *et al.,* 1985; Klei *et al.,* 1985). The enzymes from different sources had similar substrate specificity but differed in molecular weight, isoelectric point, and electrophoretic mobility in polyacrylamide gels and did not antigenically cross-react. However, most PGAs have a similar subunit configuration, structure and substrate range as *E. coli* PGA. This indicates divergent evolution although they have evolved beyond any obvious sequence homology.

Mechanism of catalysis of PGA was elucidated in detail through solving its native structure and structure with bound complexes including substrate analogs and inhibitors. The native structure of PGA from *E. coli* has been reported (Hunt *et al.,* 1995; Duggleby *et al.,* 1995). In 2000, Hewitt *et al* solved the structure of inactive precursor mutant of *E. coli* PGA, showing the spacer peptide blocking the active-site cleft lending support to an autocatalytic mechanism of maturation. The enzyme structure solved with complexes and mutants (Done *et al.,* 1998; Brannigan *et al.,* 2000) has helped advance our understanding of the enzyme's substrate binding, specificity, mechanism of action and stability. The study reported by McVey *et al.,* (2001) study on the structure of PGA in complex with PenG sulphoxide, a poor substrate has also thrown light on the catalytic mechanism of the enzyme. They have also shown that the reaction proceeds via direct nucleophilic attack of SerB1 on the scissile amide and not as previously proposed via a tightly H-bonded water molecule acting as a "virtual" base.

PGA catalysis proceeds via a acyl-enzyme intermediate. Their mode of action is similar to proteases like chymotrypsin (Kato, 1980) though, the role of intermediary water molecule has been disputed (McVey *et al.,* 2001). The hydroxyl group of serine that is located at the N-terminal of β-subunit (Serβ1) acts as a nucleophile.

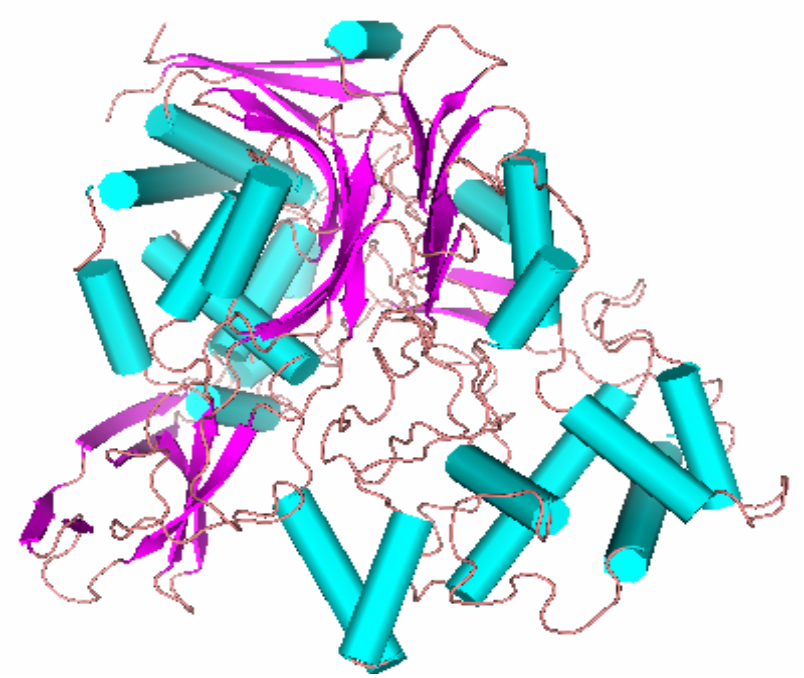

Fig. 1.7. The heteromeric PGA from *E. coli* (PDB code 1PNK). The β-sheets (magenta) which constitute the active site, are sandwiched between α-helices (cyan) on either sides (Top half in the figure). Figure generated using PyMol.

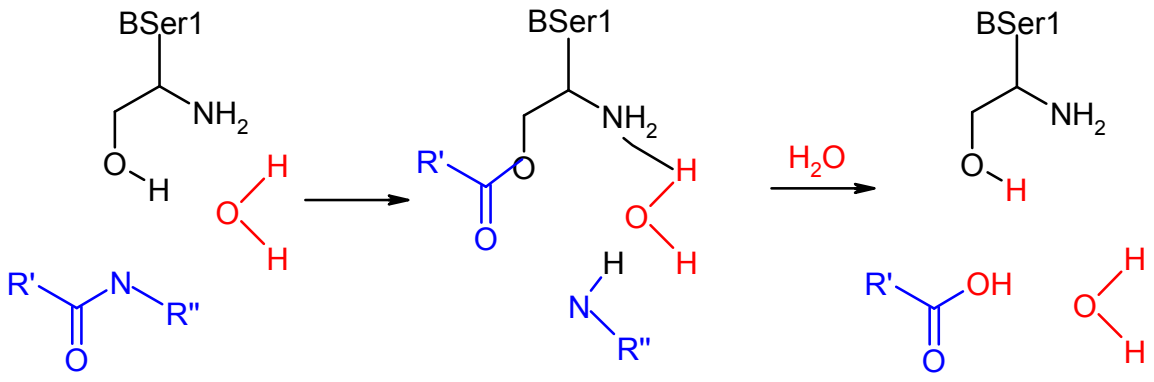

Fig. 1.8. Mechanism of catalysis of PGA (coloured black). The substrate is coloured blue, R' and R'' denote variable groups.

It is activated by its own α-amino group via a bridging water molecule, analogous to activation of serine by histidine-aspartic acid in serine proteases (Duggleby *et al.,* 1995). The serine hydroxyl oxygen forms an oxyanion tetrahedral intermediate with the acyl carbon of the substrate, which is stabilized via hydrogen bonds by the main chain amide of Ala69 and the side chain nitrogen of Asn241. The enzyme forms a covalent acyl intermediate and is subsequently deacylated by a nucleophile, through another tetrahedral intermediate to yield free enzyme and the acylation product of the nucleophile. When the nucleophilic attack is performed by water (hydrolysis), β-lactam antibiotics yield the side-chain carboxylic acid and the free β-lactam nucleus. When the acyl donor is an activated synthetic side chain like an amide or an ester, a β-lactam nucleus such as 6APA will yield a semi-synthetic β-lactam antibiotic through aminolysis. Studies have shown that PGA is specific for hydrolysis of phenylacetamide derivatives, but is more tolerant of other features in the rest of the substrate. Thus β-lactam acylases are very useful in industry.

Duggleby *et al* showed that there is no histidine equivalent that is found in serine proteases, distinguishing PGAs from them. The base is contributed by the N-terminal residue's own α-amino group. This led to the classification of these type of enzymes as a new type of hydrolases- the N-terminal nucleophile (Ntn) hydrolses (Brannigan *et al.,* 1995). Several other Ntn hydrolases have since been identified. Fermentation (DeLeon *et al.,* 2003) biochemical and other characterization studies identified residues that determine the catalysis, stability and other critical properties of the enzyme. PA from *Alcaligenes faecalis* has a very high affinity for PenG (K_m 2 μM) (Verhaert *et al.,* 1997, Svedas *et al.,* 1997) than other PGAs. For e.g., the one from *B. megaterium* ATCC14945 has a K_m of 4.5 mM (Chang and Bennet, 1967). By comparing the aminoacid sequences and also the different substrate specificities of different acylases it may be possible to identify critically important residues for strain

improvement and mutagenesis. Such studies have been conducted on *Achromobacter xylosoxidans* (Cai *et al.,* 2004) and *Kluyvera citrophila* (Martin *et al.,* 1993). Some of the studies point to the presence of arginine at or near the catalytic site (Prabhune and Sivaraman, 1990). Morillas *et al.,* (1999) have identified that α-amino group of the catalytic Serβ1 and the guanidinium group of Argβ263 are important for activity. Alkema *et al* (2002) have found that Argα145 is involved in binding of β-lactam substrates and Argβ263 is important both for stabilizing the transition state and for processing in *E. coli* PGA. Conformational studies have also been carried out on PGA (Lindsay and Pain, 1990). Modifying the N-terminal serine of the β-chain to a cysteine inactivates the enzyme, whereas Thr, Arg or Gly substitution prevents *in vivo* processing of the enzyme, underlining the importance of this residue for activity and cleavage (Duggleby *et al.,* 1995). In *Bacillus megaterium* PGA, the mutation of Lys at β427 and 430 to Ala was found to enhance stability in acidic or organic solvent environment (Yang *et al.,* 2000). The thermostability of *A. faecalis* PGA compared to other known PGAs, could be attributed to the unusual presence of two cysteines that form a disulfide bond (Verhaert *et al.,* 1997). The combined results of the inactive Nβ241A mutant structural and kinetic studies show the importance of Fα146 in the beta-lactam binding site and provide leads for engineering mutants with improved synthetic properties (Alkema *et al.,* 2000). Using selection pressure specifically designed for the compound of interest it is possible to change the specificity of PA by laboratory evolution to obtain new enzymes for industrial application (Roa *et al.,* 1994; Rajendhran and Gunasekaran, 2004). The reported results might be used to alter the substrate specificity of penicillin acylase in order to hydrolyze substrates of industrial significance other than penicillins. Greater knowledge of the enzyme's structure and specificity could facilitate engineering of the enzyme, enhancing its potential for chemical and industrial applications (Done *et al.,* 1998).

Structures of PGAs solved from other sources (*Providencia rettgeri* (Klei *et al.,* 1995), *P. rettgeri* (McDonough *et al.,* 1999)) also confirmed the conserved nature of the active site of the enzymes where, at the same time, regions elsewhere were very dissimilar. It is this property that has led to many other applications for the enzyme. *P. rettgeri* and *E. coli* PA crystal structures suggests several mutations that could potentially allow penicillin acylase to accept charged beta-lactam side chain R-groups and to function as a cephalosporin acylase and thus be used in the manufacture of semi-synthetic cephalosporins (McDonough *et al.,* 1999; Oh *et al.,* 2004).

The physiological function of this enzyme is not clear. Valle *et al* (1986), reported the nucleotide sequence of the regulatory region of this gene, the identification of a functional promoter and transcriptional start point. Oh *et al* (1987), observed that the synthesis of active PGA and precursor processing in *E.coli* are affected by growth temperature. In *E. coli*, penicillin acylase activity was found to confer the ability to use penicillin G as a metabolic substrate, by detaching the phenylacetic group which can be used as a carbon source (Merino *et al.,* 1992). In *Pseudomonas fluorescens*, the nucleus of the benzylpenicillin (PenG) molecule is reported to be utilized as carbon, nitrogen and energy source (Johnsen *et al.,* 1977). The regulation of PGA expression is controlled by both temperature and phenylacetic acid (Valle *et al.,* 1991). It is envisaged that PGA may function during the free-living mode of the organism as a scavenger enzyme for phenylacetylated compounds to metabolize aromatic compounds to generate a carbon source.

1.1.5.1.2 Penicillin V acylase

PVA reversibly cleave the amide bond between the side chain phenoxymethyl group and the β-lactam nucleus of PenV, without affecting the amide bond of the β-lactam nucleus. PVA are mostly found in fungi. They have been reported from *Beijerinckia indica var.* (Ambedkar *et al.,* 1991) *Penicillium, Fusarium* sp., *Pseudomonas*

acidovorans. PVA are mostly produced intracellularly (Sudhakaran and Borkar, 1985). The production is either constitutive or enhanced by phenoxyacetic acid in growth medium. The molecular weight ranges from 88,000 (Schneider and Roehr, 1976), 83,200 in *Fusarium* sp.SKF 235 to 140,000 in *Bacillus sphaericus*, and their subunit composition varies from monomer to tetramer. In 1991, Ambedkar *et al* isolated *Beijerinckia indica var. penicillanicum* mutant UREMS-5, which produced 168% more PVA than *B. sphaericus*.

PVA differ from PGA in reaction conditions, substrate specificity, etc. The optimum pH values for PVA range between pH 5.6 - 8.5, as opposed to 6.5 - 8.5 for PGA (Margolin *et al.,* 1980; Schumacher *et al.,* 1986). This can be advantageous in 6APA production since the chemical degradation of 6APA is less at lower pH values (Shewale and Sudhakaran, 1997). Also, compared to PenG, PenV is more stable in aqueous solutions and at the conditions of extraction. From the clinical point of view, the advantages of PenV over PenG are resistance to stomach acids so that they can be taken orally, resistance to penicillinase and broader range of activity against some Gram-negative bacteria, making PenV/PVA the preferred system over PenG/PGA (Shewale and Sudhakaran, 1997). However, PGA is still more often used than PVA for want of new and better strains.

For PVA, the gene from *B. sphaericus* (Olsson *et al.,* 1985) has been cloned and studied in biochemical and structural (Suresh *et al.,* 1999) detail. This PVA and *E. coli* PGA are very different from each other in their molecular properties. PVA is much simpler in architecture than PGA. PVA is a homotetramer of 148 kDa whereas *E coli* PGA is a 80 kDa heterodimer. PGA is produced as an inactive precursor which needs extensive post-translational modifications to form an active enzyme. PGA is usually periplasmic whereas PVA is cytoplasmic. More importantly, the two enzymes do not have detectable aminoacid sequence homology. Despite this, when PVA

structure was solved, it was discovered that the two not only have a good structural similarity- they share the Ntn hydrolase fold- the structurally and biochemically equivalent atoms in both enzymes (the oxyanion hole) were found to overlap. The geometry of the active site was similar. However, the active and substrate binding sites of PVA is bigger and more polar to accommodate PenV. According to sequence similarity, PVA belongs to choloylglycine hydrolase family of Ntn hydrolase superfamily. PVA crystal structure demonstrated that the N-terminal nucleophile is a cysteine. DNA sequence revealed that Cys is the fourth aminoacid from N-terminal methionine, indicating that the three preceding residues including Met were removed during maturation, a post-translational processing shared with other Ntn hydrolases.

1.1.5.2 Cephalosporin acylases

Cephalosporin acylases (CAs) act on β-lactams with a cephalosporin nucleus, such as cephalosporin C and /or the more preferred substrate glutaryl 7-aminocephalosporanic acid to produce 7-aminocephalosporanic acid (7-ACA) and β-lactams with a charged side chain (Fritz-Wolf *et al.,* 2002). Cephalosporin C acylase from *Pseudomonas* sp. strain N176, a heterodimer of 25 and 58 kDa, has been crystallized (Kinoshita *et al.,* 2000). Like PGA, the enzyme is a heterodimer of two nonidentical subunits, α and β, which are derived from a nascent precursor polypeptide that is cleaved proteolytically through a two-step autocatalytic process upon folding. The two subunits of the acylase, separately are inactive (Li *et al.,* 1999). CA works using the same mechanism as PGA except for involving two catalytic dyads. His and Glu residues in the beta chain are involved in catalysis (Kim *et al.,* 2003; Mao *et al.,* 2004). Histidine interacts indirectly with O^{γ} through a hydrogen bond relay network involving the α-amino group of the serine and a bound water molecule. The crystal structures of intracellular heterodimeric CA from *Pseudomonas diminuta* (Fritz-Wolf *et al.,* 2002; Kim *et al.,* 2000) and *Pseudomonas*

sp. resemble the Ntn-hydrolase fold of the *E. coli* PGA structure, but their overall structures are different elsewhere (Kim *et al.,* 2000). The acylase from *Pseudomonas* sp. 130 is highly active on glutaryl-7ACA and glutaryl 7-aminodesacetoxycephalosporanic acid, but much less active on cephalosporin C and PenG. According to MEROPS database, both PGA and CA have been grouped under Peptidase family S45 which contains self-cleaving precursor proteins of Ntn hydrolases. However, unlike PGA (Duggleby *et al.,* 1995) whose Ser gets inactivated with phenylmethyl sulphonyl fluoride, neither the cephalosporin acylase precursor nor its mature enzyme was found to be affected by this reagent (Park *et al.,* 2004).

7-ACA is obtained from the natural antibiotic cephalosporin C, either chemically or by a two-step enzymatic process involving the enzymes D-aminoacid oxidase and glutarylamidase. The chemical production is expensive and produces harmful by-products. Cephalosporin C acylases (CCA) are very interesting from an industrial point of view (Kim *et al.,* 2000). However, the problem with enzymatic cleavage using CA is that it has low substrate specificity for cephalosporin C than glutaryl-7ACA. Studies have been conducted on improving the performance of *P. diminuta* CA (Kim *et al.,* 2000) and redesigning the enzyme to produce 7-ACA from cephalosporin C in a single enzymatic step (Fritz-Wolf *et al.,* 2002). By site-directed mutagenesis relative activity of *Pseudomonas* sp. N176's CCA on cephalosporin C could be further improved to 6% as that of glutaryl 7-ACA (Ishii *et al.,* 1995). Structure of CA in native form and in complex with phosphate, ethylene glycol and glycerol has been studied recently. An enzyme-substrate complex model might help us to predict mutants of glutarylamidase that deacylate cephalosporin C into 7-ACA. The industrially used cephalosporin producing fungus *Acremonium chrysogenum* has provided a new tool, promoting the design of alternative biosynthetic pathways making it possible to obtain new antibiotics and to improve cephalosporin production (Diez *et al.,* 1996). CA was also found to be a Ntn hydrolase.

Fig. 1.9. A PVA monomer from *B. sphaericus.* PDB ID 2PVA. The structural make up of PVA is simpler than PGA.

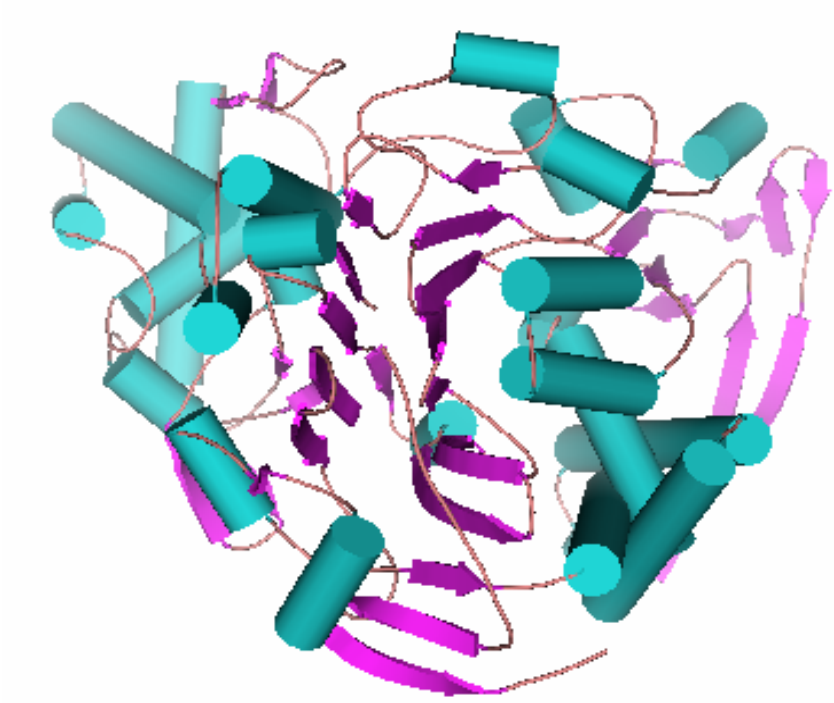

Fig. 1.10. Heterodimeric CA from *Brevundimonas diminuta* PDB ID (1FM2). The N-terminal residue is in the centre of the figure.

1.1.6 Ntn hydrolase superfamily

Ntn hydrolase superfamily of proteins are characterised by a distinct αββα fold (Ntn fold) (Brannigan *et al.,* 1995). In all the structures elucidated so far, the two central anti-parallel β-sheets are sandwiched between two layers of anti-parallel α-helices. Between them, the β-sheets have a packing angle of from 5º in aspartyl glucosaminidase to 35º in proteasome. Eight totally conserved secondary structure units are found (Oinonen and Rouvinen, 2000). The arrangement of structural elements indicates a common ancestor. However, the composition of this core varies as do the oligomeric states. For example, PVA is a tetramer of a single type of subunit whereas proteasome comprises 28 subunits of two types α and β making up a mammoth four-layered αββα barrel. Each layer has seven subunits. The outer α-layers do not have catalytic activity. The catalytic β-chains of proteasome have a Thr as their Ntn residue. Members of the family whose three-dimensional structures are known are listed in the table.

D-aminopeptidase A	Fanuel *et al.,* 1999
aspartylglucosaminidase	Oinonen *et al.,* 1995, Guo *et al.,* 1998
cephalosporin acylases	Kim *et al.,* 2001
conjugated bile acid hydrolase	Rossocha *et al.,* 2005
gamma-glutamyltranspeptidase	Okada *et al.,* 2006
glucosamine 6-phosphate synthase	Isupov *et al.,* 1996
glutamine PRPP amidotransferase	Smith *et al.,* 1994
glutaryl 7-aminocephalosporanic acid acylase	Lee *et al.,* 2000
L-aminopeptidase-DAla-esterase/amidase	Bompard-Gilles *et al.,* 2000
penicillin G acylase	Duggleby *et al.,* 1995
penicillin V acylase	Suresh *et al.,* 1999
20S proteasomes	lowe *et al.,* 1995, Groll *et al* 1997

Based on sequence homology with *B. sphaericus* PVA, Pei and Grishin (2003) have grouped peptidase U34 family with Ntn hydrolase family. It is purported to also include acid ceramidases, isopenicillin N acyltransferases and choloyglycine hydrolases (Kim *et al.,* 2000; Oinonen and Rouvinen, 2000; Pei and Grishin, 2003; Suzuki and Kumagai, 2002).

All Ntn hydrolases catalyze amide bond hydrolysis but their substrates vary diversely. As a result, the shape, size, nature of interacting residues and their locations differ in the binding pocket. The mechanism is like serine proteases, but instead of a catalytic triad, a single N-terminal residue functions as a nucleophile and catalytic base. Till date the nucleophile has been only one of the three-Ser, Thr and Cys, whose reactivity is influenced by neighbouring residues. The reaction proceeds though a covalent intermediate via a transition state, which is stabilized by residues from oxyanion hole formed normally by two residues. The catalytic nucleophile residue at the N-terminal is revealed by autocatalysis. Even though the nucleophilic residue differs (PGA-Ser, PVA-Cys, Proteasome-Thr), it occupies a spatially similar position in these proteins. In the oxyanion hole all the enzymes contain equivalent critical groups and a similar catalytic arrangement indicating similar mechanistic design of catalysis. Among the members there is lack of any discernible sequence similarity.

Post-translational autoproteolysis is a mechanism used to activate many proteins via self-catalyzed peptide bond rearrangements, which play an essential role in a wide variety of biological processes. They include activation cascades such as blood coagulation and fibrinolysis, cell death, embryonic development, protein targeting and degradation, viral protein processing, zymogen activation (Neurath, 1986), caspase (Salvesen and Dixit, 1999). Post-translational editing mechanisms were first uncovered in prokaryotes in 1992 by Thony-Meyer *et al.,* among others in *E. coli* PGA. Autocatalytic processes were described in prokaryotes by Perler *et al* in 1997.

Earlier, non-protease zymogens were believed to be incapable of autoproteolysis. In Ntn hydrolases, the processing is generally intramolecular. Propeptide processing in the proteasome from *Thermoplasma acidophilum* is autocatalytic, but is probably intermolecular (Seemuller *et al.,* 1996). Precursor structures are reported for glycosylasparaginase (Xu *et al.,* 1999), PGA (Hewitt *et al.,* 2000) and β-subunit of proteasome (Ditzel *et al.,* 1998), which has helped to decipher processing mechanisms. PVA from *B. subtilis* and CBH from *Clostridium perfringens* however, possess their Ntn residue at the second position, requiring nothing but removal of N-formyl methionine from the precursor to activate the enzyme.

1.1.7 Choloylglycine hydrolases

This group of Ntn hydrolases comprise PVA and CBH which share extensive sequence and structural similarity (Christiaens, 1992) (Fig. 1.12). Their Ntn Cys is revealed by the simple removal of N-terminal Met. CBH is a 3α,7α,12α-trihydroxy-5β-cholan-24-oylglycine amidohydrolase (bile salt hydrolase, choloyltaurine hydrolase, glycocholase). CBHs are a class of microbial enzymes hydrolyzing the amide linkage that conjugates bile acids to glycine or taurine (Hylemon, 1985). CBH activity was detected in many autochthonous gastrointestinal microbiota of animals including *Bifidobacterium* (Grill *et al.,* 1995, Tanaka *et al.,* 2000), *Clostridium* (Batta *et al.,* 1984, Coleman *et al.,* 1995), *Lactobacillus* (Elkins and Savage, 1998; Christiens *et al.,* 1992, Lundeen and Savage, 1990) and *Bacteroides* (Kawamoto *et al.,* 1989).

Bile acids are produced *de novo* in the liver from cholesterol. The steroid nucleus is conjugated through an amide bond at the carboxyl C-24 position to one of the two aminoacids, glycine or taurine to facilitate biliary excretion and concentrated in the gall bladder (Baron and Hylemon, 1997). These conjugated bile acids are secreted via the common bile duct into the duodenum in those salt forms. Though the released bile salts are absorbed back into blood, a portion of it evades absorption and reacts

with the microbial flora of the intestinal tract where they undergo biotransformation in a number of ways. The hydrolysis of conjugated bile acids is one of the most common microbial bile salt transformations. Conjugated bile acids aid in digestion, emulsification and absorption of fats and lipids from the small intestine. Bile salts inhibit HIV infection (Herold *et al.,* 1999) and induce apoptosis (Gumpricht *et al.,* 2005; Payne *et al.,* 1995). They may act as gall-stone-dissolving agents (Batta *et al.,* 1984). Extensive bile salt metabolism is implicated in steatorrhoea and tumour production. Bile acids may be regulators of gene expression in the liver and intestines and modulate a variety of other functions. Bile acids are reported to be ligands for farnesoid X receptor (Wang *et al.,* 1999).

The advantage this enzyme confers on the harbouring bacteria is not clear. The autochthonous microbiota might have evolved CBH related functions to gain advantage over allochthonous species in anaerobic environments. Though uptake of conjugated bile acids is regulated by bacteria, which in high levels is toxic to the cell, the enzyme also helps in reducing toxicity (Floch *et al.,* 1971; Baron, 1997; Ellkins and Savage, 1998). Though it was believed that CBH protects the cells that produce it from the toxicity of conjugated bile salts, recent reports are contradictory. CBH from *Listeria monocytogenes* is reported to be a virulence factor (Dussurget *et al.,* 2002).

Deconjugated bile salts are excreted more rapidly than conjugated ones (Gilliland and Speck, 1977). Since free bile acids are excreted from the body this will increase the synthesis of new bile salts from cholesterol leading to a reduction in the total cholesterol concentration in the body resulting in lower serum cholesterol levels (Chikai *et al.,* 1987; Tannock *et al.,* 1997; DeSmet *et al.,* 1998). The possibility of using bile salt deconjugation by the intestinal microbes to reduce the level of serum cholesterol levels *in vivo* has received great attention in recent years (DeSmet *et al.,* 1998), especially with regard to hypercholesterolemic patients. In research labs, the

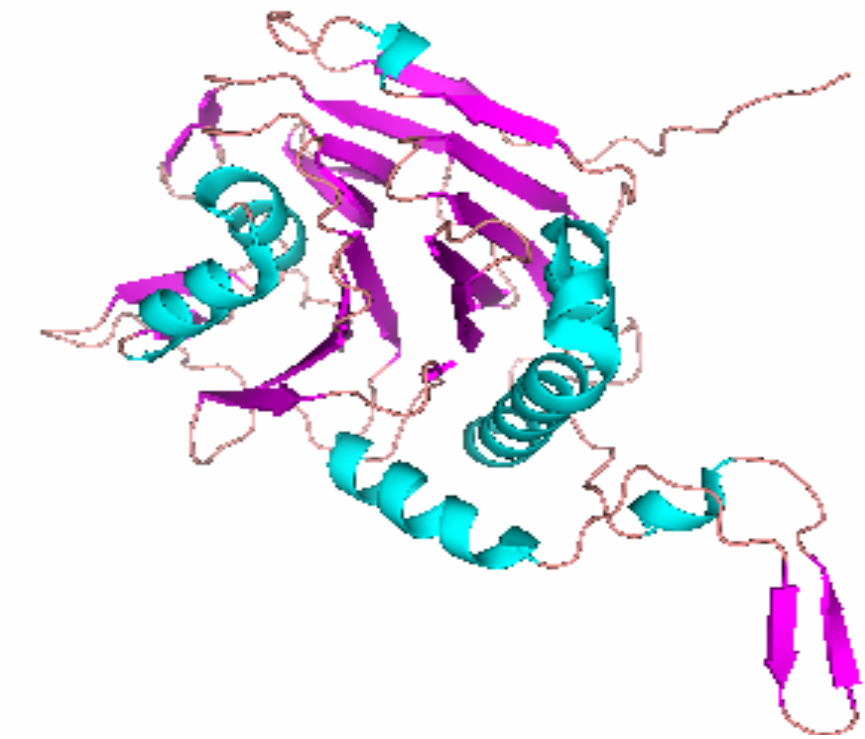

Fig. 1.11. CBH monomer from *Clostridium perfringens* (PDB code 2BJF).

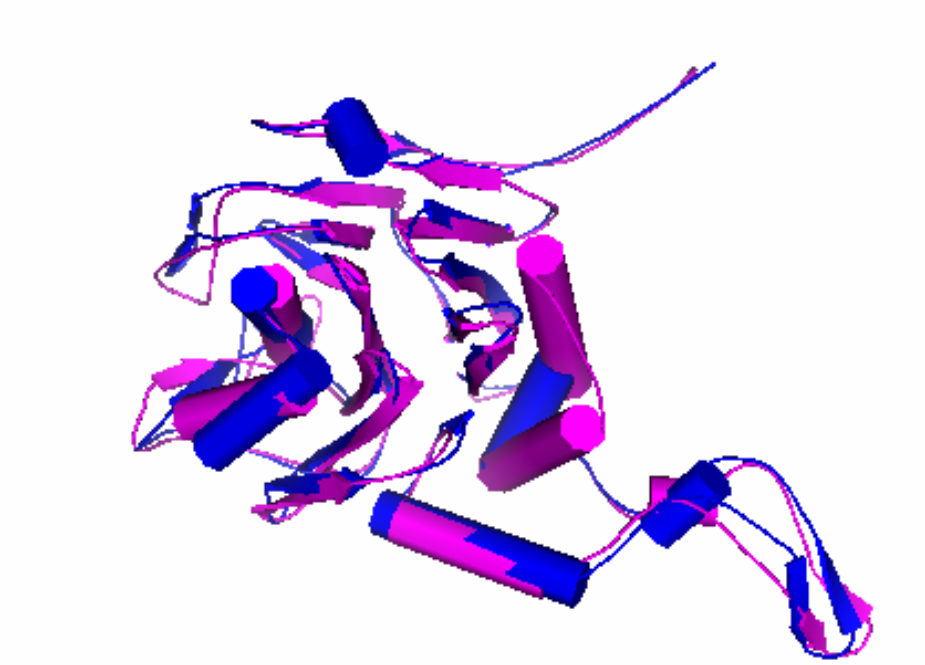

Fig. 1.12. Superposed monomers of PVA (2PVA) (magenta) and CBH (2BJF) (blue) clearly show the structural similarity between the two enzymes. The Ntn residue and sandwished β sheets are in the centre of the figure. The extensions in the structure interact with other monomers forming globular tetrameric proteins.

enzyme is used for deconjugation of bile acids for structural analysis and clinically to quantify bile acids secreted in biological fluids. Though the *in vivo* role of PAs are yet to be elucidated, the remarkable sequence similarity between PVA and CBH provides a clue to the evolutionary relatedness of the enzymes.

1.1.8 Hypothetical proteins

The advent of numerous genome sequencing projects has caused a flooding of genome data, awash with information about potential proteins. Picking protein targets for various studies has been rendered much easier with the advent of bioinformatics and various programs that are available to study and screen sequences. The basic local alignment search tool (BLAST) (Altschul *et al.,* 1997) is a very powerful and useful program that sifts through vast databases and returns any protein or gene that is similar to the query. Similarly, sequence alignment programs like ClustalW (Thompson *et al.,* 1994) enable us to zero in on conserved- and so, critical- residues. Such programs are invaluable to access and meaningfully extract needed information from the ever-increasing pool of targets. Such information can predict sequences that are not known to code for any known protein. Such 'hypothetical proteins' are aplenty. They are considered very interesting targets to study, especially the ones that seem to be conserved over a large number of organisms. Not only will knowing the function of the gene product be interesting, but it will also give us an idea of the evolutionary path of these products. The protein YxeI from the gram positive bacterium *B. subtilis* ATCC 33234 was selected as it had good sequence similarity with PVA from *B. sphaericus* (Christiaens, 1992) which has been studied previously.

1.1.9 Three-dimensional structure of proteins and X-ray crystallography

Activities of enzymes are directly related to their three-dimensional conformation, which is dictated by its aminoacid sequence. Differential activities of similar enzymes can be traced back to small differences in their sequences. This means that enzymes

that do not have adequate activities can be improvised by changing a few crucial aminoacids in its sequence. The seriousness of just one point mutation is exemplified in sickle cell anaemia where substitution of a glutamic acid to valine at position 6 in β-globin gene of hemoglobin leads to impairment of function. Phenylketonuria is caused by a single aminoacid mutation in the enzyme phenylalanine hydroxylase. However, identification of such aminoacid residues is difficult as enzymes are made up of a multitude of residues and many are oligomeric. This task will be much easier if we know the active site of the enzyme and the structure-function relationships of different aminoacids. This can be achieved by solving the three-dimensional structure of proteins by NMR or X-ray crystallography. Though a lot of information can be collated through various chemical and physical studies on macromolecules, fine details like catalytic mechanism cannot be understood until the atomic level structure is known. The molecular interactions between the substrate and the enzymes may be studied by ligand binding studies. Post-translational modifications, if any, can also be studied. Site-directed mutagenesis will let us know the various important active site residues. Once the atomic level structure is known, it is easier to identify and select residues for site-directed mutagenesis. Solving structures of unknown proteins might help assign a function to them or stumble on a hitherto unknown structure or function. Structure can be used to explain observed activities of naturally occurring proteins and also repercussions of changes in disease-related proteins. Structural details of important proteins from pathogenic organisms will help us to design molecules that might regulate them, like inhibitors. This is called rational drug design because it significantly reduces the number of molecules that need to be tested by utilizing structural information.

After the discovery of X-rays by Roentgen, Max von Laue discovered diffraction of X-ray by crystals in 1912. The usefulness of the property was promptly made use of to study crystals of small molecules. It was not until 1958 that the first protein crystal

structure, that of myoglobin, was solved by Kendrew and co-workers. Then it took years to solve the structure. With the advent of computers and superior digitized data collection equipment and synchronization of the whole process from data collection to refinement, today structures can be solved in a matter of months or even weeks. As protein structures began to be solved, the protein data bank (PDB) was established at Brookhaven National Laboratory, New York in 1971. From then, it has served as a repository of structures solved around the world. Today, it has over 40,000 structures and is maintained by Research Collaboratory for Structural Bioinformatics (RCSB) in collaboration with European Bioinformatics Institute (Macromolecular structure Database) and Protein Data Bank Japan. It can be accessed over the internet at www.pdb.org.

Part II

1.2 Malaria

1.2.1 Prevalence

Malaria is an endemic disease in developing countries in tropical and subtropical regions. Approximately 40% of the world's population lives in areas prone to malaria. Each year, there are about 500 million cases and over 2 million deaths from malaria. The mortality levels are greatest in sub-Saharan Africa, where children under 5 years of age account for 90% of all deaths due to malaria. In India, malaria is endemic except at elevations above 1800 meters and in some coastal areas (Sharma, 1996a). Periodic epidemics of malaria occur every five to seven years (Sharma *et al.,* 1994). In 2005, 2.5 to 3.5 billion people were at possible risk of transmission of *Plasmodium falciparum* and *P. vivax* (Guerra *et al.,* 2006). Distribution of malaria is influenced by temperature, precipitation and relative humidity of an area (Pampana, 1969; Bouma and van der Kaay, 1996). Due to acquired immunity to malaria in some humans, the correlation between rates of morbidity and mortality, and malaria transmission rates cannot be accurately established (Brewster, 1999). Resistance to anti-malarial drugs

and insecticides, the decay of public health infrastructure, population movements, political unrest and environmental changes are contributing to the spread of malaria. The need of the hour is to develop new and effective methods of vector control, new drugs and vaccines to combat disease and improved diagnostics. Malaria has received increased attention and several new schemes to curb the disease like Global Fund to Fight AIDS, Tuberculosis and Malaria, Multilateral Initiative on Malaria in Africa, National Malaria Eradication Programme in India, Medicines for Malaria, Malaria Vaccine Initiative, Mapping Malaria Risk in Africa and Plasmodium Genome Sequencing Project and Roll Back Malaria campaign have beed initiated.

1.2.2 The pathogen

Human malaria is caused by infection with intracellular *Plasmodium* parasites which is transmitted to man by the female anopheles mosquito. The four species that cause the disease in humans are *P. falciparum, P. vivax, P. ovale* and *P. malariae*. The disease caused by each species is different in terms of response to drugs, morbidity and mortality, the length of the incubation period, behaviour in different mosquito phases and in man (Kreier *et al.,* 1976). *P. falciparum* is the most virulent species. It causes malignant tertian malaria, which is responsible for maximum deaths due to malaria (Pampana, 1969). *P. vivax* remains in the body longer than *P. falciparum*, causing a more gradual health deterioration, the course of which is more predictable. At elevated temperatures, Plasmodium take less time to complete the extrinsic cycle. *P. vivax* and *P. falciparum*, which have the shortest extrinsic incubation times transmit faster and are more common than *P. ovale* and *P. malariae*. Also, higher temperatures increase the number of blood meals taken and the number of times eggs are laid by the mosquitoes (Martens *et al.,* 1995). 65% of malarial infections in India are caused by *P. vivax* and 35% are caused by *P. falciparum* (Kabilan, 1997). *P. malariae* causes the third most common type of malaria in the world, although it

grows slower than the other three species. *P. ovale* is the least common and least pathogenic of the four human malaria species (Kreier *et al.,* 1976).

1.2.3 Life cycle of *Plasmodium*

In the mosquito the two gametocytes from the human host, taken up with a blood meal, fuse to form the ookinete or egg which develops in the midgut. It develops into sporozoites, which circulate and end up at the salivary glands from where they can be injected into a human during the next blood meal completing the extrinsic cycle. In the human host, the sporozoites asexually reproduce to form merozoites in liver cells, which then spread through the blood and invade red blood cells (RBC). Inside the RBCs, the merozoites multiply ferociously eventually breaking the RBCs open and invading new ones. This phase causes fevers and other symptoms which we call malaria. Some of these merozoites differentiate into gametocytes which are picked up by feeding female Anopheline mosquitos.

The main symptom of malaria is a fever or paroxysm which occurs in a cyclic cold shivering, hot and sweating stages. In addition, a patient might experience chills, headache, malaise, weakness, hepatomegaly, splenomegaly, and dehydration which could lead to complications like anemia, anorexia, nausea and diarrhea. Deaths from malaria are normally caused by cerebral, renal or pulmonary failure or a combination of these. After the first fever attack, relapses occur with a pattern dependent on the species of the parasite (Pampana, 1969).

1.2.4 Drug resistance

The earliest methods to control malaria involved the eradication of mosquitoes, especially using insecticides like DDT (dichloro-diphenyl-trichloroethane) and use of treated bed nets. Malaria eradication programmes around the world were very successful in the beginning until the mosquitoes circumvented the problem by

developing resistance (Sharma, 1996a). The pathogen itself has become resistant to chloroquine and other widely used antimalarials. Once a parasite mutates into a form that can resist the effects of an anti-malarial drug, that form is naturally selected for as it rapidly multiplies and spreads from host to host. Mechanisms developed by the parasite to evade an inhospitable environment may differ widely between species. *P. falciparum* has become resistant to chloroquine in many parts of the world and there are now strains of multi-drug resistant *P. falciparum* that were first discovered in Asia but now spreading around the world (Kidson and Indaratna, 1998). Artemisinin, a product of the tree *Artemisia annua* is a promising medicine and is now used to treat parasites resistant to known drugs.

1.2.5 Resistance to infection

In individuals who are heterozygous for sickle-cell hemoglobin, the internal environment of RBCs does not favour the development of merozoites (Wakelin, 1996). This infected person does not suffer from disease nor can spread it. The Duffy antigen, which is expressed on the surface of RBCs, is necessary for *P. vivax* to enter RBCs. Individuals lacking this antigen do not develop the disease. Such people, who are infected with the parasite but do not have the disease have acquired immunity (Wakelin, 1996). Much research is being conducted currently into the mechanisms of this acquired immunity to malaria in order to create a malaria vaccine. However, acquired immunity is not foolproof against infection due to antigenic variation in the parasite. The parasites display a large diversity in antigens that vary between species, strains, stages, and during the course of an infection. A person immune to one type of pathogen might be prone to a different one not recognised by the immune system (Wakelin, 1996; Kabilan, 1997).

1.2.6 Genome sequence

An international effort was launched in 1996 to sequence the *P. falciparum* genome

with the expectation that the genome sequence would open new avenues for research. After the success of the project along with advances in sequencing technology, genomes of *P. vivax* and other related parasites are being sequenced (Gardner *et al.,* 2002). The sequencing of the genomes of malarial parasite, the vector- mosquito and the host- human, has provided a shot in the arm for understanding molecular mechanisms and treating/ preventing the disease. The genome of *P. falciparum* 3D7 has been sequenced (Gardner *et al.,* 1998; Gardner *et al.,* 2002; Bowman *et al.,* 1999) and analyzed by Gardner *et al* (2002). The 23-megabase nuclear genome consists of 14 chromosomes ranging in size from approximately 643 to 3290 Kb and encodes about 5300 genes. The AT content of the genome 80.6%, was found to be maximum among genomes sequenced to date and it is 90% in introns and intergenic regions. The average gene density in *P. falciparum* is 1 gene per 4-5000 bases. Introns were predicted in 54% of *P. falciparum* genes.

1.2.7 Vaccine

A large proportion of genes are devoted to immune evasion and host–parasite interactions. Genes involved in antigenic variation are concentrated in the subtelomeric regions of the chromosomes (Gardner *et al.,* 2002). The genome was also found to contain low-complexity regions. These could be variable immunodominant epitopes of transmembrane proteins (Reeder and Brown, 1996). This enables the parasite to evade the immune response of the host by switching among different antigenic phenotypes. Although, the protozoan itself undergoes a lot of antigenic variation, thereby making any vaccine prospects bleak, the genome sequence will stimulate vaccine development by the identification of hundreds of potential antigens that could be scanned for desired properties such as surface expression or limited antigenic diversity. This could be combined with data on stage-specific expression to identify potential antigens that are expressed in one or more stages of the life cycle. To date, about 30 *P. falciparum* antigens are being evaluated

for use in vaccines, and several have been tested in clinical trials. Partial protection with one vaccine has recently been attained in a field setting.

1.2.8 Structural genomics

The structural genomics consortia is an ambitious project to solve the structures of several selected important proteins coded by the genome. Discovering the structure of proteins provides invaluable assistance in understanding the molecular mechanisms of drug targets. Many clinically important drugs are small, highly hydrophobic molecules. The structure will shed light on the affinity of these types of molecules for sites in proteins and on important regions/ residues in the target proteins, which could be exploited for screening and designing drugs using structure-function relationships. The targets selected for the present study are calmodulin, Macrophage migration inhibitory factor and translationally controlled tumour protein.

1.2.9 Calmodulin

Many proteins are sensitive to intra and extracellular calcium levels. Troponin C was the first such protein discovered. Its structure is remarkably similar to calmodulin except for the length of the linker connecting the two calcium-binding globular domains. Similar motifs have also been discovered in other calcium-sensitive proteins. Calmodulin is so named as it is a calcium modulated protein. It is abundant in the cytoplasm of cells of all higher organisms and is highly conserved through evolution implying a very important role for it. Calmodulin acts as an intermediary protein that senses calcium levels and relays signals to various proteins. For instance, calmodulin binds and activates kinases and phosphatases that play significant roles in cell signaling, ion transport and cell death.

Calmodulin is a small dumbbell-shaped protein composed of two globular domains connected together by a flexible linker (Fig. 1.13). It contains four EF hands and

identical sites capable of binding calcium even at micromolar concentrations. Each end binds two calcium ions. Upon binding of calcium, non-polar surfaces of calmodulin are exposed which then bind to non-polar regions on the target proteins wrapping it from either side using non-polar interactions usually involving methionines. The generic nature of non-polar grooves enable calmodulin to act as a versatile regulatory protein and bind to numerous targets. The target proteins come in a range of shapes and sizes and encompass a wide array of functions. The structure of calmodulin has been studied from various sources. Calmodulin structure from the malarial parasite will enable us to exploit any critical differences between different organisms, specifically, between humans and the parasite that may be exploited to develop drugs.

1.2.10 Macrophage migration inhibitory factor

Cytokines are the messengers of the vertebrate immune system. The macrophage migration inhibitory factor (MIF), a major proinflammatory cytokine with many unusual properties, was characterized at a molecular level from T lymphocytes by Weiser *et al.,* in 1989. MIF is an important immune system regulator in humans and plays an active role in inflammation. It inhibits macrophage migration and is associated with delayed hypersensitivity type reactions. Originally named for its inhibition of mononuclear cell migration *in vitro*, localizing macrophages to sites of delayed-type hypersensitivity reactions, MIF is now recognized as a pivotal proinflammatory mediator in systemic reactions such as those induced by bacterial endotoxins. In addition to the immune system, MIF is expressed in many nonhematopoietic tissues such as the brain. It is a pituitary hormone and endogenous antagonist of glucocorticoid action (Bernhagen *et al.,* 1993; Calandra *et al.,* 1995). In what appears to be a novel pathway of secretion, MIF is secreted by cells inspite of the absence of a signal sequence. In another interesting observation, the cytokine seems to lack a membrane receptor (atleast not yet identified), but interacts with a intracellular

signaling protein. Despite lacking a receptor, MIF can be endocytosed by immune and other target cells. It interacts with the transcription factor Jab1, a transcriptional coactivator which is an intracellular re-gulatory protein. MIF is the only cytokine known to be induced rather than inhibited by glucocorticoids.

Structure of MIF from different sources and with complexes have been reported (Suzuki *et al.,* 1996, Lubetsky *et al.,* 1999, Taylor *et al.,* 1999, Orita *et al.,* 2001, Zang *et al.,* 2002). It is a trimer although in physiological conditions it was found to exist as monomer and dimers also. Each monomer of 13 kDa is structurally comprised of two antiparallel helices and a four stranded sheet revealing a trimeric assembly with an inner pore created by beta-stranded sheets from each subunit, the significance of which is ill-understood. MIF has been shown to contain glutathione S-transferase activity (Blocki *et al.,* 1992). However, crystal structure (Suzuki *et al.,* 1996) (Fig. 1.14) showed that they are different eventhough anti-MIF antibodies were shown to cross-react with GST. But it was shown to possess similarities with other bacterial isomerases 4-oxalocrotonate tautomerase and 5-(carboxymethyl)-2-hydroxymuconate isomerase (Sun *et al.,* 1996; Murzin, 1996). It was found to possess phenyl pyruvate tautomerase activity. MIF is also the only cytokine to also possess enzymatic activity despite being less than 120 aminoacids in length. However, the substrates are all synthetic- no physiological substrate has yet been identified. Many compounds have been shown to inhibit tautomerase activity. Such specific inhibitors of this molecule could be good candidates as antiinflammatory therapeutics. The N-terminal proline is necessary for the phenyl tautomerase activity (Lubetsky *et al.,* 1999; Taylor *et al.,* 1999). The use of N-terminal residue for catalysis is a property shared by the Ntn hydrolase enzymes.

Zang *et al* (2002) have shown the conservation of both biological activity and molecular structure between eukayotic pathogen *Brugia malahi* and its human host

despite the considerable phylogenetic divide among these organisms. The human and nematode MIF homologues share a tautomerase enzyme activity, which is in each case abolished by the mutation of the N-terminal proline residue. This remarkable similarity shows how parasites have developed efficient strategies to evade and manipulate host defenses by co-evolving with their immune systems. MIF is an important modulator of immune system with enzymatic properties. It is critically involved in the host immune and stress response during acute and chronic inflammatory reactions and infections. Anti-MIF antibody could be used therapeutically in animal models in a number of inflammatory diseases like Sepsis (Calandra *et al.,* 1998), adult respiratory distress syndrome (Donnelly and Bucala, 1997), rheumatoid arthritis (Mikulowska, 1997), glomerulonephritis (Lan *et al.,* 1997) etc. Inhibitors of this protein could be a valuable antinflammatory therapeutic agent in diseases involving inflammation like malaria. Such an important protein is an obvious candidate as a drug target.

1.2.11 Translationally controlled tumor protein

Endoperoxide-containing antimalarials such as artemisinin and its derivatives artemether and artesunate are becoming increasingly important to treat multidrug-resistant strains of *Plasmodium falciparum*. Because these drugs are structurally unrelated to the classical quinoline and antifolate antimalarials, there is little or no cross-resistance. Like quinoline antimalarials, artemisinin appears to be selectively toxic to malaria parasites by interacting with heme, a byproduct of hemoglobin digestion, which is present in the parasite in high amounts.

Regulation of gene expression at the translational level has been demonstrated for many important cellular proteins, and various mechanisms are known to be involved. One such protein, translationally controlled tumor protein (TCTP), is a known target of artemisinin. It reacts with artemisinin *in situ* and *in vitro* in the presence of hemin

and appears to bind to hemin. The function of the malarial TCTP and the role of this reaction in the mechanism of action of artemisinin await elucidation (Bhisutthibhan *et al.,* 1998). TCTP is variously described as “P21”, “Q23”, P23 (Boehm *et al.,* 1989) and TCTP (Gross *et al.,* 1989). It was named so when it was observed that its synthesis is under translational control and from the source of the first known cDNA sequence, a mammary tumour (Gross *et al.,* 1989). However, now it is known that its synthesis is not exclusively regulated at the translational level. It is widely expressed in mammalian tissues (Sanchez *et al.,* 1997; Chung *et al.,* 2000; Thiele *et al.,* 2000). TCTP shows a high degree of conservation between all eukaryotic kingdoms and wide spread expression indicating that it is an important cellular protein.

The exact physiological function of this protein is yet to be found although several interesting observations have been made. Yeast TCTP is similar to the Mss4/Dss4 family of proteins, which interact with Rab proteins (Thaw *et al.,* 2001). P23 has been reported to be a tubulin-binding protein (Gachet *et al.,* 1999). It is preferentially expressed in proliferating cells of the polyp *Hydra vulgaris* (Yan *et al.,* 2000). It might be a calcium-binding protein (Sanchez *et al.,* 1997; Bhisutthibhan *et al.,* 1999; Xu *et al.,* 1999). It could be involved in IgE-dependent histamine and interleukin-4 release in allergy (Schroeder *et al.,* 1996) and could act as a B-cell growth factor (Kang *et al.,* 2001). Its expression is highly regulated in response to alterations of various physiological conditions like growth induction of mammalian cells (Boehm *et al.,* 1989; Bommer *et al.,* 1994), activation of macrophages (Walsh *et al.,* 1995), increase in cytoplasmic calcium concentration (Xu *et al.,* 1999), circadian variations in plants (Sage-Ono *et al.,* 1998), different stress responses (Sturzenbaum *et al.,* 1998), and induction of apoptosis (Baudet *et al.,* 1998). Here, the haem and artemisinin-binding activity of malarial TCTP (Bhisutthibhan *et al.,* 1998; Bhisutthibhan and Meshnick, 2001) is taken into consideration in the pursuit of new anti-malarials.

Fig. 13. Calmodulin from chicken (PDB ID 1UP5) (Rupp *et al.,* 1996).

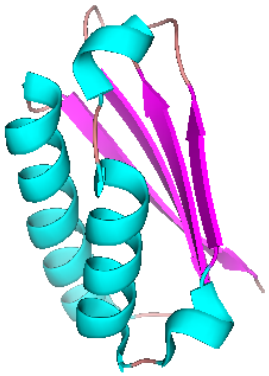

Fig. 14. MIF from rat liver (Suzuki *et al.,* 1996) (1FIM)

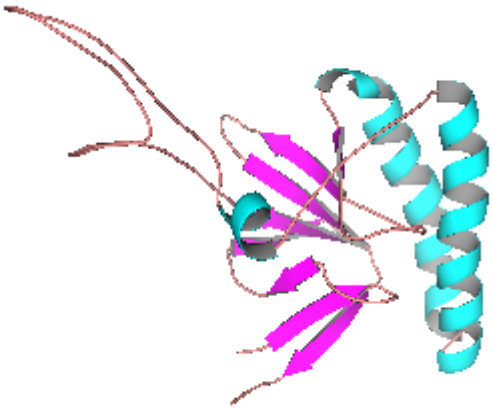

Fig. 15. Human TCTP monomer (2HR9) (Feng *et al.,* to be published)

1.3 Scope and Objective

PVA application properties improved using directed evolution or site-directed mutagenesis can be used not only for enhancing their catalytic efficiency but also to expand their substrate specificity to accommodate other related, more useful β-lactams. The work is the continuation of that quest. PVA also makes a preferred target for research since it has all the essential structural and biochemical features of PGA without being as complex in terms of structure and post-translational modifications. The expression and production of active enzyme are also much easier.

In the work described here, comparative studies have been conducted on PVA from *Bacillus subtilis* (*Bsu*PVA) and *Bacillus sphaericus* (*Bsp*PVA). Although sharing good sequence and structural similarity *Bsu*PVA is less efficient compared to *Bsp*PVA, which is more conformationally stable too. Kinetic studies carried out on the two enzymes showed that *Bsu*PVA has less affinity for PVA than *Bsp*PVA. The association constant for PVA also showed that *Bsu*PVA has lesser affinity for substrate. The two also differ in the optimal conditions of activity and stability. The study shows how and why *Bsp*PVA is better than *Bsu*PVA and has helped to identify factors important for a better PVA.

To understand the structural basis of this difference, structure of *Bsu*PVA has been solved. Structure of *Bsp*PVA was already known. The similarities in the three-dimensional structure between the two enzymes as elucidated by X-ray crystallography and the differences in their biochemical and conformational stabilities has enabled us to significantly close in on residues that seem to be so crucial for catalysis, paving way for a detailed understanding of the structure – function relationship. Both the enzymes are remarkably similar to CBH, both in sequence and structure (Rossocha *et al.*, 2005). Inhibition studies indicate that *Bsp*PVA is sensitive to the presence of various bile salts, natural substrates of CBH, whereas, *Bsu*PVA

was not significantly affected. This shows that *Bsp*PVA represents an intermediate between CBH and PVAs. Interestingly, *Bsp*PVA shows CBH activity, justifying the close-relatedness of their sequences. The study has provided a platform for elucidating functional details of PVA while highlighting the phylogenetic and evolutionary relationships between members of the choloylglycine hydrolase family-between PVA and conjugated bile salt hydrolases. Extensive studies on PGA and PVA have not resulted in any conclusive evidence for the physiological function of the protein. The remarkable similarity between these PVAs and CBH might just provide us the opportunity to arrive at some conclusion.

Ever since the genome sequence of *Plasmadium falciparum* was made available, several proteins have been targetted for structure elucidation in the hope that they can be exploited to design drugs or devise vaccine strategies to control the pest. Such work is fraught with difficulties due to peculiar features of the parasites genome. This work reports attempts made on understanding and targeting calmodulin-like proteins, a macrophage migration inhibitory factor and a translationally controlled tumour protein from another species of *Plasmodium*.

CHAPTER – II

BIOCHEMICAL CHARACTERIZATION OF YXEI AS A PENICILLIN V ACYLASE

Summary

Recombinant *E. coli* BL21 cells, containing the *yxeI* hypothetical protein gene from *Bacillus subtilis* grown in Luria Bertani medium and induced with Isopropyl thiogalactoside, overproduced a protein that was purified using phenyl sepharose column. It was found to be a homotetramer with a native molecular weight of 148,000. The protein showed penicillin V amidase activity (PVA) and was inhibited by the transition metal ions Cu^{2+}, Zn^{2+}, Fe^{2+} and Co^{2+}. The reducing agent dithiothreitol enhanced amidase activity. Chemical modification and mutation studies proved that cysteine was an active site residue. Modification of arginine reduced amidase activity. The optimum activity was between pH 6.6 - 7.5 and the catalytic residues had estimated pKa values of 6.5 and 8.5. The enzyme had an apparent K_m of 40 mM at pH 6.0 for Penicillin V and 0.67 mM for the synthetic substrate 2-nitro-5-(phenoxyacetamido)-benzoic acid (NIPOAB) at pH 7.0.

2. 1 Introduction

Post-genomics era has seen a plethora of genes sequenced from various species hitherto functionally uncharacterized. High-throughput gene sequencing has simply outpaced any characterization attempts. Some of these uncharacterized genes have been found spread over a large number of species. Such 'conserved hypothetical proteins' are mostly believed to be involved in important basic functions of the cell. They, therefore, make potentially good targets to study as they can contribute to our basic understanding, unlike genes that are species-specific. Especially so in model organisms like *Bacillus subtilis* or *Eshcherichia coli*, which still have several

uncharacterized genes. Complete characterization of their full proteome complement is essential for a systems approach.

The gene of YxeI was originally sequenced as part of an international project for the sequencing of the entire *Bacillus subtilis* genome. The gene *yxeI* lies in the region of DNA of the *bacterium B. subtilis* occurring between the *iol* and *hut* operons and has been reported to code for a hypothetical protein (Yoshida *et al.,* 1995). The open reading frame (ORF) is annotated as a hypothetical protein /choloylglycine hydrolase and a highly conserved putative penicillin amidase, based on sequence. The protein is predicted to contain the domains of penicillin V acylase (PVA) and Conjugated bile acid hydrolase (CBH). Homology with other bacterial CBH and PVA is high (Tanaka *et al.,* 2000). A Basic Local Alignment Search Tool (BLAST) search of the sequence against various databases revealed that the protein had significant levels of homology with both PVA from *Bacillus sphaericus* (*Bsp*PVA) and CBH from various sources including *Clostridium perfringens* and *Bifidobacterium longum*, whose crystal structures have been solved, and a number of hypothetical proteins from different organisms.

The physiological role of penicillin acylase in the host organisms is still not clearly established, despite years of research. Conjugated bile acid hydrolases have been thought to help the host bacteria present in the mammalian intestinal flora deconjugate the conjugated bile salts, thereby detoxifying them. Both the enzymes, however, have commercial applications- penicillin acylases are used in the industrial production of semisynthetic penicillins and CBHs are used clinically for assaying levels of bile acids in biological fluids. Interest in YxeI arose primarily because of the PVA activity of the protein. The present chapter describes the biochemical characterization of YxeI from *Bacillus subtilis*.

2. 2 Materials and Methods

2. 2. 1 Cloning

YxeI from *B. subtilis*, cloned and transformed into *E. coli*, was available for the study through a collaboration. The chromosomal DNA of *B. subtilis* was amplified by PCR using the following forward and reverse oligonucleotide primers synthesized in automatic DNA synthesizer at University of York (Applied Biosystems 373).

5' GGGACTGAT**CATATG**TGCACAAGTCTTAC 3'

3' TCTCATAAGTACTGGAATAAATT**CCTAGG**AGTTA 5'

The primers were designed to have restriction sites for the enzymes Nde I and Bam HI (shown in bold) (New England Biolabs). The purified PCR product was restriction digested and cloned into plasmid pET26b (Invitrogen) and transformed into *E. coli* XL-1 cells. The protein was expressed in *E. coli* BL21 (DE3) cells after further transformation. DNA sequencing was done at MWG Biotech, Germany. This clone was used for protein preparation, characterization and structural studies. Two mutants C_1A and C_1S were also engineered using appropriate base substitution in the primers.

2. 2. 2 Expression and purification of enzyme

Luria Bertani medium containing 30 μg ml^{-1} kanamycin was inoculated with 5% overnight shake flask cultures of *E. coli* BL21 (DE3)-pET26-*yxeI* cells. The cells were grown in Erlenmeyer flasks at 37 ^oC in shaker cultures at 200 rev min^{-1} till they attained an optical density of 0.8 at 600 nm. The mid-logarithmic growth phase culture was supplied with isopropyl-β-D-thiogalactoside (IPTG) at a final concentration of 1 mM to induce production of the enzyme. The cells were allowed to incubate at 30 ^oC for another 4 hours with shaking (200 rev min^{-1}). The culture medium was centrifuged at 10 000*g* in a Sorvall RC 5B refrigerated centrifuge for 20 min to sediment the cells and the supernatant was discarded. The cells were

weighed and stored frozen overnight. The cells were re-suspended in 10 ml of 50 mM potassium phosphate buffer pH 6.0 containing 1 mM ethylene diamine tetra acetic acid (EDTA) and 0.5 mM dithiothreitol (DTT) (buffer *A*) and sonicated in a Biosonik III sonic oscillator at 5 × 1 min at 20KHz, 300W, 10 min intervals between pulses. The enzyme was maintained on ice during sonication and all subsequent steps were carried out at 4 ^{o}C unless otherwise specified. The sonicate was centrifuged at 10 000*g* for 20 min and the cell debris was removed. The supernatant was mixed with 7 mg ml^{-1} streptomycin sulphate and stirred in the cold for 1 hour, to precipitate and remove nucleic Acids. The resulting sample was centrifuged for 30 min at 8000*g* to remove the precipitated DNA. The supernatant was mixed slowly with ammonium sulphate (AS) in the cold till a final concentration of 80% saturation was attained. After centrifugation (10 000*g*, 20 min), the precipitate was dialyzed against buffer *A* containing 24% AS. This sample was loaded at 4 ^{o}C on a phenyl sepharose column (phenyl sepharose CL 4B, Sigma, USA) that had been pre-equilibrated with buffer *A* containing 24% AS. The column was washed with 50 ml of the same buffer. The bed volume of the column was 20 ml. The protein was eluted with buffer *A*, as 30 min fractions at a column flow rate of 5 ml hr^{-1}. The fractions were checked for enzyme activity and the active fractions were subjected to sodium dodecyl sulphate polyacrylamide gel electrophoresis (SDS-PAGE). Fractions showing pure protein were pooled and dialyzed against 50 mM potassium phosphate buffer containing 10 mM DTT and concentrated by ultrafiltration using a PM-10 membrane in an Amicon unit. A 12% SDS-PAGE was run to check the purity of the protein as described by Laemmli (1970). The final total yield of the homogeneous protein was >10 mg per liter of cell culture. The purified enzyme was aliquoted (0.5 ml, 10 mg ml^{-1}) and stored at -20 ^{o}C. The C1A and C1S mutants were also purified using the same procedure.

2. 2. 3 Protein estimation

Protein concentration of samples was estimated by the method of Lowry *et al* (1951) using bovine serum albumin (BSA) as the calibration standard.

2. 2. 4 Determination of molecular weight

The molecular weight of native protein was determined using Gel filtration chromatography and High Performance Liquid Chromatography. Gel filtration chromatography was performed on a Sephadex G200 (Pharmacia) column. The marker proteins (Sigma) used were Thyroglobulin (MW 669000), β-amylase (200000), Alcohol Dehydrogenase (150000), BSA (66000) and Carbonic anhydrase (29000). The native molecular weight was calculated from the ratio of elution volume (Ve) of the protein to void volume (Vo) of the gel filtration column with reference to protein markers of known molecular weights. The column was equilibrated with 50 mM pH 7.5 potassium phosphate buffer and run at a flow rate of 4 ml hr^{-1} at 4 ^{o}C.

High performance liquid chromatography (HPLC) separations were performed on a Waters 2690 separations module equipped with a waters 2487 dual wavelength absorbance detector operated in the 20 –21 nm range. An octadecyl silica column 50×5 mm was eluted with 50 mM potassium phosphate buffer pH 7.0 after loading sample. Fractions were collected manually at the detector outlet. The molecular weight was calculated from the retention time in the case of HPLC. The markers (Sigma) used were BSA (66000), Alcohol Dehydrogenase (150000), β-amylase (200000), Cytochrome-C (12400) and Ovalbumin (45000).

The subunit molecular weight of the protein was determined by SDS-PAGE. Electrophoresis was performed on the protein samples (~5-10 µg) under reducing conditions on a 12% polyacrylamide gel in a Biorad unit. Gels were stained with

0.25% Coomassie brilliant blue R250 in 40% (v/v) methanol and 10% (v/v) glacial acetic acid. Electrophoresis was conducted at 25 ^{o}C at 200 V (constant voltage) till the bromophenol blue tracking dye reaches the end of the gel. The apparent molecular weight was calculated by comparing the migration of the protein with that of marker proteins of known molecular weights.

The subunit molecular weight of the protein was also determined using Matrix Assisted Laser Desorption Ionisation Mass Spectrometry using a sinipinic acid matrix at the CSL facility, York. Protein samples were prepared by buffer exchange overnight by dialysis against deionised water at 4 ^{o}C.

2. 2. 5 Determination of the isoelectric point of the protein

The isoelectric point of the protein was determined in a Biorad unit at a constant voltage of 400 V for 8 h at 4 ^{o}C using ampholines in the pH range 3.5 – 10.25. The markers were bought from Biorad.

2. 2. 6 Penicillin V Acylase assay

Penicillin V (PenV) was a kind gift from Hindustan Antibiotics Limited, Pimpri, India. The assay of penicillin acylase activity was carried out spectrophotometrically by measuring the amount of 6-amino penicillanic acid (6APA) released when 100 mM PenV, pre-incubated for 2 min, was incubated for 10 min with the enzyme at 40 ^{o}C at pH 6.6 using the method of Shewale *et al* (1987). One unit of penicillin acylase activity was defined as the amount of enzyme required to liberate 1 μmol of 6APA per minute using potassium salt of phenoxymethyl penicillanic acid as substrate. The reaction was initiated with the addition of the enzyme in a total reaction volume of 0.5 ml and subsequently quenched with equal volume of citrate phosphate buffer (CPB) pH 2.5. All assays were carried out in triplicates. Colour reactions were performed using p-dimethyl amino benzaldehyde (PDAB) reagent (1 g PDAB dissolved in 170

ml methanol and 0.01% hydroquinone as stabilizer). The intensity of the colour was read at 415 nm exactly after 2 min of addition of an equal amount of PDAB to samples quenched with CPB. Standard graphs were drawn using pure 6APA (sigma) (Figure 2.6).

Olsson *et al* (1985) reported the use of 6-nitro-3-(phenoxyacetamido) benzoic acid (NIPOAB) as a substrate for measuring the hydrolytic activity of *B. sphaericus* PVA. The compound has been further studied by Kerr (1993) using PVA from the fungus *Fusarium oxysporum* and also by Alkema *et al* (1999). The compound NIPOAB was synthesized by Schotten-Bauman reaction and the end product purified by crystallization.

In the case of NIPOAB, the reaction mixture contained enzyme and different concentrations of the substrate in 1 ml of 50 mM potassium phosphate buffer pH 7.0 at 30 ^{o}C. The rate of change of absorbance at 405 nm was recorded. Activity was calculated using an extinction coefficient of 8980 M^{-1} cm^{-1} for the reaction product 5-amino-2-nitrobenzoic acid. At that wavelength, absorbance due to the substrate was relatively negligible. Dimethyl sulphoxide was used in minimal amounts to dissolve NIPOAB. Advantage of this substrate is the absence of any end product inhibition unlike PenV where end-product inhibition is reported.

2. 2. 7 Determination of optimum conditions for penicillin acylase activity

The progress of PenV hydrolysis over time was monitored for 2 hours at 40 ^{o}C. The assay was carried out as outlined above. Samples were removed at suitable time intervals, reaction arrested using CPB and the product reacted with PDAB for 2 min.

The enzyme was assayed at various pHs between 1.0 to 12.0 at 40 °C as described above. The buffers used were glycine-HCl (1.0 - 3.0), CPB (4.0 – 6.0), potassium

phosphate (7.0), Tris-HCl (8.0 –9.0) and glycine-NaOH (10.0 - 12.0). The pHs of the buffers were adjusted at 25 ^{o}C. All the buffers had the same final ionic strength of 100 mM in the reaction mixture. Different buffers such as potassium phosphate, sodium phosphate, Piperazine-1,4-bis(2-ethanesulfonic acid) and sodium cacodylate were tested near the optimal pH. Activity was measured in triplicates with a 10 min reaction time, 100 mM PenV and 2 min colour development with PDAB. The pH stability of the enzyme was studied by incubating the enzyme in the corresponding buffers for different time periods at room temperature and the residual activity measured as outlined above at 40 °C at pH 7.0 using 100 mM potassium phosphate buffer.

The enzyme was assayed for PVA activity at different temperatures over the range 30 – 70 ^{o}C. The temperature stability of the enzyme was studied by incubating the enzyme at different temperatures for 30 min to 4 h, at pH 7.0 and residual activity measured at 40 °C. PenV (potassium salt) was used as the substrate in these studies. Standard assay conditions also had 10 mM DTT in the reaction mixture.

2. 2. 8 Effect of DTT and EDTA

PVA was assayed after incubating with different concentrations of the reducing agent DTT and the chelating agent EDTA for 15 min at room temperature. PVA assayed without the addition of DTT or EDTA served as control.

2. 2. 9 Effect of divalent metal ions

PVA samples (150 µg) were diluted with 50 mM potassium phosphate buffer pH 6.6 and incubated with various divalent metal ions for 15 min at room temperature (25 ^{o}C). PVA assay was then done in triplicates at 40 ^{o}C for 10 min after saturating with 100 mM PenV and 2 min reaction of the samples with PDAB to quantify the residual activity by detection of the chromogenic Schiff base formed.

2. 2. 10 Substrate specificity

The hydrolase activity was checked with different β- lactam antibiotics as substrates, purchased from Sigma, USA. Penicllin V, Penicillin G, Ampicillin, Amoxicillin, Cephalosporin C Zinc salt and Cephalosporin G were tested. A typical incubation mixture contained substrate at a concentration of 50 mM as free acid or sodium salt in 100 mM potassium phosphate buffer pH 6.6. Enzyme samples were diluted in the same buffer and assayed by initiating the reaction with addition of enzyme to different substrates. After incubating at 40 ^{o}C for 10 min, the solutions containing the potential alternate substrates were quenched and the presence of products was determined. Each substrate was assayed in triplicates, along with appropriate controls from which the addition of enzyme was withheld. In the case of NIPOAB, the reaction mixture contained 10 μg of enzyme with 500 μM NIPOAB in 1 ml of 100 mM phosphate buffer pH 7.0. The rate of change in absorption at 405 nm was recorded. Bile salts tested were sodium salts of glycocholic acid, glycodeoxycholic acid, glycochenodeoxycholic acid, taurocholic acid, taurodeoxycholic acid and taurochenodeoxycholic acid.

2. 2. 11 Kinetic studies

Measurements of the rates of enzyme reactions as a function of substrate concentration provide information about the kinetic parameters that characterize the reaction. Two of them are most important: K_m is an approximate measure of the tightness of binding of the substrate to the enzyme and V_{max} is the theoretical maximum velocity of the enzyme reaction. Measurements are made at several substrate concentrations while holding all other conditions constant.

The kinetic studies were carried out using PenV and the synthetic substrate NIPOAB as substrates. Reactions with PenV were performed at 40 ^{o}C. Substrate

concentrations typically ranged from a K_m of 0.2 to 5 units. After 10 min, reactions were quenched at which point an estimated less than 5 % of the substrate had been consumed. Initial rates (V_o) were determined in triplicates and fitted to standard Lineweaver-Burk (LB) plot to determine values of K_m and V_{max}. The kinetics of the enzyme was studied at various pH. Atleast three measurements at each substrate concentration and pH were made. In the case of NIPOAB, the enzyme was allowed to react with different concentrations of NIPOAB as described earlier and the data were fitted to LB plot.

2. 2. 12 Chemical modification and CD spectra measurements

2. 2. 12. 1 Chemical modification of cysteine

Prior to chemical modification, protein samples were extensively dialyzed against deionised water to remove any DTT present. The cysteine residues of the enzyme were modified using Ellman's reagent - 5,5'-dithiobis-(2-nitrobenzoic acid) (DTNB) (Sigma, USA). Samples (150 µg) were incubated for different time intervals with different concentrations of DTNB (0.5-10 mM) in 100 mM Tris buffer pH 8.0. Excess reagent was removed by passing through Sephadex G-25 columns.

The apparent first-order rate constant of inactivation, K_{app}, depends upon the concentration of DTNB according to the relationship

$K_{app} = K [M]^n$

where K is the second-order rate constant, [M] is the concentration of the modifier and n is the average order of the reaction with respect to concentration of DTNB. Kapp can be calculated from a semi-logarithmic plot of residual enzyme activity as a function of time. The order of the reaction can be experimentally determined by estimating K_{app} at different concentrations of DTNB. A plot of log K_{app} against [M] gives a straight line with slope equal to n, where n is the number of molecules of DTNB reacting with each active unit of the enzyme to produce an enzyme-inhibitor

complex (Levy, 1963, Ramakrishna and Benjamin, 1981). Kinetic studies were conducted on 80% modified enzyme.

2. 2. 12. 2 Chemical modification of arginine

The enzyme was treated with arginine modifying reagent phenylglyoxal (Takahashi, 1968) at various concentrations (100 µM – 10 mM) for different time periods (2 min – 1 h) and the residual activity measured. The alpha-dicarbonyl reagent phenylglyoxal was dissolved in ethanol and incubated at various concentrations with the enzyme in 50 mM potassium phosphate buffer pH 8.0. Samples were removed after definite time intervals and assayed for PVA activity as outlined above after removing the excess reagent by passing through a Sephadex G-25 column (10 x 0.5 cm).

2. 2. 12. 3 Substrate protection studies

Substrate protection studies for cysteine modification were conducted by incubating the enzyme with different concentrations of PenV before modifying with 2 mM DTNB for 6 min and measuring the residual activity.

Substrate protection studies for arginine modification were conducted thus: The enzyme was incubated with different concentrations of PenV in ice cold conditions for 10 min. A concentration of 0.1 mM phenylglyoxal was then added and allowed to incubate for 2 min and the residual activity was measured. Kinetic studies were conducted on 50% modified enzyme to determine the K_m and V_{max} values.

2. 2. 12. 4 Circular dichroism measurements

Far UV CD spectra were recorded in a Jasco-J715 spectropolarimeter at room temperature using a cell of 0.1 cm pathlength. Triplicate scans were run at 1 nm resolution, 1 nm bandwidth and a scan speed of 200 nm /min. Data were averaged to reduce noise and the baseline was subtracted. The sensitivity was 20 mdeg and the

response time was 2 sec. Each spectrum obtained was the average of 3 scans with the baseline subtracted spanning 250 to 200 nm in 0.1 nm increments. The CD spectrum of the enzyme was recorded in 50 mM potassium phosphate buffer pH 7.0 and compared with that of the treated enzyme. Protein concentration used was around 3 µM. The secondary structure composition was calculated using k2d software available at http://www.embl-heidelberg.de/~andrade/k2d/

2. 2. 13 Bile salt hydrolase assay

CBH activity was measured by estimating glycine or taurine produced on hydrolysis of glycine or taurine-conjugated bile acids. Samples were incubated at 37 ^{o}C with 100 mM substrate in 50 mM potassium phosphate buffer containing 10 mM DTT in a total volume of 100 µl. 50 µl of this was removed after 10 min incubation and mixed with 50 µl 15% TCA and centrifuged. 50 µl of the supernatant was boiled for 14 min in the presence of 50 µl 2% ninhydrin reagent (Sigma, USA) (Moore, 1968), rapidly cooled for 3 min under running water. The volume was made up to 2 ml and the absorbance was read at 570 nm. Glycine (Sigma, USA) was used as the standard. All substrates were procured from Sigma, USA.

2. 3. Results and Discussion

2. 3. 1 Overexpression and purification

The recombinant *E. coli* cells, containing the y*xeI* gene cloned from the bacterium *B. subtilis* NCIMB 11621 into plasmid pET26, grown in Luria Bertani medium, overproduced a protein that had a molecular weight of 148,000 as estimated from gel filtration chromatography. The recombinant protein cloned with a 6 × histidine tag for affinity purification on Nickel- Nitrilo tri acetate matrix, aggregated on purification and storage. Though aggregation could be reduced by adding glycerol, keeping optimal conditions of enzyme action in mind (Arroyo *et al.,* 1999), the protein without the His tag was eventually used for our studies. Optimal conditions of expression were found to be 1 mM IPTG at 30 ^{o}C for 4 h after induction. The protein was purified using phenyl sepharose column chromatography. The specific activity of the purified protein was 5 μmol mg^{-1} min^{-1}. The protein remained active for atleast a month when stored at –20 ^{o}C in aliquots. Purification details for a typical 1 L culture are summarised in Table 2. 1.

Table 2. 1: Purification of PVA from recombinant *E. coli*

Purification step	Total amt of protein (mg)	Activity (U)	Sp act (U/mg)	Yield (%)
Crude extract	1980	634	0.32	100
Phenyl sepharose	20	101	5.06	16

2. 3. 2 Estimation of molecular weight

SDS-PAGE of YxeI under reducing conditions showed a single band at MW_{calc} = 37,000 (Fig. 2. 1). The molecular weight of the subunit of the enzyme was found to be 37,008 as determined by MALDI as can be predicted from the sequence. The native enzyme was found to have a molecular weight of 148,000 as determined by gel filtration chromatography and HPLC (Fig. 2. 2), indicating that the protein is composed of four identical monomers. The native molecular weight was further supported by observation from crystallographic data (Rathinaswamy *et al.,* 2005). The molecular weight of the closely related homotetrameric PVA from *B. sphaericus* is 140,000 (Olsson *et al.,* 1985, Pundle and SivaRaman, 1997). Various molecular weights have been reported for related CBH and are elaborately discussed by Tanaka *et al* (2000). Crystallographic studies also showed a tetrameric association for CBH.

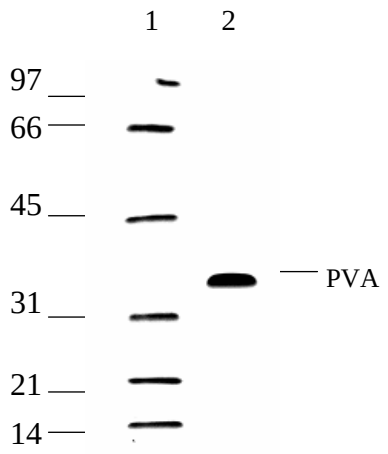

Fig. 2. 1. SDS-PAGE of YxeI: A 12% gel stained with Coomassie brilliant blue R250. The molecular weight of the markers (lane 1) is shown on the left of the lane, in kDa. Lane 2 shows single band of PVA after purification on Phenyl sepharose column.

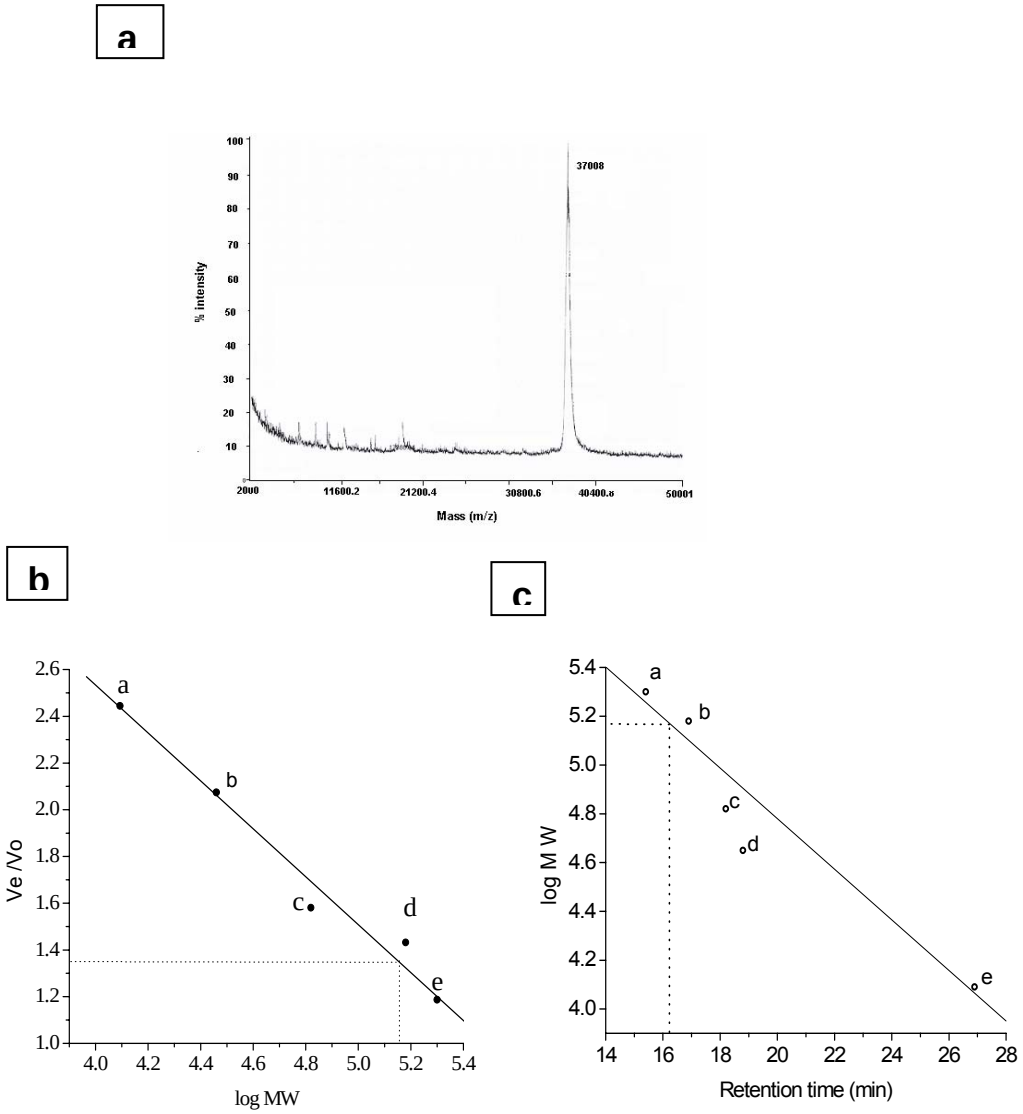

Fig. 2. 2: Molecular weight determination by **a)** MALDI

b) Gel filtration chromatography- plot of V_e/V_o versus log (molecular weight) where V_e and V_o are elution volumes of individual proteins and column void volume respectively. The marker proteins (Sigma) used were a. Cytochrome-C (Mr 12400), b. Carbonic anhydrase (29000), c. BSA (66000), d. Alcohol Dehydrogenase (150000) and β-amylase (200000).

c) HPLC – plot of log (molecular weight) versus retention time of proteins in the column. The markers (Sigma) used were a. β-amylase (200000), b. Alcohol Dehydrogenase (150000), c. BSA (66000), d. Ovalbumin (45000) and e. Cytochrome-C (12400).

2. 3. 3 Determination of pI

The isoelectric point of the protein was found to be 5.3, which is in agreement with the value predicted using YxeI protein sequence deduced from our nucleotide sequence.

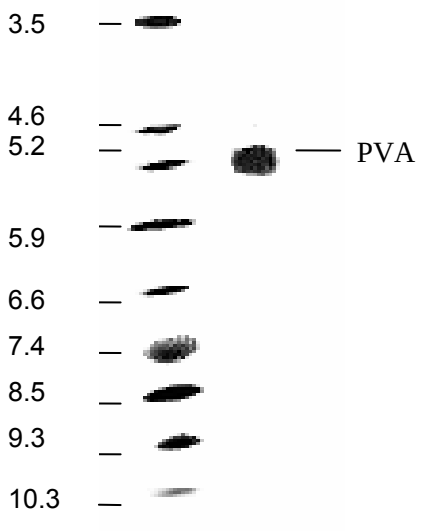

Fig. 2. 3: Isoelectric focussing of purified YxeI: The pI of the markers are shown on the left of lane 1. Lane 2 shows PVA.

2. 3. 4 N-terminal sequence information

The amino terminal sequence of the protein was found to be Cys-Thr-Ser-Leu-Thr-Leu. Comparison with the DNA-deduced sequence shows the loss of N-terminal methionine. The N-terminal aminoacid residue determined was to be a cysteine, the N-formyl methionine being lost during processing. Autocatalytic processing is a characteristic feature of Ntn hydrolases, whereby the amino group of their active Ntn residue is revealed. The sequence of our protein differs from the translated sequence reported by Yoshida *et al* (1995) at four residues – alanine-69, phenylalanine-70, methionine-91 and serine-219 were glycine, isoleucine, threonine and proline, respectively. The total number of aminoacids was 327. CD spectra revealed that the protein had 6% alpha helix and 46% beta strands. The complete aminoacid sequence deduced from nucleotide sequence is presented overleaf:

CTSLTLETADRKHVLARTMDFAFQLGTEVILYPRRYSWNSEADGRAHQTQYAFIGMGRKLG
NILFADAFNESGLSCAALYFPGYAEYEKMIREDTVHIVPHEFVTWVLSVCQSLEDVKEKIRSLT
IVEKKLDLLDTVLPLHWILSDRTGRNLTIEPRADGLKVYDNQPGVMTNSPDFIWHVTNLQQYT
GIRPKQLESKEMGGLALSAFGQGLGTVGLSGDYTPPSRFVRAVYLKEHLEPAADETKGVTA
AFQILANMTIPKGAVITEEDEIHYTQYTSVMCNETGNYYFHHYDNRQIQKVNLFHEDLDCLEP
KVFSAKAEESIHELN

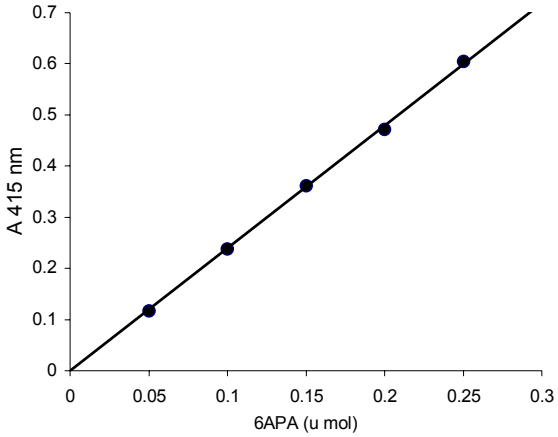

Fig. 2. 4. Standard graph of 6APA detection. Different moles of pure 6APA were reacted with PDAB for 2 min as described in methods and the Schiff base formed was quantified by reading the resultant yellow colour at 415 nm.

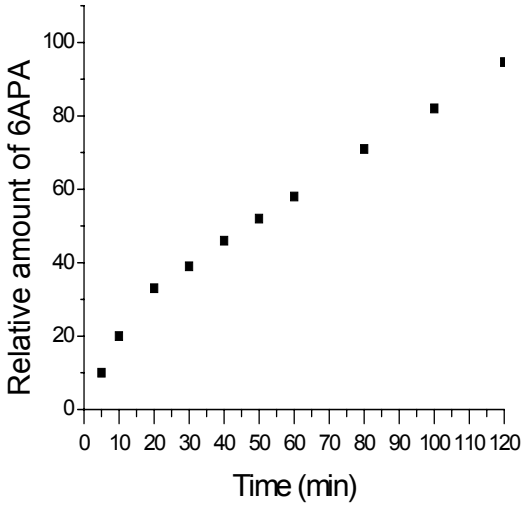

Fig. 2. 5: Time course of PVA activity. Purified enzyme was subjected to assay as described above and the amount of 6APA produced was quantified to study the variation of enzyme activity with time.

2. 3. 5 Optimum pH and stability

The enzyme was active in the pH range from pH 5.5 to 9.0 with maximal penicillin acylase activity between pH 6.6 and 7.5 at 40 ^{o}C when incubated for 10 min, using substrate PenV (Fig. 2. 6). At pH 9.0, there is a sudden drop in activity. The protein was stable at pH 8.0 where it showed only 5% loss of activity after incubation at 25 ^{o}C for 2 h.

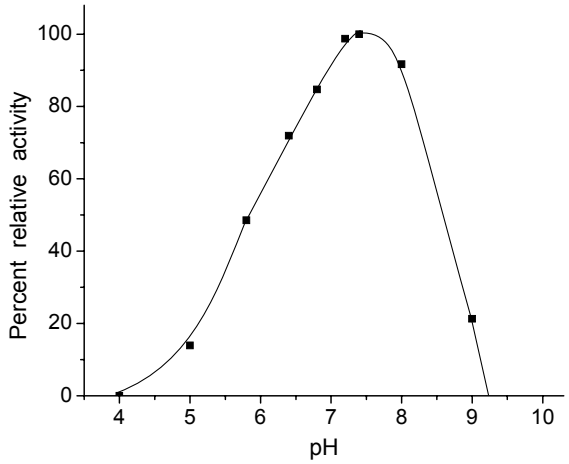

Fig. 2. 6: Relative activity of *Bsu*PVA plotted as a function of pH

2. 3. 6 Optimum temperature and stability

The enzyme was stable at the optimum temperature of 40 °C; at the end of 4 h, it showed 80% residual activity. It steadily lost activity at higher temperatures and at 50 °C, it retained only 40% activity at the end of 4 h. At 60 °C and higher, the enzyme was rapidly inactivated (Fig. 2.7). Though the enzyme was unstable at higher temperatures, CD spectra did not show any significant changes in the secondary structure composition of the protein when heated at 55 ^{o}C for 15 min at pH 7. PVA was assayed at different temperatures retaining other standard conditions; V_{max} increased with temperature (Table. 2. 7) in the range where enzyme was stable.

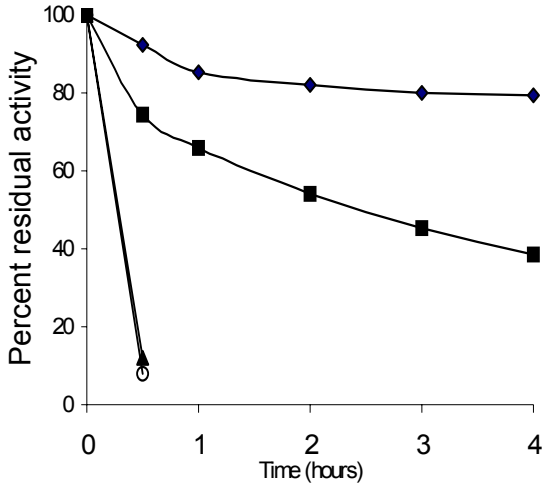

Fig 2. 7 : Effect of temperature on PVA activity. The activity was measured after incubation for different time periods at the following temperatures: —♦— 40 °C —■— 50 °C —▲— 60 °C —○— 70 °C

Temp (°C)	V_{max} (μmol mg^{-1} min^{-1})
30	2.8
35	3.5
40	5.06

Table 2. 2: PVA activity is shown as a function of temperature. PVA activity was assayed at different temperatures and V_{max} calculated.

2. 3. 7 Effect of reducing agents and chelating agents on activity

Presence of 10 mM DTT was found to enhance enzyme activity by 12%, indicating the presence of an active sulfhydryl group in the enzyme. Therefore, DTT was used at a concentration of 10 mM throughout the experiments, from sonication onwards, unless otherwise indicated. EDTA inhibited the activity of PVA in a concentration-dependant manner. At 1 mM, it decreased PVA activity by 4% (Table 2. 3).

In the case of CBH, Grill *et al* (1995) reported that the presence of DTT enhanced enzyme activity indicating that the thiol groups were present at important sites and a reduced state was necessary for activity. Nair *et al* (1967) have also reported the isolation of a choloylglycine hydrolase from *C. perfringens*, which has an active sulfhydryl group. CBH from *Bifidobacterium longum* was inhibited by thiol enzyme inhibitors indicating essential cysteine residues. PVA is also known to be oxygen sensitive. Presence of DTT enhanced penicillin acylase activity in YxeI, indicating the presence of active sulfhydryl group in the enzyme, which as shown from chemical modification and mutation studies, is a cysteine.

2. 3. 8 Effect of divalent metal ions on activity

The Group 2A metals Ca^{2+} and Mg^{2+} had no appreciable effect on activity. The enzyme was inhibited by the transition metals Cu^{2+}, Zn^{2+}, Fe^{2+}, Ni^{2+}, Mn^{2+} and Co^{2+} (Table 2. 3).

2. 3. 9 Substrate specificity

Based on significant sequence similarity between this protein and penicillin V acylase from *B. sphaericus*, the enzyme was tested with penicillin and various related β-lactam antibiotics for its hydrolytic activity. We found that the enzyme showed maximum hydrolytic activity with phenoxymethyl penicillin. It did not exhibit significant activity when benzyl penicillin was used as substrate. There was no measurable cephalosporin acylase activity. It did not hydrolyze ampicillin or amoxicillin. The synthetic substrate 2-Nitro-5-(phenoxyacetamido)-benzoic acid (NIPOAB) has been reported to be a good chromogenic substrate for PVA (Kerr, 1993). On testing it with YxeI, it was found to give significant reactivity. However, the enzyme did not show any hydrolytic activity against the conjugated bile salts tested.

Table 2. 3: PVA activity in the presence of various metals, reducing and chelating agents.

Additive	Concentration (mM)	Percent residual activity
Cu^{2+}	5	5
	10	6
Zn^{2+}	5	53
	10	37
Ni^{2+}	5	67
	10	26
Fe^{2+}	5	61
	10	72
Mn^{2+}	10	91
Co^{2+}	5	93
	10	81
DTT	5	107
	10	112
EDTA	1	96
	5	89
	10	69

2. 3. 10 Kinetic constants

Kinetic studies were conducted on the enzyme and the experimental data were analyzed by LB plots. The apparent K_m of the enzyme for PenV was 40 mM and the V_{max} was 5.06 µmol mg^{-1} min^{-1}. The K_m for NIPOAB was 0.63 mM and V_{max} was 1.2 µmol mg^{-1} min^{-1}.

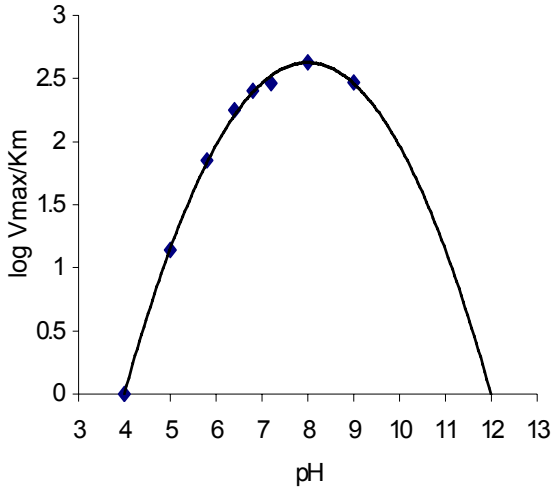

Fig. 2. 8: Plot of log V_{max}/K_m at different pH. V_{max} and K_m were calculated in the pH range where PVA was active.

The buffers used were of constant ionic strengths, which eliminated variation in activity contributed by ionic strength. There were two ionizable groups in the free enzyme with apparent pKa 6.5 and 8.5. The pKa of 6.5 indicated probable involvement of ionization of a histidine or a carboxyl group in non-polar environment. The pKa of 8.5 could be contributed by changes in the microenvironment of basic aminoacid. This could be arginine as indicated by chemical modification, sequence alignment and structure studies. Figure 2. 8 shows the pH rate profile of YxeI.

2. 3. 11 Aminoacid modification studies

2. 3. 11. 1 Modification of cysteine

Sequence similarity searches showed that YxeI was similar to proteins that have been characterized as Ntn hydrolases, which have a catalytically active N-terminal residue. The presence of the reducing agent DTT, enhanced the enzyme activity acknowledging the importance of a sulfhydryl group. Thus, cysteine could be one of

the active site residues involved in the PVA activity, as in *B. sphaericus* PVA. Therefore, cysteine modification using DTNB was tried.

Enzyme inactivation followed pseudo first-order kinetics. K_{app} was calculated from time versus log (percent residual activity) plot. The reaction order was calculated from the plot of log of DTNB concentration versus respective K_{app}. Linear fit of the plot gave a slope of 0.96 indicating the reaction of DTNB with one cysteine residue per mole of enzyme (Fig 2. 9a, 2. 9b). The enzyme mutants in which the N-terminal cysteine was mutated to alanine or serine did not show any penicillin acylase activity, indicating that the N-terminal cysteine was a catalytic residue.

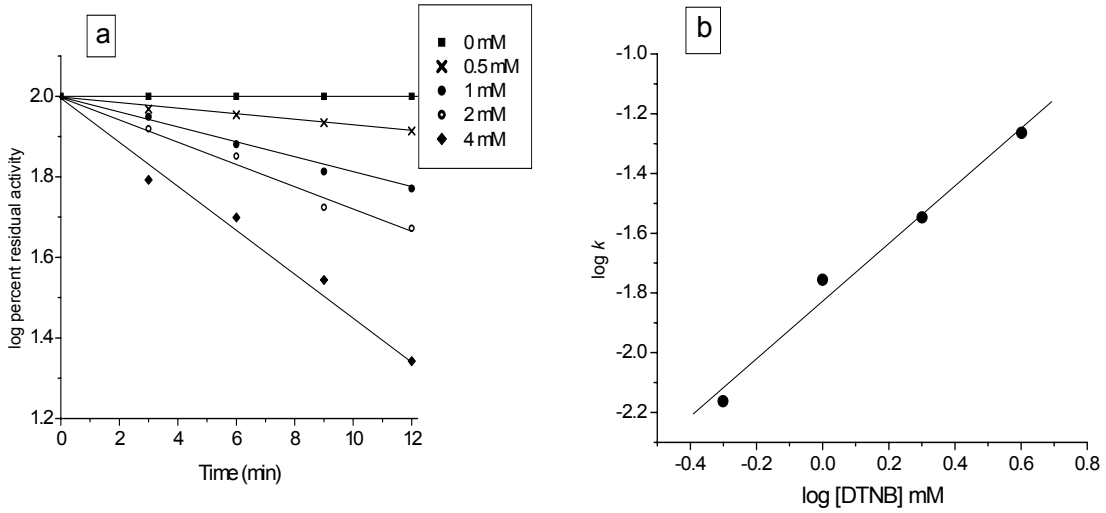

Fig. 2. 9: Chemical modification of cysteine

2. 3. 11. 2 Kinetic studies on partially inactivated PVA

Kinetic studies on PenV with 80% modified enzyme showed that K_m remained constant whereas V_{max} was reduced (1.1 μ mol min^{-1}) as determined using LB plots indicating modification of aminoacid residue at the substrate binding site.

2. 3. 11. 3 Modification of arginine

Enzymes acting on anionic substrates have essential basic aminoacids (Riordan, 1977). Pundle *et al* (1997) have shown the involvement of lysine in *B. sphaericus* PVA activity. An arginine residue was found in the vicinity of Cys1 in the active site of the enzyme structure of YxeI (Chapter 3). Both Cys and Arg were among the active residues of the closely related penicillin acylase from *B. sphaericus* (Suresh *et al.,* 1999). The aminoacid sequence analysis with BLAST showed that Cys and Arg are among the invariant residues among these proteins, which share sequence similarity with those of the Ntn hydrolase family. Sequence alignments indicated Arg17 was conserved among various proteins and was subsequently found to be important for product binding in CBH (Rossocha *et al.,* 2005).

Modification of arginine residues with phenylglyoxal, which eliminates charge in the cationic residues, rapidly reduced the activity (Fig. 2. 10). A concentration of 2 mM phenylglyoxal reduced the enzyme activity by 47% in 5 min, indicating that Arg was indeed very important for catalytic activity. The reduction in enzyme activity was protected upto 80% by adding 50 mM PenV.

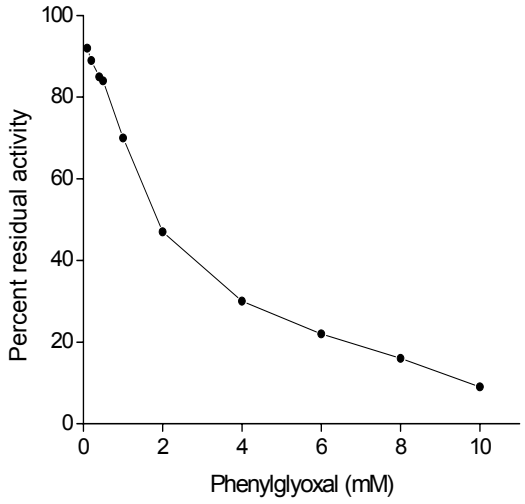

Fig. 2. 10: PVA activity as a function of phenylglyoxal concentration

The CD spectra of the modified enzyme did not show any change in secondary structure from the untreated active enzyme (Fig. 2. 11). This showed that the reduction in activity is not due to disruption in secondary structure but due to modification of the active site aminoacid residue. Protection offered by the substrate against modification indicated that those residues might be involved in substrate binding or activity.

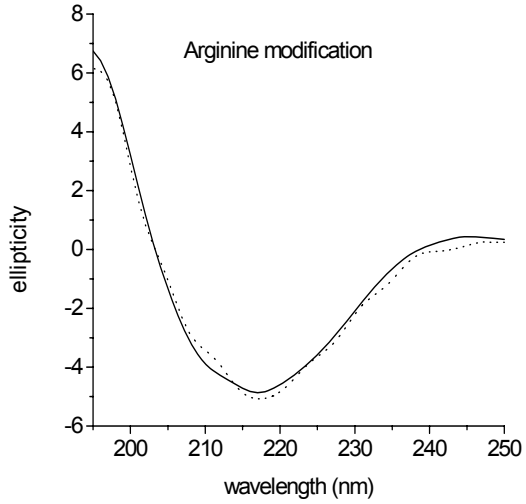

Fig. 2. 11: CD spectra of PVA. —— native enzyme ------- enzyme modified with phenylglyoxal.

In conclusion, YxeI was found to posess PVA activity. Molecular weight and subunit composition was found to be similar to the closely related PVA from *B. sphaericus* (*Bsp*PVA) which also shares 40% sequence homology. However, it has comparatively lesser affinity for PenV. Chemical modification and site-directed mutagenesis experiments of PVA from *Bacillus subtilis (Bsu*PVA) confirm cysteine1 as the nucleophilic residue pointing to the fact that this enzyme belongs to the Ntn hydrolase family. These observations are further confirmed from the crystal structure, described in the next chapter.

CHAPTER III

CRYSTALLOGRAPHIC STUDIES ON YXEI FROM *B. SUBTILIS* CHARACTERISED AS A PVA

Summary

The single crystal X-ray structure of penicillin V acylase from *Bacillus subtilis* has been determined at 2.5 Å resolution. The protein was crystallized using the hanging drop vapour diffusion method at a concentration of 10 mg ml^{-1}. The precipitant solution contained 4M sodium formate in 100 mM Tris-HCl buffer pH 8.2. Diffraction data were collected using Rigaku copper rotating anode X-ray generator on a R-AXIS IV^{++} Image Plate system under cryo conditions up to a resolution of 2.5 Å. Data processing was done using *Denzo* and *Scalepack*. The crystals belonged to the orthorhombic space group $C222_1$ having unit cell dimensions *a*= 111.0, *b*= 308.0 and *c*= 56.0 Å. It forms a symmetric homotetramer, in agreement with gel filtration studies. The Matthews number estimated, assuming one dimer per asymmetric unit was 3.23 Da $Å^{-3}$ and corresponded to 62% solvent content. The structure has been solved by molecular replacement method using *Bacillus sphaericus* PVA (PDB code 3PVA) as the search model. The final R factor is 16. The structure comprises a typical $\alpha\beta\beta\alpha$ Ntn fold.

Introduction

X-ray crystallography is one of the most powerful methods to elucidate atomic level three dimensional structures of proteins. This has practical implications for some industrially important enzymes like penicillin acylase. Site-directed mutagenesis experiments can be more carefully planned for altering specific desired traits once the structure is known and structure-function relationship established. In PVA, such

experiments can be carried out, particularly, to increase the acylase efficiency in the synthesis of semi-synthetic penicillins, and introduce specificity for cephalosporins, one of the most promising antibiotic class.

Ntn (N- terminal nucleophile) hydrolases are a superfamily of proteins that are functionally varied but share a common $\alpha\beta\beta\alpha$ fold, called the Ntn-fold. Though this group shares remarkable structural similarity, the primary sequences of these proteins are devoid of any recognizable sequence similarity (Brannigan *et al.,* 1995). Most of the family members could be identified as Ntn hydrolases only after their structures were solved. Known members include l-aminopeptidase D-ala-esterase/amidase (Bompard-Gilles *et al.,* 2000. PDB accession number 1B65), penicillin G acylase (Duggleby *et al.,* 1995), proteasome (Groll *et al.,* 2000, 1GOU), putative plant-type asparaginase (Michalska *et al.,* 2006, 1K2X)), conserved protein MTH1020 from *Methanobacterium thermoautotrophicum* (Saridakis, *et al.,* 2002, 1KUU), conjugated bile acid hydrolase (Rossocha *et al.,* 2005, 2BJF), recently1–3: glutamine PRPP amidotransferase and PVA (Suresh *et al.,* 1999).

Since this family of proteins lack obvious sequence similarity, evolutionary or structural relatedness cannot be established until the structure is solved. For example, the sequence similarity between penicillin acylase and proteasome is as low as 8% and that between the PVAs from *B. sphaericus* and *B. subtilis* is 40%, notwithstanding remarkably similar structure and mechanism. In this group, the active amino terminal nucleophile has been found to be differing- serine (PGA), threonine (proteasomes) or cysteine (PVA /CBH). PVA belongs to the choloylglycine hydrolase family which comprises CBH and PVA.

The crystal structure of a penicillin V acylase was first solved from *B. sphaericus* (PDB code 3PVA) (Suresh *et al.,* 1999). It was found to belong to the then newly

classified superfamily of proteins called the Ntn hydrolases which on post-translational autocatalytic cleavage exposes the N-terminal amino group of the nucleophile residue and this free terminal amino group in turn acts as the base in catalysis. The sequence of the hypothetical protein YxeI from *B subtilis* was found to be 40% similar to *Bsp*PVA. Biochemical studies proved penicillin acylase activity for the protein. PVA exhibits maximum sequence similarity with other PVAs as well as with CBHs - the enzymes that catalyse the hydrolysis of bonds conjugating bile acids to glycine or taurine. This chapter reports the crystallization and X-ray diffraction analysis of a newly characterized PVA from *B. subtilis*. The structure has been solved using Molecular Replacement (MR) method inputting *Bsp*PVA as the model.

3.2 Materials and methods

Structure can be put to use for applications like drug discovery or for basic research. Proteins are fine targets for drugs since they are functional molecules, which allow functions to be fine-tuned without causing any heritable change in the cell. Knowing the structure provides invaluable information for rational drug design. On a fundamental level, structure–function relationships throw light on incompletely understood cellular mechanisms. Two widely used methods of determining protein structure are Nuclear Magnetic Resonance (NMR) and X-ray crystallography and to a lesser extent cryo electron microscopy and theoretical modelling. Though NMR has the advantage of studying proteins in their soluble state and does not have the disadvantage of requirement of crystals, which is a major bottle-neck with X-ray crystallography, it cannot be used for molecules bigger than 30 kDa. In such cases X-ray diffraction is the method of choice. Apart from the requirement of protein in crystalline form, another drawback with this method as far as macromolecular crystallography is concerned, is the large solvent content of protein crystals as compared to small molecule counterparts. Therefore, protein crystals are fragile and are labile to dehydration. Proteins, membrane and other hydrophobic proteins in

particular, also have solubility problems, whereas nucleation and crystal growth require high degree of supersaturation, which depends on equilibrium solubility of the protein. Different variables affecting the solubility of the protein can be used to manipulate supersaturation in the system, thereby, influencing the rates of nucleation and growth. A variety of chemicals can be used as precipitants. The biological macromolecular crystallization database http://wwwbmcd.nist.gov:8080/bmcd/bmcd.html provides an exhaustive list of crystallisation conditions for different macromolecules.

X-ray crystallography requires a source for producing X-rays, a single phi-axis goniostat, and an area detector for measuring the location and intensity of diffraction. In home sources, a collimated X-ray beam is produced using a rotating anode X-ray generator or a sealed tube. The metal that the anode is made of determines the wavelength of resulting X-rays. In rotating anode generators, it is usually copper with a wavelength of 1.542 Å. The heat produced in the anode is carried away by chilled water supply. When X-rays impinge atoms on a regular crystal lattice, they produce an interference pattern. Nowadays, the reflections data are recorded as simple digital images in a desktop computer. In synchrotrons, high intensity X-rays are produced by the particle accelerators and the reflections are recorded on a charge coupled device (CCD) detectors. The resolution is often better than home sources and data collection time is much lesser. They are particularly useful with very large molecules or small crystals (Drenth, 1994). The electron density of the molecule is calculated by inverse transform of phased reflection data.

3.2.1 Crystallization

Protein crystallisation was used first as a method of purification which led to the establishment of enzymes as proteins (though non-protein enzymes were discovered later). Though protein crystallisation is presently mainly associated with

crystallography, the phenomenon also occurs in other contexts such as in purification of protein and diseases like madcow. For crystallographic studies, a single, high-quality crystal is needed. Protein diffraction data need to be collected from a single crystal to avoid problems from scaling multiple data sets which leads to error in final structure. This means that a protein crystal should be large enough and diffract till the required amount of data is collected. Sometimes crystals grow from multinucleation sites, or there can be twinning, some crystals do not diffract or diffract poorly for reasons still unclear. The fact that crystal surfaces are flat and uniform show underlying order and regularity in arrangement of individual molecules that constitute the crystal. Such order is required for XRD studies. Crystals are regular repeating array of molecules in three- dimensional lattices.

Protein crystallization is largely a trial and error process. Factors thought to influence crystallization include pH, temperature, ionic strength of salts present, presence of substrates/ analogs (for enzymes), impurities, pressure, gravity, mixing, and above all the precipitating agent. The thermodynamic variables of temperature, pressure, and composition are typically used to alter the solubility of proteins. Temperature directly affects protein solubility. Generally proteins are more soluble at higher temperatures. This is reversed in the presence of high salt concentrations. Protein solubility will change dramatically as pH is altered by even 0.5 pH units; however, some systems are sensitive to pH changes as small as 0.1 pH units. Many proteins are not stable near their isoelectric point and require crystallization at pH values far from the pI. When salts are used as precipitants, crystallisation can be achieved by salting in and salting out phenomena.

Protein crystallization can be carried out using a number of methods: vapour diffusion, liquid-liquid diffusion, dialysis, or microbatch. In microbatch, small droplets of protein and precipitant are dispensed under oil and allowed to equilibrate. Vapour

diffusion is the most common method used. It can be performed with hanging or sitting drop (Ducruix & Giege, 1992; McPherson, 1982). Small droplets of protein and precipitant are mixed and allowed to equilibrate with the precipitant well solution in an air-tight chamber. Slowly, due to difference in concentration, water vaporizes from the drop, and the precipitant concentration increases till a level optimal for crystallization is reached depending on well solution (Rhodes, 1993; McRee, 1993).

Drops were set up on coverslips siliconised with Sigmacote (Sigma) using 1 µl each of protein (PVA) and precipitant solution and allowed to equilibrate in multiwell trays rendered air-tight using silicone grease. Concentration of protein was estimated using the method of Lowry *et al* (1951). A number of conditions were tried for crystallisation - ammonium sulphate and polyethylene glycols of different molecular weights, 2-methylpentan-2,4-diol and various other salts by varying parameters of precipitant concentration, pH, temperature, concentration of protein etc.

3.2.2 Data collection

Growing diffraction quality crystals is considered to be the most crucial stage in the study of X-ray structure of macromolecules. However, there are several bottlenecks down the line. Data collection requires an X-ray source. At present, data are collected in-house using home sources. A copper anode generator produces X-rays with a wavelength of 1.5418 Å. Goniometer mounting can be done in thin walled glass capillaries for room temperature data collection and in cryo loops for cryogenic collection. The crystal is properly aligned in the path of the beam by viewing through a CCD camera. For data collection at low temperatures, a jet of liquid nitrogen is sprayed on the crystal from close quarters. Sensitive detectors are helpful with proteins that do not give adequately bright intensities. The crystal to detector distance has to be carefully adjusted in order not to miss any spots, without compromising resolution and appropriate separation of spots. X-rays are considered

to be reflected against lattice planes and the lattice plane distance *d* and the diffraction angle θ are related by Bragg's law $2d \sin\theta = n\lambda$.

Alternatively particle accelerators like synchrotrons are used as X-ray source. Synchrotrons are very powerful sources. They were first used for particle physics, but custom-made ones for biological macromolecules are being built such as the third generation Spring-8 in Japan and diamond in UK. Today, synchrotron radiation is used in nearly half of the new structures that are solved. The benefits of synchrotron radiation include substantial increase in resolution over those available with laboratory sources and the ability to study crystals that are too small or have a unit cell too large to be studied using home X-ray sources. (Structural Biology and Synchrotron Radiation: Evaluation of Resources and Needs - Report of BioSync- The Structural Biology Synchrotron Users Organization, 1997). Though synchrotron sources with high intensity radiation were used, crystals were often damaged due to the intensity of radiation. Help arrived in the form of cryogenics. Data collection done at temperatures as low as –160 °C minimise radiation damage to crystal. Crystals grown normally are soaked momentarily in a cryoprotectant solution before being mounted on the goniometer using a loop. The data is then collected at cryogenic temperatures. Cryoprotectants help in preventing crystalline ice formation which would otherwise damage the crystal when frozen. Different cryoprotectants used are: salts at high concentration, organic solvents such as glycerol. A variety of cryoprotectants are also commercially available.

In-house X-ray diffraction data from the crystal were collected using Rigaku Cu rotating anode generator at National Chemical Laboratory, Pune, on a Raxis IV^{++} Image plate detector to a resolution of 2.5 Å, under cryo conditions. The beam was focussed using osmic mirrors. The detector is a X-ray storage phosphor image plate

which can be used repeatedly. 350 frames of data were collected with an oscillation angle of 0.5°.

3.2.3 Data processing

Different frames of data are read, peaks searched and auto-indexed. The program *DENZO* of HKL package was used for data indexing, integrating and processing. Scaling and merging was done using *SCALEPACK* (Otwinowski & Minor, 1997).The HKL suite is a package of programs intended for the analysis of X-ray diffraction data collected from single crystals. It consists of three parts: *XdisplayF* for visualization of the diffraction pattern, *Denzo* for data reduction and integration, and *Scalepack* for merging and scaling of the intensities obtained by *Denzo* or other programs.

3.2.4 Solvent content

Mathews number, V_M (Matthews, 1968), is an estimation of number of molecules per unit cell and is calculated by using the formula

V_M = unit cell volume / ($M \times Z$)

Where Z is the number of molecules in the unit cell and M is molecular weight of the protein in daltons. For proteins, V_M is usually between 1.7 and 3.5 $Å^3$ Da^{-1}, mostly ~2.15 $Å^3$ Da^{-1}. The solvent content of the crystal is equal to (1 – (1.23/ V_M)).

3.2.5 Structure solution

The phase problem in crystallography is determining the phase angle of each reflection. There are basically 3 techniques used to solve phase problem- Isomorphous replacement (heavy atom method), Multiwavelength anomalous dispersion and Molecular replacement. In isomorphous replacement method a heavy atom derivative of the crystal, which should be isomorphous to the native crystals is used to calculate phases. In multiple isomorphous replacement, more than one

heavy atom derivative is used. In multiwavelength anomalous dispersion technique, data are collected on the same crystal using different wavelengths. A protein containing a natural heavy atom or proteins with selenomethionine instead of methionine can be used.

Molecular replacement technique is the simplest of all: It makes use of available structure of a protein (phasing model) that has good sequence homology to the one being studied. This makes use of the fact that primary sequences of proteins determine their three-dimensional structure and therefore, proteins possessing homologous sequences could be expected to share structural homology as well. Several programs employ this technique including *MOLREP* and *AMoRe* (Automated MOlecular REplacement) (Navaza, 1991), which was used in the present case. *Bsp*PVA, which has 40% sequence similarity was used as the search model.

3.2.6 Structure refinement

Structure refinements are carried out to minimise errors in phase estimates. Crystallographic R factor provides an index of the correctness of the structure and is calculated using the formula

$$R\text{-}factor = \frac{\sum_{(h,k,l)} \| F_{obs}(h,k,l) | - | F_{calc}(h,k,l) \|}{\sum_{(h,k,l)} | F_{obs}(h,k,l) |}$$

As a result of refinement, the difference between the calculated and observed structure factors are minimised. The structure was refined using the maximum likelihood program *REFMAC* (Murshudov *et al.,* 1997), implemented in the CCP4 suite. Restrained refinement involves restraints on bond lengths, angles, torsion angles and van der Waals contact. The noncrystallographic symmetry is made use of

to refine the molecules in the asymmetric unit. 5% reflections are set aside for cross-validation. Visualisation of density maps and graphics were done using *QUANTA* (Accelrys).

3.2.7 Analysis of structure

The Ramachandran plot (Ramachandran *et al*., 1963, Ramachandran and Sasishekaran, 1968) gives the stereochemistry of the folding of main chain. The dihedral angles Φ and Ψ assume values that home them in the allowed regions of the plot. Any deviation from the allowed regions needs careful analysis. *PROCHECK* (Laskowski, 1993) implemented in the CCP4 suite was used to check the geometry of the model. Crystal contacts were calculated using *CONTACT* and the buried surface area by *AREAIMOL* implemented in CCP4. Graphical representations were constructed using Pymol.

3.3 Results and Discussion

3.3.1. Crystallization

The recombinant protein was purified using procedures explained in Chapter 2. The initial crystallization trials using conventional precipitants such as different polyethylene glycols, ammonium sulphate and 2-methyl pentan-2,4-diol did not yield good quality crystals. On further screening for favourable conditions, the protein eventually crystallized using sodium formate as precipitant. Crystals were grown by vapour diffusion at 291 K. Concentration of the protein sample was 10 mg ml^{-1}. The reservoir solution contained 4 M sodium formate solution in 100 mM Tris-HCl buffer pH 8.6. The protein was dialysed against 100 mM NaCl and hanging drops containing 1 µl of protein and 1 µl of well solution were set up. The crystals grew in a week's time. A single crystal measuring 0.54 mm in the longest dimension was used to collect data. Crystals with different morphology also grew at slightly different pHs and buffers, but were of poor quality (Rathinaswamy *et al.,* 2005). The crystals belonged to the space group $C222_1$. Crystallization pH is in the active range of the enzyme.

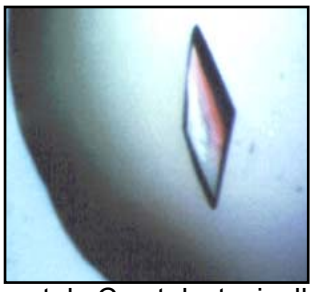

Fig. 3.1: A *Bsu*PVA crystal. Crystals typically measured ~0.5 mm in the longest dimension.

3.3.2. Data collection and data quality

Diffraction data were collected in-house at 113 K. The cryoprotectant used was 30% glycerol in crystal growth buffer. A single crystal, scooped using a cryoloop was momentarily soaked in cryoprotectant solution and immediately flash frozen in a

stream of liquid nitrogen and mounted on the goniometer head. The diffraction data up to a Bragg spacing of 2.5 Å were recorded on a R-AXIS IV^{++} Image Plate system, mounted on Rigaku rotating anode X-ray generator operated at 50 kV and 100 mA. The crystal was rotated through 0° to 180° in oscillations of 0.5°, and 5 min exposure per frame. The crystal to detector distance was kept at 260 mm. The Cu $K\alpha$ radiation was monochromated and focussed using osmic mirrors and the data collection control and initial Indexing were done using program *CRYSTALCLEAR* (Rigaku).

The protein crystallized in orthorhombic space group $C222_1$ with cell dimensions *a*= 111.0, *b*= 308.0 and *c*= 56.0 Å and unit cell volume 1913716 Å^3. The completeness of the data was 98.8% (97.8% for the last shell) and the R merge 0.084 (0.196) with a total of 114421 reflections of which 33573 were unique. The crystal had a mosaicity of 0.7. Diffraction pattern is shown in Fig.1b. Data were processed for the 354 images collected. The signal to noise ratio was 11.11 (4.14). The *HKL* program package *DENZO* and *SCALEPACK* (Otwinowski & Minor, 1997) was used for integrating, processing, scaling and merging the reflections. Data collection and processing statistics are tabulated in Table 3.1.

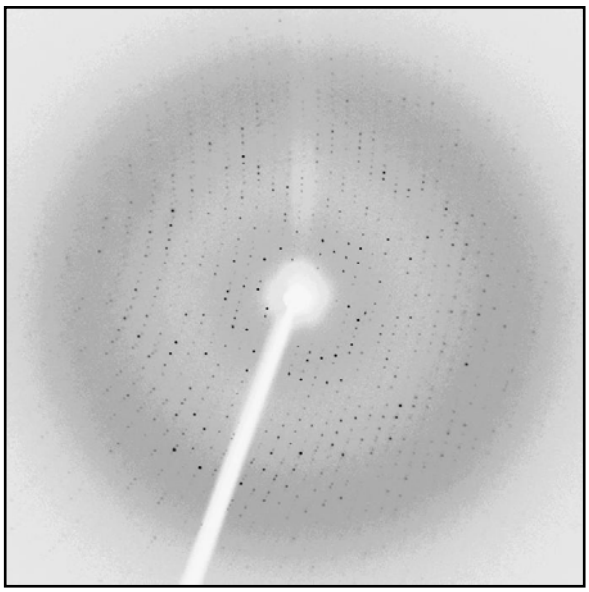

Fig. 3.2: A typical diffraction pattern of the crystal

Table 3.1 Summary of crystal properties and diffraction data statistics

Experimental Conditions	
Source	Rigaku rotating anode generator
Wavelength (Å)	1.5418
Detector	R-AXIS IV $^{++}$
Temperature (K)	113
Crystal to detector distance (mm)	250
Crystallization conditions	4*M* sodium formate, 0.1 *M* Tris buffer pH 8.6
Crystal Parameters	
Space group	$C222_1$
Unit cell parameters (Å)	
a	110.96
b	307.95
c	56.00
Data Processing	
Resolution (Å)	50 - 2.5 (last shell)
Data completeness (%)	98.8 (97.8)
Number of measured reflections	114421
Number of unique reflections	33573
Molecules per asymmetric unit	2
Matthews number	3.23
Merging R# factor	0.08 (0.20)
I / sigma	11.11 (4.14)
Mosaicity (°)	0.7

(Values in parentheses are for the highest resolution shell.)

$R_{merge} = \Sigma_{hkl} \Sigma_i |I_i(hkl) - \langle I(hkl) \rangle| / \Sigma_{hkl} \Sigma_i I_i(hkl)$

3.3.3. Solvent content of crystals

Matthews number (V_M) (Matthews, 1968) was calculated assuming a dimer in the asymmetric unit. The estimated V_M was 3.23 $Å^3$ Da^{-1}, corresponding to 62% solvent content. The crystal packing parameter is within the range commonly observed for globular proteins. The enzyme in solution was found to be a tetramer with a molecular weight of approximately 148,000 as estimated by gel fitration chromatography. Thus it could be expected that a crystallographic 2-fold related dimers of the tetramer existed.

3.3.4. Structure determination by Molecular replacement

The *AMoRe* program package (Navaza, 1994) implemented in the CCP4 suite (Collaborative Computational Project, Number 4, 1994) was used to solve the structures by MR method. A dimer of *Bsp*PVA was used as a model, with appropriate changes in the sequence. A CBH from *Clostridium perfringens*, whose crystal structure is known, also had good similarity with the protein. However, it was available only later and *Bsp*PVA had slightly higher similarity. The CLUSTAL alignment (Thompson *et al.,* 1994) of the sequences of *3*PVA and 2BJF with *Bsp*PVA is shown in Fig. 2. Rotation and translation functions were calculated followed by a rigid body fit. Details about the molecular replacement solutions are given in Table 3.2. As expected from Matthews number, the asymmetric unit turned out to be a dimer and the two dimers of the stable tetramer were indeed related by a crystallographic 2-fold axis. For diffraction data between 50 and 2.5 Å, the model gave clear solutions with a correlation coefficient of 46.9 and an R factor of 48.8%. The electron-density map was of sufficient quality to trace the polypeptide chains, excluding residues 199-208.

Table 3.2a Details of the molecular replacement solutions. Resolution used for rotation function and initial translation is 10.0 – 3.0 Å

	Eulerian angles			Corre-lation factor	Translations (fractional)				
Soln.	α	β	γ	Cc	Tx	Ty	Tz	Cc	R_{factor}
1	18.56	35.25	13.22	17.0	0.3602	0.2993	0.3486	34.0	55.8
2	51.00	12.07	336.50	13.8	0.3529	0.0599	0.2050	31.3	56.8
3	21.58	65.16	185.59	13.2	0.0656	0.4767	0.3324	24.2	59.9
4	149.33	21.02	234.00	11.8					

Table 3.2b

Translation function fixing one solution and searching for the second (10 - 3 Å)

Soln.	Tx	Ty	Tz	Cc	R_{factor}
1	0.3602	0.2993	0.3486	Fixed	
2	0.8530	0.0600	0.7050	45.1	51.8

Table 3.2c

Rigid body fit (10 - 3 Å)

Soln.	α	β	γ	Tx	Ty	Tz	Cc	R_{factor}
1	18.68	36.17	13.28	0.3603	0.2993	0.3468		
2	57.73	12.53	331.29	0.8529	0.0601	0.7062	62.2	46.4

Fig. 3.3 Alignment of the aminoacid sequences of penicillin V acylases from *B. subtilis* and *B. sphaericus* using the program CLUSTALW-1.82 (Thompson *et al.,* 1994) "*" denotes that the residues in that column are identical, ":" conserved substitutions, "." semi-conserved substitutions.

```
3PVA   CSSLSIRTTDDKSLFARTMDFTMEPDSKVIIVPRNYGIRLLEKENVVINNSYAFVGMGST 60
BsuPVA CTSLTLETADRKHVLARTMDFAFQLGTEVILYPRRYS-WNSEADGRAHQTQYAFIGMGRK 59
2BJF   CTGLALETKDGLHLFGRNMDIEYSFNQSIIFIPRNFK-CVNKSNKKELTTKYAVLGMGTI 59
       *:.*::.* *   ::.*.**:  . . .:*: **.:     : :     ..**.:***

3PVA   DITSPVLYDGVNEKGLMGAMLYYATFATYADEPKKGTTGINPVYVISQVLGNCVTVDDVI 120
BsuPVA LGNI-LFADGINESGLSCAALYFPGYAEYEKTIRADTVHIVPHEFVTWVLSVCQSLEDVK 118
2BJF   FDDYPTFADGMNEKGLGCAGLNFPVYVSYSKEDIEGKTNIPVYNFLLWVLANFSSVEEVK 119
           . : **:**.**  * * :. :. * .    ... *    .:  **.   ::::*

3PVA   EKLTSYTLLNEANIILGFAPPLHYTFTDASGESIVIEPDKTGITIHRKTIGVMTNSPGYE 180
BsuPVA EKIRSLTIVEKKLDLLDTVLPLHWILSDRTGRNLTIEPRADGLKVYDNQPGVMTNSPDFI 178
2BJF   EALKNANIVDIPISENIPNTTLHWMISDITGKSIVVEQTKEKLNVFDNNIGVLTNSPTFD 179
       * : . .:::          .**: ::* :*..:.:*     :.:. :  **:**** :

3PVA   WHQTNLRAYIGVTPNPPQDIMMGDLDLTPFGQGAGGLGLPGDFTPSARFLRVAYWKKYTE 240
BsuPVA WHVTNLQQYTGIRPKQLE----------AFGQGLGTVGLPGDYTPPSRFVRAVYLKEHLE 228
2BJF   WHVANLNQYVGLRYNQVPEFKLGDQSLTALGQGTGLVGLPGDFTPASRFIRVAFLRDAMI 239
       ** :**. * *:  :           ..:*** * :*****:**.:**:*..: :.

3PVA   KAKNETEGVTNLFHILSSVNIPKGVVLTNEGKTDYTIYTSAMCAQSKNYYFKLYDNSRIS 300
BsuPVA PAADETKGVTAAFQILANMTIPKGAVITEEDEIHYTQYTSVMCNETGNYYFHHYDNRQIQ 288
2BJF   KNDKDSIDLIEFFHILNNVAMVRGSTRTVEEKSDLTQYTSCMCLEKGIYYYNTYENNQIN 299
          .:: .:   *:** .: : :* . * * : . * *** ** :.  **:: *:* :*.

3PVA   AVSLMAENLNSQDLITFEWDRKQDIKQLNQVN 332
BsuPVA KVNLFHEDLDCLEPKVFSAKAEESIHELN--- 317
2BJF   AIDMNKENLDGNEIKTYKYNKTLSINHVN--- 328
          :.:  *:*:  :  .:. .   .*:.:* :
```

3.3.5. Structure refinement

The three-dimensional structure of PVA obtained using molecular replacement method was refined at 2.5 Å resolution (50 - 2.5 Å). The initial atomic coordinates for the molecules were obtained from that of *Bsp*PVA model. Refinement was carried out using the program *REFMAC*. After each refinement cycle, the model was visually inspected using the program *QUANTA* using ($2F_o - F_c$) and ($F_o - F_c$) difference maps. The two monomers in the asymmetric unit were labelled A and B; they were symmetrically related and B could be generated from A through non-crystallographic symmetry. Atomic coordinate superpositioning was carried out using *LSQKAB*. The non-crystallographic symmetry was made use of to restrain the molecules A and B

together. 5% reflections were set aside for R free. All data from 50 Å to 2.5 Å were used applying a bulk-solvent correction.

After the electron density maps were calculated, side chain conformations were progressively fitted into the densities and refined. The structure was subjected to several rounds of computational refinement and map calculation with CCP4 and manual model inspection and modification with QUANTA. This process was repeated till R_{free} and R_{cryst} converged. Hydrogen atoms were used if present in file. The program PROCHECK was run to check the geometry of the model. The free R factor calculated from reflections set aside at the outset was used to monitor the progress of refinement in the correct direction. In the regions where the maps were not well defined initially, and the residue not fitting the density even after a few cycles, the residues were deleted, fresh maps generated and the residues rebuilt progressively into the densities.

The interactive X-SOLVATE module of QUANTA was used to add water molecules. When the R_{cryst} value reached 25%, water molecules were placed into 3σ peaks in (F_o - F_c) maps using QUANTA when they were within a suitable hydrogen-bonding distance of the existing model (2.5 – 3.5 Å). After refinement, water molecules whose positions were not supported by the electron density at 1σ contouring in a weighted ($2F_o$ - F_c) map were deleted. Waters which tend to reach the limiting value of 100 set for B-factor were also deleted from the coordinate file. Non-crystallographic symmetry constraints were maintained throughout the refinement.

3.3.6. The model

In all 31,859 reflections were used. Mean B factor was 44. The final model, refined to 2.5 Å, incorporates 5504 non-hydrogen atoms. The total number of water is 215. A

stretch of 10 aminoacid residues could not be fitted due to insufficient electron density, and are absent in the final model. These residues form part of a loop and their B-factor was very large to begin with. The final R factor of the model is 15.6% (free R factor = 21.2%). The coordinates of the final model and the merged structure factors have been deposited with the Protein Data Bank (Bernstein *et al.,* 1977).

Analysis of the geometry of the model using the program PROCHECK (Laskowski *et al.,* 1993) were favourable with 91.4% of the 327 residues in the most favoured regions of the Ramachandran (phi-psi) plot (Ramachandran *et al*., 1963, Ramachandran and Sasishekaran*,* 1968). 8.1% residues are located in the additionally allowed regions and 0.5% in generously allowed regions. There are no residues in the disallowed regions of the plot. The overall G-factor is –0.32 indicating good sterochemistry for the model.

Table 3.3

Refinement statistics

No. of non-H protein atoms	5504
No. of solvent atoms	215
Resolution range	50 - 2.5
σ cutoff	None
R (%)	15.6
Rfree (%)	21.2
R.m.s. deviation from ideal values	
Bond lengths (Å)	0.032
Bond angles (°)	2.378
Ramachandran plot statistics	
Most favoured (%)	91.4
Additionally allowed (%)	8.1
Generously allowed (%)	0.5
Disallowed region (%)	0.0
R.m.s.d. between monomers A and B (Å)	0.123

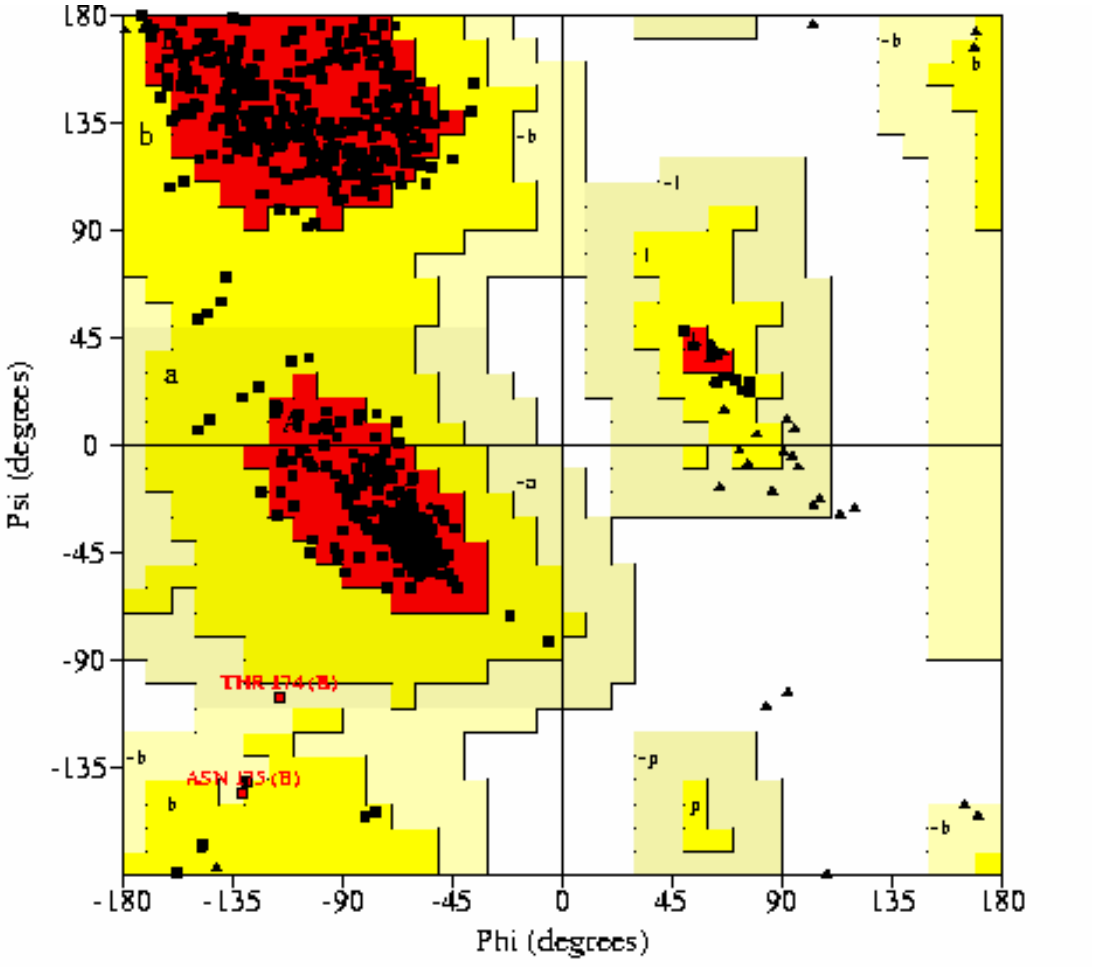

Fig. 3.4 Ramachandran plot. Triangles and squares represent glycine and non-glycine residues respectively.

3.3.7. Primary structure

The functional unit of *Bsu*PVA is a homotetramer, as observed in gel filtration studies, with 327 residues per monomer. The N-terminal is cysteine, as expected. The crystallization conditions did not include any reducing agents; therefore Cys1 is present in the oxidized form of cysteic acid. The sequence shows similarity to PVAs and CBHs. This is described in detail in Chapter 8. The sequence is different from the one reported before (Chapter 2) and the changes are retained in the structure.

Alignment with choloylglycine hydrolases whose structures are known shows that the oxyanion hole members are invariant.

3.3.8. Secondary structure

Each monomer contains two antiparallel β-sheets sandwiched between two sets of α-helices on either sides in the form αββα organization, the classical Ntn fold.

3.3.9. Tertiary structure

Two monomers related by a two-fold symmetry form a dimeric asymmetric unit. The monomer has a single globular domain with approximate dimensions of 47 x 44 x 47 Å. A loop consisting of residues 320 - 329 stretches out 19 Å, and another loop consisting of residues 210-214 stretches > 13 Å into the other dimer. The C-terminus 323-329 and the loop region extend into another subunit. The B values are ~ 35 $Å^2$. The core is composed of two sandwiched anti-parallel β-sheets that contain the N-terminus and the oxyanion hole residues and are flanked by α-helices on either sides. The N-terminal β-sheet is made up of 6 anti-parallel β-strands and the other β-sheet II comprises 7 anti-parallel β-strands. The β-sheets are flat and the angle between the two sheets is 30º. Leu207 and Gly218, highly conserved in the loop in 2BJF (Rossocha *et al.,* 2005) are found interacting with other subunits at surface in this protein. The intervening loops that connect the secondary structural elements are short and ordered and principally comprise residues with flexible side chains. There are a total of 10 loops. The β-sheet constituents are predominantly hydrophobic in nature. The aminoacid residues whose ϕ and φ angles were found in generously allowed regions, are in loops or surface – numbers 197, 177, 175, 44, 96, 11, 271, except 174.

3.3.10 The fold and the active site

*Bsu*PVA contains the classical 4-layered Ntn hydrolase fold as expected from sequence similarity and conserved residues. This fold was first observed in PGAs. Since then the fold has been found in many other proteins leading to the classification of a new superfamily of proteins- the Ntn hydrolases (Brannigan *et al.,* 1995). Whereas in PGA, two different subunits form part of the Ntn fold, in PVA, it is from a single subunit. This active site also includes Cys1, the N-terminal nucleophile. It is highly conserved among related sequences and CBH. The geometry is identical in all monomers and is similar to CBH and *Bsp*PVA. The conserved reisdues forming the oxyanion hole are found in relatively similar positions as in PVA /CBH. From sequence similarity with homologous Ntn hydrolases, the oxyanion hole residues can be assumed to be Cys1, Tyr 81 and Asn175.

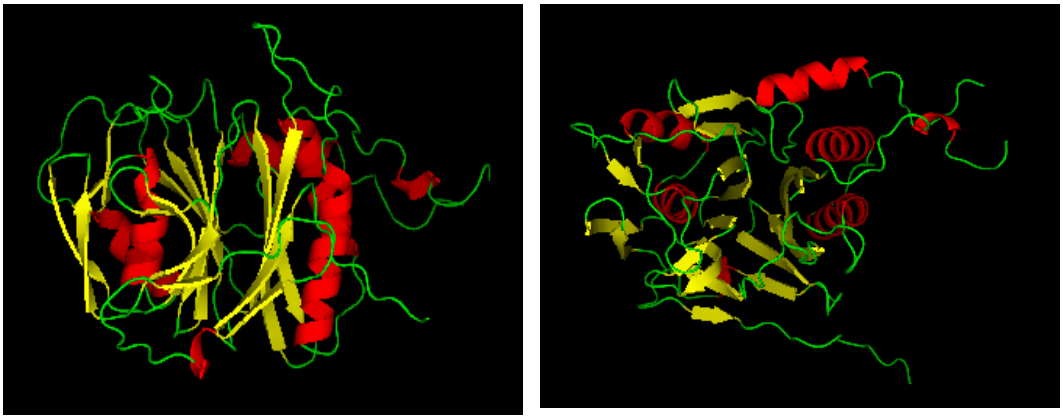

Fig. 3.5 Monomer view of Ntn fold

3.3.11. Quaternary structure

Overall structure shows that *Bsu*PVA, like *Bsp*PVA, forms a symmetric homotetramer. The overall dimensions of the tetramer are 98 Å × 95 Å × 56 Å. The asymmetric unit contains two identical subunits A and B that are related by a non-

crystallographic symmetry. The functional molecule appears to be a dimer of this dimer with a two-fold symmetry. The subunits C and D were generated by a symmetry operation on A and B respectively using PDBSET implemented in CCP4 suite. Structural superpositioning of chains A and B shows that the RMSD for the C_α of aminoacids is 0.122. The surface area buried on oligomerization was calculated from the difference in accessible surface areas in the subunit and the oligomer using AREAIMOL (CCP4). The total solvent accessible surface area and the surface area buried upon association of the subunits were computed to be 45,532 $Å^2$ and 13,692 $Å^2$ respectively. About 26% of the accessible surface area is buried upon subunit association. The loops are slightly different in arrangement from CBH. The residues 181-220 interact to form the tetramer. Each monomer has residues that interact with the other three monomers of the functional molecule. During dimer formation, the residues that are in close contact with the other subunit are Thr184, Tyr86, Gln188 and Thr224. Trp181 of both the subunits are in close contact.

3.3.12. Solvent structure

A total of 215 water molecules were found for each subunit. These waters were found within a radius of 2.5 - 3.5 Å and constitute the primary hydration shell. Secondary hydration shell is constituted by waters at a distance of 7 Å. All water molecules either had contact with themselves or with protein molecules. Invariant water molecules are the ones which have 1.8 Å between the oxygens of the constituent waters.

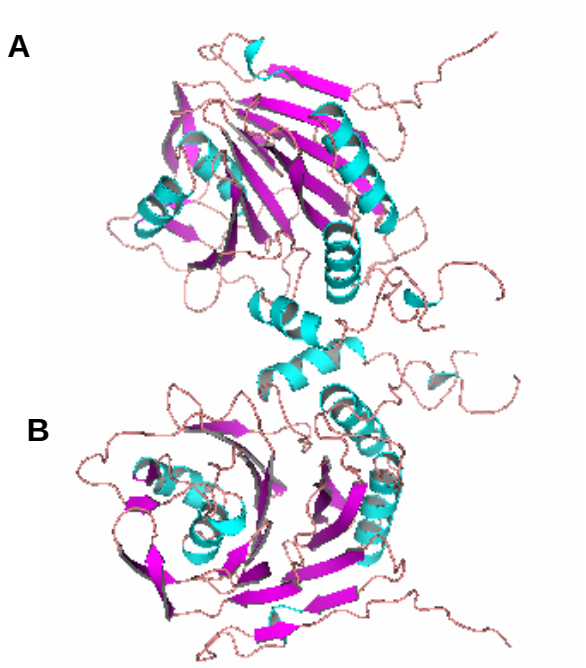

Fig. 3.6 Dimer in the asymmetric unit of *Bsu*PVA

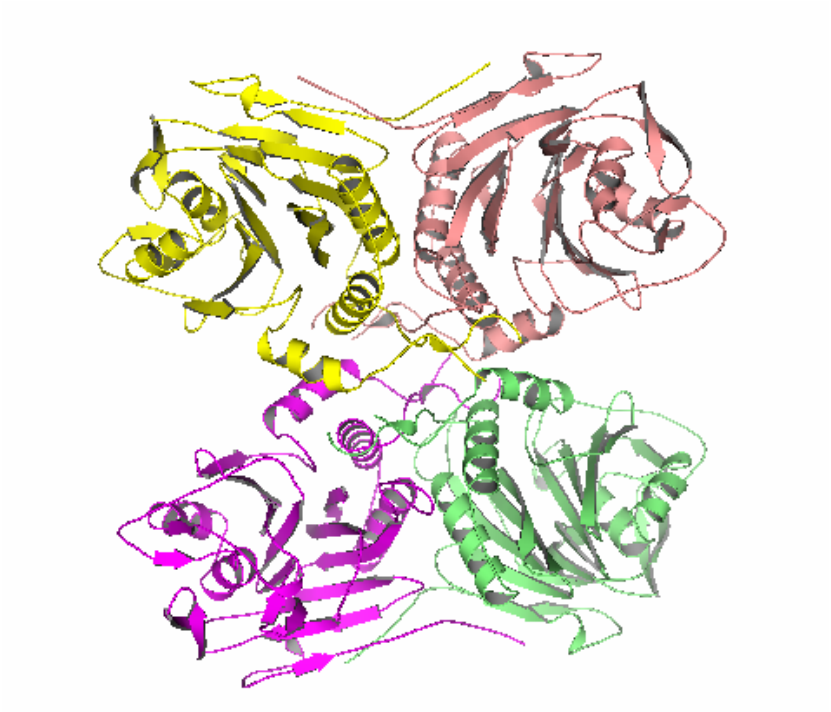

Fig. 3.7 Tetramer of *Bsu*PVA

3.3.13. Crystal packing

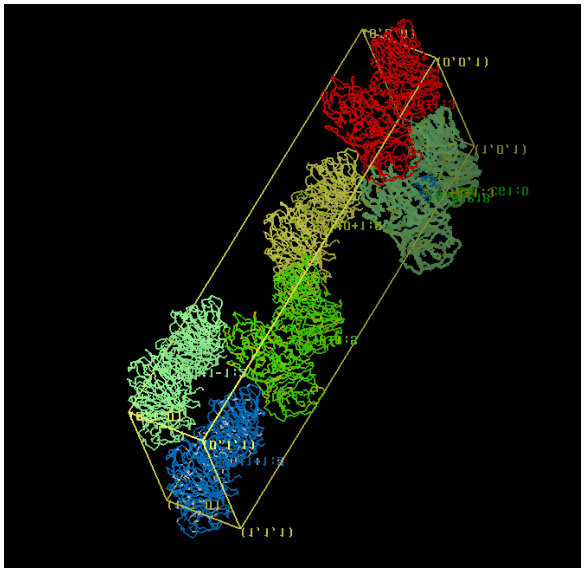

Fig. 3.8. Crystal packing diagram for PVA showing a single cell

3.3.14. Structural comparison with similar proteins in DALI database

Structural analysis using DALI algorithm (http://www.ebi.ac.uk/dali/) (Holm & Sander, 1995) returned 16 matches that were structurally homologous to *Bsu*PVA. Superposition of such proteins showed that the residues that make up the oxyanion hole are structurally well conserved and occupy similar positions in the tertiary structure. Least-square superpositions of the C_α coordinates of the monomers (restrained refinement) show remarkable similarity with CBH from *Clostridium perfringens* and *Bsp*PVA crystal structures and revealed C_α r.m.s.d values of 1.158 Å and 2.62 Å respectively. However, differences were also noted. In BJF, there was shortening of the α-helix at residue 249. The continuation of this loop which ends in another α-helix, starts earlier than the others by 242-249. The regions composed of residues 84-86 and 134 -137 are also different. Prolines found in the vicinity of loops in CBH (198) and *Bsp*PVA (209) might contribute to more order in the loops in the respective structures whereas *Bsu*PVA lacks an equivalent proline residue.

The secondary structural elements overlay closely in the conserved motif region. They are slightly deviant in the outer regions of the molecule. The corresponding region of loop 238-245 of 2BJF is slightly away from the complementary regions in 2PVA and YxeI, which overlay closely. Unlike the other two molecules, loop starts from 250 in BJF, shortening the α-helix. *Bsu*PVA further extends at C-terminal. There are six α-helices: 180I-185N, 116L-122K, 105F-112V, 245E-259M, 225P-238H and 180I-185N. There are 2 β-sheets composed of individual strands:

32 → 28
54 ← 59
72 → 69
77 ← 82
147 → 142
154 ← 159
167 → 162
303 → 300
288 ← 293
283 → 275
13 ← 21
7 → 3

other βstrands are contributed by

39 → 35
50 → 47
100 → 98
129 → 126

Table 3.4 Structural alignment statistics

PROTEIN	STR ID	Z	RMSD	Similar	total	%ID
penicillin v acylase	3pva-A	46.9	1.2	316	334	40
glutaryl 7-aminocephalosporanic acid acylase	1fm2-B	15.0	3.5	221	520	11
penicillin amidohydrolase	1ajq-B	14.7	3.3	212	557	12
proteasome	1pma-P	10.5	3.3	159	203	8
proteasome	1pma-A	9.2	3.3	156	221	10
20s proteasome	1ryp-2	9.1	4.0	159	233	6
Unknown protein	1kuu-A	9.1	3.6	163	202	12
hslv (*Escherichia coli*)	1ned-A	8.4	2.9	141	180	10
20s proteasome	1ryp-1	8.2	3.3	146	222	10
proteasome alpha-type subunit 1	1q5q-A	7.7	3.4	147	219	9
putative bacterial enzyme	1txo-A	2.9	4.3	121	230	9
phosphatase 2c human	1a6q	2.9	4.3	129	363	5
glucosamine 6-phosphate synthase domain	1gdo-A	2.7	4.2	104	238	12
glutamine amidotransferase	1ecf-B	2.4	5.7	116	500	8
6-pyruvoyl tetrahydro	1b66-A	2.2	4.0	85	138	5
aspartylglucosaminidase	1apy-B	2.2	3.9	95	141	9

STR ID: PDB code, Similar: No of residues that are similar to PVA in the sequence

Conclusion

Though very similar, CBHs have an Asn instead of Tyr conserved at position 82. It is interesting that subtle changes in specificity of aminoacids lead to different activities. Given close sequence homology, it appears possible that small crucial changes in sequence might lead to cross-reactivity between these choloylglycine members (PVA /CBH). Crystal structures of members of Ntn superfamily share an Ntn fold, including

the newly solved structure of CBH from *Clostridium perfringens*. In these structures, oxyanion residues conserved at primary level are also conserved at tertiary level. Such evidences prompted us to check YxeI for potential PVA activity. Biochemical analyses show that YxeI is a PVA. The crystal structure provides unequivocal evidence for the same.

CHAPTER – IV

FLUORIMETRIC AND KINETIC STUDIES OF *Bsu*PVA

Summary

The decrease in fluorescence intensity upon titration with the substrates NIPOAB and PenV was made use of to calculate binding constants for these substrates at different temperatures. The association constants were found to be 8.93×10^2 M^{-1} and 2.51×10^5 M^{-1} for PenV and NIPOAB, respectively at 40 °C. The ligand associations were found to be enthalpically driven with a favourable entropic contribution. The accessibility of Trp fluorophores and its local environment were investigated using acrylamide, potassium iodide (KI) and cesium chloride (CsCl). The Stern-Volmer plots of native enzyme showed downward curvature in quenching experiments with KI and upward curvatures with CsCl and acrylamide. Acrylamide was more efficient than both CsCl and KI. Complete quenching by acrylamide in native protein indicates that all the Trps lie in flexible, accessible environments. Presence of Gdn HCl increased the accessibility of the fluorophores to KI but CsCl was a poor quencher even after unfolding of protein.

4.1. Introduction

The functions of most proteins, especially those of enzymes, depend on their ability to bind various ligands. Such binding studies, based on fluorescence and CD spectroscopy, often provide information about both structure and function. The high sensitivity of fluorescence spectroscopy makes it amenable to study binding of ligands with very high affinity. The aminoacid Trp is a very sensitive fluorophore that can be used to follow changes undergone by the whole protein. Trp residues in the vicinity of active sites can be monitored to study ligand binding because a ligand may physically interact with Trp by changing its polarity or accessibility to the solvent;

alternatively, it can interact with a remote site on the protein, induce conformational changes in the protein that then alters the microenvironment of the Trp resulting either in enhancement or quenching of fluorescence or a red or blue shift in the emission spectrum. Eventhough it is not straight forward to obtain inference from these results when more than one Trp is present in the protein, or, when the protein is oligomeric, it is comparatively straightforward when applied to binding studies, since the effects can be quantified by following changes at one fixed wavelength of the emission spectrum. Accessibility of Trps in the protein to soluble quenching agents can be studied from which one can predict the average microenvironment around the Trps. This chapter describes the determination of association constants for the enzyme's substrates and determination of thermodynamic parameters for their binding at different temperatures. Tryptophan environment has been characterized using solute quenchers.

4. 2. Materials and Methods

4. 2. 1. Materials

Acrylamide was procured from Sigma (St. Louis, USA). Sodium thiosulphate and buffers were from Qualigens. Cesium chloride (CsCl) was procured from Sisco Research Laboratories. Potassium iodide (KI) and methanol were from Merck. All buffers and solutions were filtered through a 0.45 µM filter (Sartorius). All quenching solutions were prepared as 5 M stocks of the quencher. KI was dissolved in 200 µM potassium thiosulphate solution to prepare the 5 M stock. All solutions were filtered and centrifuged before use. Buffers were prepared as 1 M stocks, pH adjusted at room temperature and filtered.

4. 2. 2. Preparation of protein samples

Production and purification of the protein, enzyme assay and protein estimation were carried out as described in Chapter 2. For the fluorescence studies, protein was dialyzed against 100 mM NaCl and centrifuged (10 000*g*, 10 min). The clear supernatant was used for the studies.

4. 2. 3. Fluorescence measurements

Fluorescent chromophores such as phenylalanine, tyrosine and tryptophan present in proteins, get excited on absorption of energy. The return of the excited residue to ground state involves dissipation of excess energy by nonradiative processes like photoionization, intersystem crossing, exciplex formation, excited state proton and electron transfer etc. The resulting light emission enables us to follow conformational changes in protein using these sensitive fluorophores. Fluorescence can be studied in terms of

i) fluorescence excitation spectrum which represents fluorescence intensity as a function of the wavelength of exciting radiation

ii) fluorescence emission spectrum represents fluorescence intensity as a function of emission wavelength. The emission is due to transition from lowest vibrational level of the excited state to the ground state. Spectral characteristics of this emission is sensitive to chemical reactions or solvent perturbations that has occurred in the excited state.

iii) Quantum yield of fluorescence which is the ratio of numbers of quanta emitted to quanta absorbed (Quantum yield = quanta emitted/ quanta absorbed).

Quantum yield depends on the amount of internal and external conversion. The excited chromophore can transfer energy to other solute or solvent molecules by different mechanisms or by internal conversion when the interaction leads to modification of potential energy surfaces.

Fluorescence quenching refers to external conversion processes. The complex between chromophore and quencher can be formed in two ways leading to two types of quenching.

a) Dynamic or differential quenching must take place during excited state. The intensity of fluorescence emission is determined by the statistical chance of meeting between excited fluorescence and quencher

b) Static quenching equilibrium is established in ground state.

In static model the quencher approaches the chromophore, indole ring of Trp, by describing a path while the protein behaves as a rigid sphere whereas in dynamic quenching the buried Trps are quenched by the solute quencher whose manouvre through the solution is facilitated by dynamic state of the protein which is supposed to have fluid-like character (Eftink, 1997).

Studies were conducted on *Bsu*PVA by monitoring the fluorescence emission spectra. Steady-state fluorescence measurements were made on a Perkin Elmer LS 50 B fluorimeter with slit width of 7 nm for both the monochromators. 2 ml samples

were maintained at constant temperature (± 0.1°C) in a quartz cuvette with the help of a Julabo F 25 circulating cryobath. Samples were excited at 280 nm and the emission spectra were recorded from 300 to 400 nm. All samples were checked for inner filter effect. The fluorescence of buffers, quenchers and various additives were measured at identical wavelengths and corrected for in the observed fluorescence of samples. Corrections were also made for any dilutions due to addition of solutions to samples. Interference due to ionic strength were minimised by using a low concentration of buffer.

4. 2. 4. Determination of binding constants

The binding of non-fluorescent substrate to the enzyme was studied by intrinsic fluorescence titrations. Emission at a particular wavelength can be used instead of the whole spectra as relative signals are studied during binding. Change in fluorescence intensity after the binding of substrate was monitored at λ_{max} of the protein (333 nm). Corrections were made to compensate for the dilution effect upon addition of the substrate. At the highest concentration of substrate, volume change was less than 5% of the solution in the cuvette. To 2 ml of the protein sample (200 μg) in 50 mM potassium phosphate buffer pH 7.0, 2-5 μl aliquots of substrate stock solution were added in increments and the fluorescence intensity monitored before and after addition. The binding reactions were carried out at various temperatures thermoregulated (± 0.1°C) in a quartz cuvette with the help of a Julabo F25 circulating cryobath between 20 – 45 °C. Enzyme activity on the substrates was negligible at these substrate concentrations; it did not interfere with determination of the association constants. The fluorescence of buffers and substrates were measured at identical wavelengths and corrected for in the observed fluorescence. Linear fits and graphs were generated using Microcal Origin 6.1 software.

The fluorescence intensity of PVA saturated with substrate (F_∞) was extrapolated from the plot F_o /(F_o-F_c) against 1/[C] where F_o and F_c are the fluorescence of the enzyme in the absence and presence of substrate at a given concentration, C. The association constants (K_a) for the protein-substrate interactions were determined from the titration data by assuming the relation that pKa of the complex equals the value of [C] when log [(F_c-F_o)/ (F_∞-F_c)] = 0. The abscissa intercept of the log [(F_o-F_c)/(F_c-F_∞)] versus log[C] plot was used to calculate K_a.

Free energy changes of association (ΔG) were determined by the equation

$\Delta G = -RT \ln K_a$

Changes in enthalpy (ΔH) were determined from the vant-Hoff plots (ln K_a against 1000/T) by using the equation

$\ln K_a = (-\Delta H/RT) + \Delta S/R$

The slope of the plot equals ($-\Delta H/R$) from which the enthalpy change was calculated. The entropy change was obtained from the equation

$\Delta G = \Delta H - T\Delta S$.

4. 2. 5. Solute perturbation studies

4. 2. 5. 1. Solute quenching

Fluorescence quenching can be used to study the environment of Trp (Lehrer, 1971). Quenching of fluorescence upon addition of various solute quenchers was monitored at 333 nm. Corrections were made to compensate for the dilution effect upon addition of quencher. At the highest concentration of the quencher, volume change was less than 5% of the total volume of the solution in the cuvette. The fluorescence intensity change is linear at these dilutions. Acrylamide (a neutral quencher), KI (anionic quencher) and CsCl (cationic quencher) were used. The iodide solution contained sodium thiosulphate (200 µM) to supress tri-iodide formation, which otherwise would interfere with spectra due to its absorbance at a wavelength of 350 nm. Defined

amounts of the quencher (2-5 µl aliquots) from a stock of 5 M were used to titrate 2 ml protein solution in the cuvette. All quenching experiments were carried out in 50 mM phosphate buffer pH 7 at 30 °C. Quenching studies were repeated on enzyme treated with Gdn HCl buffered with 50 mM potassium phosphate buffer pH 7. The corrected fluorescence signal was calculated using the formula ($F_o \times$ total volume in µl) / 2000, where F_o is the observed fluoresence intensity.

4. 2. 5. 2. Analysis of fluorescence quenching data

Accessibility of the quenchers to the fluorophores depends on exposure as well as lifetime. Accessibility of residues are reflected in the Stern-Volmer constant. The fluorescence data were analyzed using Stern-Volmer (SV) and modified Stern-Volmer equations:

$F_o/F_c = 1 + K_{sv}[Q]$

$F_o/(F_o-F_c) = 1/f_a + 1/f_a K_q [Q]$

Where F_o and F_c are the fluorescence intensities at λ_{max} in the absence and presence of the quencher at concentration [Q], respectively. f_a is the fractional degree of fluorescence at concentration [Q], *Ksv* is the effective quenching or Stern-Volmer constant and (F_o-F_c) is the difference between fluorescence intensities in the absence and presence of quencher. The plot of F_o/F_c versus [Q] is linear and the slope, K_{sv} is the product of lifetime and bimolecular rate constant K_q.

From the ordinate intercept of the modified SV plot (double reciprocal plot of $F_o/(F_c-F_o)$ versus 1/[Q]), where F_o and F_c are the fluorescence intensities of the free protein and of the protein at a quencher concentration [Q], F_∞ the fluorescence intensity at infinite concentration of quencher was obtained. SV plots were constructed using F_o/F_c versus [Q]. Linear fits of the data and graphs were generated using Microcal Origin 6.1 software.

4. 3. Results and Discussion

*Bsu*PVA has four Trp residues per monomer. When excited at wavelength 280 nm, the fluorescence emission spectrum showed maximum intensity between 330 and 350 nm indicating that it contained two populations of Trp. One of the populations is in nonpolar environment or buried while the other one is in a polar environment. Tryptophans completely exposed to aqueous solutions show a λ_{max} around 356 nm whereas those in hydrophobic milieu have a λ_{max} around 330 nm (Eftink, 1997).

4. 3. 1. Determination of association constants

The intrinsic fluorescence intensity of *Bsu*PVA decreased upon binding of substrates. There was a small blue shift upon binding of PenV. Titration of the enzyme with PenV resulted in quenching of the intrinsic fluorescence with a pronounced decrease in the emission maximum at the red end of the peak (Fig. 4.1). Since fluorescence of Trp is influenced by its microenvironment, changes in fluorescence in the presence of PenV shows changes in hydrophilic environment of Trp.

The slope of the plot of log $[\Delta F/(F_c-F_\infty)]$, versus log[C] was unity for both substrates (PenV and NIPOAB) indicating formation of one-to-one complex. There was also a large difference in entropy. Temperature dependence of association constants (K_a) was made use of to determine the thermodynamic parameters. The values of K_a for the binding of PenV were determined at different temperatures. Fig. 4.1 shows the pattern of quenching. The association decreased with increasing temperature indicating that the affinity of the enzyme for PenV decreased with increase in temperature (Table 4.1). Binding experiments repeated for NIPOAB indicated that the patterns of binding of the two substrates are different. The K_a for PenV was much lower than that for NIPOAB. For PenV, the K_a decreased with increase in temperature corresponding to a negative change in enthalpy (ΔH). The increase in the affinity was accompanied by a positive entropy change in this case (Table 4.2).

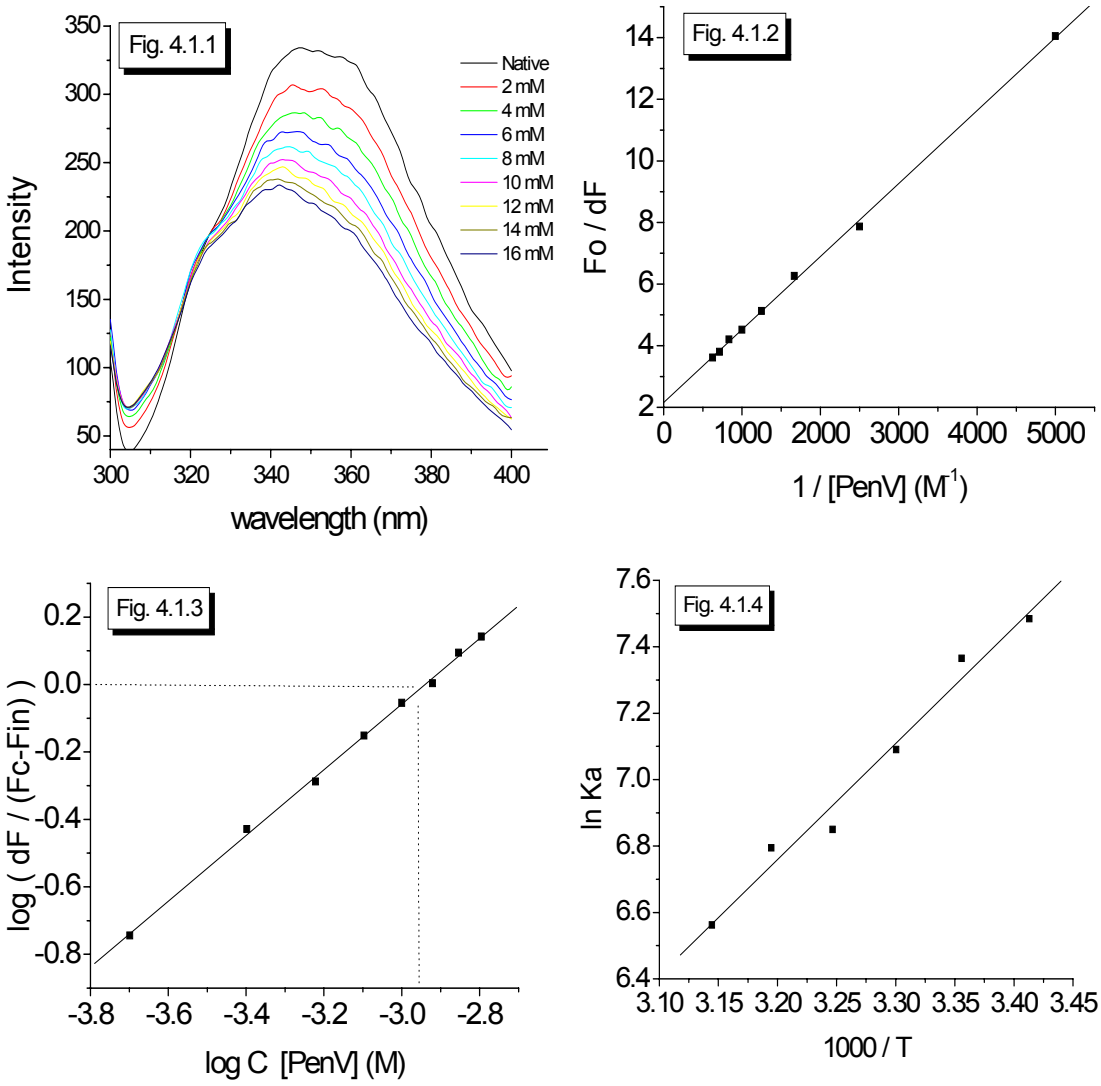

Fig. 4. 1: Determination of association constants and thermodynamic parameters for the binding of PenV to *Bsu*PVA

Fig. 4. 1. 1: Fluorescence emission spectrum on titration with PenV

Fig. 4. 1. 2: $F_o/ \Delta F$ versus 1/[PenV] (M^{-1}) plot. dF indicates (F_o-F_c) or (ΔF)

Fig. 4. 1. 3: log ($\Delta F/ (F_c-F_\infty)$) versus log C plot. fin denotes F_∞

Fig. 4. 1. 4: vant-Hoff plot for the binding of PenV to *Bsu*PVA

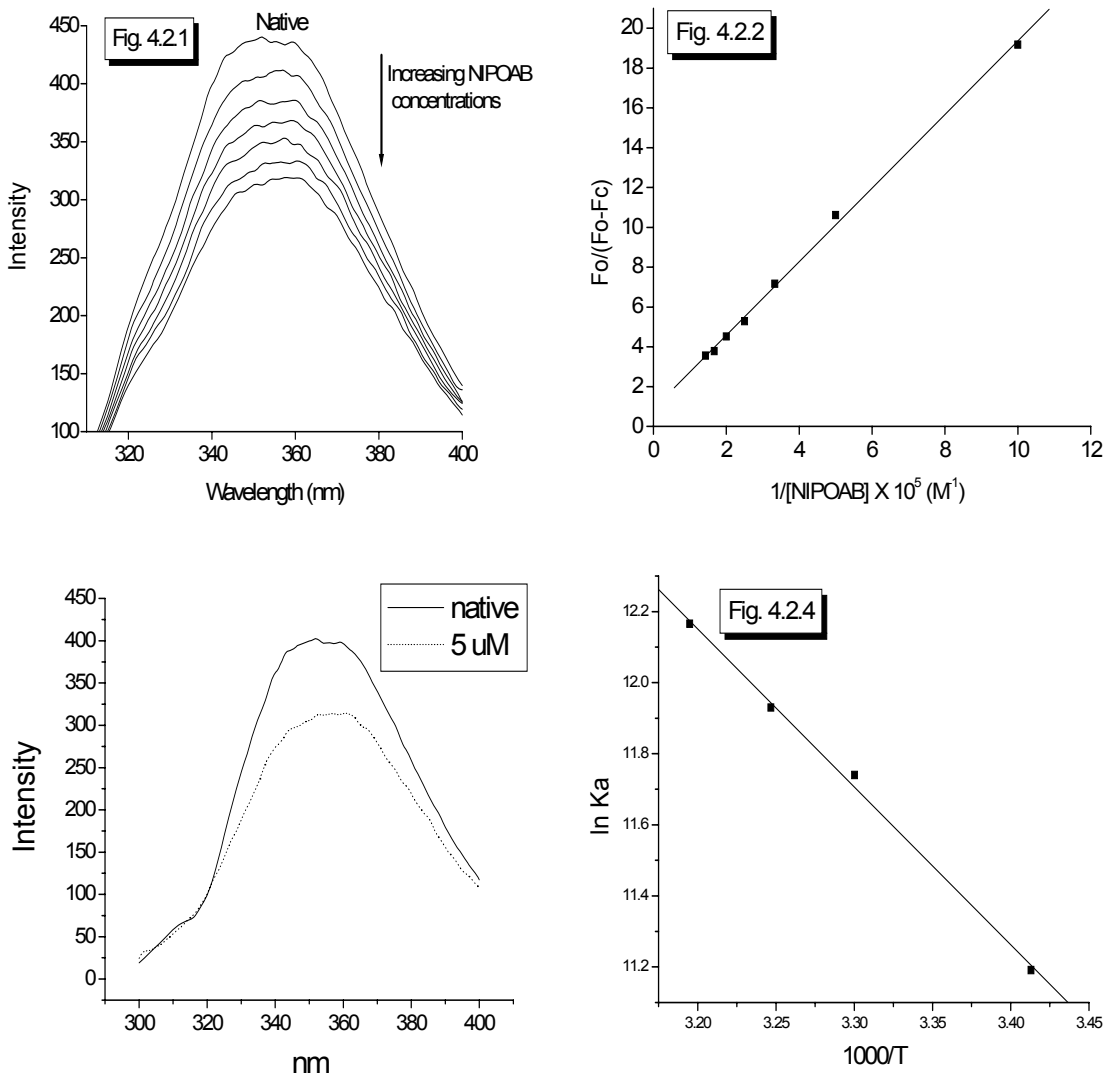

Fig. 4. 2: Binding studies with NIPOAB on *Bsu*PVA

Fig. 4. 2. 1: Fluorescence emission spectrum on titration with 1μM aliquots of NIPOAB

Fig. 4. 2. 2: $F_o/ \Delta F$ versus 1/[NIPOAB] (M^{-1}) plot. dF indicates (F_o-F_c) or (ΔF)

Fig. 4. 2. 3: log ($\Delta F/ (F_c-F_\infty)$) versus log C plot. Fin denotes F_∞

Fig. 4. 2. 4: vant-Hoff plot for the binding of NIPOAB to *Bsu*PVA

Table 4. 1: Association constants for the binding of PenV and NIPOAB to *Bsu*PVA at different temperatures.

Temp (^{o}C)	PenV ($\times 10^{2}$ M^{-1})	NIPOAB ($\times 10^{4}$ M^{-1})
20	17.8	7.25
30	12	12.55
35	9.44	15.17
40	8.93	19.21

Table 4. 2: Thermodynamic parameters for the binding of substrates to *Bsu*PVA at 40 ^{o}C.

Ligand	K_a (M^{-1})	ΔH (kJ mol^{-1})	-ΔG (kJ mol^{-1})	ΔS (J mol^{-1} K^{-1})
PenV	8.93×10^{2}	-29.1	17.68	-36.95
NIPOAB	1.92×10^{5}	45.73	31.05	46.91

4. 3. 2. Solute quenching

Acrylamide was the most efficient quencher of the native protein at room temperature. Addition of acrylamide resulted in 100% quenching of fluorescence with no shift in the emission maximum of the native protein. The modified SV plot was linear while the direct SV plot showed upward curvature. This indicates static and dynamic quenching. In the modified SV plots, the value of fa^{-1} was given by the Y-intercept. Accordingly, the fraction of Trps accessible to quenchers (fa) in the free

protein was expressed in values relative to the Trp residues contributing to the initial fluorescence of the protein. Acrylamide is an uncharged and soluble molecule and is capable of effectively quenching indole derivatives present in aqueous environment. It does not quench the fluorescence of completely buried Trp residues, but quenches the surface-exposed and partially buried Trp residues. The holes formed in the protein to allow quenching with acrylamide should be as large as to allow a molecule as big as acrylamide to diffuse through. Thus quenching gives an idea about the flexibility of the molecule also. Complete quenching of fluorescence by acrylamide indicated that all the four Trp residues are accessible in *Bsu*PVA. The SV constant was calculated to be 14.38 and the quenching constant was 9.2.

Trp environment was studied also using anionic (iodide) and cationic quenchers (cesium ion). Titration of protein with CsCl and KI resulted in quenching of the native protein with no shift in the emission maximum showing that there was no change in protein conformation upon binding of quenchers. KI showed 23% quenching while cesium ion showed very little quenching (5%). The modified SV plots for both the quenchers were linear while the direct SV plot showed curvature. The downward curvature of the SV plot for KI indicates that all the Trps are not accessible to polar phase. The SV plot for CsCl curved upwards. All Trps were thus not accessible to ionic quenchers. Higher quenching efficiency of KI compared to CsCl is an indication of the presence of an average electropositive environment around Trp.

Quenching of enzyme denatured with 1 and 6 M Gdn HCl led to marginal increase in quenching compared to native enzyme. KI and CsCl showed 55% and 25% quenching respectively in the presence of 1 M Gdn HCl. However, CsCl showed lesser quenching of even fully unfolded PVA in 6 M Gdn HCl. This may be an effect of charge repulsion due to presence of excess Gdn HCl rather than due to accessibility of Trp to CsCl.

Table 4. 3: Quenching parameters for PVA from *B subtilis* on denaturation with Gdn HCl.

Protein	Quencher	K_{sv}	K_Q	F_a (eff)	% quenching
*Bsu*PVA	Acrylamide	14.38	9.2	1.19	100
alone	KI	1.29	17.28	0.23	23
	CsCl	1.12	37.68	0.095	9.5
*Bsu*PVA +	Acrylamide	21.49	13.59	1.54	100
1.0 M	KI	13.63	26.34	0.55	55
Gdn HCl	CsCl	4.03	17.2	0.25	25
*Bsu*PVA +	Acrylamide	29.29	43.85	0.76	76
6.0 M	KI	12.89	28.56	0.46	46
Gdn HCl	CsCl	6.36	271.85	0.055	5.5

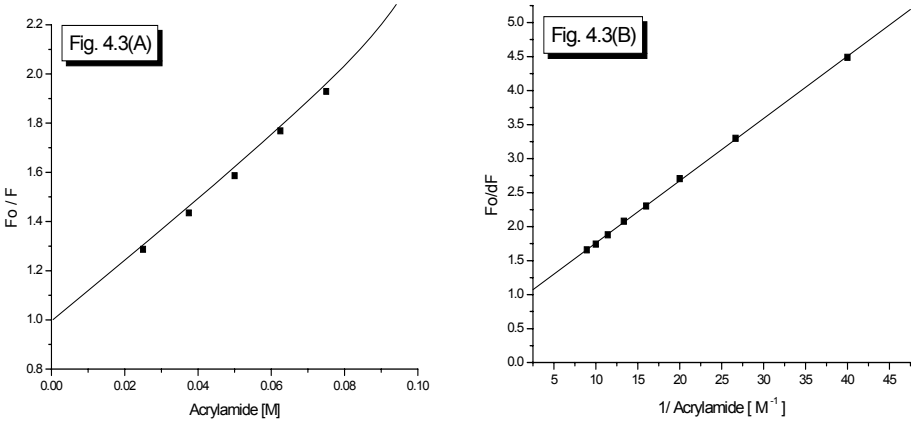

Fig. 4. 3: Quenching of fluorescence of native PVA by acrylamide.

(A) SV and (B) modified SV plots

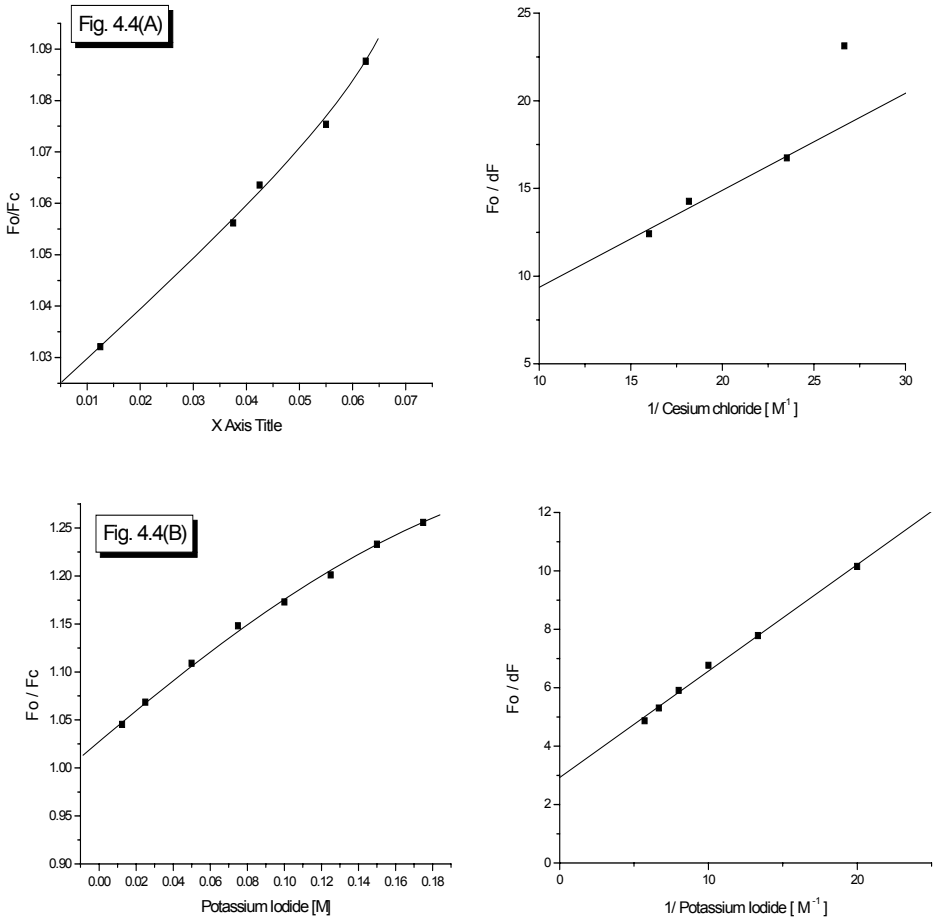

Fig. 4. 4: SV and modified SV plots for quenching of native PVA by A) KI B) CsCl

Fluorescence measurement studies show that *Bsu*PVA has higher association constant for NIPOAB (2.51 $\times 10^5$ M^{-1}) than PenV (8.93 $\times 10^2$ M^{-1}) which explains the higher affinity towards the synthetic substrate NIPOAB (apparent K_m 0.6 mM) than for Penicillin V (PenV) (40 mM). Trps appear to be in both hydrophobic and polar environments but completely accessible to the neutral quencher acrylamide. The average charge of Trp microenvironment is positive. In continuation, conformational stability studies were also conducted using Trp fluorescence and CD spectroscopy. The results from these studies are presented in the next chapter.

CHAPTER V

STUDIES ON CONFORMATIONAL STABILITY OF *Bsu*PVA USING FLUORIMETRY AND CIRCULAR DICHROISM

Summary

Temperature, pH and guanidine hydrochloride (Gdn HCl)- induced conformational changes were studied in *Bsu*PVA, by monitoring the changes observed in Trp emission. Increasing temperatures progressively quenched fluorescence intensity. Temperature related changes were partially reversible as evidenced by partial restoration of PVA activity. Molecular aggregation was observed at higher temperatures when the protein solution was incubated at acidic pH. The loss of fluorescence and enzyme activity were both reversible even at extreme alkaline pH but not at acidic pH. PVA showed presence of solvent-accessible nonpolar clusters at acidic pH as evidenced by the binding of 1-anilinonaphthalene-8-sulphonic acid (ANS). It could be inferred from circular dichroism spectra that the secondary structure of the protein was preserved at extremes of pH and at temperatures as high as 55 ^{o}C. The enzyme was irreversibly inactivated at a concentration of 2 M Gdn HCl. The loss of PVA activity and structure was complete at 6 M Gdn HCl.

5.1 Introduction

Physiological functions of proteins are linked to their three-dimensional structures and native conformations. Since three-dimensional structures of proteins are stabilized by disulphide bridges and non-covalent interactions such as hydrogen bonds, ionic and hydrophobic interactions and van der Waals forces, those conditions that interfere with such interactions tend to destabilize proteins, affecting their native and active conformation. This can be caused by increase in temperature,

pH changes and denaturation by chemical agents like urea and Gdn HCl. Perturbations in structure throw light on how proteins might behave at a given condition and thus supply probable explanations for observed effects. Unlike using crystallography which has the limitation of requiring protein in crystal form, by using fluorescence and circular dichroism (CD) spectroscopy, dynamic studies on proteins can be conducted in solution itself under varied conditions of temperature, pH, ionic strength, denaturation etc. Progressively the protein denaturation can be monitored. Surface properties can be mapped using dyes and fluorimetric assays can be performed for detecting the binding of different ligands. Moreover, comparatively lesser sample is required for these methods, an advantage when protein is not available in large quantities.

Atoms are perpetually in motion because of thermal agitation or vibration. Since crystallographic experiments are carried out in solid state the dynamics of the protein to a large extent are not captured. However, regions of protein that are not discernable in electron density can be considered as mainly due to disorder arising from dynamics. Dynamics is necessary for substrate binding and release. Binding and release of substrates cannot be achieved without destroying the crystal structure. Moreover, native states of proteins are actually an ensemble of different states that are energetically stable and viable. Structural dynamics of the protein can be studied depending on the accessibility of Trps to soluble quenching agents, monitoring Gdn HCl induced changes etc.

The crystal structures of two penicillin V acylases, one from *Bacillus subtilis* and the other from *Bacillus sphaericus* are known. Until now, there are no reports of biophysical studies on any PVA. It is shown in Chapter 4 that together with crystal structure, these studies can be powerful tools for gathering information on the interaction of substrate with the protein and to elucidate its structure-function

relationship. Such studies in tandem with conformational stability studies are important for the biotechnological applications of the enzyme. This chapter describes the studies on conformational stability of *Bsu*PVA conducted using fluorescence and CD spectroscopy.

5. 2 Materials and Methods

5. 2. 1 Materials

Guanidine hydrochloride (Gdn HCl) and 1-anilino-8-naphthalene sulfonic acid (ANS) were procured from Sigma (St. Louis, USA). Sodium thiosulphate and buffers were from Qualigens. Methanol was from Merck. All buffers and solutions were filtered through a 0.45 µM filter (Sartorius). All solutions were filtered and centrifuged before use. Gdn HCl was prepared as 8 M solution in deionised water, adjusted the pH to 7 and then filtered. Buffers were prepared as 1 M stocks, pH adjusted at room temperature and filtered. ANS was prepared fresh every time at a concentration of 10 mM in methanol and centrifuged before use. All the other reagents were also prepared fresh before use.

5. 2. 2 Preparation of protein samples

Production and purification of the protein, enzyme assay and protein estimation were carried out as described in Chapter 2. For the fluorescence studies, protein was dialyzed against 100 mM NaCl and centrifuged (10 000*g*, 10 min). The clear supernatant was used for the studies.

5. 2. 3 Fluorescence measurements

Details of collection of fluorescence emission spectra are given in Chapter 4.

5. 2. 4 Hydrophobic dye binding studies

ANS is a fluorescent molecule used as a hydrophobic extrinsic probe for examining subtle changes in nonpolar character of proteins at the surface. ANS has a weak

fluorescence at around 515 nm at acidic pH. The ANS fluorescence intensity increases significantly upon binding to exposed hydrophobic patches on proteins with a concomitant blue shift of λ_{max} to 495 nm. The fluorescence yield is high in apolar environment and water molecules quench fluorescence of ANS. This property can be made use of to detect surface exposed nonpolar patches in proteins (Daniel & Weber, 1966, Cardamone & Puri, 1992). Since Trp residues are usually buried inside the protein and are not exposed unless unfolding takes place, subtle changes on surface of the protein can be easily traced by following its fluorescence. It is very useful to detect molten globule states which are partially folded states of protein characterized by accessible ordered hydrophobic surfaces (Semisotnov *et al.,* 1991). Assessment of ANS binding can also be applied to study the interaction between a protein and its ligand (Masui & Kuramitsu, 1998).

Protein samples were allowed to react with the hydrophobic dye ANS and the spectra recorded. 15 µl aliquots of 10 mM ANS stock were used for 2 ml samples. The samples were excited at wavelength 375 nm and the emission spectra were recorded from 400 to 550 nm. Bandwidths were kept at 5.0 for both excitation and emission monochromators. ANS blanks were also run simultaneously and were subtracted from the respective spectra of the samples.

5. 2. 5 Rayleigh light scattering studies

When light travels in transparent solids, liquids and especially in gases, the light is scattered by particles much smaller than its own wavelength. This is known as Rayleigh scattering and the amount of scattering of a beam of light is dependent upon the size of the particles and the wavelength of the incident light and the scattering coefficient of light in the medium. The intensity of the scattered light, varies inversely with the fourth power of the wavelength according to Rayleigh law. The

intensity I of light scattered by a single small particle from a beam of light of wavelength λ and intensity I_0 is given by:

$$I = I_0 \frac{(1+\cos^2\theta)}{2R^2} \left(\frac{2\pi}{\lambda}\right)^4 \left(\frac{n^2-1}{n^2+2}\right)^2 \left(\frac{d}{2}\right)^6$$

where R is the distance to the particle, θ is the scattering angle, n is the refractive index of the particle, and d is the diameter of the particle (Ditchburn, 1953). This property can be used to detect presence of any aggregates in the protein solution. PVA suspended in 50 mM potassium phosphate buffer pH 7 was studied under various conditions for Rayleigh light scattering. The excitation and emission wavelengths were fixed at 400 nm or 350 nm with excitation and emission slit widths at 5.0 and 2.5 and scattering was recorded for 30 s at intervals of 1 s.

5. 2. 6 Circular Dichroism

Circular dichroism refers to the phenomenon where different quantities of left and right polarised light are absorbed by molecules when circularly polarised light is incident upon them. This is a property exhibited by all optically active molecules. Biological molecules like sugars and aminoacids are examples of molecules exhibiting CD. The secondary structures of proteins and nucleic acids also exhibit signature CD spectra. The CD spectra of proteins in the ultraviolet region is commonly used to follow secondary structural changes and to estimate the fractions of different types of secondary structure present. Though spatial coordinates of the secondary structural elements cannot be estimated using CD, it is an invaluable tool in following conformational changes in protein. Along with fluorescence study, which is also conducted on proteins in solution, CD analysis nicely complements solid state studies like X-ray crystallography.

Near UV (250 - 300 nm) CD signals are contributed by the aromatic aminoacid sidechains and disulfide bonds. The CD signals they produce are sensitive to the

overall tertiary structure of the protein. The aminoacids responsible for the signal are phenylalanine (250 - 270 nm), tyrosine (270 - 290 nm) and tryptophan (280 - 300 nm). Weak signals are contributed by disulfide bonds throughout the near-UV CD spectrum. The contributions from individual aminoacids can vary and it is not feasible to separate the contributions of individual aromatic residues from the spectra.

Far UV CD (200 – 250 nm) spectra were recorded in a Jasco-J715 spectropolarimeter at room temperature using a cell of 0.1 cm pathlength. Scans were run at 1 nm resolution, 1 nm bandwidth and a scan speed of 200 nm/min. The sensitivity was 20 mdeg and the response time was 2 sec. The spectra obtained were the average of 5 scans with the baseline subtracted. Temperature was maintained using a circulating Julabo waterbath. 200 μl samples were used for recording the spectra. Near UV CD spectra were also collected by extending the range to 250 to 300 nm. A cuvette of pathlength 1 cm was used with the same settings. CD spectra were simultaneously recorded for appropriate blanks containing only buffer and subtracted from those of the respective samples. The changes in far UV CD spectra were monitored by following changes in ellipticity at 222 nm. Mean residue ellipticity was calculated as follows

Mean Residue Ellipticity = $(100 \times \theta \times Mr) / (l \times c \times N)$ deg cm^2 $dmol^{-1}$

Where θ is ellipticity in mdeg, *Mr* is the molecular weight of the protein, *l* is the length of the light path in cm, *c* is the concentration in mg mL^{-1} and *N* is number of aminoacids.

5. 2. 7 Temperature treatment

The stability of the enzyme at different temperatures was studied by incubating 2 ml samples of protein in 50 mM potassium phosphate buffer pH 7 for 15 min at different temperatures (30 to 55 °C) with the help of a variable circulating cryobath and the

collecting emission spectra in the range 300 to 400 nm. Samples were allowed to renature at room temperature and the spectra were re-recorded at 30 °C. Enzyme samples treated identically were tested for PVA activity as outlined in Chapter 2. ANS binding studies were carried out as described above. In a similar manner, far and near UV CD spectra were recorded for selected samples after heating and then cooling.

5. 2. 8 Effect of pH variation

PVA was incubated at room temperature in different buffers at varying pH from 1.0 to 12.0. The buffers used were glycine-HCl in the pH range 1.0 to 3.0, citrate phosphate in the pH range 4.0 to 6.0, potassium phosphate for pH 7.0, Tris from 8.0 to 9.0 and glycine-NaOH from 10.0 to 12.0. Protein was incubated for 2 h in 100 mM concentration of different buffers and spectra recorded as outlined above at 30 °C. Experiments were repeated with samples incubated at different temperatures for 15 min. ANS binding at different temperatures was also studied as previously described. The pH of samples incubated in buffers of different pH were adjusted to pH 7 and the spectra and ANS binding were studied at 30 °C. CD spectra were also recorded as described above for selected samples. All the samples were checked for PVA activity and aggregation.

5. 2. 9 Denaturation by Guanidine hydrochloride

PVA was incubated for 4 h with different concentrations of Gdn HCl at room temperature. Spectra and ANS binding were studied as outlined above. CD spectra were also recorded. For renaturation studies, samples were first incubated in different concentrations of Gdn HCl in a total volume of 100 μl and then renatured by diluting out Gdn HCl to different residual concentrations by making up the solution to 2 ml and equilibrating for 24 h. The spectra were recorded and ANS binding was studied for renatured samples. Rayleigh light scattering studies were also carried out

on these samples. Aggregation was checked by using scattering at 400 and 350 nm. PVA activity assays were carried out on all the samples.

5. 3 Results and Discussion

5. 3. 1. Temperature stability of *Bsu*PVA

The effects of thermal treatment on the conformation of protein were studied at pH 7 using Trp fluorescence intensity changes. Increase in temperature reduced the fluorescence intensity of the protein linearly, without any shift in λ_{max}. At 65 °C, fluorescence intensity reduced to 55% of the original (Fig. 5. 1). The protein regained intensity upon cooling with a little loss in intensity at higher temperatures. There was a remarkable reduction in PVA activity with temperatures above 55 °C (Fig. 5. 2). The loss of activity at this temperature could not be reversed completely by allowing the enzyme to cool to room temperature.

There was no aggregation observed as no change was recoded in light scattering intensity. The protein did not bind ANS at any of the temperatures tested or after it was allowed to cool to 30 ^{o}C, indicating that no hydrophobic patches were accessible to solvent. Fluorescence was studied at 55 °C at different pH from 1 to 12. The trend appeared to be the same as that of the enzyme kept at room temperature. Compared to room temperature, there was reduction in intensity at all of the pH studied compared to 55 °C.

The decrease in fluorescence intensity may be due to thermal deactivation of fluorophores. The primary amine group of lysine is known to quench fluorescence (Brand & Withold, 1967). *Bsu*PVA has 16 lysine residues per monomer. Thermal quenching of fluorophores indicates that such groups are repositioned due to increase in temperature, in such a way as to effectively quench Trp fluorescence. If the heat in the system is converted into excess chemical potential energy, weak bonds might collapse with ensuing alterations in the three-dimensional structure.

Such conformational changes often lead to exposure of buried Trp residues to aqueous environment resulting in changes in the intensity of emission spectra accompanied by shift in the emission maximum (λ_{max}). Such changes were not observed upon raising temperature till 65°C, ruling out unfolding in this range.

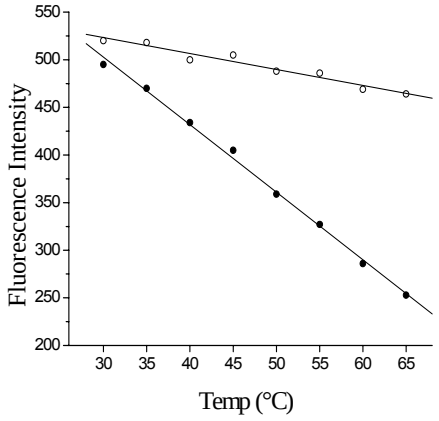

Fig. 5. 1: Fluorescence intensity as a function of temperature -●- upon heating and -o- upon cooling.

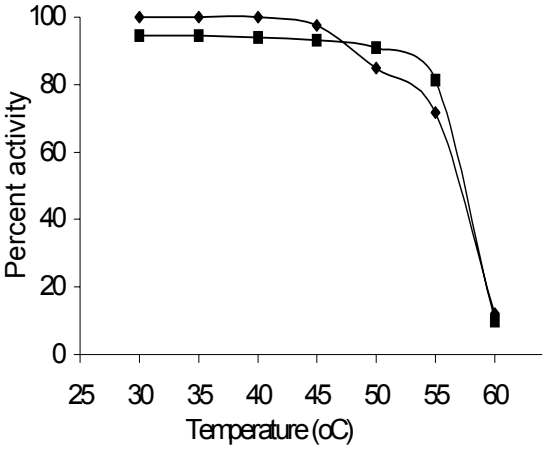

Fig. 5. 2: PVA activity measured as percentage of original activity upon heating -♦- and subsequent cooling -■- plotted as a function of temperature.

Far UV CD (200–250 nm) of native PVA exhibited characteristic spectrum of αβ proteins at pH 7, with minima at 218 nm and 222 nm. There was no significant change in the secondary structure composition at pH 7 and 55 °C when compared to the spectrum at room temperature. However, when the heated protein was cooled, there was a split in minima (Fig. 5.3). Near UV CD spectrum showed negative minima at 284 to 294 nm showing contributions from tyrosine and tryptophan side chains and a positive maximum at 259 nm where the signal contribution is mainly due to phenylalanine (Fig. 5.4). There was gradual loss of native structure on heating. At 70 °C, there was complete loss of structure as indicated by significant decrease in negative minima. After cooling, negative ellipticity decreased further; there was no discernible tertiary structure indicating that the loss of structure at 70 °C is irreversible. This is in contrast to fluorescence intensity, which is regained upon cooling. Therefore, changes occuring in microenvironment of Trps on heating is reversible though the overall tertiary structure was lost.

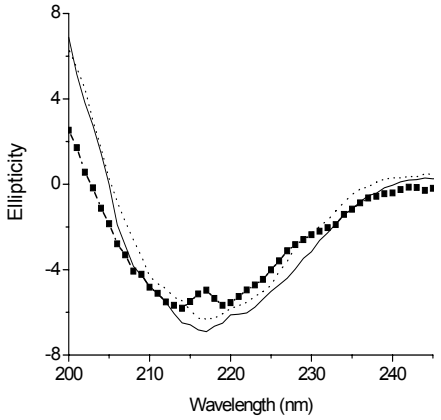

Fig. 5. 3: CD spectra of PVA — at room temperature, - - at 55 ^{o}C, - -■- - after cooling.

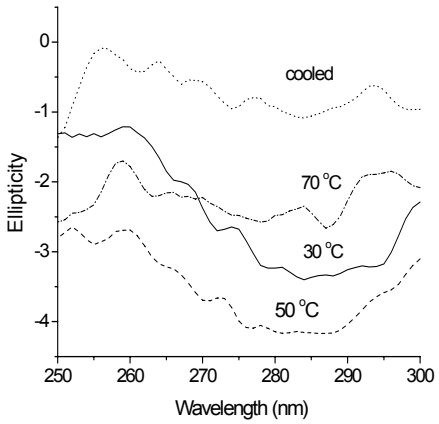

Fig. 5. 4: Near UV CD spectra of PVA at different temperatures. ——30 °C −−−50 °C −···− 70 °C ---- cooled.

5. 3. 2 Stability of *Bsu*PVA in different pH and presence of molten globule state

Fluorescence intensity increased with increase in pH till pH 9 and then started dropping beyond pH 9 (Fig. 5.5). The enzyme was stable in a wide range of pH from 5 to 12 as indicated by reversible loss of PVA activity (Fig. 5.6). the loss of activity was irreversible.

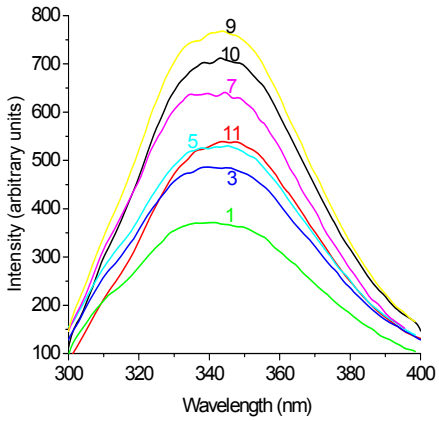

Fig. 5. 5: Fluorescence spectrum of *Bsu*PVA at different pH at room temperature.

It is well-known that the intensity of Trp fluorescence decreases on protonation of neighbouring water molecules or in the presence of protonated acidic groups. In the

zwitterionic states, the residues aspartic and glutamic acid act as dynamic quenchers. Protonation of imidazole rings of histidine residues with p*K* of 6.5 may also cause reduction in fluorescence intensity (Bushueva *et al.,* 1974). Evidences from crystal structures suggest that there is a histidine (His182) residue next to Trp181. Trp181 sidechains from subunits A and B (and C and D) are only 3.457 Å away from each other and are solvent accessible. This indicates possibility of energy transfer between the residues (Ercelen *et al.*, 2001). However, it should be remembered that Trp found in a given environment in the crystal structure might change conformations due to dynamics in solution, even if only for a fleeting moment. In strong alkaline conditions, deprotonation of amino group of aminoacid residues occur. The ε-amino group of lysine, guanidino group of arginine and phenol group of tyrosine are also known to quench the fluorescence of Trp residues in their deprotonated form (Bushueva, 1975 & Steinberg, 1971) which explains decrease in intensity at extreme alkaline pH. Deprotonation might induce charge destabilization in the local environment by inducing unfavourable changes in the native state like electrostatic repulsions, breakage of salt bridges or formation of isolated buried charges, leading to loss of function. The loss in activity above pH 10 could also be due to unfolding of the protein as indicated by decrease in 330/350 intensity ratio.

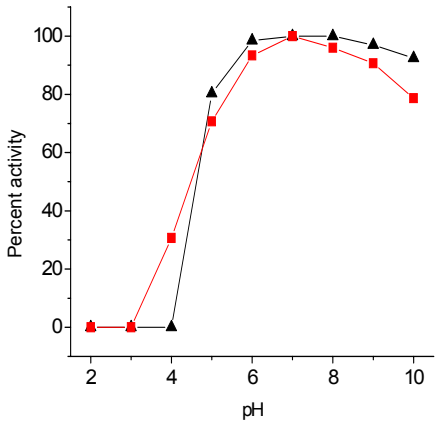

Fig. 5. 6: Relative activity of PVA as a function of pH. —▲— after incubation at respective pH. —■— after readjusting the pH to 7.

The CD spectrum of native PVA at pH 7, was typical of a protein with β-sheet and α-helix structure (Fig. 5. 7). At pH 1 and 12, there was splitting of the far UV CD spectra around 219 nm in the room temperature sample. Incubation at 55 °C for 15 min at pH 1, 7 or 12 did not affect the secondary structure but the splitting in the spectra at extreme pH was reversed indicating the formation of compact molecule though slight rearrangement of structure might be possible. There was some rearrangement of the structure with prominent minima present at 216 and 222 nm at pH 12 whereas the minima were at 216 and 224 nm at pH 1 which might involve a native-like molten globule state. Due to the rearrangement, there was exposure of hydrophobic patches at pH 1, but not at pH 12 (see below). The CD spectrum in the aromatic region (250-300 nm) was featureless for the acid-denatured (pH 1) whereas pH 7 showed structural features with a negative minimum at 284 nm (Fig. 5. 8). Thus, at pH 1, PVA has intact, although rearranged, secondary structure but no defined tertiary structure.

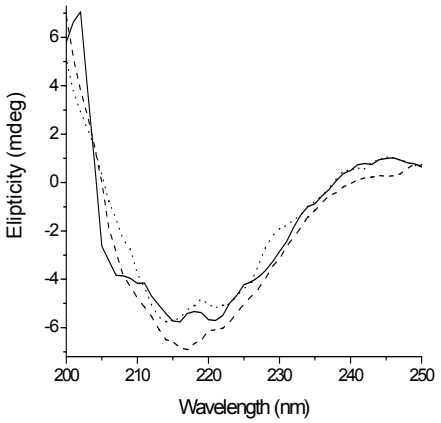

Fig. 5. 7: CD spectra of PVA at different pH ·····pH 1 −−− pH 7 —— pH 12

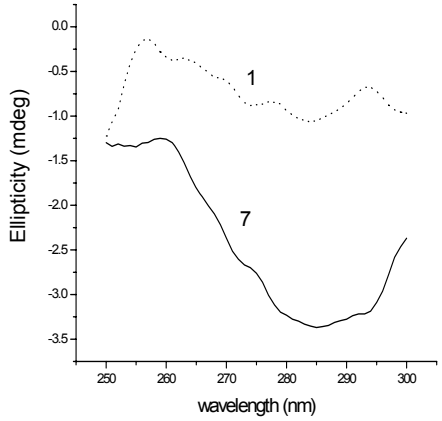

Fig. 5. 8: Near UV CD spectra of PVA at −−− pH 1 and ——pH 7.

No aggregation of the protein was observed in Rayleigh light scattering studies when excited at 400 nm at different pH and 30 °C. However, aggregation was observed when the experiment was repeated with protein incubated at 55 °C, in pH range of 3-5 (Fig. 5. 9). The observed effects may be because the protein solution is closer to its isoelectric point which is 5.3. Here, there was very little aggregation at lower temperatures but substantial aggregation was observed at 55 °C (Data not shown). Aggregation is indicative of the fact that the protein is not in its native conformation.

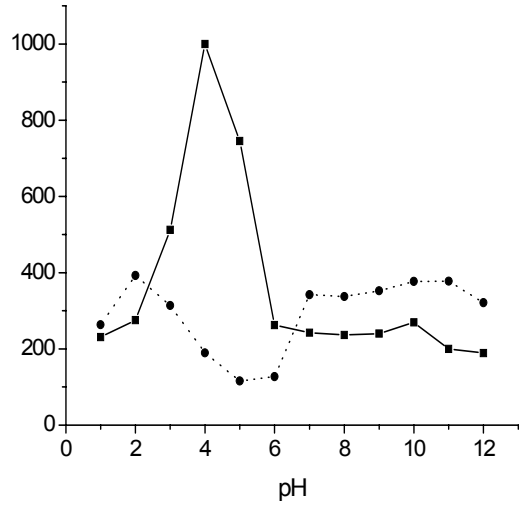

Fig. 5. 9: Aggregation of PVA at ——55 ^{o}C as compared to aggregation at ----30 ^{o}C.

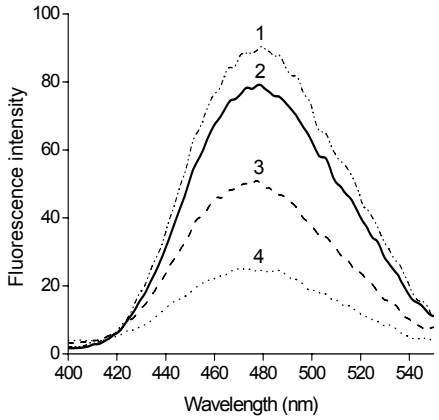

Fig. 5. 10: ANS binding of PVA at acidic pH −···− 1 —— 2 −−−3 ---- 4.

At pH 1-4, there was increase in fluorescence intensity of ANS as well as blue shift of λ_{max} to 480 nm, both of which indicate exposure of hydrophobic surfaces on PVA (Fig. 5. 10). Maximum binding of ANS was at pH 1; it gradually decreased with increase in pH upto 4. This binding occured at 30 °C. Same pattern of ANS binding was observed when similar experiment was conducted at 55 °C; no further increase in ANS binding was observed after heating for 15 min. This showed that irrespective

of the temperature, there was perturbance in the hydrophobic pockets at pH 1-4 and the binding is contributed mainly by a protonated environment and is independent of temperature. Due to change in pH there could be a change in polarity of the Trp environment. So, apart from hydrophobic interaction, there could also be electrostatic forces in play helping the binding of ANS to the protein (Zhengping *et al.,* 2005).

There was no binding of ANS to protein upon readjustment at pH 7, showing that the binding is pH dependant and that the changes caused in the hydrophobic pockets are reversible. ANS binding indicated rearrangement of the globular structure of the protein. Very mild change in ANS binding indicated that there is no substantial change in the structure around hydrophobic pockets due to pH. This is also confirmed from the spectrum of the refolded protein. Interestingly, the renatured protein has a sharp λ_{max} at 333 nm indicating only buried Trp residues in nonpolar environment. Protein also regained its original intensity (Data not shown).

Many proteins exist in stable conformations that are neither fully folded nor unfolded. One of these states is the molten globule state, characterized by partly folded species with high proportion of native-like secondary structure but lacking persistent tertiary interactions. The main chain folds similarly and as compactly as the native state but there is a high degree of freedom for the side chains and the intramolecular non covalent bonds are fewer. These partly folded intermediates can be made to accumulate in equilibrium by mild concentrations of chemical denaturants, low pH, covalent trapping or by protein engineering. The molten globule can be experimentally found at conditions which show a high content of native-like secondary structure, overall compactness with buried but highly mobile aromatic side-chains, exposure of hydrophobic surface, as indicated by dye binding ability and susceptibility to aggregation. Forming molten globule state by globular protein molecules is a general trend (Ohgushi & Wada, 1983).

Although ANS is widely used to study structural changes, there are reports that ANS can distort structure by itself. This calls for careful interpretation of observations lest simple ANS distortion will be attributed to other parameters, especially pH. In horse heart cytochrome *c*, it was found that ANS induced a native-like secondary structure in the acid-unfolded protein while disrupting tertiary structure, thus stabilizing a molten globule state at acidic pH (Ali *et al.,* 1999). In pectate lyase C also ANS was found to induce partially folded molecular species (Kamen & Woody, 2001). Electrostatic interaction mainly between negatively charged ANS and positively charged aminoacid residues in acid-unfolded proteins results in a compact molten globule-like state (Haskard & Li-Chan, 1998, Matulis & Lovrien, 1998).

5. 3. 3 Effect of Guanidine hydrochloride

In presence of Gdn HCl, the 330/350 ratio of fluorescence intensity decreased with increased concentration of the denaturant indicating increased exposure of Trp residues to the polar environment (Fig. 5.11). The decrease in the ratio from 0.94 to 0.85 and increase in intensity at 350 nm indicated unfolding of protein. Unfolding of enzyme was maximum in 2 M Gdn HCl and with higher concentrations, only emission of exposed Trp increased. There was no ANS binding on treatment with Gdn HCl or after removal of Gdn HCl indicating that there was no exposure of hydrophobic patches during unfolding or refolding.

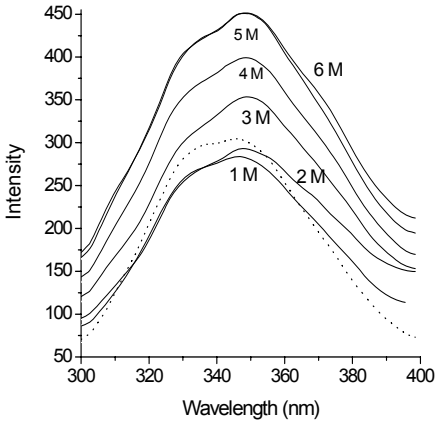

Fig. 5. 11: Fluorescence spectra of PVA treated with different concentrations of Gdn HCl ----- untreated protein.

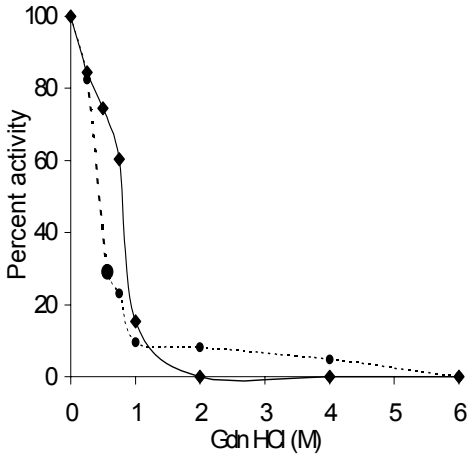

Fig. 5. 12: Hydrolase activity of PVA on PenV as a function of Gdn HCl concentration. —♦— denatured enzyme - -♦- - after removal of Gdn HCl.

The enzyme lost significant activity when the concentration of the denaturant reached 1 M (Fig. 5.12). The far UV CD data showed disturbances in the secondary structure as Gdn HCl concentration increased (Data not shown). There was rearrangement at

1 M Gdn HCl. Loss of secondary structure was complete at 2M, where the protein lost activity fully. At 1 M Gdn HCl, the positively charged guanidinium group of Gdn HCl might interact with negatively charged active site residues, resulting in reduced activity without major change in the conformation of the protein. An aspartic acid residue found in the active site of PVA could interact with Gdn HCl (Chapter 3). Also at low concentrations, Gdn HCl is known to confer effective charge shielding (Monera *et al.,* 1994).

The enzyme was renatured by diluting Gdn HCl-treated enzyme samples with 50 mM potassium phosphate buffer, pH 7 so that the samples eventually had slightly varied insignificant residual concentrations of Gdn HCl. The unfolded protein, on renaturation, regained partial structure as indicated by increase in 330/350 ratio of fluorescence though the fluorescence intensity was significantly lower when compared with untreated enzyme. However, inactivation of hydrolase activity was not completely reversible. The duration and temperature of incubation with Gdn HCl prior to refolding is reported to affect the yield of native protein on renaturation (Kathir *et al.,* 2005).

*Bsu*PVA was unstable in Gdn HCl solutions. This indicated the importance of ionic bonds in maintaining the overall structure of the functional enzyme. It was also unstable in acidic pH at high temperatures. These properties of *Bsu*PVA were compared with a related hydrolase, *Bsp*PVA which is described in the next part of the thesis.

CHAPTER – VI

COMPARATIVE STUDIES ON RELATED HYDROLASES- Part-I

Specificity and Substrate Binding of the PVA from *Bacillus sphaericus*

Summary

Titration with PenV and NIPOAB caused slight but progressive blue shift in emission maximum of the spectrum and also led to quenching of fluorescence intensity. The binding constants for PenV and NIPOAB were calculated to be 2.74×10^4 M^{-1}, and 3.99×10^4 M^{-1} respectively at 40 ^oC, which is comparatively higher than that of *Bsu*PVA. Acrylamide was by far the most efficient quencher (81% quenching in native protein), as in the case of *Bsu*PVA. Quenching by KI and CsCl were 20% and 14% respectively.

6.1 Introduction

In the present and the next chapter of the thesis, comparative studies conducted on a related hydrolase- PVA from *Bacillus sphaericus* (*Bsp*PVA) is reported. The present chapter describes substrate binding studies conducted on the enzyme using fluorimetry and tryptophan environment. The substrates studied were PenV and NIPOAB. Solute quenching studies were conducted using the neutral acrylamide and the ionic quenchers KI and CsCl. Data are presented in comparison with the results obtained on *Bsu*PVA.

6. 2 Materials and Methods

6. 2. 1 Materials

Various materials used and solution and stock preparations are as described in 4. 2. 1. section of Chapter 4.

6. 2. 2 Cloning

*Bsp*PVA was cloned and expressed in *E. coli* as described by Chandra *et al* (2005).

6. 2. 3 Production and purification of enzyme

The recombinant cells were grown in Luria Bertani medium containing 50 μg ml^{-1} ampicillin till they attained OD_{600} of 0.8. Expression of the recombinant protein in the mid-logarithmic growth phase *E. coli* cells was induced with 1 mM isopropyl thiogalactoside. The cells were allowed to incubate at 30 °C for further 4 hours with shaking at 200 rpm. The culture medium was centrifuged at 10 000*g* in a Sorvall RC 5B refrigerated centrifuge for 20 minutes to sediment the cells and the supernatant was discarded. The cells were weighed and stored frozen overnight. Cells were suspended in 50 mM potassium phosphate buffer, pH 6.0 containing 1 mM ethylene diamine tetraacetic acid (EDTA) and 10 mM dithiothreitol (DTT) (buffer *A*) and sonicated using a Biosonik III sonic oscillator for 5 x 1 min at 20 KHz, 300 W, with 10 min intervals between pulses. Samples were always held on ice. After centrifugation (10 000*g* for 20 min), ammonium sulphate (AS) was slowly added to the supernatant to a final concentration of 80% saturation. The precipitate was dissolved in buffer *A* and dialyzed against 24% AS in buffer *A* (buffer *B*) and purified on a phenyl sepharose column (CL 4B, Sigma) that had been pre-equilibrated with buffer *B*, using buffer *A* for elution. The fractions were checked for enzyme activity and positive fractions were subjected to Polyacrylamide Gel Electrophoresis under denaturing conditions. Pure fractions were pooled, dialyzed against buffer *A* and concentrated

by ultrafiltration in an Amicon unit using PM-10 membrane. Protein was dialyzed against 100 mM NaCl and centrifuged (10 000*g*, 10 min) immediately before use, to remove any precipitate. Amount of protein in the samples was estimated by the method of Lowry *et al* (1951) using bovine serum albumin (Sigma) as the calibration standard.

6. 2. 4 Pencillin V acylase assay

Assay for penicillin acylase activity with the substrate PenV was carried out at pH 5.8 at 40 °C as described by Shewale *et al* (1987). Full details are given in Chapter 2 section 2. 2. 6.

6. 2. 5 Fluorescence measurements

Steady-state fluorescence measurements were made on a Perkin Elmer LS 50 B fluorimeter as described in section 4. 2. 3. of Chapter 4.

6. 2. 6 Determination of binding constants

Association constants for PenV and NIPOAB were determined at various temperatures and thermodynamic parameters were calculated. The details of procedures are given in Chapter 4 section 4. 2. 4.

6. 2. 7 Solute quenching

Fluorescence quenching studies on the protein upon addition of the quenchers acrylamide, potassium iodide and cesium chloride, were carried out in 50 mM phosphate buffer pH 7 at 30 °C. The fluorescence signal was corrected for dilution upon addition of quenchers. The data were analyzed using Stern-Volmer and modified Stern-Volmer equations described in section 4. 2. 5. 2 of Chapter 4.

6. 3 Results and Discussion

The fluorescence emission spectrum of the enzyme showed maximum at 333 nm indicating that Trp residues lie in a predominantly hydrophobic environment with low mobility. Though Kyte-doolittle plot showed that the three Trps in *Bsp*PVA- at positions 181, 235 and 319 are all in aqueous milieu (data not shown), emission maximum of fluoresence indicated that they are indeed in hydrophobic environment. This is in contrast to *Bsu*PVA where three of the four Trps are predicted to be in relatively polar environment accessible to the aqueous milieu. This is also clear from the fluorescence spectra of the two enzymes; *Bsp*PVA has a sharp peak at 333 nm whereas *Bsu*PVA has a plateau from 330-350 nm.

6. 3. 1 Determination of binding constants

Binding of substrate PenV and the synthetic substrate NIPOAB resulted in reduction of fluorescence intensity. This was made use of to determine the binding constants for both the substrates. The binding and resultant decrease in intensity were linear. Binding of substrate induced a conformational change in the enzyme as evidenced from the blue shift of the λ_{max} from 333 nm in normal protein to 330 nm for protein in the presence of PenV. Association constants were calculated at different temperatures and vant-Hoff plots were constructed. Thermodynamic parameters for the association at different temperatures were calculated (Table 6.1). The association constant for PenV (2.7×10^4 M^{-1}) was lesser than that for NIPOAB (4×10^4 M^{-1}) at 40 ^oC. As temperature increased, association increased for both the substrates. The association was found to be enthalpically driven.

Free energy of binding (ΔG) was negative for both the substrates. This means that the binding of substrates to the enzyme is a spontaneous process and the values indicate that both substrates are equally favoured. Enthalpy (ΔH) was positive indicating that the process of binding is endothermic.

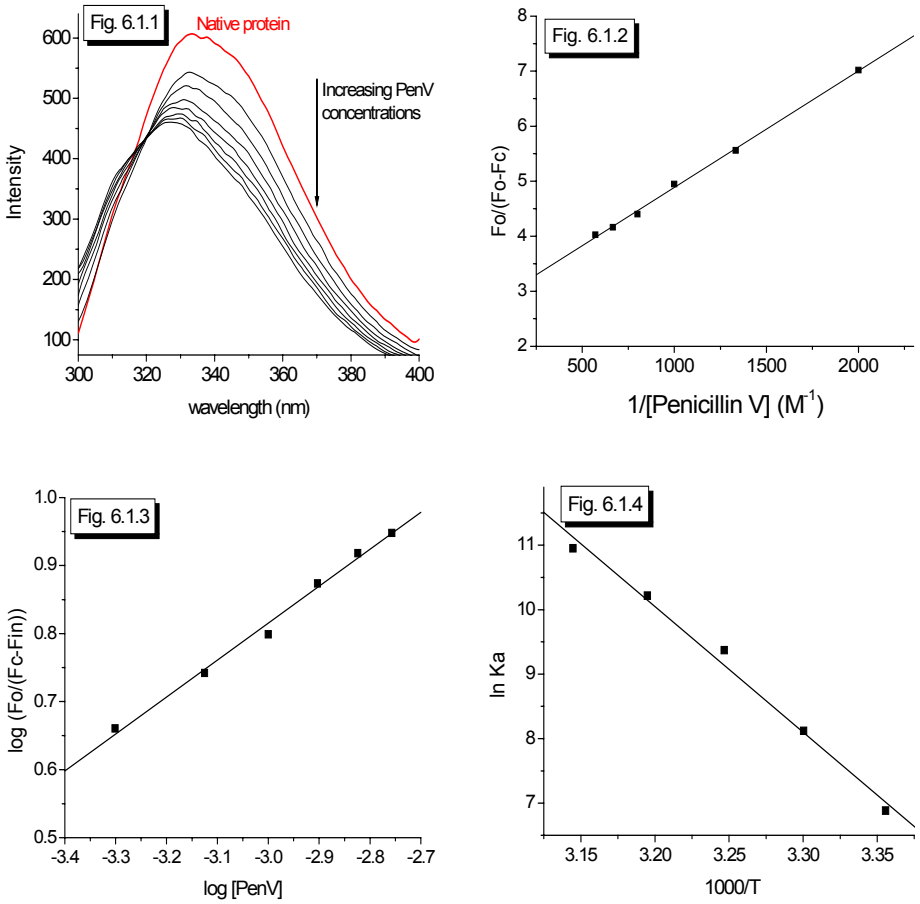

Fig. 6. 1 Determination of association constants and thermodynamic parameters for the binding of PenV to *Bsp*PVA at 40 °C

Fig. 6. 1. 1: Fluorescence emission spectrum on titration with 250 μM aliquots of PenV

Fig. 6. 1. 2: Fo/ ΔF versus 1/[PenV] (M^{-1}) plot. dF indicates (Fo-Fc) or (ΔF)

Fig. 6. 1. 3: log (ΔF/ (Fc-F_∞)) versus log C plot. Fin denotes F_∞

Fig. 6. 1. 4: vant-Hoff plot for the binding of PenV to *Bsp*PVA

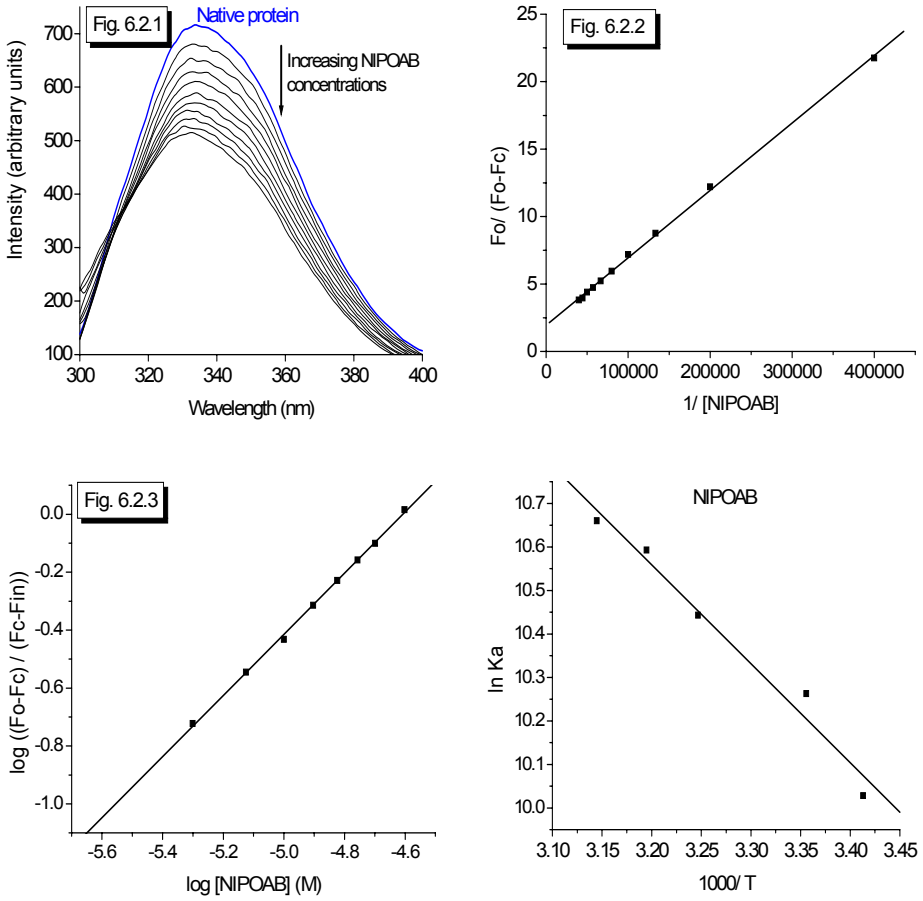

6. 2: Binding studies on *Bsp*PVA with NIPOAB

Fig. 6. 2. 1: Fluorescence emission spectrum on titration with NIPOAB

Fig. 6. 2. 2: $F_o/ \Delta F$ versus 1/[NIPOAB] (M^{-1}) plot. dF indicates (F_o-F_c) or (ΔF)

Fig. 6. 2. 3: log $\Delta F/ (F_c-F_\infty)$ versus log C plot. Fin denotes F_∞

Fig. 6. 2. 4: vant-Hoff plot for the binding of NIPOAB to PVA

Table 6.1: Thermodynamic parameters for the binding of PenV and NIPOAB at 40 °C

40 °C	$K_a \times 10^4$ (M^{-1})	$-\Delta S$ (J mol^{-1} K^{-1})	$-\Delta G$ (kJ mol^{-1})	$-\Delta H$ (kJ mol^{-1})
PenV	2.74	601.26	-26.59419	161.6
NIPOAB	3.985	148.53	-27.56904	18.92

6. 3. 2 Quenching studies

Solute perturbation studies were conducted using the neutral quencher acrylamide, cationic cesium chloride and anionic potassium iodide. Acrylamide was the most effective quencher of the three. It gave 81% quenching while KI and CsCl gave only 20 and 14% quenching respectively. The SV constants and quenching constants are summarised in Table 6.2. SV plot of acrylamide showed linearity (Fig. 6.3). The less than complete quenching indicates that there are some tryptophans that are not accessible to the quenchers. The SV plot showed downward curvature and biphasic quenching by KI and CsCl indicating that the quenching is static and the population of Trp is heterogenous (Fig. 6.4). The environment around tryptophans seems to be partly positive and negative. The Trp accessibility of *Bsp*PVA showed Trp in an average slightly electropositive environment as accessibility to iodide ion was found to be more than cesium ion. Since these proteins have more than one Trp, the emission signal is heterogenous and therefore, the slope of SV plot is considered to be the quenching constant (Eftink & Ghiron, 1977).

Acrylamide is also known to react with sulfhydryl groups in proteins (Cavins & Friedman, 1968). It is to be noted that both *Bsu*PVA and *Bsp*PVA have active cysteinyl sulfhydryl groups. Acrylamide may induce structure distortions. It inactivated aldolase from rabbit muscle at 3.5 M (Dobryszycki *et al.,* 1999). It has been reported

that acrylamide denatures proteins at higher temperatures in which case, the SV plot will be upper curving (Eftink & Ghiron, 1977). However, such distortions were not observed in PVA in the concentration range of acrylamide used as evidenced by absence of any red shift in the fluorescence spectrum.

Table 6. 2: Quenching by different solutes

Quencher	Ksv	KQ	f_a	% quenching
Acrylamide	12.87	17.43	0.81	81
KI	1.47	24.7	0.2	20
CsCl	0.51	12.2	0.14	14

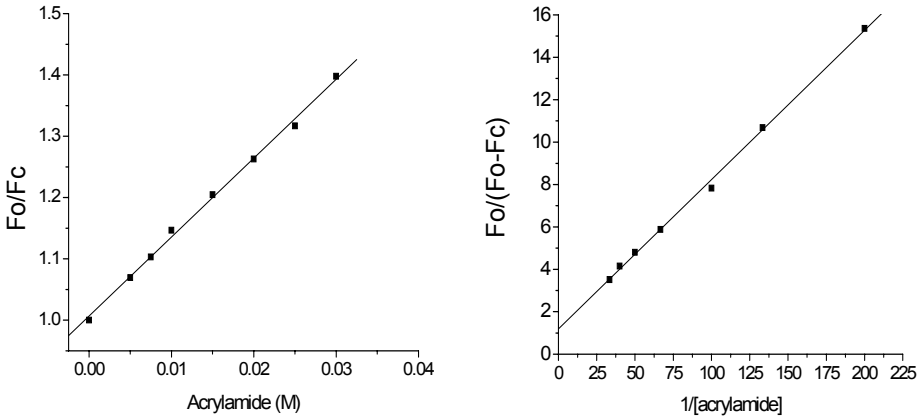

Fig. 6. 3. : SV and modified SV plot for quenching of *Bsp*PVA by acrylamide.

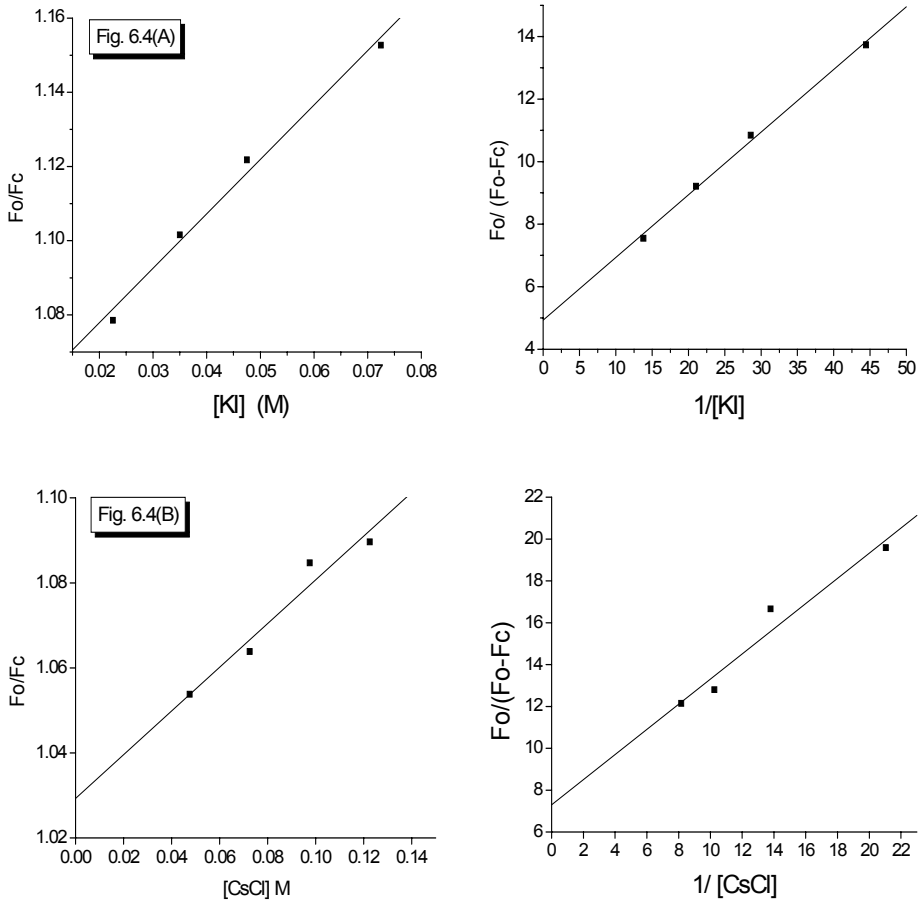

Fig. 6. 4 : SV and modified SV plot for quenching of *Bsp*PVA by A) KI and B) CsCl.

In contrast to *Bsu*PVA, all the Trp in *Bsp*PVA lie in hydrophobic environments with low mobility. Efficiency of acrylamide towards quenching of Trp in native *Bsp*PVA is less as compared to *Bsu*PVA where it is complete. The association constants of the substrates are higher for *Bsp*PVA. This also follows the fact that the K_m of this enzyme (10 mM) is much lower than *Bsu*PVA (40 mM). This shows that *Bsp*PVA is a more efficient enzyme in PenV hydrolysis than *Bsu*PVA. The conformational stability of *Bsp*PVA is described in the next chapter.

CHAPTER – VII

COMPARATIVE STUDIES ON RELATED HYDROLASES: Part–II

Comparison with the Conformational Stability of *Bsp*PVA

Summary

Tryptophan fluorescence intensity decreased with increase in temperature. Both decrease in intensity and PVA activity were partially reversible. After cooling, they were 85% and 90% of the initial values respectively. There was decrease in ellipticity values with increase in temperature as seen from the far UV CD spectra pointing to disturbances in secondary structure. Upon incubation in acidic pH range 1-4, the protein showed presence of molten globule as indicated by ANS binding. This range also had good PVA activity. Far UV CD showed loss of secondary structure at extreme acidic and alkaline pH. Increasing concentrations of Gdn HCl resulted in decreased fluorescence intensity with decrease in 333/355 ratio. There was substantial loss of activity (80%) at 1 M Gdn HCl. Secondary structure losses started from 0.75 M and at 6 M Gdn HCl, there was complete loss of secondary structure.

7. 1. Introduction

*Bsu*PVA has been studied in comparison with other related hydrolases based on structure, conformation and biochemical characteristics. *Bsp*PVA is the other PVA whose crystal structure is available. The biochemical characteristics of *B*spPVA have been already reported. However, conformational changes of the enzyme in solution have not been studied. This enzyme being significantly similar to *Bsu*PVA, comparative studies on their behaviour in solution will help elucidate structural basis of observations. This chapter reports conformational stability of *Bsp*PVA as a function of temperature, pH and Gdn HCl concentration. This is the first instance of such studies on the choloylglycine hydrolase family of the Ntn hydrolase superfamily.

7. 2. Materials and Methods

7. 2. 1. Materials

The materials and preparation of solutions are described in chapter 5 under Materials and Methods section 4. 2. 1.

7. 2. 2. Preparation of protein samples

Production and purification of the protein, enzyme assay and protein estimation were carried out as described in Chapter 6. The recombinant cells were grown in Luria Bertani medium containing 50 μg ml^{-1} ampicillin. Expression of the recombinant protein was induced with 1 mM IPTG. Protein was purified on phenylsepharose column. Pure protein samples were dialyzed against 100 mM NaCl and centrifuged (10 000*g*, 10 min) immediately before use, to remove any precipitate.

7. 2. 3. Assay of Penicillin V acylase activity

Assay for penicillin acylase activity against PenV was carried out at pH 5.8 at 40 °C as described earlier.

7. 2. 4. Fluorescence measurements

Steady-state fluorescence measurements were made on a Perkin Elmer LS 50 B fluorimeter as previously described (Chapter 4).

7. 2. 5. Hydrophobic dye binding studies

ANS binding studies were carried out with samples treated as in chapter 5 section 5. 2. 4. and were excited at wavelength 375 nm and the emission spectra were recorded from 400 to 550 nm.

7. 2. 6. Circular dichroism

Far and near UV CD spectra were recorded in a Jasco-J715 spectropolarimeter at room temperature as outlined in Chapter 5.

7. 2. 7. Light scattering studies

Aggregation of the protein was studied under various conditions using Rayleigh light scattering. The excitation and emission wavelengths were fixed at 400 nm and scattering was recorded for 30 s in 1 s intervals.

7. 2. 8. Effect of temperature

The stability of the enzyme at different temperatures was studied by holding 2 ml samples of protein in 50 mM potassium phosphate buffer pH 7 at required temperature with the help of a variable circulating cryobath and the spectra collected from 300 to 400 nm. Samples were slowly heated and spectra collected at different temperatures. Samples were allowed to cool and the spectra were recorded again. Similarly treated enzyme samples were tested for PVA activity as outlined in 2.1. ANS binding studies were carried out as described above. Far and near UV circular dichroism spectra were recorded for selected samples after heat treatment as well as cooling. The effect of temperature was studied for every 5 °C rise and decrease in temperature from 25 to 65 °C and back to 25 °C at pH 7.

7. 2. 9. Effect of pH

PVA was incubated at room temperature in the following buffers: glycine-HCl in the pH range 1.0 to 3.0, citrate phosphate in the pH range 4.0 to 6.0, potassium phosphate for pH 7.0, Tris from 8.0 to 9.0 and glycine-NaOH from 10.0 to 12.0. after incubation for 2 h in 100 mM concentration of buffers, spectra were recorded as previously outlined at 30 °C. ANS binding was also studied as previously described. These samples, incubated in different pH buffers, were adjusted to pH 7 and the

spectra and ANS binding were studied at 30 °C. CD spectra were collected for selected samples. All samples were parallely checked for PVA activity and aggregation.

7. 2. 10. Effect of guanidine hydrochloride

There are various techniques to monitor unfolding of proteins- Ultraviolet difference spectroscopy, CD, optical rotation, fluorimetry and NMR. Denaturation using urea or guanidine hydrochloride can be used to estimate the conformational stability ΔG_D of the protein. Denaturation curves for different proteins obtained under identical conditions are helpful in measuring differences in their conformational stabilities because of aminoacid sequence or chemical modification inspite of significant similarities between them, especially, in relation to three-dimensional structure. From the denaturation curves, it is possible to unravel the mechanism of folding and to predict whether the protein is made of single domain or if it is made up of more than one domain. The extent of reversibility of Gdn HCl denaturation is dependent on time for which the protein is allowed to equilibrate in the denaturant and pH at which the denaturation and refolding are conducted (Pace, 1986).

Most globular proteins unfold in a two-state mechanism:

F (folded state) $\leftrightarrow$ U (unfolded state)

The spectroscopic property at each concentration used for the calculation, *y*, is the ratio of fluorescence intensities at emission λ_{max} of native and denatured protein. Where y_u and y_f are values of parameters obtained at unfolded and folded by extrapolation from linear portions of unfolding curve at low and high unfolding concentrations.

For a two-state mechanism,

$f_f + f_u = 1$

Where f_f and f_u denote fraction of the protein in folded and unfolded conformations respectively.

$y = y_f f_f + y_u f_u$

Therefore,

$f_u = (y\text{-}y_f) / (y_u - y_f)$

$f_f = (y_u\text{-}y)/(y_u\text{-}y_f)$

The equilibrium constant K_u is calculated using the relation

$K_u = e^{-\Delta Gu / RT} = f_u/f_f = (y\text{-}y_f)/ (y_u\text{-}y)$

Where ΔG_u is the energy of unfolding.

In linear extrapolation, the simplest method of estimating ΔG_u^{H2O} (energy of unfolding in the absence of denaturant), linear dependence of ΔG_u on denaturant concentration observed in transition region is assumed to continue to zero concentration.

$\Delta G_u = \Delta G_u^{H2O} - m$ [Denaturant]

The difference in conformational stability is estimated by multiplying the difference between the $D_{1/2}$ values by m, where m is the slope of the

$\Delta G_u = \Delta G_u^{H2O} - m$[Denaturant]

plot and $D_{1/2}$ is the denaturant concentration where unfolding is halfway.

PVA was incubated for 4 h with different concentrations of Gdn HCl at room temperature. For renaturation studies, samples were incubated in different concentrations of Gdn HCl in a total volume of 100 μl and renatured by diluting out Gdn HCl to slightly different residual concentrations by making up the solution to 2 ml and equilibrating for 24 h. Fluorescence spectra, CD spectra and ANS binding were studied for both denatured and renatured samples. Light scattering studies were also carried out. Aggregation was checked at 400 nm. PVA activity assays were carried out on all the samples. The methods used are described in detail in chapter 4.

7. 3. Results and Discussion

7. 3. 1. Temperature stability of *Bsp*PVA

The fluorescence intensity at 333 nm decreased with increase in temperature (Fig. 7. 1). The change in intensity was gradual and linear in the temperature range tested. At 70 °C, the intensity was 63% as that of the enzyme at 25 °C. As temperature was increased, the 333/350 emission intensity ratio, which is indicative of folded conformation, decreased marginally (0.03). On gradual cooling from 70 ^{o}C to 25 ^{o}C, the intensity again increased, but the final intensity was 85% of the initial intensity. This might indicate some minor changes in the Trp environment in the enzyme structure or thermal inactivation of fluorophores though loss in hydrolase activity was not documented. Upon cooling from 70 ^{o}C to room temperature and then assaying, there was a loss of 10% activity underlining the minor changes during cooling.

Far UV CD data showed that ellipticity was gradually lost during heating at pH 7 (Fig. 7. 2). At 45 °C, there was significant transition at 218 and 222 nm. The negative ellipticity peak at 218 nm disappeared at 50 °C. On gradually cooling the protein again, ellipticity increased but the final ellipticity was 10% lesser than that of the native protein. This trend is similar to fluorescence where intensity after cooling was less than the initial intensity. The secondary structure showed a change in alpha helix content upon cooling; the negative peak became pronounced at 222 nm.

There was no evidence of aggregation at any of the temperatures tested either upon heating or cooling, though there was marginal increase in scattering upon heating, as indicated by Rayleigh light scattering studies. There was no ANS binding indicating that there is no exposure of surface hydrophobic pockets.

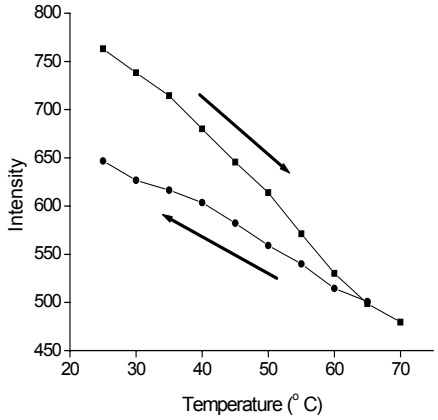

Fig. 7. 1: Intensity at emission maxima as a function of temperature upon heating to 70 °C and cooling back to room temperature.

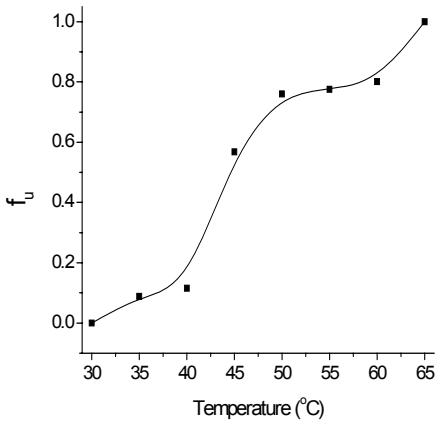

Fig. 7. 2: Far UV CD: Fraction unfolded calculated using ellipticity at 222 nm at different temperatures.

7. 3. 2. Effect of pH variation

The effect of pH was studied from pH 1 to 12 in 100 mM buffers at 30 °C. To investigate the functional stability of PVA at different pH, we determined its acylase activity on PenV at 40 °C as a function of pH. The enzyme retains more than 80% of its activity over the whole range of pH from 1 to 12 after 4 h of incubation. On readjustment of pH to 7, the enzyme on the acidic side (pH 2 - 6) regains activity

whereas in the alkaline range does not regain full activity. This indicates that there is a slight irreversible modification of the protein in alkaline pH. The activity profile of PVA is shown in (Fig. 7. 3). The structural changes under these conditions were studied using fluorescence spectroscopy, CD spectroscopy and ANS binding. Emission spectrum collected in wavelength range 300 - 400 nm upon excitation at 280 nm showed that the intensity was minimum at pH 5. It increased towards the acidic range. On the other side towards neutral and alkaline pH, it increased till pH 7 and there was no significant change thereafter.

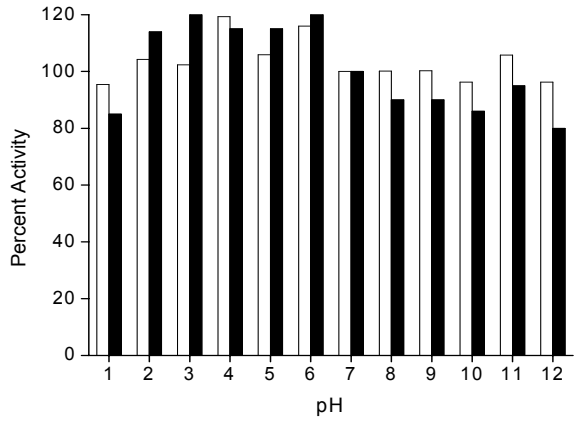

Fig. 7. 3: Activity profile of *Bsp*PVA after incubation at different pH (∏) and after readjusting the pH to 7 (■).

There was significant ANS binding at the acidic pH range in *Bsp*PVA at 30 °C (Fig. 7. 4). The binding was maximum at pH 1 and decreased upon increase in pH till 4, where there was very little ANS fluorescence. The λ_{max} was 488 nm for pH 1-2 which shifted to 495 at pH 4.

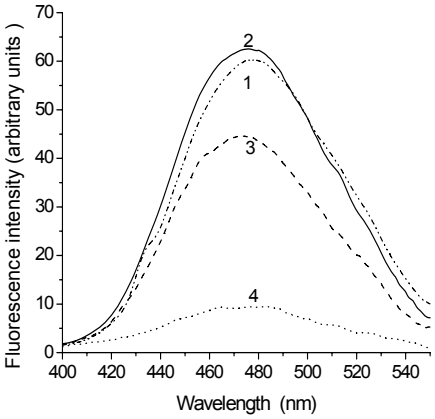

Fig. 7. 4: ANS binding of *Bsp*PVA at acidic pH: −···− 1 —— 2 −−−3 ---- 4

Enzyme treated at pH 3 exhibited preserved secondary structure as seen from the CD data. At pH 4, there was significant loss of secondary structure and negligible binding of ANS showing lack of molten globule species, but activity was found to be maximum indicating that exposure of hydrophobic patches alone does not affect the activity.

There were some interesting observations made in the protein structure at different pH, which are described below. PVA incubated at pH 5 showed considerable loss in secondary structure. This is also where fluorescence intensity and 333/355 ratio was low for the protein. Since the isoelectric point of the protein is 5.2, the protein is unstable at this pH. At pH 6, there was shift in the ellipticity mimimum to 225 nm from 218 nm at pH 7. The protein showed maximum negative ellipticity at 218 nm at pH 7 in far UV CD spectrum. At pH 9, where the enzyme showed least activity, far UV CD spectrum showed minimum at 221 nm indicating rearrangement in the secondary structure elements (Fig. 7.5). There was a dramatic decrease in structural features at pH 11 as compared to pH 9. This may be because pH 11 is strongly alkaline and

might lead to charge repulsion between delicately balanced electrostatic charges leading to instability.

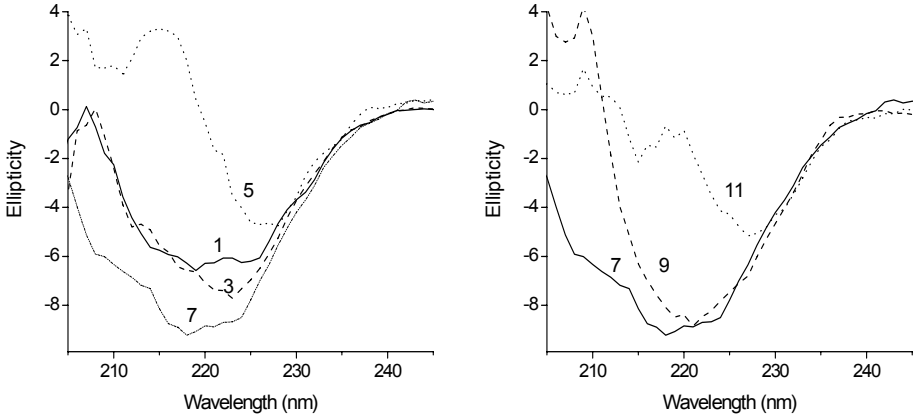

Fig. 7. 5: Far UV CD spectrum of *Bsp*PVA at different pH

From the above results it is seen that the fluorescence and CD data are very different from the activity trend of the enzyme for the hydrolysis of PenV. For instance, loss of secondary structure does not lead to loss in activity at pH 1 and 3. At pH 1, though there was significant activity, fluorescence intensity was minimum. Therefore, the active state of the enzyme is dependent on the protonated-deprotonated forms of active residues rather than the overall secondary structure or tertiary conformation of the protein. There was no aggregation at any of the pH tested at 30 ^{o}C. The protein also did not show any aggregation till 65 °C.

Fluorescence spectra showed that apart from change in the intensity of the protein in the acidic and alkaline pH range, there is no major change in the Trp environment of the protein (Data not shown). It is well-known that Trp fluorescence intensity decreases on protonation of water or neighbouring protonated acidic groups. In the zwitterionic states, aspartic and glutamic acid act as dynamic quenchers. Protonation of imidazole rings of histidine residues with a pK_a of 6.5 may also contribute to reduction in fluorescence intensity (Bushueva *et al.,* 1974). In strong alkaline

conditions, deprotonation of side chain amino group of residues can occur. The ε-amino group of lysine, guanidino group of arginine and phenol group of tyrosine are also known to quench the fluorescence of Trp residues in their deprotonated form (Bushueva, 1975, Steinberg, 1971) which explains decrease in intensity at extreme alkaline pH.

Far UV CD spectra of the protein at pH 7 shows characteristic minima of αβ proteins. The negative ellipticity at 222 nm is maximum at pH 7 and gradually decreases when moving towards either side of the pH range. Though there is decrease in ellipticity, the pH range 1 and 9 showed significant conservation of secondary structure (Fig. 7.5). Comparison of the near UV CD spectra of PVA at pH 7, shows that at pH 1 the structure completely collapses. Rayleigh light scattering studies showed no aggregation at any of the pH or temperatures from 30 °C to 65 °C. The ANS binding properties of the protein was then checked at different pH. PVA strongly bound ANS at acidic pH 1-4 with resultant increase in fluorescence intensity along with a blue shift in the λ_{max} from 520 to 480 nm, indicating exposure of hydrophobic patches on the surface (Fig. 7.4). The binding was maximum at pH 1-2. There was no ANS binding in the pH range 5 to 12. The binding was lost after readjustment of pH to 7 showing reversibility of structural changes at this pH. These results indicate the presence of molten globule state of pVA in pH 1-4.

7. 3. 3. Effect of Guanidine hydrochloride

*Bsp*PVA underwent progressive unfolding when incubated with increasing concentrations of Gdn HCl. During unfolding, the fluorescence intensity decreased gradually (Fig. 7. 6). Since Trp fluorescence can be quenched by water, it decreased upon unfolding of *Bsp*PVA as buried Trps started getting exposed to aqueous environment. Polar groups of protein themselves are also capable of quenching to a

certain extent. The 333/355 ratio of the native protein which was 1.27 in the native protein, decreased to 0.76 at 6 M Gdn HCl. The emission λ_{max} underwent a significant shift from 333 nm in the native protein to 355 nm at a Gdn HCl concentration of 6 M (Fig. 7. 7).

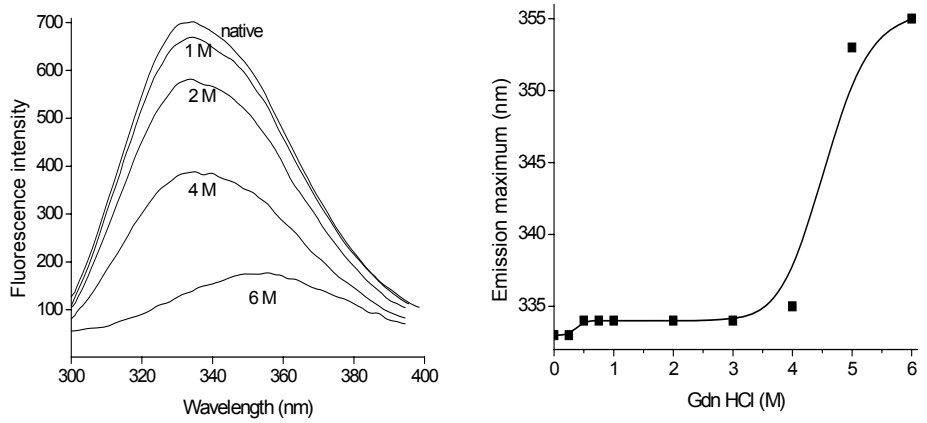

Fig. 7. 6: Fluorescence emission spectrum of *Bsp*PVA at different Gdn HCl molarities.

Fig. 7. 7: Wavelength of emission maxima at different Gdn HCl molarities.

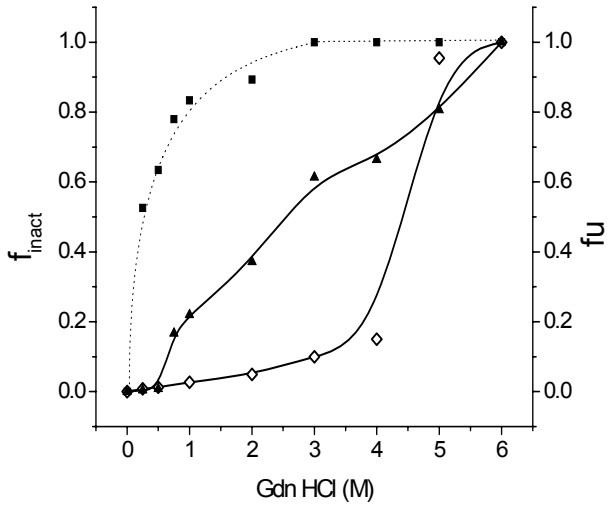

Fig. 7. 8: Effect of Gdn HCl on *Bsp*PVA. ---■---inactive fraction —◊—unfolded fraction calculated from F 333/350 ratio —▲— unfolded fraction calculated from ellipticity at 222 nm.

Hydrolase activity of PVA towards PenV decreased sharply with increasing concentrations of Gdn HCl. At 0.5 M Gdn HCl, the secondary and tertiary structures were intact but there was loss of 65% activity. At 1 M Gdn HCl, only 16% of the original activity was retained although there were no major disruptions in secondary and tertiary structures. This could be attributed to charged nature of Gdn HCl in solution which enables it to interact with active site residues of PVA. Positively charged guanidinium ion can react with negatively charged active residues. It may be remembered that *Bsp*PVA has an aspartic acid at the active site. At 3 M, there was complete loss of activity with 60% loss in secondary structure and negligible loss in tertiary structure. Secondary structure decreased gradually whereas there was a partial unfolding of the protein at 4 M Gdn HCl. Complete unfolding occured only above 4 M Gdn HCl whereas there was complete loss of activity at a concentration of Gdn HCl as less as 3 M. This showed that loss of activity at lower concentrations of Gdn HCl was independent of structural disturbances and at higher concentrations, the loss was due to modification of secondary structure (Fig. 7. 8). Thus, *Bsp*PVA lost enzyme activity much before it lost secondary or tertiary structures.

Denaturation curves were plotted with fraction of the protein inactivated (f_{inact}) and fraction unfolded (f_u) as a function of Gdn HCl concentration (Fig. 7.8). A plot of the ratio of fluorescence intensities at emission λ_{max} of native (333 nm) and denatured (355 nm) protein against Gdn HCl molarity was constructed and from the graph a two-state mechanism of unfolding was assumed. At each concentration, fraction of the protein in folded and unfolded forms were calculated using equations given in materials and methods section of this chapter. Free energy of unfolding in the transition range was calculated from these graphs and plotted as a function of Gdn HCl molarity from which the difference in free energy between the folded and unfolded states was determined (Fig. 7.9). The value of ΔG_D^{H2O} was found to be

12.29 kJ/ mol. Concentration of the denaturant required to unfold 50% of the protein molecules, $D_{1/2}$ was found to be 4.44 M at pH 7 at room temperature.

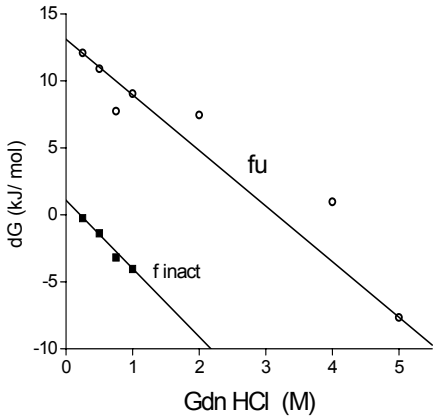

Fig. 7. 9: Free energy of unfolding as a function of Gdn HCl concentration

Upon renaturation, the enzyme regained fluorescence intensity (Fig. 7.10) and λ_{max} shifted back to 333 nm indicating that unfolding is completely reversible. There was not much recovery of activity after refolding the enzyme treated with different concentrations of Gdn HCl. There was no change in ANS binding indicating absence of exposure of any hydrophobic patches upon unfolding or refolding. Neither was aggregation observed.

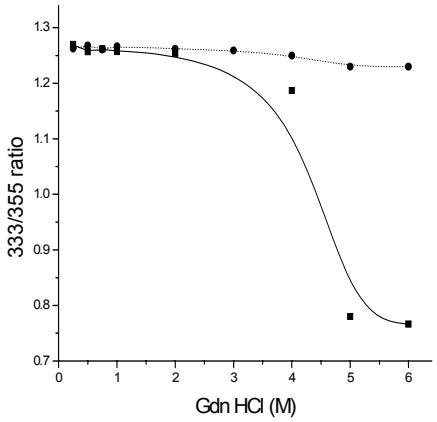

Fig. 7. 10: F 333/350 of *Bsp*PVA as a function of Gdn HCl ——♦——after unfolding and – –■– –refolding

Understanding the protein folding pathways requires structural characterization of both native structures and stable intermediate states. The crystal structure of the stable PVA from *B. sphaericus* was first solved in our laboratory. However, unstable, non-native intermediate states are less amenable to structure elucidation. This chapter has reported studies on solution dynamics in different conditions.

During our investigations using spectroscopic techniques, we found that PVA exists in a molten globule state in acidic pH conditions. Many proteins can exist in stable conformations that are neither fully folded nor unfolded. One of these states is the molten globule state, characterized by partly folded species with high proportion of native-like secondary structure but lacking persistent tertiary interactions. ANS binding is generally observed in molten globule states where hydrophobic regions that are usually buried in the native state are exposed to the polar medium due to flexibility or fluidity of the state (Semisotnov *et al.,* 1991). Forming of molten globule state is a general trend in globular proteins (Ohgushi and Wada, 1983). Most proteins are required to undergo conformational changes for functioning and molten globule states sometimes form intermediary stages during execution of a function. Typical characteristics of molten globule are observed for *Bsp*PVA at pH 1-3, viz., major retention of secondary structure, substantial distortion of tertiary structure and exposure of hydrophobic patches to the solvent.

Bychkova *et al* (1988) have hypothesised that the molten globule state is involved in the translocation of proteins across membranes. During membrane insertion of the pore-forming domain of colicin A, a bacteriocin that depolarizes the cytoplasmic membrane of sensitive cells, the acidic molten globular state could be an intermediate (van der Goot, *et al.,* 1991). The steroidogenic acute regulatory protein is believed to exist as a molten globule at reduced pH and the partially unfolded state may be critical to its biological action of moving cholesterol from outer to inner

membrane of adrenal and gonadal mitochondria for synthesis of steroid hormones (Bose *et al.,* 1999). The groEL chaperone stabilizes proteins, during their folding, in a conformation resembling the 'molten globule' state (Martin *et al.,* 1991). Protein-receptor interactions involve certain conformational changes in the molecules involved to fit each other. For example both insulin and its plasma membrane receptor (Nakagawa and Tager, 1993), antigenic peptides and immunoglobulins (Rini *et al.,* 1992), cyclosporin A and cyclophilin (Weber *et al.,* 1991) undergo small adjustments in their structure to accommodate each other. In a demonstration of structure-function relationship, the native alpha-lactalbumin structure present in milk provides nourishment and the multimeric molten globule form (MAL) in acid conditions fights tumor. Similarly, retinol-binding protein transports retinol in plasma as a complex with transthyretin. Under acidic conditions it undergoes transformation to molten globule which releases bound retinol (Bychkova, 1992). Molten globules are natural conformational states in protein folding process. However, enzymes rarely occur in an active molten globule form. PVA is now shown here to exist in molten globule form in acidic conditions which retained 80% of the enzyme activity.

Gdn-HCl and temperature induced molten globules have also been reported for some proteins. Creatine kinase was reported to exhibit an inactive molten globule form when denatured with 0.8 M Gdn-HCl. A temperature induced molten globule in the botulinum toxin has been reported (Kukreja and Singh, 2005). However, when tested under different conditions of Gdn-HCl during unfolding or refolding and at different temperatures, PVA did not exhibit any molten globule form or aggregates.

Gdn-HCl denaturation studies show that the protein is relatively unstable. It is widely acknowledged that due to high flexibility at the active sites compared to the rest of the protein, most proteins are inactivated before conformational changes occur. In this case it could also be attributed to charged nature of Gdn-HCl in solution, which enables it to interact with active site residues of PVA. The positively charged

guanidine group can react with negatively charged residues. Interestingly, PVA has an aspartic acid at the active site. At low concentrations, Gdn-HCl is known to confer effective charge shielding. The active site seems to involve hydrophobic and nonionic interactions (Monera *et al.,* 1994).

PVA is commercially used in the manufacture of semi-synthetic penicillins. Search is on for an enzyme that is more efficient in terms of yield and may function as cephalosporin acylase since semi-synthetic cephalosporin production is a complicated multi-step process. The main advantage of PVA is the operability at acidic pH. Denaturation studies indicate that the core of PVA, an Ntn hydrolase**,** which is known to be a compact $\alpha\beta\beta\alpha$-layered structure, is well-shielded. The protonation-deprotonation of active site residues in the core overrides the overall changes in secondary or tertiary conformations of the protein, as far as activity is concerned. Though the functional significance of the molten globule form *in vivo* is unclear, these observations have implications on the minimal structural requirement of the protein for activity.

Thus, PVA from *B. sphaericus* is relatively stable at high temperature and extremes of pH. It exhibits an active molten globule state in the acidic pH range 1-3. It can be a good catalyst in the production of 6APA as it gives a lot of flexibility in culture and extraction conditions because of its functional stability over a wide range of conditions. Our studies indicate that together with crystal structure, these studies can be a powerful tool to enhance the utility of such industrially important enzymes and that such studies can be used to screen and select candidates for such applications. Results presented in this chapter indicate that *Bsp*PVA is comparatively more stable in the presence of Gdn HCl and in acidic pH and at high temperatures as compared to *Bsu*PVA. Results obtained in various studies described in this as well as in the previous chapters are consolidated in the next chapter.

CHAPTER – VIII

COMPARATIVE STUDIES ON RELATED HYDROLASES: Part - III

Structure, Function and Evolution

Summary

Comparison of *Bsp*PVA and *Bsu*PVA shows that the former is a superior enzyme in terms of affinity and association constants for the substrates tested. It is more efficient in tolerating extreme temperatures and pH changes. The conformational stability in the presence of chaotrope is also better. This observation helps us to identify factors that make a protein a better PVA. The overall structure and the active site of the two enzymes superpose particularly well, pointing to minor critical changes in residues that lead to change in substrate specificity and efficiency. This throws open avenues for modification experiments to tailor a given protein to our need. The substrate cross reactivity also emphasises the evolutionary relatedness of the enzymes. Although we expected *Bsu*PVA to possess CBH activity, it could not be established with purified protein.

8.1 Introduction

The gene of YxeI was originally sequenced as part of an international project for the sequencing of the entire *Bacillus subtilis* genome. The gene *yxeI* lies in the region of DNA of the *bacterium B. subtilis* occurring between the *iol* and *hut* operons and has been reported to code for a hypothetical protein (Yoshida *et al.,* 1995). The open reading frame (ORF) is annotated as a hypothetical protein /choloylglycine hydrolase and a highly conserved putative penicillin amidase, based on sequence. Homology with other bacterial conjugated bile acid hydrolases (CBH) and PVA is high (Tanaka *et al.,* 2000). A BLAST search of the sequence against various databases revealed that the protein had significant levels of homology with both *Bsp*PVA and CBH from

various sources including *Clostridium perfringens* and *Bifidobacterium longum*, whose crystal structures have been reported, and a number of hypothetical proteins from different organisms.

The physiological role of penicillin acylase in host organisms is still not clearly established, despite years of research. Conjugated bile acid hydrolases have been thought to help the host bacteria present in the mammalian intestinal flora deconjugate the conjugated bile salts, thereby detoxifying them. Both the enzymes, however, have commercial applications- penicillin acylases are used in the industrial production of semi-synthetic penicillins and CBHs are used clinically for assaying levels of bile acids in biological fluids. Interest in YxeI arose primarily because of the similarity with *Bsu*PVA. Though recombinant expression of PVA was tried in *B. subtilis*, there is no report of any indigenous PVA. The present chapter describes the identification of PVA using sequence information, comparison with related sequences along with comparison of *Bsu*PVA with *Bsp*PVA.

Apart from helping to trace relatedness between the enzymes, which might lead to establishing a physiological role for PVAs, this comparative study also sheds light on the two PVAs from industrial stand point. This study explains the rationale behind superior PVA activity of *Bsp*PVA, and thus might help to pick out residues that could be subjected to site-directed mutagenesis to extend the substrate specificity of PVAs to cephalosporins. Using information from genomic data, YxeI has been characterized as a PVA. Observations from kinetic studies and comparison of similar studies conducted on the two proteins are discussed in this chapter.

8.2 Material and methods

8.2.1 Homology studies with other choloylglycine hydrolases

Protein Sequence analysis of YxeI was performed using *BLAST* (Altschul *et al.,* 1997) at the Swiss Institute of Bioinformatics site (http://au.expasy.org/tools/blast/) against UniProt knowledgebase using default settings. A blastp search was also done at the National Center for Biotechnology Information site (http://www.ncbi.nlm.nih.gov/BLAST/) against a nonredundant database. After selecting sequences with significant e values, redundancy was decreased using an upper cutoff of 85% sequence identity and the resulting sequences were screened and the N-terminal stretch of sequences that was not part of the alignment were removed from the analysis. All sequences began with cysteine at the N-terminal - otherwise they were removed. Multiple sequence alignment of the selected sequences was generated using the program ClustalW (www.ebi.ac.uk/clustalw) (Thompson, *et al* 1994). Phylogenetic trees were constructed using TreeView (Page, 1996) or Molecular Evolutionary Genetic Analysis (Kumar *et al*., 2004).

8.2.2 Inhibition kinetics

Kinetic studies were carried out by incubating the enzyme in different substrate concentrations in the presence of different inhibitors. The assays were carried out as described in chapter 2. Inhibitors were added to the mixture before the reaction was initiated with the addition of enzyme. The K_i vaules were calculated using LB plots.

8.2.3 Structure superpositions

Structural coordinates of the proteins were superposed using *LSQKAB* or superpose implemented in CCP4 and also manually checked using *QUANTA* (Accelrys).

8.2.4 Hydropathicity plot

A hydropathicity plot of the protein (Kyte and Doolittle, 1982) was constructed using ExPASy (Swiss Institute of Bioinformatics). Window size was set at 9 amino acids, when strong negative peaks indicate possible surface regions of globular proteins.

8.3 Results and Discussion

8.3.1 Sequence similarity to other PVAs and CBHs

Sequence homology studies indicate that the protein *Bsu*PVA is very similar to PAs and CBHs from different organisms. It shared a 40% sequence identity with *Bsp*PVA (Swissprot Accession No.P12256; PDB code 3PVA) and 39% with CBH from *Clostridium perfringens* (Swissprot Acc No. P54965; (PDB code 2BJF) whose crystal structures have been solved. It shared 32% identity with the well-characterised *Lactobacillus plantarum* CBH (Swissprot Accession No. Q06115) and 27% sequence similarity with a hypothetical protein A284L (Swissprot Accession No. P54965) from *Paramecium bursaria Chlorella* virus 1, which could also be a PVA /CBH. It has all the conserved residues of the family except for Asp20.

Phylogenetic analysis shows evolutionary links between CBH and PVA. A tree was constructed with the sequences found by BLAST as described in materials and methods section of this chapter. All members of the tree have the residues that are thought to be essential in PVA /CBH activity. Cys1, Arg17, Asn70, His141, Asp146, Asn173, Pro175 and Arg226 are conserved; a Glu substitutes Asp20 in some sequences. Another catalytically implicated residue Tyr80 varies in the sequences. (Residues are numbered starting from N-terminal cysteine of *Bsu*PVA.) Based on these observations, we have identified these hypothetical/ putative proteins that could have choloylglycine hydrolase or penicillin acylase activity. Many of these sequences, including that of *B. subtilis*, are part of genome sequencing projects. Once these proteins are fully characterised, the evolution of these enzymes can be better understood.

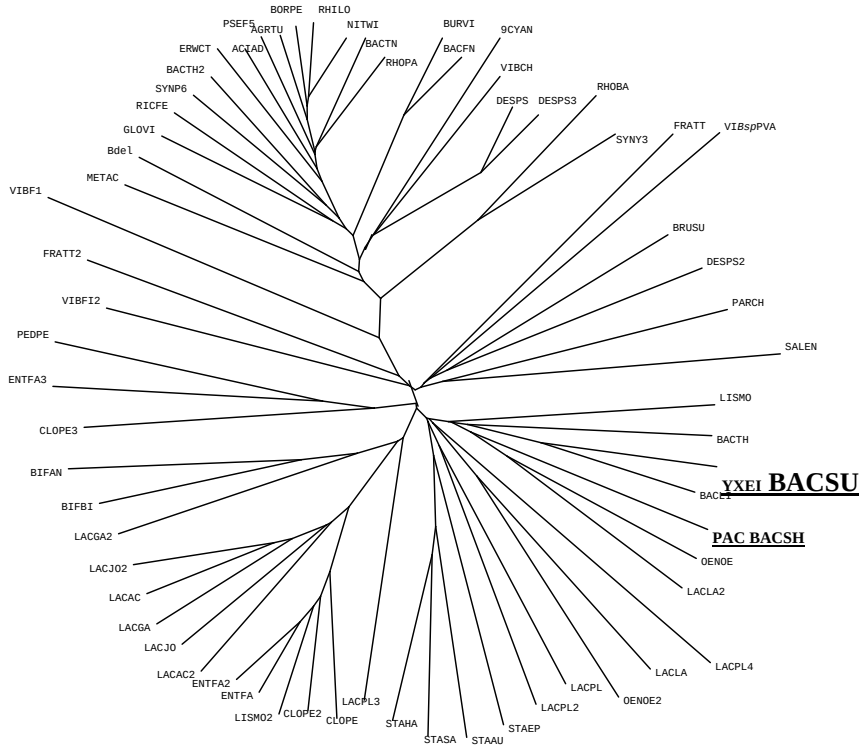

Fig. 8.1. A dendrogram showing relationships between proteins that are homologous to PVA of *B. subtilis* as found by the BLAST program. The distance of the branches corresponds to aminoacid substitutions per site. This tree was constructed using *TREEVIEW*.

The source of the proteins and their data bank accession numbers are: YXEI (Penicillin V acylase from *Bacillus subtilis*, Swissprot accession number P54948), LACLA (*Lactococcus lactis,* Trembl Acc no. Q9CGG1), GLOVI (*Gloeobacter violaceus,* Trembl Acc. No. Q7NNP2), BACTN (*Bacteroides thetaiotaomicron,* Trembl Acc. No. Q8A600), DESPS (*Desulfotalea psychrophila,* Trembl Acc. No. Q6ARU2), BACFN (*Bacteroides fragilis,* Trembl Acc. No. Q5L9F8), SYNP6 (*Synechococcus* sp., Trembl Acc. No. Q5N0N8), RHILO (*Rhizobium loti,* Trembl Acc. No. Q983W5), ACIAD (*Acinetobacter* sp., Trembl Acc. No. Q6FAR4), ERWCT (*Erwinia carotovora,* Trembl Acc. No. Q6D291), PSEF5 (*Pseudomonas fluorescens,* Trembl Acc. No. Q4KCA8), VIBF1 (*Vibrio fischeri,* Trembl Acc. No. Q5DZK1), METAC (*Methanosarcina acetivorans,* Trembl Acc. No. Q8TSP0), RICFE (*Rickettsia azadi,* Trembl Acc. No. Q4UKE3), RHOBA (*Rhodopirellula baltica,* Trembl Acc. No. Q7TU08), SYNY3 (*Synechocystis* sp., Trembl Acc. No. P72765), VIBCH (*Vibrio cholerae,* Trembl Acc. No. Q9KL70), 9CYAN (*Lyngbya majuscula,* Trembl Acc. No. Q6E7I9), BACLI (*Bacillus licheniformis,* GenBank Acc. No. 52005709), BACTH

(*Bacillus thuringiensis,* GenBank Acc. No. 49478365), LISMO (*Listeria monocytogenes,* GenBank Acc. No. 16802490), OENOE (*Oenococcus oeni,* GenBank Acc. No. 48864776), LACLA (*Lactococcus lactis,* GenBank Acc. No. 15673817), BACSH (*Bacillus sphaericus,* GenBank Acc. No. 129549), LACPL (*Lactobacillus plantarum,* GenBank Acc. No. 28379706), CLOPE (*Clostridium perfringens,* GenBank Acc. No. 18144368), STASA (*Staphylococcus saprophyticus,* GenBank Acc. No. 73661455), STAEP (*Staphylococcus epidermidis,* GenBank Acc. No. 27467268), LACPL (*Lactobacillus plantarum,* GenBank Acc. No 28377029) STAAU (*Staphylococcus aureus,* GenBank Acc. No 57286722), BRUSU (*Brucella suis,* GenBank Acc. No 23348317), STAHA (*Staphylococcus haemolyticus,* GenBank Acc. No 70725298), ENTFA (*Enterococcus faecium,* GenBank Acc. No 46518306), ENTFA (*Enterococcus faecalis,* GenBank Acc. No 29375146), LACPL (*Lactobacillus plantarum,* GenBank Acc. No 28379847), LACGA (*Lactobacillus gasseri,* GenBank Acc. No 12802353), LISMO (*Listeria monocytogenes,* GenBank Acc. No 16804106), LACGA (*Lactobacillus gasseri,* GenBank Acc. No 23003120), LACJO (*Lactobacillus johnsonii,* GenBank Acc. No 10732793), LACAC (*Lactobacillus acidophilus,* GenBank Acc. No 58337369), DESPS (*Desulfotalea psychrophila,* GenBank Acc. No 50876071), CLOPE (*Clostridium perfringens,* GenBank Acc. No 60417955), VIBFI (*Vibrio fischeri,* GenBank Acc. No 59713424), LACAC (*Lactobacillus acidophilus,* GenBank Acc. No 58337197), LACJO (*Lactobacillus johnsonii,* GenBank Acc. No 42519073), BIFBI (*Bifidobacteium bifidum,* GenBank Acc. No 40074455), OENOE (*Oenococcus oeni,* GenBank Acc. No 48865090), CLOPE (*Clostridium perfringens,* GenBank Acc. No 18144753), BIFAN (*Bifidobacterium animalis,* GenBank Acc. No 46486762), FRATT (*Francisella tularensis,* GenBank Acc. No 56708296), PARCH (*Paramecium bursaria chlorella virus 1,* GenBank Acc. No 9631852), ENTFA (*Enterococcus faecalis,* GenBank Acc. No 29377466), LACPL (*Lactobacillus plantarum,* GenBank Acc. No 28379105), PEDPE (*Pediococcus pentosaceus,* GenBank Acc. No 48870357), FRATT (*Francisella tularensis,* GenBank Acc. No 56708187), RHOPA (*Rhodopseudomonas palustris,* GenBank Acc. No 39934948), SALEN (*Salmonella enterica,* GenBank Acc. No 29141908), NITWI (*Nitrobacter winogradskyi,* GenBank Acc. No 75675071), BORPE (*Bordetella parapertussis,* GenBank Acc. No 33597843), Bdel (*Bdellovibrio bacteriovorus,* GenBank Acc. No 42522252), AGRTU (*Agrobacterium tumefaciens,* GenBank Acc. No 1793827), VI*Bsp*PVA (*Vibrio* sp., GenBank Acc. No 75856500), BURVI (*Burkholderia vietnamiensis,* GenBank Acc. No 67548680), DESPS (*Desulfotalea psychrophila,* GenBank Acc. No 50875094), BACTH (*Bacteroides thetaiotaomicron,* GenBank Acc. No 29338566).

Fig. 8.2. CLUSTALW multiple sequence alignment of known proteins belonging to choloylglycine hydrolase family. BIFLO (*Bifidobacterium longum* CBH), LACPL (*Lactobacillus plantarum* CBH), CLOPE (*Clostridium perfringens* CBH), BACSH (*Bacillus sphaericus* PVA), BACSU (*Bacillus subtilis* PVA) and PBCV1 (*Paramecium bursaria* chlorella virus 1 hypothetical protein). The data bank accession numbers are given in the results section of the text. * indicates conserved residues. Putative functional residues conserved in all the members of the dendrogram in Fig 8.1 are highlighted.

```
BIFLO   CTGVRFSDDEGNTYFGRNLDWSFSYGETILVTPRGYHYDTVFG--AGGKAKPNAVIGVGV 58
LACPL   CTAITYQS--YNNYFGRNFDYEISYNEMVTITPR--KYPLVFRK-VENLDHHYAIIGITA 55
CLOPE   CTGLALETKDGLHLFGRNMDIEYSFNQSIIFIPR--NFKCVNKSNKKELTTKYAVLGMGT 58
BACSH   CSSLSIRTTDDKSLFARTMDFTMEPDSKVIIVPRNYGIRLLEKE-NVVINNSYAFVGMGS 59
BACSU   CTSLTLETADRKHVLARTMDFAFQLGTEVILYPRRYSWN-SEAD-GRAHQTQYAFIGMG- 57
PBCV1   CSGLRIIADDGTVVVGRTLEFGEN----------------------ILKFKKFVNGNIRG 38
        *                 *

BIFLO   VMADRPMYFDCANEHGLAIAGLNFPGYASFVHEPVEGTENVATFEFPLWVARNFDSVDEV 118
LACPL   DVESYPLYYDAMNEKGLCIAGLNFAGYADYKKYDAD-KVNITPFELIPWLLGQFSSVREV 114
CLOPE   IFDDYPTFADGMNEKGLGCAGLNFPVYVSYSKEDIEGKTNIPVYNFLLWVLANFSSVEEV 118
BACSH   TDITSPVLYDGVNEKGLMGAMLYYATFATYADEPKKGTTGINPVYVISQVLGNCVTVDDV 119
BACSU   RKLGNILFADGINESGLSCAALYFPGYAEYEKTIREDTVHIVPHEFVTWVLSVCQSLEDV 117
PBCV1   ISTPDGKLLDGMNEHGLVIFVFYFKNYAKYG-CPSQTKLNIKPTEVALFLLQKAKNVKDV 97
                  *  ** **                                          *

BIFLO   EETLRNVTLVSQIVPGQQ-ESLLHWFIGDGK-RSIVVEQMADG-MHVHHDDVDVLTNQPT 175
LACPL   KKNIQKLNLVNINFSEQLPLSPLHWLVADKQ-ESIVIESVKEG-LKIYDNPVGVLTNNPN 172
CLOPE   KEALKNANIVDIPISENIPNTTLHWMISDITGKSIVVEQTKEK-LNVFDNNIGVLTNSPT 177
BACSH   IEKLTSYTLLNEANIILGFAPPLHYTFTDASGESIVIEPDKTG-ITIHRKTIGVMTNSPG 178
BACSU   KEKIRSLTIVEKKLDLLDTVLPLHWILSDRTGRNLTIEPRADG-LKVYDNQPGVMTNSPD 176
PBCV1   KAIAKTLNVIHESYPPFTETPPMHWLVTDASGKSIVLEPLGNGELTVFDNPMGIFTNAPT 157
                           *    *         *                  ** *

BIFLO   FDFHMENLRNYMCVSNEMAEPTSWGKASLTAWGAGVGMHGIPGDVSSPSRFVRVAYTNAH 235
LACPL   FDYQLFNLNNYRALSNSTPQNSFSEKVDLDSYSRGMGGLGLPGDLSSMSRFVRAAFTKLN 232
CLOPE   FDWHVANLNQYVGLRYNQVPEFKLGDQSLTALGQGTGLVGLPGDFTPASRFIRVAFLRDA 237
BACSH   YEWHQTNLRAYIGVTPNPPQDIMMGDLDLTPFGQGAGGLGLPGDFTPSARFLRVAYWKKY 238
BACSU   FIWHVTNLQQYTGIRPKQLESKEMGGLALSAFGQGLGTVGLPGDYTPPSRFVRAVYLKEH 236
PBCV1   FPEHMESAKKALEHLSPISDP--------NAASQGTGALGLPGDFSSASRFIRLAFFSQT 209
                                      * *  * ***     ** *

BIFLO   YPQQNDEAANVSRLFHTLGSVQMVDGMAKMGDGQF-----ERTLFTSGYSSKTNTYYMNT 290
LACPL   SLSMQTESGSVSQFFHILGSVEQQKGLCEVTDGKY-----EYTIYSSCCDMDKGVYYYRT 287
CLOPE   MIKNDKDSIDLIEFFHILNNVAMVRGSTRTVEEKS-----DLTQYTSCMCLEKGIYYYNT 292
BACSH   TEKAKNETEGVTNLFHILSSVNIPKGVVLTNEGKT-----DYTIYTSAMCAQSKNYYFKL 293
BACSU   LEPAADETKGVTAAFQILANMTIPKGAVITEEDEI-----HYTQYTSVMCNETGNYYFHH 291
PBCV1   IEIPRTSAGAVNTLFHVLNNFDIPKGVVASINMNTGKHVYEKTIYTVIYNIKSKEIVFKH 269
                      *  *       *               *

BIFLO   YDDPAIRSYAMADYDMDSSELISVAR---------------- 316
LACPL   YDNSQINSVSLNHEHLDTTELISYPLRSEAQYYAVN------ 323
CLOPE   YENNQINAIDMNKENLDGNEIKTYKYNKTLSINHVN------ 328
BACSH   YDNSRISAVSLMAENLNSQDLITFEWDRKQDIKQLNQVNVMS 335
BACSU   YDNRQIQKVNLFHEDLDCLEPKVFSAKAEESIHELN------ 327
PBCV1   YNDQNIQKL-------------------------------- 278
        *    *
```

Fig. 8.3. A neighbour-joining tree

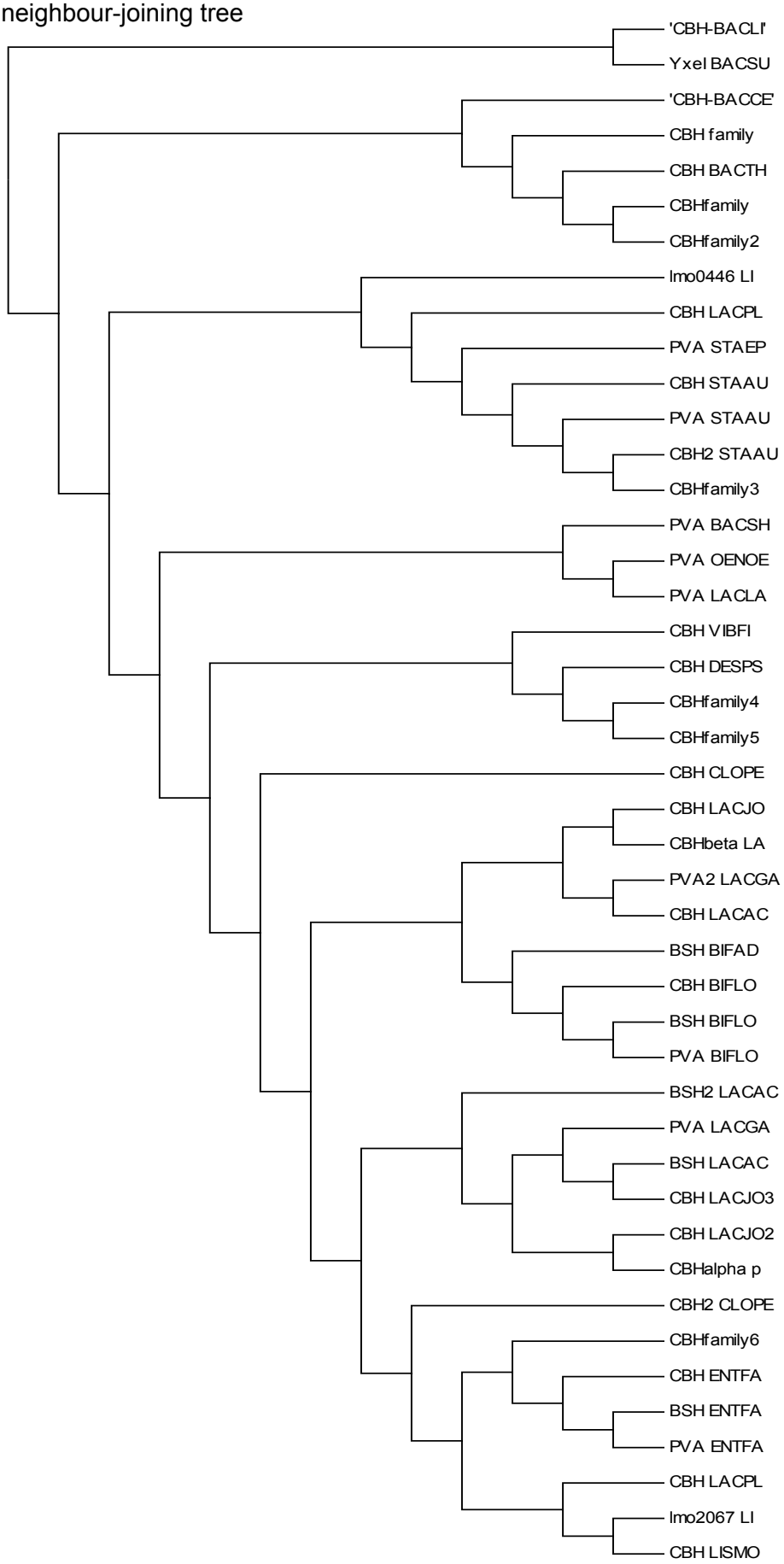

Fig: 8.4. A rooted UPGMA tree

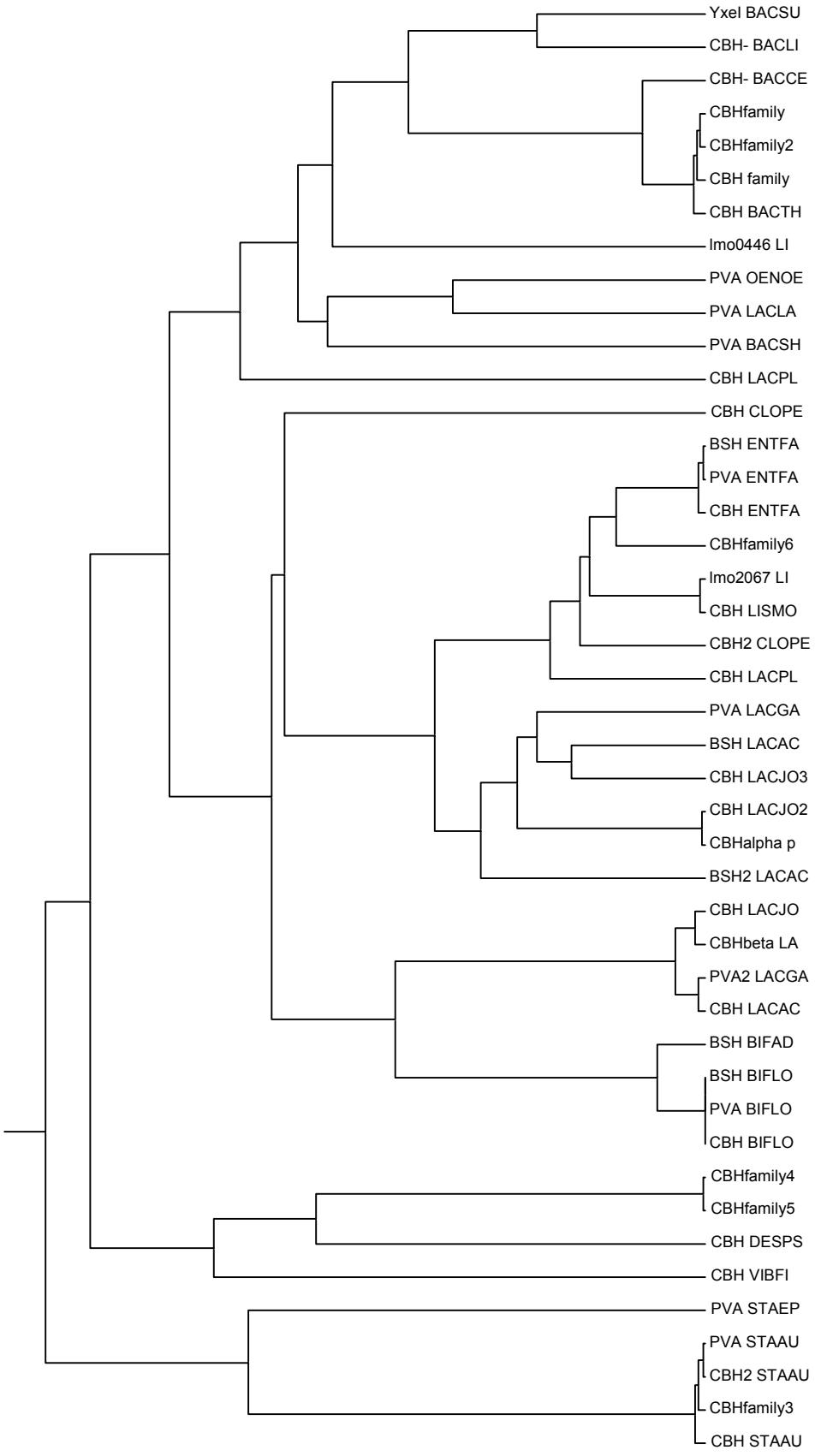

8.3.2 Structure similarities with *Bsp*PVA

The structure of *Bsu*PVA was compared to the other PVA structure that is available, that of *Bsp*PVA. The main chain of the structures overlap each other extremely well. The Cα trace shows a rms deviation of 0.88 Å. The catalytic residue Cys1 overlaps well as do Arg17, Asp20, Asp69, His143, Asp148, Asn175, Pro177 and Arg228. There are no major differences in the loops. The secondary structural elements overlap well, particularly in active site region.

Fig. 8.5: Superposition of monomers of *Bsu*PVA (blue) and *Bsp*PVA (magenta)

The different Trp emission spectra of the two proteins show that Trps lie in different environments. The Kyte-Doolittle plots shows the hydropathicity of protein residues. The sequence of *Bsu*PVA shows the presence of Trps at positions 38, 106, 142 and 179. Hopp-Woods plot (Hopp & Woods, 1981) (data not shown) shows that trytophan-38 and 179 could be in a hydrophilic local environment. From the crystal structure it is clear that Trp106 and Trp142 lie in the hydrophobic environment. Trp38 is found in the periphery of the protein and is accessible to solvent. This could be contributing to fluorescence emission at 350 nm. All the four Trps lie linearly with

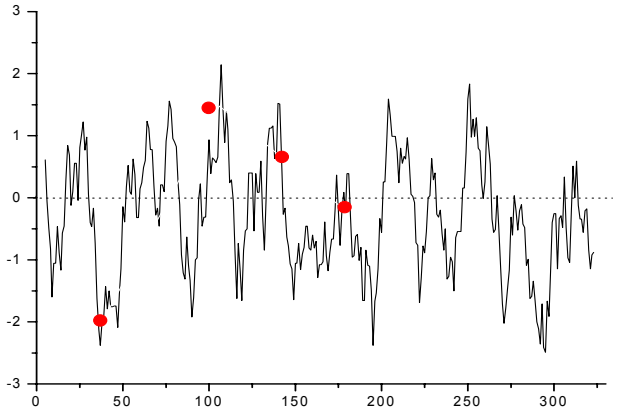

Fig. 8.6: Kyte-Doolittle plot for hydropathicity of PVA from *B. subtilis*. Trp are marked by '●'.

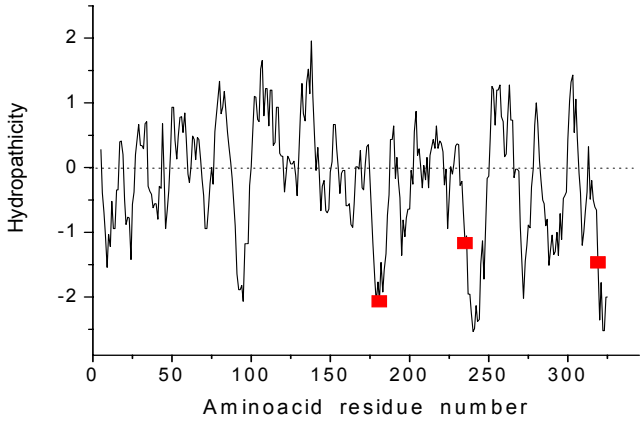

Fig. 8.7: Kyte-doolittle hydropathicity plot for *Bsp*PVA. Trp are marked by '■'.

distances between them in the range 10.3 to 15.6 Å. At distances in the range 7 to 12 the fluorescence emission spectrum of *Bsp*PVA shows maximum at 333 nm indicating that Trp lie in a hydrophobic environment with low mobility. Though the plot shows that the three Trps at positions 181, 235 and 319 are all in aqueous milieu, emission maximum of fluoresence shows that they are indeed in hydrophobic Å , there is a possibility of energy transfer (Ercelen *et al.,* 2001) between them. The distance between Trp142 and Cys1 is 11.42 Å, enabling us to follow changes at the active site through the fluorescence of Trp142. TrpA181 and TrpB181 sidechains are 3.457 Å away and solvent accessible.environment. This is in contrast to *Bsu*PVA where three of the four Trps are predicted to be in relatively polar environment

accessible to the aqueous milieu. This is also clear from the fluorescence spectra of the two enzymes; *Bsp*PVA has a sharp peak at 333 nm whereas *Bsu*PVA has a plateau from 330-350 nm. The sequence shows presence of aminoacids known to quench fluorescence in the vicinity of Trp. VMTNSPGYE**W**(181)HQTNLRAY, DFTPSARFLRVAY**W**(235)KKYTE and
QDLITFE**W**(319)DRKQDIKQLNQ

8.3.3 Comparison of the two proteins in denaturing conditions

8.3.3.1 Effect of temperature on activity and conformation

*Bsp*PVA showed better tolerance to increased temperature. *Bsp*PVA retains activity at 70 °C whereas *Bsu*PVA loses substantial activity at 60 °C. *Bsp*PVA retains significant secondary and tertiary structures at high temperatures. Thus the interactions that stabilize the two structures must be different in character or number.

8.3.3.2 Tolerance to pH changes

The optimal conditions for enzyme action were slightly different for the two enzymes. *Bsp*PVA was active at a lower pH range than *Bsu*PVA (6.6 - 7.5) highlighting differences in the nature of participating catalytic residues. The stabilities of the two proteins, as estimated by enzyme activity at different pH were different. *Bsu*PVA was unstable at acidic pH whereas, *Bsp*PVA retained significant activity. This has got to do more with the charges on groups of active residues as the secondary structure is not disturbed (Chapter 5 and 7). This shows that residues involved in stability and catalysis are different in character and charge.

Both the enzymes exist in a molten globule form in acidic pH. Under these conditions, they retain secondary structure, lose significant tertiary structure and show exposure of hydrophobic patches that are buried in native conditions. The remarkable difference between them is in their function. *Bsp*PVA is active under

these conditions whereas *Bsu*PVA is not. This shows that irrespective of changes that may occur in their structure, their function is primarily dictated by the protonation-deprotonation and environment of the active site.

8.3.3.3 Denaturation studies with guanidine hydrochloride

*Bsp*PVA was found to be more stable to Gdn HCl denaturation than *Bsu*PVA. It was unfolded only when the concentration of Gdn HCl reached beyond 4 M whereas *Bsu*PVA was unfolded much before. It appears that the hydrophobic and nonionic interactions that participate in intra or intersubunit interactions that stabilise the structure in *Bsp*PVA are stronger or numerous.

8.3.4 Affinity for substrates

*Bsp*PVA showed greater affinity for the substrate PenV. The K_m was 10 mM as opposed to 40 mM for *Bsu*PVA. The V_{max} was also higher indicating greater catalytic efficiency. The association constant, determined using Trp fluorescence (Chapter 4 and 6), was also greater for *Bsp*PVA indicating differences in the side chain of active site residues or their environment, as the main chain backbone of the two enzymes overlap particularly well.

Although in the absence of any substrate-complexed structure, the catalytic residues cannot be pin-pointed, from the structure of related PGA, equivalent residues can be identified. We can assume that the N-terminal cysteine plays the proton donor. This residue has been shown by chemical modification to be important for activity and also to bind substrate in *Bsu*PVA. Since such residues are conserved in both the proteins, the difference in binding efficiency may be due to geometric constraints.

8.3.5 Inhibition studies

Conjugated bile acids inhibited both *Bsu*PVA and *Bsp*PVA activity (Table 1 and 2). *Bsp*PVA shows significant inhibition in activity in the presence of bile salts. Conjugated forms of deoxycholic acid showed the maximum inhibition. There was no significant difference between glycine or taurine conjugated salts. Deoxycholic acid showed comparable inhibition indicating that the aminoacid moiety is not important for specificity and is not involved in binding. Chenodeoxycholic acid conjugates showed slightly lesser inhibition. Cholic acid conjugates showed the least inhibition. Competitive inhibitions indicate that bile salts compete at the substrate binding site. Phenoxyacetic acid slightly inhibited PVA activity. Cephalosporin significantly inhibited the enzyme.

Compared to *Bsu*PVA, the inhibitions are much more profound in the case of *Bsp*PVA indicating differences in the geometry of the active site and chemistry of the participating aminoacid residues in the two proteins. Inhibition suggests that PVAs can have CBH activity and vice versa. *Bsp*PVA was indeed found to have CBH activity. However, CBH activity could not be clearly established with purified *Bsu*PVA. Inhibition studies on *Bsu*PVA showed that the inhibitions very very feeble and so the inhibition constants could not be calculated. The only exception was cephalosporin which showed good inhibition. The percent residual activity in the presence of inhibitors compared to untrated enzyme, is tabulated in Table 8.2.

Table 8.1 Kinetics studies for *Bsp*PVA

Substrate/ Inhibitor	K_m / K_i
Penicillin V	10
Glycocholic acid	0.5
Glycodeoxycholic acid	0.04
Glycochenodeoxycholic acid	0.09
Taurocholic acid	0.58
Taurodeoxycholic acid	0.042
Taurochenodeoxycholic acid	0.05
Deoxycholic acid	0.044
Phenoxyacetic acid	10
Cephalosporin G	0.04

Table 8.2 Kinetics studies for *Bsu*PVA

1 mM	Percent activity
Glycodeoxycholic acid	95
Taurodeoxycholic acid	94
Deoxycholic acid	95
Phenoxyacetic acid	94
Amoxicillin	90
Cephalosporin C	35
Cephalosporin G	21

8.3.6 Similarities with CBH

Given close sequence homology, it appears possible that small crucial changes in sequence might lead to cross-reactivity between (PVA/CBH) of these choloylglycine hydrolase members. The newly solved CBH structure of *Clostridium perfringens* enables us to corroborate with structure. The active site cleft of these two PVAs are similar to the one from *C. perfringens*, showing possibility of cross-reaction between

substrates. Interestingly, *Bsp*PVA also showed CBH activity, confirming the evolutionary relatedness of these enzymes. Subtle changes in specificity and structure lead to different activities. The important conserved residues for activity, in CBHs, are found at similar positions in *Bsu*PVA also. It has four out of the five residues (Cys1, Asp20, Asn173 and Arg226) that are conserved in the oxyanion hole among the members of choloylglycine hydrolase family, implying structural similarity between them. The exception is Tyr81, which is common between *Bsu*PVA and other PVAs, whereas CBHs have Asn conserved at that position.

```
3PVA  CSSLSIRTTDDKSLFARTMDFTMEPDSKVIIVPRNYGIRLLEKENVVINNSYAFVGMGST
BsuPA CTSLTLETADRKHVLARTMDFAFQLGTEVILYPRRYS-WNSEADGRAHQTQYAFIGMGRK
2BJF  CTGLALETKDGLHLFGRNMDIEYSFNQSIIFIPRNFK-CVNKSNKKELTTKYAVLGMGTI

3PVA  DITSPVLYDGVNEKGLMGAMLYYATFATYADEPKKGTTGINPVYVISQVLGNCVTVDDVI
BsuPA LGNI-LFADGINESGLSCAALYFPGYAEYEKTIRADTVHIVPHEFVTWVLSVCQSLEDVK
2BJF  FDDYPTFADGMNEKGLGCAGLNFPVYVSYSKEDIEGKTNIPVYNFLLWVLANFSSVEEVK

3PVA  EKLTSYTLLNEANIILGFAPPLHYTFTDASGESIVIEPDKTGITIHRKTIGVMTNSPGYE
BsuPA EKIRSLTIVEKKLDLLDTVLPLHWILSDRTGRNLTIEPRADGLKVYDNQPGVMTNSPDFI
2BJF  EALKNANIVDIPISENIPNTTLHWMISDITGKSIVVEQTKEKLNVFDNNIGVLTNSPTFD

3PVA  WHQTNLRAYIGVTPNPPQDIMMGDLDLTPFGQGAGGLGLPGDFTPSARFLRVAYWKKYTE
BsuPA WHVTNLQQYTGIRPKQLE----------AFGQGLGTVGLPGDYTPPSRFVRAVYLKEHLE
2BJF  WHVANLNQYVGLRYNQVPEFKLGDQSLTALGQGTGLVGLPGDFTPASRFIRVAFLRDAMI

3PVA  KAKNETEGVTNLFHILSSVNIPKGVVLTNEGKTDYTIYTSAMCAQSKNYYFKLYDNSRIS
BsuPA PAADETKGVTAAFQILANMTIPKGAVITEEDEIHYTQYTSVMCNETGNYYFHHYDNRQIQ
2BJF  KNDKDSIDLIEFFHILNNVAMVRGSTRTVEEKSDLTQYTSCMCLEKGIYYYNTYENNQIN

3PVA  AVSLMAENLNSQDLITFEWDRKQDIKQLNQVN
BsuPA KVNLFHEDLDCLEPKVFSAKAEESIHELN
2BJF  AIDMNKENLDGNEIKTYKYNKTLSINHVN
```

Fig. 8.8: Alignment of residues according to their structural alignments. A stretch of 10 residues which could not be fitted into the structure are absent in *Bsu*PVA.

Fig. 8.9: Superposition of monomers of *Bsu*PVA (3PVA) (blue) and 2BJF (green).

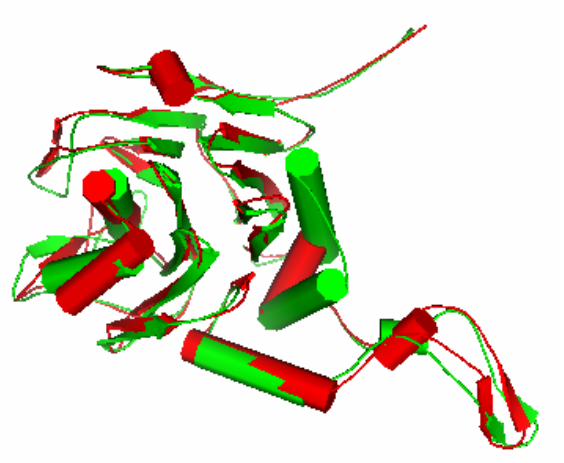

Fig. 8.10: Superposition of monomers of *Bsp*PVA (red) and 2BJF (green).

The superpositions of structures of *Bsu*PVA with *C. perfringens* CBH (PDB code 2BJF) shows remarkable similarity. The main chain of the structures overlap each other extremely well. The Cα trace shows a rms deviation of 2.62 Å. The catalytic residues Cys1, Arg17, Asp20, Asp67, His141, Asp146, Asn173, Pro175 and Arg226 overlap well.

Another similarity between *Bsu*PVA and CBHs is that the N-terminal nucleophile is revealed by a simple removal of N-formyl methionine, unlike *Bsp*PVA, which involves autoproteolysis to remove three residues at the N-terminus. This property could be of particular advantage in studying structure-function relationships of different aminoacids using site-directed mutagenesis as it represents a simpler model devoid of autoproteolytic processing requirements. *Bsp*PVA also shows good similaity to CBH. Phylogenetic analysis show that *Bsp*PVA could be an evolutionary intermediate during the divergence of PVAs and CBHs from a common precursor. The secondary structural elements overlap well particularly in active site region.

Conclusion

The advantage CBHs confer on the harbouring bacteria is still debated. Despite several years of extensive research, the physiological function of PAs also is not clear. Work on PGA suggested that they might function during the free-living mode of the organism as a scavenger for phenylacetylated and other aromatic compounds to generate a carbon source. The similarity between PVA and CBH gives us an opportunity to understand the physiological role of these enzymes better. Comparative studies on two PVAs reported here gives insights into structure-function relationships of different aminoacid residues and, even when active site aminoacids are conserved how their environment and binding sites can change the properties of the enzymes including their specificity.

CHAPTER – IX

STUDIES ON MALARIAL PROTEINS

Summary

Three calmodulin–like proteins from *Plasmodium falciparum,* MALP71.69, PF14_0181 and PF10_0301 were identified from PlasmoDB, the database for *Plasmodium* genome. All three genes were transformed into *E. coli*. Two of the genes could be expressed, but were insoluble. Solubilization and purification using various methods were attempted. Another protein, macrophage migration inhibitory factor (MIF) was purified, refolded and crystallisation attempted. A very crystalline precipitate was obtained. Translationally Controlled Tumour Protein from *P. knowlesii* was purified and crystallized using sodium citrate. Diffraction data were collected at the European Synchrotron Radiation Facility in France. The crystal diffracted very well to a resolution of 2.1 Å.

9. 1. Introduction

Malaria is an endemic disease in tropical countries and accounts for the death of more than a million people, especially children, every year and infects about 500 million. Malaria is caused by the protozoan *Plasmodium*; the most virulent species is *Plasmodium falciparum*. The vector, which spreads the parasite, is the mosquito *Anopheles gambiae*. The earliest methods to control malaria involved the eradication of mosquitoes, especially using insecticides like DDT. But the mosquitoes have circumvented the problem by developing resistance. The protozoan itself undergoes lot of antigenic variation, thereby making any vaccine prospects bleak. The sequencing of the genomes of malarial parasite, the vector- mosquito and the host-human, has provided a shot in the arm for understanding molecular mechanisms and treating / preventing the disease. Discovering the structure of proteins through X-ray

crystallographic studies provides invaluable assistance in the understanding of molecular mechanisms of important drug targets. The structure will shed light on the affinity of candidate drug molecules for sites in proteins and on important regions / residues in the target proteins, which could be exploited for screening and designing new drugs. The targets selected for the study were calmodulin-like proteins and the Macrophage migration inhibitory factor (MIF) apart from a group of translationally controlled tumour proteins (TCTPs).

Calmodulin is a protein that is modulated by levels of calcium in cells. It relays signals to a multitude of target proteins. The structure of calmodulin is known in various organisms. The structure of this important protein from the malarial parasite will enable us to exploit any critical differences between different organisms, specifically, between humans and the parasite, to develop drugs. Three proteins that had good sequence similarity with calmodulin were studied.

The macrophage migration inhibitory factor is an important immune system regulator in humans and plays an active role in inflammation. It inhibits macrophage migration and is associated with delayed hypersensitivity type reactions. It is also a phenyl pyruvate tautomerase. Studies using anti-migration inhibitory factor antibody have shown that it is beneficial in many inflammatory diseases like sepsis, adult respiratory distress syndrome, rheumatoid arthritis, glomerulonephritis etc. Inhibitors of this protein could be valuable anti-inflammatory therapeutic agents in diseases involving inflammation like malaria. This enzyme uses its N-terminal residue for catalysis, a property shared by a superfamily of enzymes called the N-terminal nucleophile hydrolases.

Artemisinin and its derivatives are important new antimalarial drugs. Artemisinin, the first drug of this class, was originally identified as a component of a Chinese herbal

remedy. Because these drugs are structurally unrelated to the classical quinoline and antifolate antimalarials, there is little or no cross-resistance. Like quinoline antimalarials, artemisinin appears to be selectively toxic to malaria parasites by interacting with heme, a byproduct of hemoglobin digestion, which is present in the parasite in high amounts. Recently, one of these target proteins was identified as a translationally controlled tumor protein (TCTP) homolog. The function of the malarial translationally controlled tumor protein and the role of this reaction in the mechanism of action of artemisinin await elucidation (Bhisutthibhan *et al.,* 1998).

9. 2. Materials and methods

9. 2. 1. Bacterial strains

The BL21 strain used for transformation is derived from *E. coli* and lacks the Lon and OmpT proteases. It is optimsed for high-level protein expression from T7 RNA polymerase-based expression systems. BL21 CodonPlus RIL strains (Stratagene) contain extra copies of rare *E. coli* tRNA genes for optimal expression of proteins encoded by rare codons. Kanamycin, chloramphenicol and various buffers and salts were procured from Sigma. Plasmid purification kits were bought from Promega Wizard or Qiagen. PCR cleaning kit was from Promega. DNA Ligase was from New England Biolabs.

9. 2. 2. Cloning of MAL7P1.69, PF14_0181 and PF10_0301

The following forward and reverse primers were synthesized at MWG Biotech, Germany. Forward 5' CATGCCATGGTATATAATTCTTTTCTAGTTCG 3'

Reverse 5' CCG CTCGAGTGAATTATTTAAAAGGTAAAAAATTG 3'

The required fragment of DNA was amplified by PCR. The mixture contained 200 µM of each dNTP, 65 ng of *P. falciparum* 3D7 DNA, 1 unit pfu polymerase, 10 pmol of forward and reverse primers in 1× NEB Thermopol buffer made upto a total of 50 µl with nuclease- free water. A standard 30-cycle amplification was performed, involving

a initial heating at 95 °C for 2 min followed by 30 cycles of 95 °C for 30 s, 45 °C for 30 s, 68 °C for 3 min and finally 68 °C for 10 min. Electrophoresis was performed in 1% agarose gels in Tris-Acetate-EDTA buffer at 120 V. Gels were stained with ethidium bromide and photographed under a UV trans-illuminator. The band of interest was spliced from the agarose gel and DNA extracted using a Promega Wizard column. The purified PCR product was digested with NcoI and XhoI in a total volume of 50 μl by incubating at 37 °C overnight. The restriction digested vector and insert were ligated using T4 DNA ligase (NEB) by incubating for 2 h at room temperature.

25 μl of novablue supercompetent cells (Novagen) was incubated with 5 μl of the ligation mixture on ice for 30 minutes. The cells were heat shocked at 42 °C for 90 s. Cells were then suspended in 500 μl of SOC medium (invitrogen) and incubated at 37 °C for 30 min. Cells were pelleted out, resuspended in 100 μl medium and plated onto Luria Bertani agar plates containing 30 μg ml^{-1} kanamycin and incubated overnight at 37 °C. 5 ml overnight culture was prepared from individual colonies. The plasmid was prepared using a Promega wizard kit and digested as described before and electrophoresed on a 1% agarose gel to ascertain the presence of insert. 1 μl of this plasmid preparation was used to transform 50 μl of *E. coli* BL21 codonplus cells.

For the cloning of PF14_0181 gene, the forward and reverse primers were synthesised at MWG Biotech, Germany.

Forward 5' TATCATGCCATGGGCATTGTAGATAAGCAA 3'

Reverse 5' TTTCCGCTCGAGCGAAAGAATTTTTTCTACAAATAC 3'

Novablue colonies transformed using the recombinant plasmid were screened for the insert and their plasmid preparation was used for transforming BL21 codonplus cells.

For the cloning of PF10_0301 gene, the primers used were

Forward 5' TATCATGCCATGGAGGTGAATTTC 3'

Reverse 5' TTTCCGCTCGAGACATAAATTTTTAATCATTTTCG 3'

Same procedures were followed as above for transforming BL21cells. The gene of interest was present in the correct orientation as shown by sequencing.

9. 2. 3. Expression

Cells grown in Luria Bertani medium containing 30 μg ml^{-1} kanamycin inoculated with 5% overnight culture were allowed to grow at 37 °C with shaking at 200 rev min^{-1} till they obtained an optical density of 0.6 at 600 nm. Cells were induced with 1mM IPTG and allowed to incubate at 30 °C for a further 4 h with shaking. The cells were pelleted out by centrifuging at 8000*g* for 30 min and the pellets frozen. Cells were thawed on ice and suspended in lysis buffer and sonicated on ice for two bursts of 10 s each with 10 s interval at an amplitude of 14 microns. A 12% SDSPAGE was run to check the presence of the protein of interest in the total and soluble fractions.

9. 2. 4. Denaturation purification

Cells were suspended in buffer containing 100 mM NaH_2PO_4 10 mM Tris HCl (buffer *A*) pH 8.0 containing 6 M Gdn HCl. The suspension was sonicated and spun at 8000*g* for 30 min. The supernatant was mixed with 50% Ni-NTA column and allowed to stand for 1 hour. After allowing the liquid to flowthrough and the column was washed twice with wash buffer *A* containing 8 M urea pH 6.3. Eluted the protein 4 times with buffer *A* containing 8 M urea pH 5.9 and then 4 times with buffer *A* containing 8M urea pH 4.5. Samples from various steps were run on a 12% SDS-Polyacrylamide gel.

9. 2. 5. Dynamic light scattering studies on MIF

In DLS, scattering of light when a monochromatic beam of light is incident on the sample is recorded at right angles. DLS studies were carried out on filtered protein sample containing 0.5 mg ml^{-1} in 100 mM NaCl, 10 mM Tris pH 8.5, 1 mM DTT at 20 °C using settings for globular proteins on a DynaPro instrument (Protein Solutions) for monochromatic beam of light of wavelength 825 nm. Data were analysed with Dynamics software.

9. 2. 6. Purification of MIF by Gel filtration

A prepacked superdex 75 column equilibrated with 20 mM Tris pH 8.5 100 mM NaCl 1 mM DTT was run on Akta FPLC at a maximum pressure of 0.35 MPa at 1 ml min^{-1}. The protein was concentrated, filtered, loaded and eluted using the same buffer used for equilibration.

9. 2. 7. Refolding of MIF

Purified MIF (1 mg) was resuspended in 3:30 ml of 6 M Gdn HCl/ 20 mM sodium dihydrogen phosphate in the presence of 1 µM DTT for 2 h. This was dialysed against 1 L of sodium phosphate and DTT pH 7.2 for 24 h. Dialysis repeated thrice in 5 L 20 mM sodium dihydrogen phosphate pH 7.2 for 24 h. The protein was then concentrated using centricons (amicon).

9. 2. 8. MALDI

The molecular weight of the protein was estimated on a sinapinic acid matrix using a Applied Biosystems Voyager system 4071.

9. 2. 9. Circular dichroism

Circular dichroism studies were carried out on a Jasco J-810 instrument. The settings were 2 nm band width, 1 s response time. Five accumulations were carried out at

100 nm min^{-1}. Measurements were carried out at room temperature in a cell with a pathlength of 0.1 cm.

9. 2. 10 Purification of TCTP

Recombinant *E. coli* cells, containing the protein with a His tag and AcTEV protease site, were grown in LB medium at 37 °C at 200 rpm till they attained an optical density of 0.6 at 600 nm. They were induced with 1 mM IPTG and incubated at 30 °C for 4 h with shaking. The cells were pelleted out and sonicated. The clear supernatant containing the protein was loaded on 5 ml HisTrap Nickel column (Amersham) at a flow rate of 1 ml min^{-1} at a pressure of 0.3 MPa on Akta FPLC (Amersham). The protein was eluted with an imidazole gradient. Fractions were checked for purity on a 12% SDS-PAGE. Fractions containing pure protein were pooled and digested using AcTEV Protease to cleave the tag. The tag was then removed by allowing the digestion mixture to pass again through a nickel column. The tag was retained on the column whereas the protein flowed through the column unbound. The fractions were then pooled, concentrated and purified further using superdex 75 16/60 column on Akta FPLC equilibrated with 20 mM HEPES buffer pH 7.5, 100 mM NaCl and 1mM DTT and concentrated to 10 mg ml^{-1}.

9. 2. 11. Crystallization of TCTP

Hanging drops were set up using 1 μl each of protein (10 mg ml^{-1}) and well solution made up of 1.36 M sodium citrate in 100 mM HEPES buffer pH 7.5. Rod shaped crystals grew in 4 days. A single crystal was scooped up from the drop, momentarily soaked in well solution containing 20% hexanetriol and flash frozen in liquid nitrogen.

9. 3. Results and Discussion

9. 3. 1. Cloning of Calmodulin-like proteins

The *Plasmodium falciparum* strain 3D7 is derived from NF54 line by dilution (Rosario, 1981). There are several putative calmodulin-like proteins in the *Plasmodium falciparum* genome database (www.plasmodb.org). Of these, three calmodulins that have single exons were selected namely, MALP71.69, PF10_0301 and PF14_0181 (Table 9.1). The aim of the investigation was to clone the proteins in order to overexpress them, purify and crystallise to study the X-ray crystal structure.

Gene name	Chromosome	Description
MAL7P1.69	7	calmodulin, putative
PF10_0301	10	calmodulin, putative
PF14_0181	14	calmodulin

Table 9.1: Specifications of calmodulins that were selected from *Plasmodium falciparum*.

MALP71.69 gene product has an estimated molecular mass of 30.1 kDa. This protein has a deduced length of 249 aminoacids and is slightly longer compared to the other calmodulins. PCR products amplified using Pfu DNA polymerase (Fig. 9.1) and pET28a vector were both digested separately with NcoI and XhoI. Ligation was then carried out with T4 DNA ligase. Ligated products were transformed with XL-1 novablue supercompetent cells. Transformants were picked up and analysed for the presence of insert. The plasmid was sequenced using T7 polymerase and the correct sequence of the gene ascertained. These cells were grown, plasmid harvested which was then used to transform competent BL-21 cells for expression.

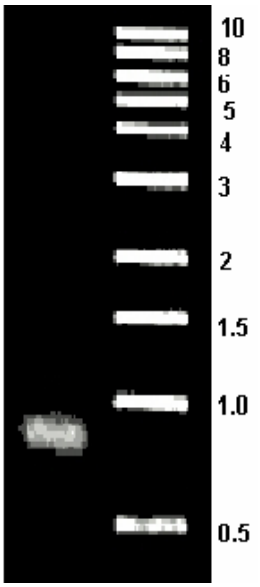

Fig. 9.1.: Amplification of MALP71.69. Lane 1 shows PCR-amplified product of MALP71.69. Lane 2 shows molecular mass markers (Promega). On the right, the masses are given in kbase.

MALP71.69 was first transformed in the BL-21* strain and C41, but showed no expression. Since the BL21 expression host series of *E. coli*, are protease deficient, when Rare, RareS and RIG of the BL-21 strains were used, they showed good overexpression of the protein. The BL21-CodonPlus series of strains (Stratagene) are variants of the BL21-Gold cells and contain extra copies of rare *E. coli* tRNA genes. This modification allows for high-level expression of many proteins that are difficult or impossible to express in conventional *E. coli* hosts due to the presence of rare codons like arginine codons AGA and AGG, isoleucine AUA, leucine CUA, and proline CCC thereby resolving the problem of codon bias for organisms like *Plasmodium* whose genome is AT-rich. However, the protein was totally insoluble in all the strains in which it was expressed and attempts to solubilise it were unsuccessful (Fig. 9.2). The protein could not be purified using different conditions of sonication, growth or temperature. Temperature of induction was varied from 30 to 16 °C. Lower temperatures have been reported to enable proper folding of proteins.

The period of induction was also varied. Triton X-100 was tried during sonication and with different buffers and at different pH and in the presence of EDTA. Presence of lysozyme during sonication did not make any difference either. The speed of shaking during cell growth was varied. Presence of calcium did not help in the solubilisation of the protein. IPTG was also tried at different concentrations. Rich medium containing metals was unsuccessfully tried for growth. The protein was denatured in urea or guanidine hydrochloride (Qiagen) and tried for solubilisation. The protein was soluble after Gdn HCl treatment and heating.

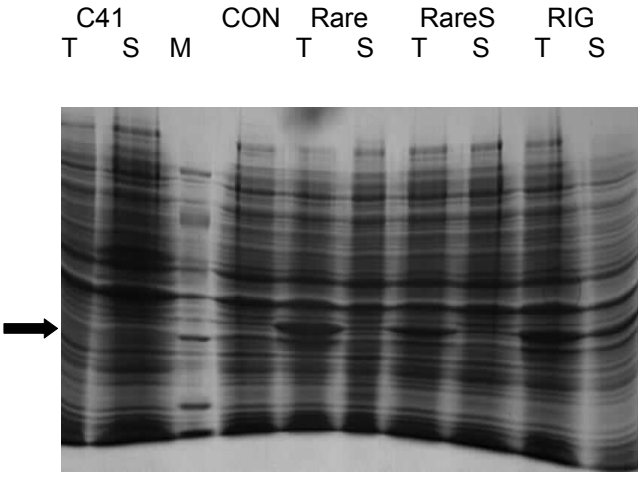

Fig. 9.2: Expression of MAL7P1.69. T indicates total cell sonicate and S indicates the soluble fraction. Lane containing molecular weight markers is indicated by M. Uninduced cells were used as control (CON).

9.3. 2. Cloning PF14_0181

Calmodulin like proteins present on chromosome 14 (gene PF14_0181) was cloned in pET28a and overexpression was achieved in BL-21*. It showed expression when induced with IPTG at 30 °C for 4 hours, but was insoluble. Again, this protein was totally insoluble and attempts to solubilise it were unsuccessful (Fig. 9.3). Reducing the temperature to 16 °C and incubation overnight did not produce any improvement in solubility.

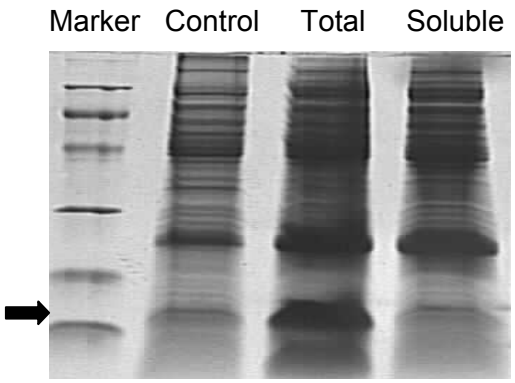

Fig. 9.3: Expression of PF14_0181. The protein is present in the total fraction (Lane 3) of sonicated cells (indicated by arrow) but is absent in the soluble fraction (Lane 4). Uninduced cells served as the control (Lane 2).

9. 3. 3. Cloning PF10_0301

The calmodulin gene from chromosome 10 (PF10_0301) was amplified using PCR (Fig. 9.4). DNA was amplified using pfu polymerase with specific primers and cleaned the PCR product with the Promega kit. Digestion was with NcoI and XhoI, vector used was pET28a and successfully transformed in XL-1 blue cells. It, however, did not express in the strains.

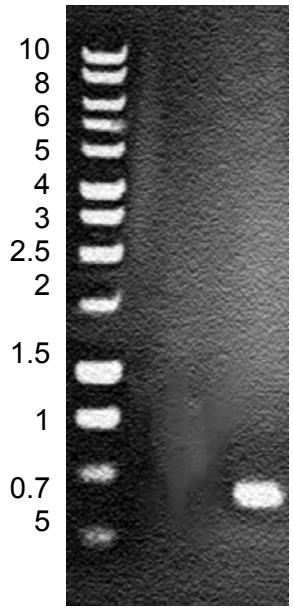

Fig. 9.4: Amplification of PF10_0301. Lane 1 shows molecular mass markers (Promega). On the left, the masses are given in kbase. Lane 2 shows PCR-amplified product of PF10_0301.

9. 3. 4. Purification and crystallisation trials of macrophage migration inhibitory factor

Macrophage migration inhibitory factor was available in a purified form through a collaboration. It was screened for crystallisation conditions using the commercially available screens as well as some other conditions, mainly based on ammonium sulphate (AS) precipitation. The commercial screens that were tried were Hampton crystal screen 1 and Hampton crystal screen 2, Clear Strategy Screen (Molecular Dimensions Inc.) at pH 5.6 and 8.6, PEG Ion Screen, Stura footprint and the Hampton Index Screen. Crystallisation trials with AS showed granular precipitate in the pH range 4.6- 6.0 and at concentration of AS at 1.5 to 2.5 M. Various additives were tried in combination with AS. Preliminary conditions did not yield any crystals. Investigation using Dynamic Light Scattering showed presence of precipitate (Fig. 9.5). The hydrodynamic radius of the precipitate was calculated to be 3.99 nm, indicating the presence of hexamers of MIF.

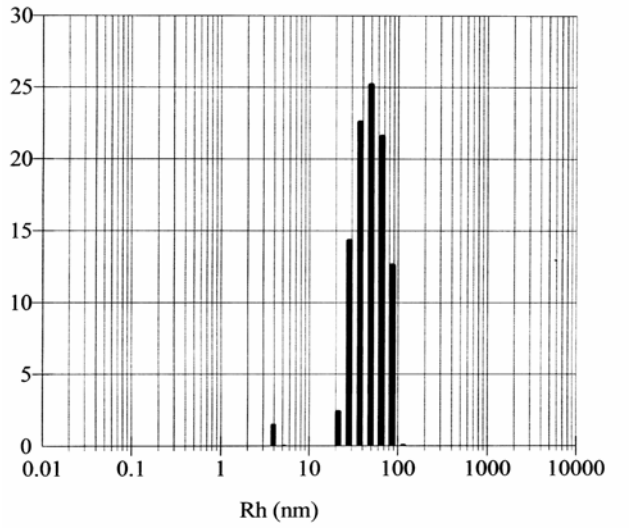

Fig.9.5 DLS regularisation histogram of MIF. This size distribution histogram shows presence of aggregates in the protein sample.

The protein was then purified on a gel filtration column (a native PAGE showed that the protein was rid of precipitates (Fig. 9.6), this sample was then used for crystallisation experiments. The protein was also refolded using the procedure outlined in methods section of this chapter and the resultant sample used for crystallisation (Fig. 9.7). The molecular weight of refolded monomeric MIF as calculated from SDS_PAGE and ascertained from MALDI as 14055 (Fig. 9.8). Refolding of MIF was followed using CD. Far UV CD spectra were recorded in the range 185 – 250 nm. The refolded protein showed good structural features (Fig. 9.9). A very crystalline precipitate was obtained with ammonium sulphate (Fig. 9.10). This could be reproduced but could not be further improved. The inability of the protein could arise from the fact that the protein was several months old. Proteins develop a tendency not to crystallise on keeping.

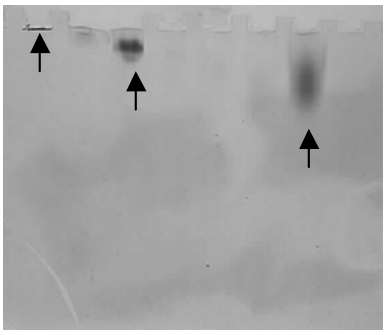

Fig. 9.6 : Native PAGE showing purification of MIF from aggregates. Arrows indicate different protein fractions from the column.

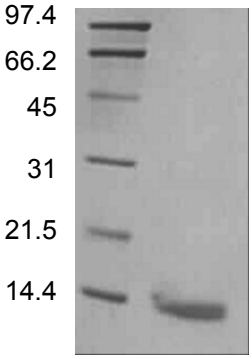

Fig. 9.7: Purified and refolded MIF. Left lane shows mass of molecular markers in kDa. The pure protein is shown in the second lane.

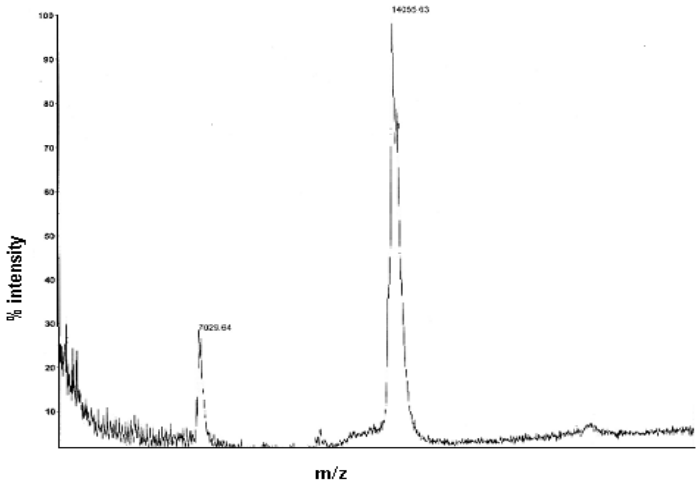

Fig. 9. 8: Molecular weight determination by MALDI.

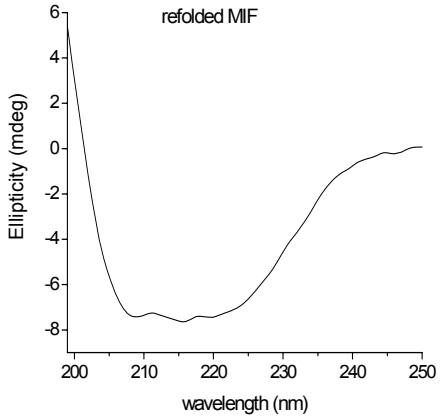

Fig. 9.9: CD spectra of MIF. The refolded MIF shows good secondary structural features

Fig. 9. 10 : Crystalline precipitate of MIF. This was reproducible, but could not be further improved.

9. 3. 5. Expression, purification, crystallisation and X-ray diffraction studies on the translationally controlled tumour protein

TCTP homologs from different species namely, *falciparum, vivax, knowlesii, yoelii, Berghii,* were overproduced and purified. The clones gave excellent expression. Recombinant TCTP from *P. knowlesii* cloned into E. coli cells was expressed and purified on a HisTrap HP (Amersham Biosciences) Ni-NTA matrix. The tag was removed by digestion with AcTEV protease and passing through nickel column. It was further purified on a superdex 75 gel filtration column (Fig 9.11). The molecular weight was estimated by MALDI to be 20458. CD showed good secondary structural features (Fig. 9.12).

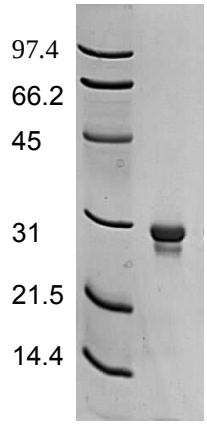

Fig. 9.11.: Purified and digested TCTP. Left lane shows molecular mass markers in kDa.

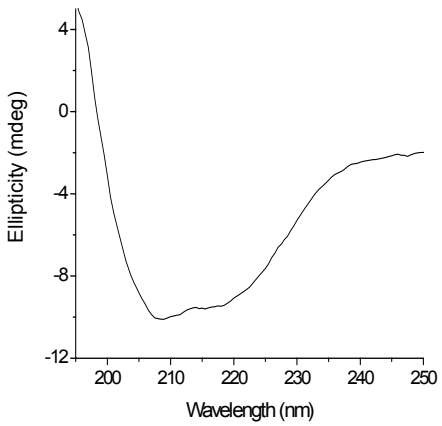

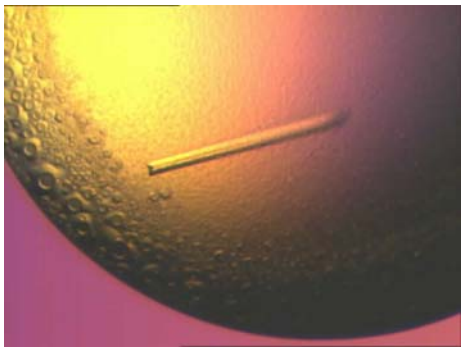

Fig. 9.12: Far UV CD of purified TCTP showing good secondary structural features.

Fig. 9.13 : A TCTP crystal.

The TCTP homolog from *P. knowlesii* was taken up for crystallisation. Preliminary conditions were screened using Hampton, Marek, PEG ion and Stura screens and ammonium sulphate and citrate. Needles were obtained with citrate as the precipitant. The fine tuned condition was supplied through a research collaboration. The protein gave good diffraction quality, long rod-shaped, crystals with 1.36 M sodium citrate in 100 mM HEPES buffer pH 7.5 (Fig. 9.13). The concentration of protein was around 10 mg ml^{-1} in 20 mM HEPES pH 7.5 with 100 mM NaCl and 1mM DTT. The diffraction data were collected on the crystal at the European Synchrotron Radiation Facility at Grenoble, France. The crystal diffracted very well to a resolution of 2.1 Å.

The study helps in highlighting the challenges while working with eukaryotic proteins and the problems pertaining to malarial proteins in particular. Of particular concern is the problem of insolubility of recombinant proteins when expressing in prokaryotic host systems. Since the genome of plasmodium was sequenced completely, it has thrown a myriad of opportunities for understanding and combating the pathogenic organism. However, the practical difficulties in handling the proteins highlight how daunting the task actually is.

Appendix

Purification, crystallization, data collection and processing of FemX from *Weissella viridescens* and purification of FemB from *Staphylococcus aureus*

Introduction

The imprudent use of broad spectrum antibiotics has resulted in the prevalence of bacteria that are resistant to a wide variety of antibiotics. This problem can be overcome by designing drugs that are very specific for target pathogens. Methicillin resistant *Streptococcus aureus* is one of the most serious pathogens. One group of the candidate targets in this organism could be the factor essential for methicillin resistance, which is very important for the survival of the bacteria and is specific to a small subgroup of Gram positive organisms, making it a very specific and vital target. FemABX family of proteins are non-ribosomal peptidyl transferases and have an active role to play in the synthesis of the interchain pentapeptide of the peptidoglycan of the bacterial cell wall. FemX is believed to be responsible for the addition of the first glycine of the pentapeptide (Rohrer *et al*, 1999), while FemA and FemB catalyse the second and third, and the fourth and fifth additions, respectively (Tschierske *et al*, 1999). Among the three enzymes involved in the peptidoglycan synthesis pathway, the structure of *S. aureus* FemA (Benson et al., 2002) and *Wiesella viridescens* FemX (Biarrotte-Sorin *et al*, 2004) have been reported before we could complete the structure analysis.

Expression and purification FemX

The gene for the FemX peptidyl transferase cloned in a vector containing ampicillin and kanamycin as the selectable markers was obtained from the authors (Hegde & Shrader, 2001), with a 6×His affinity tag at the C-terminal. 30 mg ml^{-1} kanamycin and 100 mg ml^{-1} ampicillin stocks were prepared and ultrafiltered using a 2 μm filter. Recombinant *E. coli* cells were inoculated in 50 ml Luria-Bertani medium containing 0.1% glucose, 30 μg ml^{-1} kanamycin and 100 μg ml^{-1} ampicillin and incubated in a shaker at 200 rev min^{-1} at 37 °C overnight. From the overnight cell culture, 2 ml of the medium was transferred to 100 ml LB media with ampicillin and kanamycin and incubated for 4 h at 37 °C. This culture was induced with 0.1 mM isopropyl thiogalactoside and allowed to shake for 4 h at 30 °C. The cells were harvested by centrifugation at 8000 rev min^{-1} for 20 min at 4 °C and stored frozen till further processing.

The frozen cells were thawed and suspended in potassium phosphate buffer 50 mM pH 7.5 containing 20 mM imidazole and 250 mM NaCl (buffer *A*). Henceforth, the enzyme was maintained on ice. The suspension was sonicated thrice for 1 minute with 5 minute intervals. This was centrifuged at 8000 x*g* for 30 min and the cell debris was removed. The supernatant was mixed with 7 mg ml^{-1} streptomycin sulphate and stirred in the cold for 1 h, to precipitate and remove DNA. The resulting sample was centrifuged for 30 min at 8000 x*g* to remove the precipitated DNA. The nickel affinity column was equilibrated with buffer *A* and washed with 50 ml of potassium phosphate buffer 50 mM pH 7.5 containing 35 mM imidazole and 250 mM NaCl (buffer *B*). Loaded the supernatant and passed 50 ml of buffer *B*. The protein was eluted with potassium phosphate buffer 50 mM pH 7.5 containing 250 mM imidazole and 250 mM NaCl. The absorbance of the fractions was read at 280 nm and the fractions containing the protein checked for purity using SDS-PAGE and finally the pure fractions were pooled and concentrated. It was further dialysed against potassium phosphate buffer 50 mM pH 7.5 to remove imidazole.

Crystallization of FemX

FemX was dialyzed against 100 mM sodium chloride. The protein was crystallized by the hanging drop vapour diffusion method at a concentration of 10 mg ml^{-1} with 1 μl of protein solution to which 1μl of precipitant was added to set up the drop. The precipitant that gave the crystal was 20% polyethylene glycol (MW 8000) at pH 6.0. Other precipitants tried yielded extremely thin and very small crystals. The crystals grew in 10 days time at 18 °C. They were thin long needles or diamond shaped thin plates. The quality of the crystals deteriorated very quickly upon exposure to X-rays. It was extremely difficult to collect data either at room temperature or by freezing the crystal. Eventually good data could be collected at room temperature from a long crystal in two stages by translating the crystal to expose two different edges of the crystal for two data sets.

Data Collection and processing for FemX

Data were collected by keeping the detector at 200 mm and giving 0.5° oscillation to the crystal. Exposure time chosen was 2 min. The mosaicity of the crystal was 0.7. The unit cell dimensions determined were found to be *a*= 42.48 Å, *b*= 102.09, *c*= 47.44 Å and β=102.63 in a monoclinic space group P21. The processed and scaled data from the two sets gave R merge 0.106 (0.218) for the resolution range 50-3.0 Å and completion 82.4 (85%). At this stage, the same crystal structure was reported

by another group in the same unit cell (Biarrotte-Sorin, 2004) and so the work was abandoned.

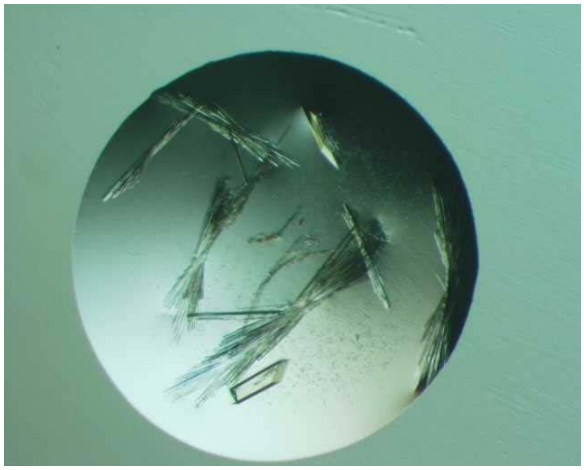

Fig. 1: Crystals of FemX.

Expression and purification of FemB

Since FemX structure was solved, we switched over to studies on FemB as FemA structure also has been reported earlier. FemB from *Staphylococcus aureus* was cloned into *E. coli* (Rohrer *et al*, 1996). The recombinant *E. coli* cells containing the plasmid were obtained from the authors, grown from 5% overnight cultures in shaker cultures with Luria-Bertani medium grown till they attained an optical density of 0.8 at 595 nm. The cells were then grown in shaker cultures at 200 rpm for five hours. Isopropyl thiogalactoside was added at a final concentration of 1 mM to induce the production of the enzyme. The cells were allowed to incubate at 30 ^{o}C for another 4 hours at 200 rev min^{-1}. The culture medium was centrifuged at 8000 x*g* in a Sorvall centrifuge for 20 min and the supernatant was discarded. The cells were weighed and frozen. The recombinant protein was purified using nickel NTA column. The purified protein had a subunit molecular weight of ~50,000. MALDI and amino-terminal sequencing were carried out at Indian Institute of Science, Bangalore. The protein aggregated on purification. The soluble portion was quickly set up for extensive crystallisation trials. None of the crystallisation conditions were successful. The crystals that did appear were tested for diffraction. They turned out to be salt crystals. Further investigations conclusively proved all the protein was precipitated and there was no protein in the purified protein sample used for crystallization, which explains why no protein crystals were grown in any of the conditions. The next batch of protein is under preparation.

REFERENCES

Benson, T.E., Prince, D., Mutchler, V., Curry, K., Ho, A., Sarver, R., Hagadorn, J., Choi, G. and Garlick, R. (2002). X-ray crystal structure of Staphylococcus aureus FemA. *Structure (Camb.)* **10**: 1107–1115.

Biarrotte-Sorin, S., Maillard, A. P., Delettré, J., Sougakoff, W., Arthur, M. and Mayer, C (2004). Crystal Structures of *Weissella viridescens* FemX and Its Complex with UDP-MurNAc-Pentapeptide Insights into FemABX Family Substrates Recognition. *Structure* **12**:257-267.

DeLano, W.L. (2002). *The PyMOL Molecular Graphics System*, DeLano Scientific, San Carlos, CA.

Hegde, S.S. and Shrader, T.E. (2001). FemABX family members are novel nonribosomal peptidyltransferases and important pathogen-specific drug targets. *J. Biol. Chem.* **276**:6998–7003.

Rohrer, S. and Berger-Bächi, B. (2003). FemABX peptidyl transferases: a link between branched-chain cell wall peptide formation and beta-lactam resistance in gram-positive cocci. *Antimicrob. Agents Chemother.* **47**:837–846.

Rohrer, S., Ehlert, K., Tschierske, M., Labischinski, H. and Berger-Bächi, B. (1999). The essential *Staphylococcus aureus* gene fmhB is involved in the first step of peptidoglycan pentaglycine interpeptide formation. *Proc. Natl. Acad. Sci. USA* **96**:9351–9356.

Tschierske, M., Mori, C., Rohrer, S., Ehlert, K., Shaw, K. J. and Berger-Bachi, B. (1999). Identification of three additional femAB-like open reading frames in *Staphylococcus aureus*. *FEMS Microbiol. Lett.*, **171**:97-102.

REFERENCES

Abraham, E.P. (1981). The β-lactam antibiotics. *Sci. Am*. **244**: 64-74.

Abraham, E.P. (1987). Cephalosporins 1945-1986. *Drugs* **34**:1-14.

Acar, J.F., Sabath, L.D. and Ruch, P.A. (1975). Antagonism of the antibacterial action of some penicillins by other penicillins and cephalosporins. *J. Clin. Invest*. **55**:446-53.

Ali, V., Prakash, K., Kulkarni, S., Ahmad, A., Madhusudan, K.P. and Bhakuni, V. (1999). 8-Anilino-1-naphthalene sulfonic acid (ANS) induces folding of acid unfolded cytochrome *c* to molten globule state as a result of electrostatic interactions. *Biochemistry* **38**:13635-13642.

Alkema, W. B. L., Floris, R. and Janssen, D. B. (1999). The use of chromogenic reference substrates for the kinetic analysis of Penicillin Acylases. *Anal. Biochem*. **275**:47-53.

Alkema, W.B., de Vries, E., Floris, R., Janssen, D.B. (2003). Kinetics of enzyme acylation and deacylation in the penicillin acylase-catalyzed synthesis of beta-lactam antibiotics. *Eur J Biochem*. **270**:3675-83.

Alkema, W.B.L., Hensgens, C.M.H., Kroezinga, E.H., de Vries, E., Floris, R., Laan, v.d., J.-M., Dijkstra, B.W. and Janssen, D.B. (2000). Characterization of theβ-lactam binding site of penicillin acylase of *Escherichia coli* by structural and sitedirected mutagenesis studies. *Protein Eng*.**13**:857-868.

Altschul, S. F., Madden, T. L., Schaffer, A. A., Zhang, J., Zhang, Z., Miller, W. and Lipman, D. J. (1997). Gapped BLAST and PSI-BLAST: a new generation of protein database search programs. *Nucleic Acids Res*. **25**:3389-3402.

Ambedkar, S. S., Deshpande, B.S., Sudhakaran, V.K. and Shewale, J.G. (1991). *Beijerinckia indica* var. penicillanicum penicillin V acylase: enhanced enzyme production by catabolite repression-resistant mutant and effect of solvents on enzyme activity. *J. Ind Microbiol*. **7**:209-214.

Ambedkar, S.S., Deshpande, B.S. and Shewale, J.G. (1997). Separation of cephalosporin C acylase and penicillin V acylase from *Aeromonas* ACY 95 by chemical treatment. *Proc. Biochem.* **32**:305-307.

Antignac, A., Boneca, I.G., Rousselle, J.C., Namane, A., Carlier, J.P., Vazquez, J.A., Fox, A., Alonso, J.M. and Taha, M.K. (2003). Correlation between alterations of the penicillin-binding protein 2 and modifications of the peptidoglycan structure in *Neisseria meningitidis* with reduced susceptibility to penicillin G. *J Biol Chem*. **278**:31529-31535.

Arroyo M., de la Mata, I., Acebal, C. and Castillón, P. (2003). Biotechnologicalapplications of penicillin acylases: state-ofthe-art. *Appl. Microbiol. Biotechnol*., **60**:507-514.

Arroyo, M., Torres, R., de la Mata, I., Castillon, M. P. and Acebal, C. (1999). Interaction of penicillin V acylase with organic solvents: catalytic activity modulation on the hydrolysis of penicillin V. *Enz. Microb. Tech*. **25**:378-383.

Barbero, J.L., Buesa, J.M., Gonzalez de Buitrago, G., Mendez, E., Pez-Aranda, A. and Garcia, J.L. (1986). Complete nucleotide sequence of the penicillin acylase gene from *Kluyvera citrophila*. *Gene* **49**:69-80.

Baron, R.L. (1997). Computed tomography of the bile ducts. *Semin Roentgenol.* **32**:172-187.

Baron, S.F. and Hylemon, P.B. (1995). Expression of the bile acid-inducible NADH:flavin oxidoreductase gene of *Eubacterium sp.* VPI 12708 in *Escherichia coli*. *Biochim Biophys Acta*. **1249**:145-154.

Baron, S.F., Franklund, C.V. and Hylemon, P.B. (1991). Cloning, sequencing, and expression of the gene coding for bile acid 7 alpha-hydroxysteroid dehydrogenase from *Eubacterium sp*. strain VPI 12708. *J Bacteriol*. **173**:4558-4569.

Batta, A.K., Salen, G. and Shefer, S. (1984). Substrate specificity of cholylglycine hydrolase for the hydrolysis of bile acid conjugates. *J Biol Chem*. **259**:15035-15039.

Bennett, J.W. and Chung, K.T. (2001). Alexander Fleming and the discovery of penicillin. *Adv Appl Microbiol*. **49**:163-184.

Berman, H.M., Westbrook, J., Feng, Z., Gilliland, G., Bhat, T.N., Weissig, H., Shindyalov, I.N. and Bourne P.E., (2000). The Protein Data Bank. *Nucleic Acids Res.* **28**:235-242.

Bernhagen, J., Calandra, T., Mitchell, R.A., Martin, S.B., Tracey, K.J., Voelter, W., Manogue, K.R., Cerami, A. and Bucala, R. (1993). MIF is a pituitary-derived cytokine that potentiates lethal endotoxaemia. Nature. **365**:756-759.

Bhisutthibhan, J. and Meshnick, S.R. (2001). Immunoprecipitation of [(3)H]dihydroartemisinin translationally controlled tumor protein (TCTP) adducts from Plasmodium falciparum-infected erythrocytes by using anti-TCTP antibodies. *Antimicrob Agents Chemother*. **45**:2397-2399.

Bhisutthibhan, J., Philbert, M.A., Fujioka, H., Aikawa, M. and Meshnick, S.R. (1999). The *Plasmodium falciparum* translationally controlled tumor protein: subcellular localization and calcium binding. *Eur J Cell Biol*. **78**:665-670.

Bhisutthibhan, J., Xing-Qing, P., Hossler, P. A., Walker, D. J., Yowell, C. A., Carlton, J., Dame, J. B. and Meshnick, S R. (1998). The *Plasmodium falciparum* translationally controlled tumor protein homolog and its reaction with the antimalarial drug artemisinin. *J. Biol. Chem.* **273**:16192-16198.

Blocki, F.A., Ellis, L.B. and Wackett, L.P. (1993). MIF protein are theta-class glutathione S-transferase homologs. *Protein Sci*. **2**:2095-2102.

Bock, A., Wirth, R., Schmidt, G., Schumacher, G., Lang, G. and Buckel, P. (1983). The two subunits of penicillin acylase are processed from a common precursor. *FEMS Microbiol. Lett.* **20**:141-144.

Bohm, H., Benndorf, R., Gaestel, M., Gross, B., Nurnberg, P., Kraft, R., Otto, A. and Bielka, H. (1989). The growth-related protein P23 of the Ehrlich ascites tumor: translational control, cloning and primary structure. *Biochem Int*. **19**:277-286.

Bommer, U.A., Lazaris-Karatzas, A., De Benedetti, A., Nurnberg, P., Benndorf, R., Bielka, H. and Sonenberg, N. (1994). Translational regulation of the mammalian growth-related protein P23: involvement of eIF-4E. *Cell Mol Biol Res*. **40**:633-641.

Bompard-Gilles, C., Villeret, V., Davies, G.J., Fanuel, L., Joris, B., Frere, J.M., Van Beeumen, J. (2000). A new variant of the Ntn hydrolase fold revealed by the crystal structure of L-aminopeptidase D-ala-esterase/amidase from *Ochrobactrum anthropi*. *Structure Fold Des*. **8**:153-162.

Bomstein, N. J. and Evans, W. G. (1965). Automated colorimetric determination of 6-

aminopenicillanic acid in fermentation media. *Anal. Chem*. **37**:576–578.

Borek, D. and Jaskolski, M. (2000). Crystallization and preliminary crystallographic studies of a new L-asparaginase encoded by the *Escherichia coli* genome. *Acta Crystallogr D Biol Crystallogr.* D**56**:1505-1507.

Michalska, K., Bujacz, G. and Jaskolski, M. (2006). Crystal Structure of Plant Asparaginase. J. Mol. Biol. **360**:105-116.

Bose, H.S., Whittal, R.M., Baldwin, M.A. and Miller, W.L. (1999). The active form of the steroidogenic acute regulatory protein, StAR, appears to be a molten globule. *Proc Natl Acad Sci USA*. **96**:7250-7255.

Bossi, A, Cretich, M. and Righetti, P.G. (1998). Production of D-phenylglycine from racemic (D,L)-phenylglycine via isoelectrically-trapped penicillin G acylase. *Biotechnol Bioeng*. **60**:454-61.

Bouma, M.J. and van der Kaay, H.J. (1996). The El Nino Southern Oscillation and the historic malaria epidemics on the Indian subcontinent and Sri Lanka: an early warning system for future epidemics? *Trop Med Int Health*. **1**:86-96.

Bouma, M.J., Dye, C. and van der Kaay, H.J. (1996). Falciparum malaria and climate change in the northwest frontier province of Pakistan. *Am J Trop Med Hyg*. **55**:131-137.

Bowman, S., Lawson, D., Basham, D., Brown, D., Chillingworth, T., Churcher, C.M., Craig, A., Davies, R.M., Devlin, K., Feltwell, T., Gentles, S., Gwilliam, R., Hamlin, N., Harris, D., Holroyd, S., Hornsby, T., Horrocks, P., Jagels, K., Jassal, B., Kyes, S., McLean, J., Moule, S., Mungall, K., Murphy, L., Oliver, K., Quail, M.A., Rajandream, M.A., Rutter, S., Skelton, J., Squares, R., Squares, S., Sulston, J.E., Whitehead, S., Woodward, J.R., Newbold, C. and Barrell, B.G. (1999). The complete nucleotide sequence of chromosome 3 of *Plasmodium falciparum*. *Nature* **400**:532-538.

Brand, L and Withold, B. (1967). Fluorescence measurements. *Methods Enzymol*. **11**:776-856.

Brannigan, J.A., Dodson, G.G., Done, S.H., Hewitt, L., McVey, C.E., and Wilson, K.S. (2000). Structural studies of penicillin acylase. *Appl Biochem Biotechnol* **88**:313-319.

Brannigan, James A., Dodson, Guy G., Duggleby, Helen J., Moody, Peter C. E., Smith, Janet L., Tomchick, Diana R. and Murzin, Alexey G. (1995). A protein catalytic framework with an N-terminal nucleophile is capable of self-activation. *Nature*. **378**:416-419.

Brewster, D. (1999). Environmental management for vector control. Is it worth a dam if it worsens malaria? *BMJ*. **319**:651-652.

Bruggink, A. and Roy, P.D. (2001). Industrial synthesis of semi-synthetic antibiotics. *In*: Synthesis of β-lactam antibiotics. Chemistry, Biocatalysis & Process Integration (Bruggink, A., ed.). Dordrecht (The Netherlands): Kluwer Academic Publishers, pp. 13-55.

Burtscher, H. and Schumacher, G. (1992). Reconstitution in vivo of penicillin G acylase activity from separately expressed subunits. *Eur J Biochem* **205**:77-83.

Bushueva, T. L., Busel E. P., Bushuev, V. N. and Burstein, E. A. (1974). The interaction of protein functional groups with indole chromophore. I. Imidazole group. *Stud. Biophys*. **44**:129–132.

Bychkova, V.E., Berni, R., Rossi, G.L., Kutyshenko, V.P. and Ptitsyn, O.P. (1992). Retinol-binding protein is in the molten globule state at low pH. *Biochemistry*. **31**:7566-7571.

Bychkova, V.E., Pain, R.H. and Ptitsyn, O.B. (1988). The 'molten globule' state is involved in the translocation of proteins across membranes? *FEBS Lett*. **238**:231-234.

Cabaret, D., Adediran, S.A., Pratt, R.F. and Wakselman, M. (2003). New substrates for beta-lactam-recognizing enzymes: aryl malonamates. *Biochemistry* **42**:6719-6725.

Cai, G., Zhu, S., Yang, S., Zhao, G. and Jiang, W. (2004). Cloning, overexpression, and characterization of a novel thermostable penicillin G acylase from *Achromobacter xylosoxidans*: probing the molecular basis for its high thermostability. *Appl Environ Microbiol*. **70**:2764-2770.

Calandra, T., Bernhagen, J., Metz, C.N., Spiegel, L.A., Bacher, M., Donnelly, T., Cerami, A. and Bucala, R. (1995). MIF as a glucocorticoid-induced modulator of cytokine production. *Nature* **377**:68-71.

Calandra, T., Spiegel, L.A., Metz, C.N. and Bucala, R. (1998). Macrophage migration inhibitory factor is a critical mediator of the activation of immune cells by exotoxins of Gram-positive bacteria. *Proc Natl Acad Sci USA*. **95**:11383-11388.

Cardamone, M. and Puri, N. K. (1992). Spectrofluorimetric assessment of the surface hydrophobicity of proteins. *Biochem. J.* **282**:589-593.

Cavins, J. F. and Friedman, M. (1968). Specific modification of protein sulfhydryl groups with alpha,beta-unsaturated compounds. *J Biol Chem*. **243**:3357-3360.

Chandra, P.M., Brannigan, J.A., Prabhune, A., Pundle, A., Turkenburg, J.P., Dodson, G.G. and Suresh, C.G. (2005). Cloning, preparation and preliminary crystallographic studies of penicillin V acylase autoproteolytic processing mutants. *Acta Crystallogr Sect F Struct Biol Cryst Commun*. **61**:124-127.

Chiang, C and Bennett, R.E. (1967). Purification and properties of penicillin amidase from *Bacillus megaterium*. *J Bacteriol.* **93**:302-308.

Chikai, T., Nakao, H. and Uchida, K. (1987). Deconjugation of bile acids by human intestinal bacteria implanted in germ-free rats. *Lipids*. **22**:669-671.

Chilov GG, Guranda DT, Svedas VK. The role of hydrophobic interactions on alcohol binding in the active center of penicillin acylases. Biochemistry (Mosc). 2000 Aug;65(8):963-6.

Choi, K.S., Kim, J.A. and Kang, H.S. (1992). Effects of site-directed mutations on processing and activities of penicillin G acylase from *Escherichia coli* ATCC 11105. *J Bacteriol*. **174**:6270-6276.

Christiaens, H., Leer, R. J., Pouwels, P. H. and Verstrete, W. (1992). Cloning and expression of a conjugated bile acid hydrolase gene from *Lactobacillus plantarum* by using a direct plate assay. *Appl. Environ. Microbiol*. **58**: 3792-3798.

Chung, S., Kim, M., Choi, W., Chung, J. and Lee, K. (2000). Expression of translationally controlled tumor protein mRNA in human colon cancer. *Cancer Lett*. **156**:185-190.

Coleman, J. P. and Hudson, L. L. (1995). Cloning and characterization of a conjugated bile acid hydrolase gene from *Clostridium perfringens. Appl. Environ. Microbiol*. **61**:2514-2520.

Collaborative Computational Project Number. 4. (1994). The CCP4 suite: Programs for protein crystallography. *Acta Crystllogr*. D**50**:760-763.

De Leon, A., Breceda, G.B., Barba de la Rosa, A.P., Jimenez-Bremont, J.F. and Lopez-Revilla, R. (2003). Galactose induces the expression of penicillin acylase under control of the lac

promoter in recombinant *Escherichia coli*. *Biotechnol Lett*. **25**:1397-1402.

Demain, A.L. (2000). Small bugs, big business: the economic power of the microbe. *Biotechnol Adv* **18**:499-514.

Deshpande, B.S., Ambedkar, S.S., Sudhakaran, V.K. and Shewale, J.G. (1994). Molecular biology of beta-lactam acylases. *World J. Microbiol and Biotech* **10**:129-138.

Desmet, V.J., van Eyken, P. and Roskams, T. (1998). Histopathology of vanishing bile duct diseases. *Adv Clin Path*. **2**:87-99.

Diez, B., Mellado, E., Fouces, R., Rodriguez, M. and Barredo, J.L. (1996). Recombinant *Acremonium chrysogenum* strains for the industrial production of cephalosporin. *Microbiologia* **12**:359-370.

Ditchburn, R. W. (1953). Light. John Wiley and Sons. New York.

Ditzel, L., Huber, R., Mann, K., Heinemeyer, W., Wolf, D.H. and Groll, M. (1998). Conformational constraints for protein self-cleavage in the proteasome. *J Mol Biol*. **279**:1187-1191.

Dixon, M., and Webb, E. C. (1979). Enzymes, 3rd ed. Longman, London, United Kingdom.

Dobryszycki, P., Rymarczuk, M., Gapinski, J. and Kochman, M. (1999). Effect of acrylamide on aldolase structure. I. Induction of intermediate states. *Biochim Biophys Acta* **1431**:338-350.

Done, S.H., Brannigan, J.A., Moody, P.C. and Hubbard, R.E. (1998). Ligand-induced conformational change in penicillin acylase. *J. Mol. Biol.* **284**:463-475.

Donnelly, S.C. and Bucala, R. (1997). Macrophage migration inhibitory factor: a regulator of glucocorticoid activity with a critical role in inflammatory disease. *Mol Med Today* **3**:502-507.

Drenth, J. (1994). Principles of protein crystallography. Springer-Verlag; New York, pp. XIII + 305.

Ducruix, A & Giege, R (1999).(ed) Crystallization of nucleic acids and proteins- A practical approach, II ed., Oxford University Press, Oxford.

Duggleby, H.J., Tolley, S.P., Hill, C.P., Dodson, E.J., Dodson, G. and Moody, P.C. (1995). Penicillin acylase has a single amino acid catalytic centre. *Nature.* **373**:264-268.

Dussurget, O., Cabanes, D., Dehoux, P., Lecuit, M., Buchrieser, C., Glaser, P. and Cossart, P. (2002). European Listeria Genome Consortium. *Listeria monocytogenes* bile salt hydrolase is a PrfA-regulated virulence factor involved in the intestinal and hepatic phases of listeriosis. *Mol Microbiol*. **45**:1095-1106.

Eftink, M. R. (1997). Fluorescence Methods for Studying the Kinetics of Protein Folding Reactions, in Methods Enzymol. edited by L. Brand and M. Johnson, **278**:258-286.

Elander, R.P. (2003). Industrial production of β-lactam antibiotics. *Appl. Mircobiol.Biotechnol*. **61**:385-392.

Elkins, C. A. and Savage, D. C. (1998). Identification of genes encoding conjugated bile salt hydrolase and transport in *Lactobacillus johnsonii* 100-100. *J. Bacteriol.* **180**:4344-4349.

Ercelen, Sebnem., Kazan, Dilek., Erarslan, Altan and Demchenkoa, Alexander P. (2001). On the excited-state energy transfer between tryptophan residues in proteins: the case of penicillin acylase. *Biophys. Chem.* **90**:203-217.

Essack, S.Y. (2001). The development of beta-lactam antibiotics in response to the evolution of beta-lactamases. *Pharm Res* **18**:1391-1399.

Ezra, Daniel and Gregorio, Weber. (1966). Cooperative Effects in Binding by Bovine Serum Albumin. I. The Binding of 1-Anilino-8-naphthalenesulfonate. Fluorimetric Titrations. *Biochemistry* **5**:1893-1900.

Fanuel, L., Goffin, C., Cheggour, A., Devreese, B., Van Driessche, G., Joris, B., Van Beeumen, J. and Frere, J.M. (1999). The DmpA aminopeptidase from *Ochrobactrum anthropi* LMG7991 is the prototype of a new terminal nucleophile hydrolase family. *Biochem. J.* **341**:147-155.

Floch, M.H., Gershengoren, W., Elliott, S. and Spiro, H.M. (1971). Bile acid inhibition of the intestinal microflora--a function for simple bile acids? *Gastroenterol.* **61**:228-233.

Fritz-Wolf, K., Koller, K.P., Lange, G., Liesum, A., Sauber, K., Schreuder, H., Aretz, W. and Kabsch, W. (2002). Structure-based prediction of modifications in glutarylamidase to allow single-step enzymatic production of 7-aminocephalosporanic acid from cephalosporin C. *Protein Sci*. **11**:92-103.

Fuganti, C., Lanati, S. and Servi, S. (1986). Kinetic resolution of substituted 1,3-4H-5,6-dihydrooxazines with carboxylesterase NP: synthesis of (3S,1'R)-3-(1'-hydroxyethyl)-azetidin-2-one. *Bioorg Med Chem*. **2**:723-726.

Gachet, Y., Tournier, S., Lee, M., Lazaris-Karatzas, A., Poulton, T., Bommer, U.A. (1999). The growth-related, translationally controlled protein P23 has properties of a tubulin binding protein and associates transiently with microtubules during the cell cycle. *J Cell Sci.* **112**:1257-1271.

Gardner, M.J., Hall N, Fung E, White O, Berriman M, Hyman RW, Carlton JM, Pain A, Nelson KE, Bowman S, Paulsen IT, James K, Eisen JA, Rutherford K, Salzberg SL, Craig A, Kyes S, Chan MS, Nene V, Shallom SJ, Suh B, Peterson J, Angiuoli S, Pertea M, Allen J, Selengut J, Haft D, Mather MW, Vaidya AB, Martin DM, Fairlamb AH, Fraunholz MJ, Roos DS, Ralph SA, McFadden GI, Cummings LM, Subramanian GM, Mungall C, Venter JC, Carucci DJ, Hoffman SL, Newbold C, Davis RW, Fraser CM, Barrell B. (2002). Genome sequence of the human malaria parasite *Plasmodium falciparum*. *Nature* **419**:498–511.

Gardner, M.J., Shallom, S.J., Carlton, J.M., Salzberg, S.L., Nene, V., Shoaibi, A., Ciecko, A., Lynn, J., Rizzo, M., Weaver, B., Jarrahi, B., Brenner, M., Parvizi, B., Tallon, L., Moazzez, A., Granger, D., Fujii, C., Hansen, C., Pederson, J., Feldblyum, T., Peterson, J., Suh, B., Angiuoli, S., Pertea, M., Allen, J., Selengut, J., White, O., Cummings, L.M., Smith, H.O., Adams, M.D., Venter, J.C., Carucci, D.J., Hoffman, S.L., Fraser, C.M. (2002). Sequence of *Plasmodium falciparum* chromosomes 2, 10, 11 and 14. *Nature* **419**:531-534.

Gardner, M.J., Tettelin, H., Carucci, D.J., Cummings, L.M., Aravind, L., Koonin, E.V., Shallom, S., Mason, T., Yu, K., Fujii, C., Pederson, J., Shen, K., Jing, J., Aston, C., Lai, Z., Schwartz, D.C., Pertea, M., Salzberg, S., Zhou, L., Sutton, G.G., Clayton, R., White, O., Smith, H.O., Fraser, C.M., Adams, M.D., Venter, J.C. and Hoffman, S.L. (1998). Chromosome 2 sequence of the human malaria parasite *Plasmodium falciparum*. *Science* **282**:1126-1132.

Garewal, H., Bernstein, H., Bernstein, C., Sampliner, R. and Payne, C. (1996) Reduced bile acid-induced apoptosis in "normal" colorectal mucosa: a potential biological marker for cancer risk. *Cancer Res.* **56**:1480-1483.

Gilliland, S.E. and Speck, M.L. (1977). Deconjugation of bile acids by intestinal lactobacilli. *Appl*

Environ Microbiol. **33**:15-18.

Grill, J., Schneider, F., Crociani, J. and Ballongue, J. (1995). Purification and characterization of conjugated bile salt hydrolase from *Bifidobacterium longum* BB536. *Appl. Environ. Microbiol*. **61**:2577-2582.

Groll, M., Bajorek, M., Kohler, A., Moroder, L., Rubin, D.M., Huber, R., Glickman, M.H. and Finley, D. (2000). A gated channel into the proteasome core particle. *Nat.Struct.Biol*. **7**:1062-1067.

Groll, M., Ditzel, L., Lowe, J., Stock, D., Bochtler, M., Bartunik, H.D. and Huber, R. (1991). Structure of 20S proteasome from yeast at 2.4 A resolution. *Nature* **386**:463-471.

Gross, B., Gaestel, M., Bohm, H. and Bielka, H. (1989). cDNA sequence coding for a translationally controlled human tumor protein. *Nucleic Acids Res*. **17**:8367.

Guan, C., Cui, T., Rao, V., Liao, W., Benner, J., Lin, C.L. and Comb, D. (1996). Activation of glycosylasparaginase. Formation of active N-terminal threonine by intramolecular autoproteolysis. *J Biol Chem*. **271**:1732-1737.

Guan, C., Liu, Y., Shao, Y., Cui, T., Liao, W., Ewel, A., Whitaker, R. and Paulus, H. (1998). Characterization and functional analysis of the cis-autoproteolysis active center of glycosylasparaginase. *J Biol Chem*. **273**:9695-9702.

Guerra, C.A., Snow, R.W., Hay, S.I. (2006). Mapping the global extent of malaria in 2005. *Trends Parasitol.* **22**:353-358.

Gumpricht, E., Dahl, R., Devereaux, M.W. and Sokol, R.J. (2005). Licorice compounds glycyrrhizin and 18beta-glycyrrhetinic acid are potent modulators of bile acid-induced cytotoxicity in rat hepatocytes. *J Biol Chem.* **280**:10556-10563.

Guo, H.C., Xu, Q., Buckley, D. and Guan, C. (1998). Crystal structures of Flavobacterium glycosylasparaginase. An N-terminal nucleophile hydrolase activated by intramolecular proteolysis. *J Biol Chem*. **273**:20205-20212.

Haskard, Carolyn A. and Li-Chan, Eunice C. Y. (1998). Hydrophobicity of Bovine Serum Albumin and Ovalbumin Determined Using Uncharged (PRODAN) and Anionic (ANS^-) Fluorescent Probes. *J. Agric. Food Chem.* **46**:2671-2677.

Hedrick, J. L. and Smith, A. J. (1968). Size and charge isomer separation and estimation of molecular weights of proteins by disc gel electrophoresis. *Arch. Biochem. Biophys*. **126**:155-164.

Herold, B.C., Kirkpatrick, R., Marcellino, D., Travelstead, A., Pilipenko, V., Krasa, H., Bremer, J., Dong, L.J., Cooper, M.D. (1999). Bile salts: natural detergents for the prevention of sexually transmitted diseases. *Antimicrob Agents Chemother* **43**:745-751.

Hewitt, L., Kasche, V., Lummer, K., Lewis, R.J., Murshudov, G.N., Verma, C.S., Dodson, G.G. and Wilson, K.S. (2000). Structure of a slow processing precursor penicillin acylase from *Escherichia coli* reveals the linker peptide blocking the active-site cleft. *J Mol. Biol*. **302**:887-898.

Holm, L. and Sander, C. (1995). DALI: a network tool for protein structure comparison. *Trends Biochem. Sci.*, **20**:478-480.

Holt, R.A., Subramanian GM, Halpern A, Sutton GG, Charlab R, Nusskern DR, Wincker P, Clark AG, Ribeiro JM, Wides R, Salzberg SL, Loftus B, Yandell M, Majoros WH, Rusch DB, Lai

Z, Kraft CL, Abril JF, Anthouard V, Arensburger P, Atkinson PW, Baden H, de Berardinis V, Baldwin D, Benes V, Biedler J, Blass C, Bolanos R, Boscus D, Barnstead M, Cai S, Center A, Chaturverdi K, Christophides GK, Chrystal MA, Clamp M, Cravchik A, Curwen V, Dana A, Delcher A, Dew I, Evans CA, Flanigan M, Grundschober-Freimoser A, Friedli L, Gu Z, Guan P, Guigo R, Hillenmeyer ME, Hladun SL, Hogan JR, Hong YS, Hoover J, Jaillon O, Ke Z, Kodira C, Kokoza E, Koutsos A, Letunic I, Levitsky A, Liang Y, Lin JJ, Lobo NF, Lopez JR, Malek JA, McIntosh TC, Meister S, Miller J, Mobarry C, Mongin E, Murphy SD, O'Brochta DA, Pfannkoch C, Qi R, Regier MA, Remington K, Shao H, Sharakhova MV, Sitter CD, Shetty J, Smith TJ, Strong R, Sun J, Thomasova D, Ton LQ, Topalis P, Tu Z, Unger MF, Walenz B, Wang A, Wang J, Wang M, Wang X, Woodford KJ, Wortman JR, Wu M, Yao A, Zdobnov EM, Zhang H, Zhao Q, Zhao S, Zhu SC, Zhimulev I, Coluzzi M, della Torre A, Roth CW, Louis C, Kalush F, Mural RJ, Myers EW, Adams MD, Smith HO, Broder S, Gardner MJ, Fraser CM, Birney E, Bork P, Brey PT, Venter JC, Weissenbach J, Kafatos FC, Collins FH and Hoffman, S.L. (2002). The genome sequence of the malaria mosquito Anopheles gambiae. *Science*. 2002 **298**:129-149.

Hopp, T.P. and Woods, K.R. (1983). A computer program for predicting protein antigenic determinants. *Mol Immunol*. **20**:483-489.

Hubbard, S. J., Campbell, S. F. and Thoronton, J. M. (1991). Molecular recognition: Conformational analysis of limited proteolytic sites and serine proteinase protein inhibitors. *J. Mol. Biol*. **220**:507-530.

Hunt, P.D., Tolley, S.P., Ward, R.J, Hill, C.P. and Dodson, G.G. (1990). Expression, purification and crystallization of penicillin G acylase from *Escherichia coli* ATCC 11105. *Protein Eng*. **3**:635-639.

Hylemon, P. B. (1985). In H. Danielson and J. Sjovall (ed.), Sterols and bile acids. Elsevier Science Publishing Inc., New York.

Ignatova, Z., Mahsunah, A., Georgieva, M. and Kasche, V. (2003). Improvement of posttranslational bottlenecks in the production of penicillin amidase in recombinant Escherichia coli strains. *Appl Environ Microbiol*. **69**:1237-1245.

Ishii, Y., Saito, Y., Fujimura, T., Sasaki, H., Noguchi, Y., Yamada, H., Niwa, M. and Shimomura, K. (1995). High-level production, chemical modification and site-directed mutagenesis of a cephalosporin C acylase from Pseudomonas strain N176. *Eur J Biochem.* **230**:773-778.

Isupov, M.N., Obmolova, G., Butterworth, S., Badet-Denisot, M.A., Badet, B., Polikarpov, I., Littlechild, J.A. and Teplyakov, A. (1996). Substrate binding is required for assembly of the active conformation of the catalytic site in Ntn amidotransferases: evidence from the 1.8 A crystal structure of the glutaminase domain of glucosamine 6-phosphate synthase. *Structure*. **4**:801-810.

Jacoby, G.A. and Munoz-Price, L.S. (2005). The new beta-lactamases. *N Engl J Med*. **352**:380-391.

Jancarik, J. and Kim, S. H. (1991). Sparse matrix sampling: a screening method for crystallization of proteins. *J. Appl. Cryst*. **24**:409-411.

Johnsen, J. (1977). Utilization of benzylpenicillin as carbon, nitrogen and energy source by a Pseudomonas fluorescens strain. *Arch Microbiol*. **115**:271-275.

Kabilan, L. (1997). T cell immunity in malaria. *Indian J Med Res*. **106**:130-148.

Kamen, Douglas E. and Woody, Robert W. (2001). A partially folded intermediate conformation is induced in pectate lyase C by the addition of 8-anilino-1-naphthalenesulfonate (ANS). *Protein Sci.*, **10**:2123-2130.

Kang, H.S., Lee, M.J, Song, H., Han, S.H., Kim, Y.M., Im, J.Y. and Choi, I. (2001). Molecular identification of IgE-dependent histamine-releasing factor as a B cell growth factor. *J Immunol.* **166**:6545-6554.

Kasche, V., Lummer, K., Nurk, A., Piotraschke, E., Rieks, A., Stoeva, S. and Voelter, W. (1999). Intramolecular autoproteolysis initiates the maturation of penicillin amidase from *Escherichia coli*. *Biochim Biophys Acta* **1433**:76-86.

Kathir, K. M., Krishnaswamy, T., Kumar, S., Rajalingam, D. and Yu, C. (2005). Time-dependent Changes in the Denatured State(s) Influence the Folding Mechanism of an All -Sheet Protein. *J. Biol. Chem*. **280**:29682-29688.

Kato, K. (1980) Kinetics of acyl transfer by α-amino acid ester hydrolase from *Xanthomonas citri*. *Agric. Biol. Chem*. **44**:1083-1088.

Kerr, D. E. (1993). A colorimetric assay for Penicillin-V amidase. *Anal. Biochem*. **209**:332-334.

Kidson, C. and Indaratna, K. (1998). Ecology, economics and political will: the vicissitudes of malaria strategies in Asia. *Parassitologia.* **40**:39-46.

Kim, J.K, Yang, I.S, Rhee, S., Dauter, Z., Lee, Y.S., Park, S.S. and Kim, K.H. (2003). Crystal structures of glutaryl 7-aminocephalosporanic acid acylase: Insight into autoproteolytic activation. *Biochemistry* **42**:4084-4093.

Kim, Y. and Hol, W.G. (2001). Structure of cephalosporin acylase in complex with glutaryl-7-aminocephalosporanic acid and glutarate: insight into the basis of its substrate specificity. *Chem Biol.* **8**:1253-1264.

Kim, Y., Kim, S., Earnest, T.N. and Hol, W.G. (2002). Precursor structure of cephalosporin acylase. Insights into autoproteolytic activation in a new N-terminal hydrolase family. *J. Biol. Chem.* **277**:2823-2829.

Kim, Y., Yoon, K.H., Khang, Y., Turley, S. and Hol, W.G.J. (2000). The 2.0 Å crystal structure of cephalosporin acylase.*Structure* **8**:1059-1068.

Kinoshita, T., Tada, T., Saito, Y., Ishii, Y., Sato, A. and Murata, M. (2000). Crystallization and preliminary X-ray analysis of cephalosporin C acylase from *Pseudomonas* sp. strain N176. A*cta Cryst Section D: Biological Cryst* **56**:458-459.

Klei, H.E., Daumy, G.O. and Kelly, J.A. (1995). Purification and preliminary crystallographic studies of penicillin G acylase from *Providencia rettgeri. Protein Sci*. **4**:433-441.

Krier, J.P., Hamburger, J., Seed, T.M., Saul, K. and Green, T. (1976). *Plasmodium berghei*: characteristics of a selected population of small free blood stage parasites. *Tropenmed Parasitol*. **27**:82-88.

Kruskal, J.B. and Sankoff, D. (1983). Time Warps, String Edits, and Macromolecules: The Theory and Practice of Sequence Comparison. Addison-Wesley, Reading, MA.

Kukreja, R. and Singh, B. (2005). Biologically active novel conformational state of botulinum, the most poisonous poison. *J Biol Chem*. **280**:39346-39352.

Kumar, S., Tamura, K. and Nei, M. (2004). MEGA3: Integrated software for Molecular Evolutionary

Genetics Analysis and sequence alignment. *Brief. Bioinform* **5**:50-163.

Kutzbach, C. and Rauenbusch, E. (1974). Preparation and general properties of crystalline penicillin acylase from *Escherichia coli* ATCC 11 105. *Hoppe Seylers Z. Physiol. Chem*. **355**:45-53.

Kyte, J. and Doolittle, R. (1982). A simple method for displaying the hydropathic character of a protein. *J. Mol. Biol*. **157**:105-132.

Laemmli, U. K. (1970). Cleavage of structural proteins during the assembly of the head of bacteriophage T4. *Nature*. **227**:680-685.

Lan, H.Y., Bacher, M., Yang, N., Mu, W., Nikolic-Paterson, D.J., Metz, C., Meinhardt, A., Bucala, R. and Atkins, R.C. (1997). The pathogenic role of macrophage migration inhibitory factor in immunologically induced kidney disease in the rat. *J Exp Med*. **185**:1455-1465.

Laskowski, R. A., MacArthur. M. W., Moss. D. S. and Thoronton, J. M. (1993). PROCHECK: A program to check the stereo-chemical quality of protein structures. *J. Appl. Cryst*. **26**:283-291.

Lee, B. and Richards, F. M. (1971). The interpretation of protein structures: estimation of static accessiblity. *J. Mol. Biol*. **55**:379-400.

Lee, H., Park, O.K. and Kang, H.S. (2000). Identification of a new active site for autocatalytic processing of penicillin acylase precursor in *Escherichia coli* ATCC11105. *Biochem Biophys Res Commun*.**27**:199-204.

Lee, Y.S., Kim, H.W. and Park, S.S. (2000). The role of alpha-amino group of the N-terminal serine of beta subunit for enzyme catalysis and autoproteolytic activation of glutaryl 7-aminocephalosporanic acid acylase. *J Biol Chem*. **275**:39200-39206.

Lee, Y.S., Kim, H.W., Lee, K.B. and Park, S.S. (2000). Involvement of arginine and tryptophan residues in catalytic activity of glutaryl 7-aminocephalosporanic acid acylase from *Pseudomonas* sp. strain GK16. *Biochim Biophys Acta*. **1523**:123-127.

Lehrer, S. S. (1971). Solute perturbation of protein fluorescence: the quenching of the trytophyl fluorescence of model compounds and of lysozyme by iodide ion. *Biochemistry.* **10**:3254-3263.

Levy, H. M., Leber, P. D. and Ryan, E. M. (1963). Inactivation of myosin by 2,4-Dinitrphenol and protection by adenosine triphosphate and other phosphate compounds *J. Biol. Chem.* **238**:3654-3659.

Li, Y., Chen, J., Jiang, W., Mao, X., Zhao, G. and Wang, E. (1999). In vivo post-translational processing and subunit reconstitution of cephalosporin acylase from *Pseudomonas s*p. 130. *Eur J Biochem*. **262**:713-719.

Lowe, J., Stock, D., Jap, B., Zwickl, P., Baumeister, W. and Huber, R. (1995). Crystal structure of the 20S proteasome from the archaeon *T. acidophilum* at 3.4 A resolution. *Science.* **268**:533-539.

Lowry, O. H., Rosebrough, N. J., Farr, A. L. and Randall, R. J. (1951). Protein measurement by the Folin-Phenol reagent. *J. Biol. Chem*. **193**:265-275.

Lubetsky, J.B., Dios, A., Han, J., Aljabari, B., Ruzsicska, B., Mitchell, R., Lolis, E. and Al-Abed, Y. (2002). The tautomerase active site of macrophage migration inhibitory factor is a potential target for discovery of novel anti-inflammatory agents. *J Biol Chem*. **277**:24976-

24982.

Lundeen, S. G. and Savage, D. C. (1990). Characterization and purification of bile salt hydrolase from Lactobacillus sp. strain 100-100. *J. Bacteriol*. **172**:4171-4177.

Mao, X., Wang, W., Jiang, W. and Zhao, G.P. (2004). His23beta and Glu455beta of the *Pseudomonas sp*. 130 glutaryl-7-amino cephalosporanic acid acylase are crucially important for efficient autoproteolysis and enzymatic catalysis. *Protein J*. **23**:197-204.

Margolin, A.L., Svedas, V.K. and Berezin, I.V. (1980). Substrate specificity of penicillin amidase from E. coli. *Biochim Biophys Acta* **616**:283-289.

Martens, W.J.M., Niessen, L.W., Rotmans, J., Jetten, T.H. and McMichael, A.J. (1995). Potential Impact of Global Climate Change on Malaria Risk. *Environmental Health Perspectives*, **103**: 458-464.

Martin, J., Langer, T., Boteva, R., Schramel, A., Horwich, A.L. and Hartl, F.U. (1991). Chaperonin-mediated protein folding at the surface of GroEL through a 'molten globule'-like intermediate. *Nature.* **352**:36–42.

Martin, J., Prieto, I., Mancheno, J.M., Barbero, J.L. and Arche, R. (1993). pH studies to elucidate the chemical mechanism of penicillin acylase from *Kluyvera citrophila*. *Biotechnol Appl Biochem*. **17**:311-325.

Martin, L., Prieto, M.A., Cortes, E. and Garcia, J.L. (1995). Cloning and sequencing of the pac gene encoding the penicillin G acylase of *Bacillus megaterium* ATCC 14945. *FEMS Microbiol Lett*. **125**:287-292.

Masui, Ryoji and Kuramitsu, Seiki. (1998). Probing of DNA-Binding Sites of *Escherichia coli* RecA Protein Utilizing 1-Anilinonaphthalene-8-sulfonic Acid. *Biochemistry,* **37**:12133-12143.

Matthews, B. W. (1968). Solvent content of protein crystals. *J. Mol. Biol*. **33**:491-97.

Matulis, D. and Lovrien, R. (1998). 1-Anilino-8-naphthalene sulfonate anion-protein binding depends primarily on ion pair formation. *Biophys J*. **74**:422-429.

McDonough, M.A., Klei, H.E. and Kelly, J.A.(1999) Crystal structure of penicillin G acylase from the Bro1 mutant strain of *Providencia rettgeri*. *Protein Sci*., **8**:1971-1981.

McRee, Duncan E. (1993). *Practical Protein Crystallography*. San Diego: Academic Press, pp. 1-23.

McVey, C.E., Tolley, S.P., Done, S.H., Brannigan, J.A. and Wilson, K.S. (1997). A new crystal form of penicillin acylase from *Escherichia coli*. *Acta Crystallogr D Biol Crystallogr*. **53**:777-779.

McVey, C.E., Walsh, M.A., Dodson, G.G., Wilson, K.S. and Brannigan, J.A. (2001). Crystal structures of penicillin acylase enzyme-substrate complexes: structural insights into the catalytic mechanism. *J. Mol. Biol.* **313**:139-150.

Merelo, J.J., M.A. Andrade, A. Prieto and F. Morán. (1994). Proteinotopic Feature Maps. Neurocomputing. **6**:443-454.

Michaelis, L. and Menten, M. L. (1913). Die Kinetik der Invertinwirkung. *Biochem. Z.* **49**:333-369.

Mikulowska, A., Metz, C.N., Bucala, R. and Holmdahl, R. (1997). Macrophage migration inhibitory factor is involved in the pathogenesis of collagen type II-induced arthritis in mice. *J Immunol*. **158**:5514-5517.

Monera, O.D., Kay, C. M. and Hodges, R. S. (1994). Protein denaturation with guanidine hydrochloride or urea provides a different estimate of stability depending on the

contributions of electrostatic interactions. *Protein Sci*. **3**:1984-1991.

Moore, S. (1968). Amino acid analysis: aqueous dimethyl sulfoxide for the ninhydrin reaction. *J. Biol. Chem*. **243**:6281-6283.

Morillas, M., Goble, M.L. and Virden, R. (1999). The kinetics of acylation and deacylation of penicillin acylase from *Escherichia coli* ATCC 11105: evidence for lowered pKa values of groups near the catalytic centre. *Biochem J.* **338**:235-239.

Murshudov, G. N., Vagin, A. A. and Dodson, E. J. (1997). Refinement of macromolecular structures by the maximum likelihood method. *Acta Crystallogr*. D**53**:240-255.

Myers, E.W. (1991). An Overview of Sequence Comparison Algorithms in Molecular Biology. Technical Report TR 91-29, University of Arizona, Tucson, Department of Computer Science,

Nair, P.P., Gordon, M. and Reback, J. (1967). The enzymatic cleavage of the carbon-nitrogen bond in 3α,7α,12α-trihydroxy-5-ß-cholan-24-oylglycine. *J. Biol. Chem*. **242**:7-11.

Nakagawa, S.H. and Tager, H.S. (1993). Importance of main-chain flexibility and the insulin fold in insulin-receptor interactions. *Biochemistry*. **32**:7237-7243.

Navaza, J. (1994). AMoRe: An automated package for molecular replacement. *Acta Crystallogr*., A**50**:157-163.

Navaza, J. (2001). Implementation of molecular replacement in AMoRe. *Acta Crystallogr*., D**57**:1367-1372.

Navaza, J. and Saludjian, P. (1997). AMoRe: An automated molecular replacement program package. *Methods Enzymol*. **276**:581-594.

Neurath, H. (1986). The versatility of proteolytic enzymes. *J Cell Biochem*. **32**:35-49.

Oh, B., Kim, M., Yoon, J., Chung, K., Shin, Y., Lee, D. and Kim, Y. (2003). Deacylation activity of cephalosporin acylase to cephalosporin C is improved by changing the side-chain conformations of active-site residues. *Biochem Biophys Res Comm* **310**:19-27.

Ohashi, H., Katsuta, Y., Hashizume, T., Abe, S.N., Kajiura, H., Hattori, H., Kamei, T. and Yano, M. (1988). Molecular cloning of the penicillin G acylase gene from *Arthrobacter viscosus. Appl Environ Microbiol*. **54**:2603-2607.

Ohashi, H., Katsuta, Y., Nagashima, M., Kamei, T. and Yano, M. (1989). Expression of the *Arthrobacter viscosus* penicillin G acylase gene in *Escherichia coli* and *Bacillus subtilis*. *Appl Environ Microbiol*. **55**:1351-1356.

Ohgushi, M. and Wada, A. (1983). 'Molten-globule state': a compact form of globular proteins with mobile side-chains. *FEBS Lett*. **164**:21-24.

Oinonen, C. and Rouvinen, J. (2000). Structural comparison of Ntn-hydrolases. *Prot. Sci.* **9**:2329-2337.

Okada, T., Suzuki, H., Wada, K., Kumagai, H. and Fukuyama, K. (2006). Crystal structures of gamma-glutamyltranspeptidase from Escherichia coli, a key enzyme in glutathione metabolism, and its reaction intermediate. *Proc Natl Acad Sci. USA.***103**:6471-6476.

Oliver, G., Valle, F., Rosetti, F., Gomez-Pedrozo, M., Santamaria, P., Gosset, G. and Bolivar, F. (1985). A common precursor for the two subunits of the penicillin acylase from *Escherichia coli* ATCC11105. *Gene* **40**:9-14.

Olsson, A., and M. Uhlen. (1986). Sequencing and heterologous expression of the gene encoding

penicillin V amidase from *Bacillus sphaericus. Gene*. **45**:175-181.

Olsson, A., Hagstrom, T., Nilsson, B., Uhlen, M. and Gatenbeck, S. (1985). Molecular cloning of *Bacillus sphaericus* penicillin V amidase gene and its expression in *Eshcherichia coli* and *Bacillus subtilis*. *Appl. Environ. Microbiol*. **49**:1084-1089.

Orita, M., Yamamoto, S., Katayama, N. and Fujita, S. (2002). Macrophage migration inhibitory factor and the discovery of tautomerase inhibitors. *Curr Pharm Des*. **8**:1297-1317.

Otwinowski, Z. (1993). DENZO. An oscillation data processing program for macromolecular crystallography. Yale University, New Haven, CT, USA.

Otwinowski, Z. and Minor, W. (1997). Processing of X-ray Diffraction Data Collected in Oscillation Mode, *Methods in Enzymology*, Volume **276**: Macromolecular Crystallography, part A, p.307-326, Carter, Jr. C.W. and Sweet, R. M. Eds., Academic Press (New York).

Pace, C N. (1986). Determination and analysis of urea and guanidine hydrochloride denaturation curves. *Methods Enzymol.* **131**:266-280.

Page, R. D. M. (1996). TREEVIEW: An application to display phylogenetic trees on personal computers. *Comput. Appl. Biosci*. **12**:357-358.

Pampana, E. (1969). A Textbook of Malaria Eradication. London: Oxford University Press.

Patterson, A. L. (1934). A Fourier series method for the determination of the components of interatomic distances in crystals. *Phys. Rev*. **46**:372-376.

Patterson, A. L. (1935). A direct method for the determination of the components of interatomic distances in crystals. *Zeitschrift fur Kristallographie*., A**90**:517-542.

Payne, C.M., Bernstein, H., Bernstein, C. and Garewal, H. (1995). Role of apoptosis in biology and pathology: resistance to apoptosis in colon carcinogenesis. *Ultrastruct Pathol* **19**:221-248.

Pearson, W. R. Comparison of methods for searching protein sequence databases. *Prot. Sci*. **4**:1145-1160.

Pei, J. and Grishin, N.V. (2003). Peptidase family U34 belongs to the superfamily of Nterminal nucelophile hydrolases. *Prot. Sci*. **12**:1131-1135.

Prabhune, A.A. and Sivaraman, H. (1990). Evidence for involvement of arginyl residue at the catalytic site of penicillin acylase from *Escherichia coli*. *Biochem Biophys Res Commun*. **173**:317-322.

Pundle, A. and SivaRaman, H. (1997). *Bacillus sphaericus* Penicillin V Acylase: Purification, Substrate Specificity, and Active-Site Characterization. *Curr. Microbiol*. **34**:144-148.

QUANTA (1997). X-ray structure analysis user's reference. San Diego: Molecular simulations.

Rajendhran, J. and Gunasekaran, P. (2004) Recent biotechnological interventions for developing improved penicillin G acylases. *J Biosci Bioeng*. **97**:1-13.

Ramachandran, G. N. and Sasishekaran, V. (1968). Conformation of polypeptides and proteins. *Adv. Protein. Chem*., **23**:283-438.

Ramachandran, G. N., Ramakrishnan, C. and Sasisekharan, V. (1963). Stereochemistry of Polypeptide Chain Configurations. *J. Mol. Biol.* **7**:95-99.

Ramakrishna, S., and Benjamin, W.B. (1981). Evidence for an essential arginine residue at the active site of ATP citrate lyase from rat liver. *Biochem. J.* **195**:735–743.

Rathinaswamy, P., Pundle, A. V., Prabhune, A. A., SivaRaman, H., Brannigan, J. A., Dodson G. G., and Suresh, C. G. (2005). Cloning, purification, crystallization and preliminary

structural studies of penicillin V acylase from *Bacillus subtilis*. *Acta Cryst*. F**61**:680-683.

Reeder, J.C. and Brown, G.V. (1996). Antigenic variation and immune evasion in Plasmodium falciparum malaria. *Immunol Cell Biol*. **74**:546-554.

Rhodes, Gale. Crystallography Made Crystal Clear. San Diego: Academic Press, 1993 pp. 8-10, 29-38.

Rini, J.M., Schulze-Gahmen, U. and Wilson, I.A. (1992). Structural evidence for induced fit as a mechanism for antibody-antigen recognition. *Science*. **255**:959-965.

Riordan, J. F., McElvany, K. D. and Borders, Jr. C. L. (1977). Arginyl residues: anion recognition sites in enzymes**.** *Science* **195**:884-886.

Roa, A, Garcia, J.L., Salto, F. and Cortes, E. (1994). Changing the substrate specificity of penicillin G acylase from *Kluyvera citrophila* through selective pressure. *Biochem J.* **303**:869-875.

Rossmann, M. G. (2001). Molecular replacement–historical background. *Acta Crystallogr*. D**57**:1360-1366.

Rossmann, M. G. and Blow, D. M. (1962). The detection of sub-units within the crystallographic asymmetric unit. *Acta Crystallogr*. **15**:24-31.

Rossmann, M. G. and Blow, D. M. (1963). Determination of phases by the conditions of non-crystallographic symmetry. *Acta Crystallogr*. **16**:39-45.

Rossmann, M. G., Blow, D. M., Harding, M. M. and Coller, E. (1964). The relative positions of independent molecules within the same asymmetric unit. *Acta Crystallogr*. **17**:338-342.

Rossocha, M., Schultz-Heienbrok, R., Von Moeller, H., Coleman, J.P. and Saenger, W. (2005). Conjugated bile acid hydrolase is a tetrameric N-terminal thiol hydrolase with specific recognition of its cholyl but not of its tauryl product. *Biochemistry*. **44**:5739-5748.

Rupp, B., Marshak, D.R. and Parkin, S. (1996). Crystallization and preliminary X-ray analysis of two new crystal forms of calmodulin. *Acta Crystallogr D Biol Crystallogr*. **52**:411-413.

Sadasivan, C., Nagendra, H. G. and Vijayan, M. (1998). Plasticity, hydration and accessibility in Ribonuclease A. The structure of a new crystal form and its low humidity content. *Acta. Crystallogr.*, D**54**:1343-1352.

Sage-Ono, K., Ono, M., Harada, H. and Kamada, H. (1998). Accumulation of a clock-regulated transcript during flower-inductive darkness in pharbitis nil *Plant Physiol*. **116**:1479-1485.

Sakaguchi, K. and S. A. Murao. (1950). Preliminary report on a new enzyme, "penicillin-amidase". *J. Agric. Chem. Soc*. Jpn. **23**:411.

Salvesen, G.S. and Dixit, V.M. (1999). Caspase activation: the induced-proximity model. *Proc Natl Acad Sci USA.* **96**:10964-10967.

Sanchez, J.C., Schaller, D., Ravier, F., Golaz, O., Jaccoud, S., Belet, M., Wilkins, M.R., James, R., Deshusses, J. and Hochstrasser, D. (1997). Translationally controlled tumor protein: a protein identified in several nontumoral cells including erythrocytes. *Electrophoresis*. **18**:150-155.

Sander, C. and Schneider, R. (1991). Database of homology-derived protein structures. *Proteins* **9**:56-68.

Saridakis, V., Christendat, D., Thygesen, A., Arrowsmith, C.H., Edwards, A.M. and Pai, E.F. (2002). Crystal structure of *Methanobacterium thermoautotrophicum* conserved protein mth1020 reveals an ntn-hydrolase fold. *Proteins: Struct.,Funct.,Genet*. **48**:141-143.

Schneider, W.J. and Roehr, M. (1976). Purification and properties of penicillin acylase of *Bovista plumbea. Biochim Biophys Acta*. **452**:177-185.

Schumacher, G., Sizmann, D., Haug, H., Buckel, P. and Bock, A. (1986). Penicillin acylase from *E. coli*: unique gene-protein relation. *Nucleic Acids Res*. **14**:5713-5727.

Seemuller, E., Lupas, A. and Baumeister, W. (1996). Autocatalytic processing of the 20S proteasome. *Nature*. **382**:468-471.

Semisotnov, G.V., Rodionova, N.A., Razgulyaev, O.I., Uversky, V.N., Gripas A.F. and Gilmanshin, R.I. (1991). Study of the "Molten Globule" intermediate state in protein folding by a hydrophobic fluorescent probe. *Biopolymers.* **31**:119–128.

Sharma, V.P. 1996a. Re-emergence of malaria in India. *Ind J Med Res* 103: 26-45.

Sharma, V.P., Srivastava, A. and Nagpal, B.N. (1994). A study of the Relationship of Rice Cultivation and Annual Parasite Incidence of Malaria in India. *Social Sci Med* **38**:165-178.

Shewale, J. G. and SivaRaman, H. (1989). Penicillin Acylase: Enzyme production and its application in the manufacture of 6-APA. *Proc Biochem*. **24**:146-154.

Shewale, J. G., Kumar, K. K. and Ambedkar, G. R. (1987). Evaluation of determination of 6-Aminopenicillanic acid by p-dimethylaminobenzaldehyde. *Biotechnol Techniq*. **1**:69-72.

Shewale, J.G. and Sudhakaran, V.K. (1997). Penicillin V acylase: its potential in the production of 6-aminopenicillanic acid.*Enzyme Microb.Technol*. **20**:402-410.

Shimizu, M., Masuike, T., Fujita, H., Okachi, R., Kimura, K. and Nara, T. (1975). Purification and properties of penicillin acylase from *Kluyvera citrophila*. *Agr. Biol. Chem*. **39**:1225–1232.

Shimomura, K. (1996). Protein engineering of a cephalosporin C acylase from *Pseudomonas* strain N176. *Ann N Y Acad Sci*. **782**:226-240.

Smith, J.L., Zaluzec, E.J., Wery, J.P., Niu, L., Switzer, R.L., Zalkin, H. and Satow, Y. (1994). Structure of the allosteric regulatory enzyme of purine biosynthesis. *Science.* **264**:1427-1433.

Steinberg, I. Z. (1971). Long-Range Nonradiative Transfer of Electronic Excitation Energy in Proteins and Polypeptides *Annu. Rev. Biochem*. **40**:83-114.

Stellwag, E.J. and Hylemon, P.B. (1976). Purification and characterization of bile salt hydrolase from *Bacteroides fragilis* subsp. *fragilis*. *Biochim. Biophys. Acta* **452**:165-176.

Stryer, L. (1995) Biochemistry, W H Freeman and Co, New York.

Sturzenbaum, S.R., Kille, P. and Morgan, A.J. (1998). Identification of heavy metal induced changes in the expression patterns of the translationally controlled tumour protein (TCTP) in the earthworm Lumbricus rubellus1. *Biochim Biophys Acta*. **1398**:294-304.

Sudhakaran, V.K. and Borkar, P.S. (1985a). Microbial transformation of β-lactam antibiotics: enzymes from bacteria, sources and study - a summary. *Hind. Antibiot. Bull.* **27**:63-119.

Sudhakaran, V.K. and Borkar, P.S. (1985b). Phenoxymethyl penicillin acylases: sources and study - a summary. *Hind Antibiot Bull* **27**:44-62.

Sudhakaran, V.K., B. S. Deshpande, Ambedkar, S. S. and Shewale, J. G. (1992). *Proc. Biochem*. **27**:131-143.

Suresh, C.G., Pundle, A.V., SivaRaman, H., Rao, K.N., Brannigan, J.A., McVey, C.E., Verma, C.S., Dauter, Z., Dodson, E.J. and Dodson, G.G. (1999). Penicillin V acylase crystal structure reveals new Ntn-hydrolase family members. *Nat.Struct.Biol*. **6**:414-416.

Suzuki, H., Miwa, C., Ishihara, S. and Kumagai, H. (2004). A single amino acid substitution converts gamma-glutamyltranspeptidase to a class IV cephalosporin acylase (glutaryl-7-aminocephalosporanic acid acylase). *Appl Environ Microbiol*. **70**:6324-6328.

Suzuki, M., Sugimoto, H., Nakagawa, A., Tanaka, I., Nishihira, J. and Sakai, M. (1996). Crystal structure of the macrophage migration inhibitory factor from rat liver. *Nat Struct Biol*. **3**:259-266.

Svedas, V., Guranda, D., van Langen, L., van Rantwijk, F. and Sheldon, R. (1997). Kinetic study of penicillin acylase from *Alcaligenes faecalis. FEBS Lett.* **417**:414-418.

Svedas, V.K., Savchenko, M.V., Beltser, A.I. and Guranda, D.F. (1996). Enantioselective penicillin acylase-catalyzed reactions. Factors governing substrate and stereospecificity of the enzyme. *Ann N Y Acad Sci*. **799**:659-669.

Takahashi, K. (1968). The reaction of phenyl glyoxal with arginine residue in proteins. *J. Biol. Chem*. **243**:6171-6179.

Tanaka, H., Hashiba, H., Kok, J. and Mierau, I. (2000). Bile Salt Hydrolase of *Bifidobacterium longum*-Biochemical and Genetic Characterization. *Appl. Environ. Microbiol*. **66**:2502-2512.

Tannock, G. W., Bateup, J. M., and Jenkinson, H. F. (1997). Effect of sodium taurocholate on the in vitro growth of *lactobacilli. Microb. Ecol*. **33**:163-167.

Tannock, G. W., M. P. Dashkevicz, and S. D. Feighner. (1989). Lactobacilli and bile salt hydrolase in the murine intestinal tract. *Appl Environ Microbiol.* **55**:1848–1851.

Taylor, A.B, Johnson, W.H. Jr, Czerwinski, R.M., Li, H.S., Hackert, M.L. and Whitman, C.P. (1999). Crystal structure of macrophage migration inhibitory factor complexed with (E)-2-fluoro-p-hydroxycinnamate at 1.8 A resolution: implications for enzymatic catalysis and inhibition. *Biochemistry* **38**:7444-7452.

Thanassi, D. G., Cheng, L. W. and Nikaido, H. (1997). Active efflux of bile salts by *Escherichia coli*. *J. Bacteriol*. **179**:2512-2518

Thaw, P., Baxter, N.J., Hounslow, A.M., Price, C., Waltho, J.P., Craven, C.J. (2001). Structure of TCTP reveals unexpected relationship with guanine nucleotide-free chaperones. *Nat Struct Biol.* **8**:701-704.

Thiele, H., Berger, M., Skalweit, A. and Thiele, B.J. (2000). Expression of the gene and processed pseudogenes encoding the human and rabbit translationally controlled tumour protein (TCTP). *Eur J Biochem*. **267**:5473-5481.

Thompson, J. D., Higgins, D.G. and Gibson, T. J. (1994). CLUSTAL W: improving the sensitivity of progressive multiple sequence alignment through sequence weighting, position-specific gap penalties and weight matrix choice. *Nucleic Acids Res*. **22**:4673-4680.

Torres-Guzman, R., de la Mata, I., Torres-Bacete, J., Arroyo, M., Castillon, M.P. and Acebal, C. (2002). Substrate specificity of penicillin acylase from *Streptomyces lavendulae. Biochem Biophys Res Commun*. **291**:593-597.

Valle, F., Balbas, P., Merino, E. and Bolivar, F. (1991) The role of penicillin amidases in nature and in industry. *Trends Biol Sci.* **16**:36-40.

Valle, F., Gosset, G., Tenorio, B., Oliver, G. and Bolivar, F. (1986). Characterization of the regulatory region of the *Escherichia coli* penicillin acylase structural gene. *Gene* **50**:119-

122.

van der Goot, F.G., Gonzalez-Manas, J.M., Lakey, J.H. and Pattus, F.A. (1991). A 'molten-globule' membrane-insertion intermediate of the pore-forming domain of colicin A. *Nature*. **354**:408-410.

Van Langen, L. M., Oosthoek, N. H. P., Guranda, D. T., Van Rantwijk, F., Svedas, V. K. and Sheldon R. A.. (2000b). Penicillin acylase- catalyzed resolution of amines in aqueous organic solvents. *Tetrahedron Asym*. **11**:4593-4600.

Van Langen, L. M., Van Rantwijk, F., Svedas, V. K. and Sheldon R. A.. (2000a). Penicillin acylase-catalysed peptide synthesis: a chemoenzymatic route to stereoisomers of 3,6-diphenylpiperazine-2,5-dione. *Tetrahedron Asym* **11**:1077-1083.

Van Langen, L.M., Oosthoek, N.H.P., van Rantwijk, F. and Sheldon, R.A. (2003). Penicillin acylase catalysed synthesis of ampicillin in hydrophilic organic solvents. *Adv Syn Cat* **345**:797-801.

Vandamme, E.J. and Voets, J.P. (1974). Microbial penicillin acylases. *Adv. Appl. Microbiol* **17**:311-369.

Verhaert, R.M., Riemens, A.M., van der Laan, J.M., van Duin, J. and Quax, W.J. (1997). Molecular cloning and analysis of the gene encoding the thermostable penicillin G acylase from *Alcaligenes faecalis. Appl Environ Microbiol.* **63**:3412-3418.

Verhaert, R.M.D, van Duin, J. and Quax, W.J. (1999). Processing and functional display of the 86 kDa heterodimeric penicillin G acylase on the surface of phage fd. *Biochem J* **342**:415-422.

Wakelin, D. (1978). Genetic control of susceptibility and resistance to parasitic infection. *Adv Parasitol*. **16**:219-308.

Walsh, B.J., Gooley, A.A., Williams, K.L. and Breit, S.N. (1995). Identification of macrophage activation associated proteins by two-dimensional gel electrophoresis and microsequencing. *J Leukoc Biol.* **57**:507-512.

Wang, H., Chen, J., Hollister, K., Sowers, L.C. and Forman, B.M. (1999). Endogenous bile acids are ligands for the nuclear receptor FXR/BAR. *Mol Cell.* **3**:543-553.

Waterman. M.S. Introduction to Computational Biology. Chapman and Hall, London, 1995.

Waterman. M.S. Sequence Alignments. In M.S. Waterman, editor, Mathematical Methods for DNA Sequences, pages 53-92. CRC-Press, Boca Raton, FL, 1989.

Weber, C., Wider, G., von Freyberg, B., Traber, R., Braun, W., Widmer, H. and Wuthrich, K. (1991). The NMR structure of cyclosporin A bound to cyclophilin in aqueous solution. *Biochemistry* **30**:6563-6574.

Weiser, W.Y., Temple, P.A., Witek-Giannotti, J.S., Remold, H.G., Clark, S.C. and David, J.R. (1989). Molecular cloning of a cDNA encoding a human macrophage migration inhibitory factor. *Proc Natl Acad Sci USA*. **86**:7522-7526.

Wilbur, W.J. and D.J. Lipman. (1983). Rapid Similarity Searches of Nucleic Acid and Protein Data Banks. *Natl. Acad. Sci. USA* **80**:726-730.

Woodley, J.M. (2000). Advances in Enzyme Technology - UK contributions. Adv.Biochem. Eng., **70**:93-108.

Xu, Q., Buckley, D., Guan, C. and Guo, H.C. (1999). Structural insights into the mechanism of

intramolecular proteolysis. *Cell.* **98**:651-661.

Yan, L., Leontovich, A., Fei, K. and Sarras, M.P. Jr. (2000). Hydra metalloproteinase 1: a secreted astacin metalloproteinase whose apical axis expression is differentially regulated during head regeneration. *Dev Biol.* **219**:115-128.

Yang, S., Huang, H., Li, S.Y., Ye, Y.Z., Wan, L., Zhang, F.W. and Yuan, Z.Y. (2000). Enhancing Penicillin G Acylase Stability by Site-directed Mutagenesis. *Sheng Wu Hua Xue Yu Sheng Wu Wu Li Xue Bao* (Shanghai). **32**:581-585.

Yoshida, K., Fujimura, M., Yanai, N. and Fujita, Y. (1995). Cloning and sequencing of a 23-kb region of the *Bacillus subtilis* genome between the *iol* and *hut* operons. *DNA Res*. **6**:295-301.

Zang, X., Taylor, P., Wang, J.M., Meyer, D.J., Scott, A.L., Walkinshaw, M.D. and Maizels, R.M. (2002). Homologues of human macrophage migration inhibitory factor from a parasitic nematode. Gene cloning, protein activity, and crystal structure. *J Biol Chem*. **277**:44261-44267.

Zhengping, L., Chenghui, L., Yuqin, S. and Xinrui, D. (2005). Study on the interaction between protein and 8-anilino-1-naphthalenesulfonic acid by resonance light scattering technique. *Chemical J Internet*. **7**:83.